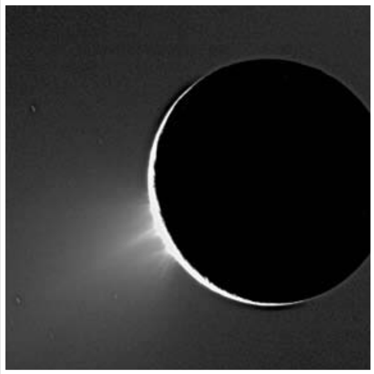 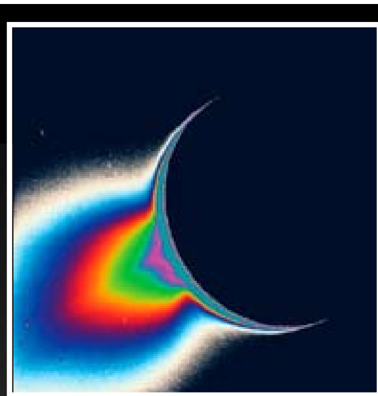  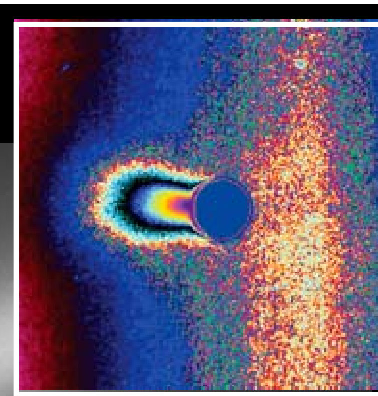

11.2.2007 (Revision 1, Edited for Public Release)

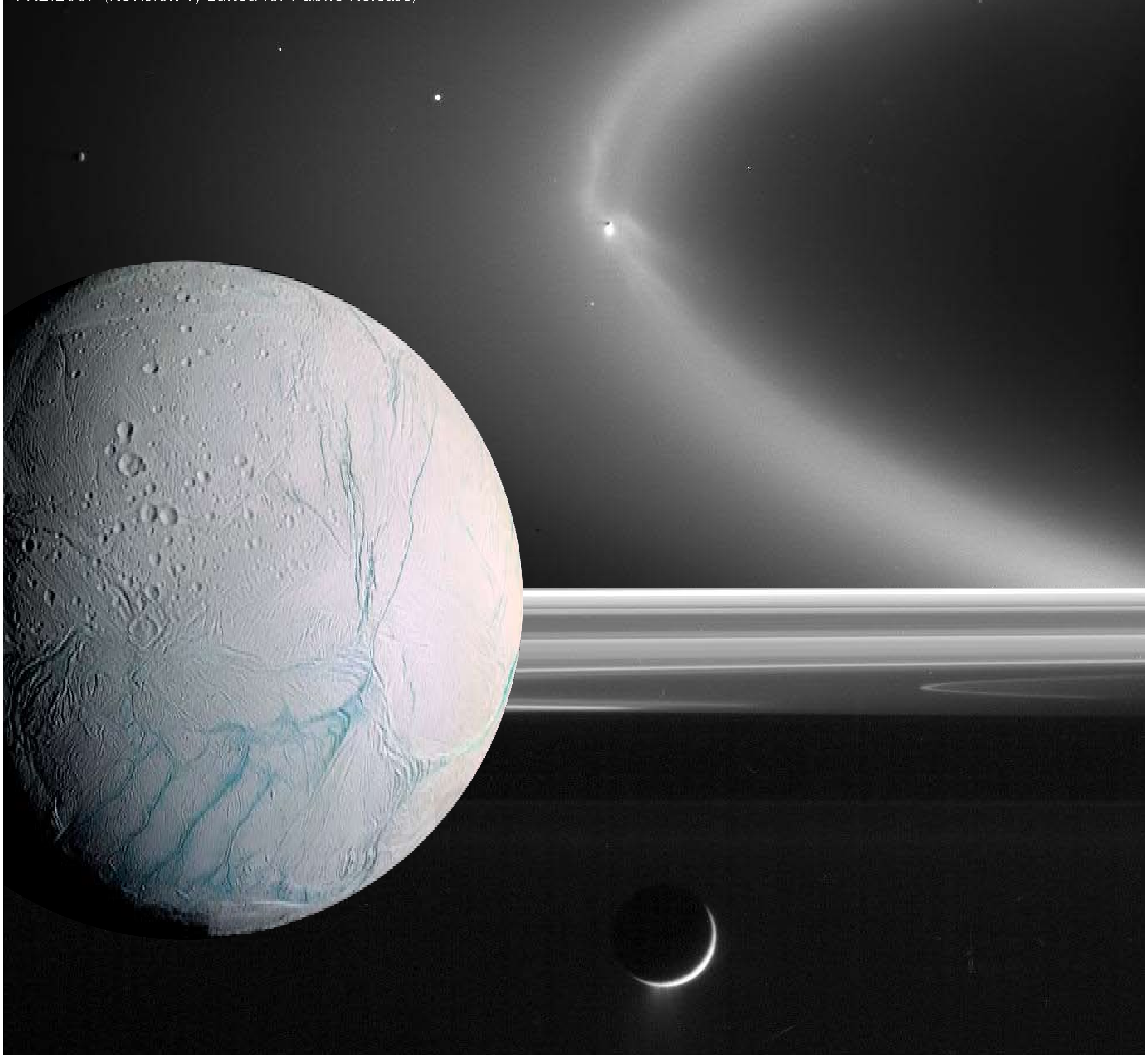

ENCELADUS

Saturn's
Active
Ice Moon

Enceladus Flagship Mission Concept Study

NASA Goddard Space Flight Center
August 29, 2007

Prepared for NASA's Planetary Science Division

Contributing Authors:

Mission Design Team

Vince Bly
David Di Pietro
David Quinn
Andrea Razzaghi
Gary Sneiderman
Steven Tompkins
Lauri Via

Science Definition Team

Amy Barr
William Brinkerhoff
Bonnie Buratti
J. Bradley Dalton
Andrew Dombard
Daniel Glavin
Paul Helfenstein
Joseph Kirschvink
Donald Mitchell
Francis Nimmo
Amy Simon-Miller
John Spencer

Andrea I. Razzaghi
Study Lead
NASA GSFC

Amy A. Simon-Miller
SDT Co-Chair
NASA GSFC

David A. Di Pietro
Mission Systems Engineer
NASA GSFC

John R. Spencer
SDT Co-Chair
Southwest Research Institute

Preface

Upon the recommendation of the NASA Advisory Council Planetary Science Subcommittee and the Outer Planets Assessment Group (OPAG), NASA Headquarters (HQ) Planetary Science Division commissioned pre-Phase A studies of Flagship missions to Europa, Ganymede/Jupiter system, Enceladus, and Titan. The purpose of these studies is to inform near term strategic decisions for the next Flagship mission. NASA's Goddard Space Flight Center (GSFC) was directed to conduct the Enceladus study.

NASA HQ appointed an Enceladus Science Definition Team (SDT) consisting of members drawn from the science community. The Enceladus SDT developed the science objectives, prioritized subobjectives, defined an example strawman payload, and worked with the mission design team to create the mission scenarios, concept of operations and instrument accommodation requirements. The SDT based science priorities on those recommended in the 2003 Decadal Survey for planetary science and on work performed by previous science teams in support of the JPL-led study documented in Titan and Enceladus $1B Mission Feasibility Report, JPL D-37401 (*Reh et al. 2007*). (The two SDT Co-Chairs provided a consolidated view of the SDT's advice as input for this study.)

The NASA GSFC assembled a mission design team (listed in **Section 5**) to develop mission architecture concepts to address the science goals identified by the SDT. A Champion Team (listed in **Section 5**), whose members have expertise in the keys areas required for this study, provided advice to the mission design team at critical decision points, and reviewed and endorsed this report.

Relative to the initial edition of the report released 29 August 2007, this Revision 1 edition contains changes that permit the report to be released to the public. It also includes editorial corrections along with a few minor technical corrections which materially affect neither the results nor the recommendations.

Table of Contents

1.0 EXECUTIVE SUMMARY

1.1 Overview

Based on existing knowledge of Enceladus and 2003 Decadal Survey goals, the Science Definition Team (SDT) developed science goals for studying Enceladus and identified the possible mission configurations that could meet those goals. Orbiters, as well as a single flyby spacecraft, were considered with the added possibility for sample return and various lander-type options. **Table 1.1-1** shows the mission configuration trade space and provides a brief assessment of science value. **Section 2** of this report outlines why low science value, high risk, or other reasons removed some configurations from further study.

Within this trade space the mission design team identified 12 possible architectures that could be developed into mission concepts to meet the stated science goals. Of those 12, three were selected for concept development because of their high science value and their ability to provide insight into the remainder of the trade space; an Enceladus orbiter with a soft lander (Enceladus-OL), an Enceladus orbiter (Enceladus-O) and a Saturn orbiter with a soft lander (Saturn-OL). These three cases were purposely selected to enable evaluation of different points in the architecture trade space and to expedite developing an understanding of basic system sizing, performance, and cost over the broad range of potential implementations. **Sections 3.3** through **3.5** of this report present these three concepts. **Section 3.6** uses these results, along with the trajectory and technology trade study work performed, to provide insight into the feasibility, advantages, and disadvantages of the other possible architectures identified.

1.2 Enceladus Science

Enceladus, a 500-km diameter moon of Saturn, is one of the most remarkable celestial bodies in the solar system, as revealed by recent discoveries from the Cassini mission. It is the only icy world in the solar system proven to have current geological activity, offer the possibly of biological potential, and provides a way to sample fresh material from its interior via active plumes. The plume source region on Enceladus provides a plausible site for complex organic chemistry and even biological processes, and fresh samples from this environment can be obtained by flying past Enceladus and sampling its plume.

Enceladus provides dynamic examples of phenomena that have been important at some time throughout the outer solar system. Also, because Enceladus is the source of the Saturnian E-ring, as well as the extensive neutral O and OH clouds that fill the middle Saturnian magnetosphere, the moon plays a pivotal role in the Saturnian system, similar in some ways to Io's role in the Jovian system. For all these reasons, a mission to Enceladus would produce valuable science that is highly relevant to NASA goals as laid out in the 2003 Decadal Survey for planetary science.

1.2.1 Science Goals

The overarching science goal for a future Enceladus mission is the investigation of its biological potential, as that ties together many inter-related disciplines and has high priority in the Decadal Survey. Second-level goals, which are essential to addressing the primary goal, are the understanding of Enceladus' tidal heating and interior structure, its composition, its cryovolcanism, and its tectonism. Of tertiary importance is the

Table 1.1-1: Full Configuration Trade Space

Configuration	Only	+ Soft Lander	+ Hard Lander(s)	+ Dumb Impactor	+ Plume Sample Return
Saturn Orbiter	Incremental science return	High science return	Seismic network adds value	Modest science return	High potential science return
Enceladus Orbiter	High science return	Highest science return	Seismic network adds value	Modest science return	High potential science return
Single Flyby	Low science return	Low science return	No way to return data	Modest science return	High potential science return
Lander Only	Low science return	N/A	No way to return data	Modest science return	High potential science return

understanding of surface processes, and the interaction of Enceladus with the rest of the Saturn system.

1.2.2 Measurement Requirements

The key measurements needed to address these science goals would:

- Characterize the surface of Enceladus with global imaging, topographic, compositional, and thermal maps
- Probe the interior structure seismically and/or with sounding radar
- Probe the interior through tidal response, electromagnetic induction signature, and high-order gravity and shape mapping
- Investigate the chemical, pre-biotic, and potential biotic evolution of Enceladus with *in-situ* chemical analysis of plume gases and solids, and surface analysis.

Cassini will continue to add to our knowledge of Enceladus through the small number of close flybys planned for the remainder of its mission. However, Cassini has limited ability to make the above measurements due to its brief time near Enceladus, the high speed of its encounters, instrumentation that is not optimized for these measurements, and its inability to perform *in-situ* surface science. Thus, the science goals defined here for a Flagship mission are not expected to be fundamentally changed by new knowledge from Cassini, unless truly unexpected discoveries are made.

1.2.3 Instrument Types

A broad suite of instruments were considered in this study to make these measurements. Remote sensing instruments include pushbroom visible, near-infrared, and thermal infrared mapping cameras, with a framing camera and an ultraviolet spectrometer as lower priority instruments. Geophysics instruments include a laser altimeter and radio science for measurement of tidal flexing and static topography and gravity, and a radar sounder when possible. *In-situ* instruments include plume dust and gas analyzers, including mass spectrometers, and for analysis of samples collected at low speed, a scanning electron microscope. Lander instruments include a comprehensive surface chemistry package and a seismometer. It is recognized that many different science instruments can be used to address the same science goals. While the instruments presented are not an exhaustive list, they provide examples of balanced science payloads and allowed for operations and mass scoping of detailed mission designs.

1.3 Mission Architecture Assessment

1.3.1 Key Challenges to Studying Enceladus

Missions to study Enceladus will present some key challenges. Those common to any mission to Saturn include designing a trajectory that will deliver the spacecraft to the Saturn system in a reasonable amount of time, with a reasonable amount of payload. Those unique to Enceladus include the large ΔV required once in the Saturn system to either orbit or land on Enceladus. Alternatively, they include methods to mitigate that large ΔV at the expense of adding to mission duration and life cycle cost. They also include methods to protect the spacecraft while it samples the plume near the Enceladus south pole. Additionally, planetary protection considerations become important not only for disposal of landers left on Enceladus, but also for orbiters which may impact Enceladus. The same is potentially true for boosters which separate between Titan and Enceladus and which may impact other icy moons within the Saturn system over the same time interval.

Risk reduction analyses were conducted to help address some of these challenges including: a) evaluation of inner planet gravity assists enroute to Saturn, b) the use of Solar Electric Propulsion (SEP) as well as chemical propulsion trajectories, c) the use of either Saturn moons between Titan and Enceladus and aerocapture to reduce the ΔV required to either orbit or land on Enceladus, d) the viability of a free-return trajectory for a sample return mission, and e) requirements for debris shielding.

The evaluation of these risks identified further considerations. The use of gravity assists at Venus drives the spacecraft thermal system, and the use of gravity assists at Earth with a spacecraft that uses a radioisotope power supply imposes special safety constraints. Also, the extended duration between launch and the start of science operations resulting from the use of multiple gravity assists drives mission reliability. Additionally, for architectures that include orbiting Enceladus (a small moon), the characterization of the gravitational field of

Enceladus is a challenge as many of the orbits about Enceladus are significantly perturbed by the size and proximity of Saturn. Furthermore, a landing on Enceladus must be conducted in a fully autonomous manner, which means the lander must be able to identify and react to surface hazards as it approaches the surface.

1.3.2 Technical Approach

Before commencing development of concept designs, the mission design team performed risk reduction and fact finding studies. This phase focused primarily on identifying trajectories for orbiting Saturn, for orbiting Enceladus and for free return for sample collection. The team also consulted with experts from other NASA centers and the Department of Energy (DOE) to examine:

- solar electric and chemical propulsion
- aerocapture to reduce ΔV requirements
- debris shielding
- radioisotope power systems

Following this initial study phase, the team performed studies in the GSFC Integrated Mission Design Center (IMDC)[1] to initiate the development of the Enceladus-OL, Enceladus-O and Saturn-OL concepts.

1.3.3 Architecture Trade Space

The architecture trade space for this study is shown in **Table 1.1-1**. Some of these options were considered to be of low science priority, such as single flybys, and were not considered any further as explained in **Section 2**. In addition, there are many ways to implement each mission concept. For example, both solar electric and chemical propulsion systems were considered. The launch vehicles considered were limited to Atlas V 551 and Delta IV Heavy due to performance needs. Within this trade space, the following technical architectures were identified:

1. Enceladus orbiter with soft lander with chemical propulsion (Enceladus-OL)
2. Enceladus orbiter with chemical propulsion (Enceladus-O)
3. Saturn orbiter with soft lander with SEP (Saturn-OL)
4. Enceladus orbiter that lands with chemical propulsion
5. Enceladus orbiter using SEP
6. Enceladus orbiter with hard impactor(s)
7. Saturn orbiter with soft lander using chemical propulsion and gravity assists
8. Saturn orbiter with soft lander using SEP and more Saturnian moon flybys
9. Saturn orbiter with hard impactor(s)
10. Sample return with or without orbiter
11. Dual launch vehicle – loosely coupled orbiter/lander
12. Dual launch vehicle – Low Earth Orbit (LEO) assembly

1.3.4 Trade Space Concept Designs

Three promising mission concepts were developed: Enceladus-OL, Enceladus-O and Saturn-OL. **Sections 3.3** through **3.5** of this report present the details of these designs. **Table 1.3-1** summarizes their salient features. No requirements for mission-specific technology development were identified for any of these concepts.

1.3.5 Remaining Architectures in Trade Space

The implications of the remaining architecture concepts in the trade space are discussed in **Section 3.6** of this report and summarized in **Table 1.3-2**.

1.4 Cost

Tables 1.4-1 to **1.4-3** show the cost estimates for the three concepts developed during this study, broken out by WBS element for fiscal year (FY) 2007 dollars.

[1] The NASA/GSFC IMDC provides engineering analyses, end-to-end mission design products and grassroots and parametric cost estimates during concept development studies, which nominally last one to one-and-a-half weeks per concept

Table 1.3-1: Summary of Trade Space Concept Designs

	Enceladus -OL	Enceladus O	Saturn –OL
Mission Description	Enceladus orbiter w/soft lander	Enceladus orbiter	Saturn orbiter w/soft lander
Instruments	Orbiter: imagers and *in-situ* Lander: imager, seismometer, sample analysis	Orbiter: imagers, radar, and *in-situ*	Orbiter: imagers and *in-situ* Lander: imager, seismometer, sample analysis
Trajectory (all use Saturn & Titan gravity assists)	VVEES + Rhea & Dione gravity assists	VVEES + Rhea gravity assists	Earth gravity assist
C_3 (km^2/s^2)	19.05	19.05	19.2
Launch Date	29 Sep 2018	29 Sep 2018	Mar 2018
Nominal Mission Duration (years)	18.3	17.3	9.5
Orbiter Science Ops (years)	2.4	2.4	1.3
Lander Science Ops (days)	5-8	N/A	5-8
Plume passages	12 @ 0.143 km/s	12@ 0.143 km/s	12@ 3.8 km/s
Number of Stages	3	2	3
Propulsion Type	Dual-mode chemical booster & orbiter Mono-prop lander	Dual-mode chemical booster & orbiter	25 kW SEP module Dual-mode chemical orbiter Bi- prop lander
∆V from Chemical Propellant (m/s)	Booster and orbiter: 4497 Lander: 415	Booster and orbiter: 4977	Orbiter: 2797 Lander: 4315
Launch Mass (kg)	6320	5810	6196
Launch Vehicle Type	Delta IV Heavy	Delta IV Heavy	Delta IV Heavy
Cost (FY07 $B)	2.8 to 3.3	2.1 to 2.4	2.6 to 3.0

Table 1.3-2: Summary of Remaining Trade Space Architectures

Remaining Architectures in Trade Space			
Architecture	**Derivation**	**Benefits**	**Drawbacks**
Enceladus orbiter that lands with chemical propulsion	Enceladus-OL or Enceladus-O	Longer lander lifetime	Complexity required for instruments and subsystems to work in two different environments, mission life
Enceladus orbiter using SEP	Orbiter from Enceladus-O and SEP from Saturn-OL	Shorter mission lifetime, ~ 15.5 years, than Enceladus-O	SEP adds complexity and expense
Enceladus orbiter with hard impactor(s)	Enceladus-OL or Enceladus-O	Low cost multipoint surface observation for enhanced geophysics	Concepts and technology for hard landers are immature
Saturn orbiter with soft lander using chemical propulsion and gravity assists	Saturn-OL with gravity assists from the Enceladus-OL	Smaller launch vehicle	Longer required mission lifetime than Saturn-OL
Saturn orbiter with soft lander using SEP and more Saturnian moon flybys	Saturn-OL with lesser moon gravity assists of Enceladus-OL	Less ΔV for the lander, slower flybys, and increased plume dwell time	Longer required mission lifetime; 2.5 to 5 years longer
Saturn orbiter with hard impactor(s)	Saturn-OL	Low cost multipoint surface observation for enhanced geophysics	Concepts and technology for hard landers are immature
Sample return with or without orbiter	Not related	Much less propellant required than Trade Space Concept Designs	Long mission (~26 years), single sample opportunity; high Earth reentry velocity
Dual launch vehicle – loosely coupled orbiter/lander	Enceladus-OL	More robust lander and orbiter	Cost
Dual launch vehicle – LEO assembly	Enceladus-OL	More robust lander and orbiter	Not Feasible

Table 1.4-1: Enceladus-OL Cost Estimate

FY07 ($M)	
Cost Element	
Project Elements:	
1.0 Project Management	**61**
2.0 Mission Sys Engr	**52**
3.0 Mission Assurance	**38**
4.0 Science	**124**
5.0 Payload	**225**
6.0 Spacecraft	**417**
7.0 Mission Ops	**270**
9.0 Ground System	**52**
10.0 System I&T	**40**
Subtotal	**1,279**
Uncertainty Range (40% to 70%)	**511 to 895**
Subtotal w/ Uncertainty	**1790 to 2173**
Reserves	**531 to 645**
Sub total w/reserves (30%)	**2320 to 2818**
Elements w/o cont:	
8.0 Launch Vehicle	**486**
11.0 E/PO	**3**
FY07 ($B)	
Mission Total Range	**2.8 to 3.3**

Table 1.4-2: Enceladus-O Cost Estimate

FY07 ($M)	
Cost Element	
Project Elements:	
1.0 Project Management	**53**
2.0 Mission Systems Engineering	**43**
3.0 Mission Assurance	**34**
4.0 Science	**54**
5.0 Payload	**128**
6.0 Spacecraft	**251**
7.0 Mission Operations	**240**
9.0 Ground System	**49**
10.0 System I&T	**24**
Subtotal	**876**
Uncertainty Range (40-70%)	**350 to 613**
Subtotal w/Uncertainty	**1225 to 1488**
Reserves	**363 to 441**
Subtotal w/reserves (30%)	**1589 to 1929**
Elements w/o cont:	
8.0 Launch Vehicle	**486**
11.0 E/PO	**2**
FY07 ($B)	
Mission Total Range:	**2.1 to 2.4**

Table 1.4-3: Saturn-OL Cost Estimate

FY07 ($M)	
Cost Element	
Project Elements:	
1.0 Project Management	**61**
2.0 Mission Sys Engr	**52**
3.0 Mission Assurance	**39**
4.0 Science	**78**
5.0 Payload	**200**
6.0 Spacecraft	**495**
7.0 Mission Ops	**137**
9.0 Ground System	**54**
10.0 System I&T	**35**
Sub total	**1,151**
Uncertainty Range (40-70%)	**460 to 805**
Subtotal w/ Uncertainty	**1611 to 1956**
Reserves	**476 to 579**
Subtotal w/reserves (30%)	**2087 to 2534**
Elements w/o cont:	
8.0 Launch Vehicle	**486**
11.0 E/PO	**3**
FY07 ($B)	
Mission Total Range:	**2.6 to 3**

1.5 Conclusions and Findings

A mission to Enceladus would produce high-value science that is highly relevant to NASA goals as laid out in the 2003 Decadal Survey and described in this report. The accessibility of subsurface water enable sampling through conventional means and without complicated drilling scenarios. The SDT defined a comprehensive set of science goals that can be met, to varying degrees, by a wide range of mission configurations.

The highest priority science goal for a future Enceladus mission is the investigation of its biological potential. Of secondary importance are the understanding of Enceladus' tidal heating and interior structure, its composition, its cryovolcanism, and its tectonism. Of tertiary importance is the understanding of surface processes, and the interaction of Enceladus with the rest of the Saturn system. Cassini can still make valuable contributions towards addressing these questions, but is limited by its instrumentation, its orbit and by its inability to land on Enceladus. Thus Cassini cannot adequately address the advanced science goals defined here.

These goals can be met most effectively by both orbiting Enceladus and landing on its surface. Orbiting Enceladus allows comprehensive mapping of its surface morphology, composition and heat flow, including detailed investigation of the active plume vents. The interior structure and tidal heating mechanisms, including the presence or absence of a subsurface ocean, can also be investigated through determination of the moon's gravity and global shape, its potential and shape Love numbers, its magnetic induction signature, and crustal structure can be probed using sounding radar. Multiple plume passages at the low orbital speed of ~150 m/s will allow collection of intact plume particles and complex organic molecules from the plume for onboard study. A lander provides the opportunity for seismometry *in-situ* chemical analysis and unique views of surface process.

The mission design team developed three promising concepts using state of the practice technology: Enceladus-OL, Enceladus-O, and a Saturn-OL, with cost estimates in the two to three billion dollar ($FY07) range. All three present the possibility of providing valuable Flagship-level science, allow the further evaluation of the full architecture trade space, and represent single points in the architecture trade space. For each case, trades can be made that affect mission lifetime and deliverable mass. In addition, common key challenges, risks and technology liens emerged, including:

- trajectory design and resultant ΔV budget
- chemical propulsion (enables more delivered mass at the cost of time)
- SEP (saves time at the expense of mass and complexity)
- aeroassist to decrease propellant mass (at the expense of complexity and mass for the aeroshell)
- deficiency of current gravity models of Enceladus

  - affects orbital stability estimates

- paucity of flight data in Saturn environment radiation model

- long required lifetimes, regardless of which trajectory is chosen

  - has implications for overall mission reliability

  - technology lien for critical spacecraft components to undergo additional long-life testing (particularly true in the case of sample return missions which could have lifetimes in excess of 25 years)

- planetary protection guidelines

- lander concerns:

  - soft landers must maintain anchoring to the surface during any sample collection and surface coupling for seismometer experiments

  - soft lander concepts that operate on battery power result in short life

  - hard impactor package needs further definition in several areas (e.g., battery sizing, thermal design, deployment approach, landing shock attenuation orienting in preferred attitude on surface, coupling to the surface, etc.)

In summary, based on SDT-defined goals and measurement requirements, the architecture trade study presented in this report found promising Enceladus mission concepts that would provide valuable, Flagship-level, science in the two to three billion dollar ($FY07) range. The three study concepts that were developed use state of the practice technology and could be developed in time to meet the proposed launch dates. Key challenges, considerations and risks have been identified, some of which are common to any mission to Saturn and some of which are unique to missions to study Enceladus. Possible mission design trades and their effects were discussed, along with insights gleaned about remaining trade space architectures. The SDT concluded that a Flagship mission to Enceladus can achieve a significant advance in knowledge and several mission concepts are identified that merit further study.

2.0 ENCELADUS SCIENCE GOALS AND OBJECTIVES

2.1 Science Goals

2.1.1 Introduction: The Importance of Enceladus

Enceladus (**Figure 2.1.1-1**) is one of the most remarkable moons in the solar system. It has captured the attention of planetary scientists since the early 1980s, when Voyager revealed Enceladus' extraordinarily high albedo and its youthful and heavily modified surface (*Smith et al. 1982*). Ground-based observations further demonstrated that Saturn's diffuse E-ring is concentrated at the orbit of Enceladus (*Baum et al. 1980*). The very short estimated lifetime of E-ring particles requires a constant source of replenishment, and speculation about geyser activity on Enceladus supplying fresh material to the ring is not new (*Haff et al. 1983*). However, it was a series of Cassini observations in 2005 that provided definitive proof that Enceladus is one of the very few solid bodies in the solar system that is currently geologically active. Multiple Cassini instruments detected plumes of gas and ice particles emanating from a series of warm fractures centered on the south pole, dubbed the "tiger stripes."

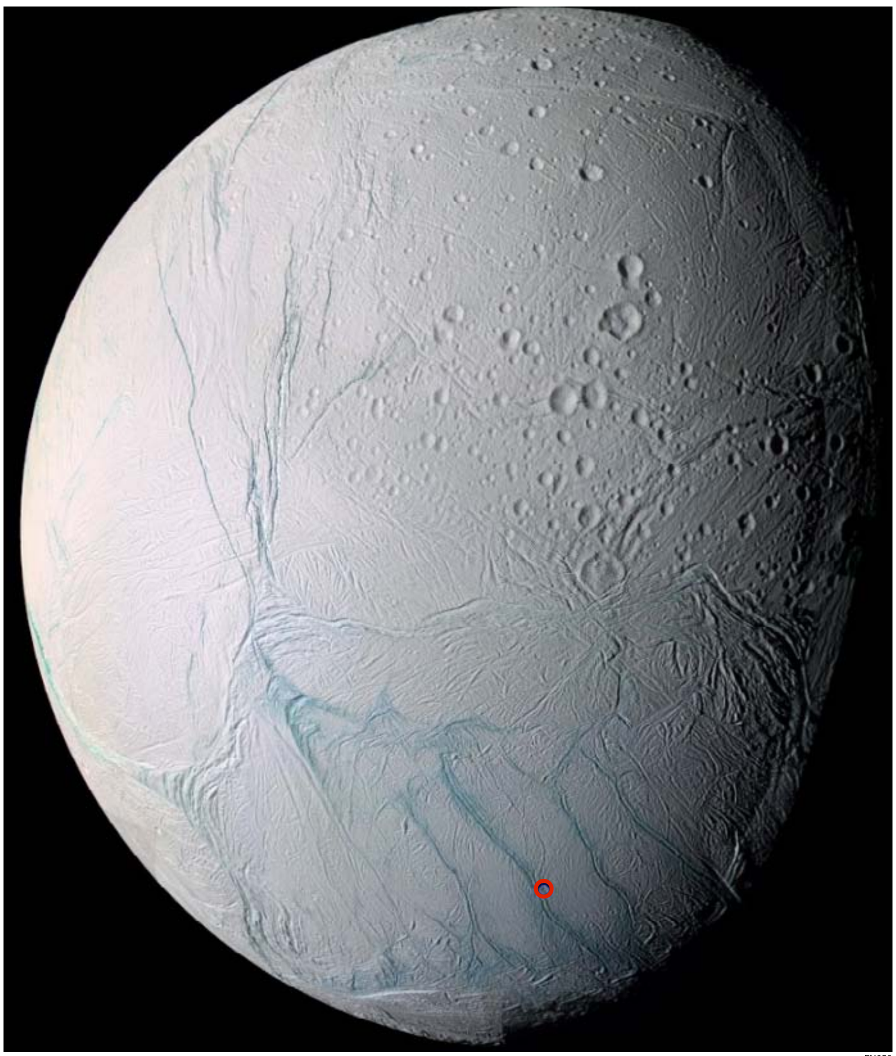

Figure 2.1.1-1: Global Cassini view of Enceladus (diameter 500 km). The active south polar region is ringed by a scalloped fracture zone and includes the four parallel "tiger stripe" fractures in its central region. The south pole itself is marked by a red circle. Credit: NASA/JPL/Space Science Institute, PIA06254.

The plume source region on Enceladus provides a warm, chemically rich, environment, perhaps including liquid water, that is a plausible site for complex organic chemistry and even biological processes. Most importantly, fresh samples from this environment can be obtained and studied by flying past Enceladus and sampling its plume, allowing investigation of Enceladus' interior and its biological potential. No other icy satellite offers this opportunity.

As the only proven example of a geologically active ice world (with the possible exception of Triton), Enceladus provides active examples of phenomena that have been important at one time or another throughout the outer solar system. These processes, including tidal heating, cryovolcanism, and ice tectonism, can be studied as they happen on Enceladus, leading to understanding that can be applied throughout the outer solar system. Finally, because Enceladus is the source of the E-ring, as well as the extensive neutral O and OH clouds that fill the middle Saturnian magnetosphere, the moon plays a pivotal role in the Saturnian system similar in some ways to Io's role in the Jovian system. For all these reasons, a mission to Enceladus would produce compelling science that is highly relevant to NASA goals (see **Section 2.1.5**).

Prioritized science goals for a future Enceladus mission are summarized in **Table 2.1.1-1** and discussed in detail below. There is no prioritization within the three broad categories, and many of the goals are inter-related (**Figure 2.1.1-2**) and require similar measurements. Detailed flow-down from these goals to specific measurements and mission requirements is given as traceability matrix in **Section 2.2.1**.

Table 2.1.1-1: Prioritized Science Goals

Priority	Goal	Section
1	Biological Potential	2.1.2.1
2	Composition	2.1.3.1
	Cryovolcanism	2.1.3.2
	Tectonics	2.1.3.3
	Tidal Heating and Interior Structure	2.1.3.4
3	Saturn System Interaction	2.1.4.1
	Surface Processes	2.1.4.2

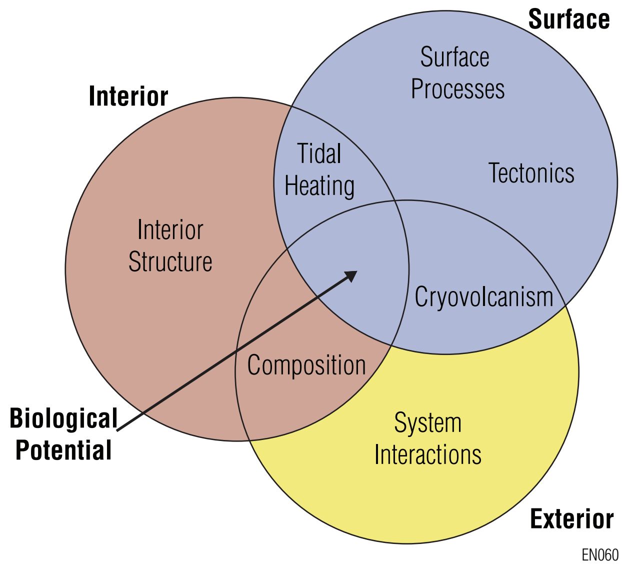

Figure 2.1.1-2: Illustration of the overlapping and interdependent nature of the science goals discussed here.

2.1.2 Priority 1 Goals

2.1.2.1 Biological Potential

The search for extraterrestrial habitable environments is a driving force in planetary exploration, as outlined in the 2003 Decadal Survey. Because Enceladus is arguably the place in the solar system where space exploration is most likely to find a demonstrably habitable environment, evaluating its biological potential is the overarching goal of Enceladus exploration. Evaluating the habitability of Enceladus involves understanding nearly all other aspects of Enceladus science, so much will be learned even if the conclusion reached is that Enceladus cannot support life as we currently understand it. In addition, though detection of extant life is perhaps unlikely, the enormous impact of such a discovery makes it worthwhile to carry some instrumentation (for instance, to measure molecular chirality) that is specifically designed for that task.

Current State of Knowledge

Despite its small relative size, there are many reasons to suspect that life might have evolved and could be supported more easily on Enceladus than on other icy moons in the outer solar system suspected of having liquid-water oceans, such as Europa or Callisto. Oxidation/reduction reactions (redox chemistry) provide the only known, and most plausible, energy partitioning and storage systems that might drive a biosphere (see discussion in *Gaidos et al.* (*1999*)). All known biochemistry is certainly dependent on electron-transport, as evidenced by the electron transport chains that permeate all of biochemistry. In terms of supporting redox-based life, the ice-covered oceans of the outer planets need to have access to both end-members of a significant redox couple, and the further apart the end-members are chemically, the more plausible are the initial steps in the evolution of metabolism (*Kirschvink and Weiss 2002*). Both end-members of the redox scale are, therefore, of equal importance.

At the reducing end of this scale it is not difficult to find suitable materials for driving a biosphere. Hot H_2 gas in the inner portion of the ancient solar nebula led to the widespread chemical reduction of Fe and Ni-bearing dust particles, which were later accreted into progressively larger objects, and processed in the core of proto-planetary bodies. Hence, all solid bodies in the solar system are intrinsically capable of providing the reducing couple for a biosphere, assuming that a suitable geological process (like silicate volcanism) is present to mix these materials with more oxidizing counterparts. On Enceladus, the chemical composition of materials in the plume and on the surface suggests the presence of a heat source hot enough to decompose ammonia into N_2 and drive reactions with hydrocarbons, implying internal temperatures on the order of 500-800 K. In turn, this suggests some form of silicate volcanism presumably driven by tidal interactions (*Matson et al. 2007*). A volcanic source near Enceladus' south pole, and a substantial body of water in an ice-covered ocean, is also consistent with the moon's shape and inferred true Polar Wander events which would have moved this effective negative mass anomaly to the body's spin axis (*Collins and Goodman 2007*; *Nimmo and Pappalardo 2006*). Similar tidal processes could plausibly supply a source of reductants on Europa (*Squyres et al. 1983*).

Gaidos et al. (*1999*) noted that for Europa, the availability of oxidants is the primary factor which makes life in ice-covered oceans difficult, particularly in situations where hydrothermal circulation in response to continuous volcanic activity will act to cycle and recycle the same fluid over billions of years on a time scale much faster than the ice dynamics; chemical equilibrium is reached quickly and virtually all significant chemical gradients disappear. *Hand et al. (2006)* have since argued that the concentration of oxidants in planetary ices may be much higher than estimated previously, but still falls short by three orders of magnitude when compared with the most energy-deprived ecosystem known on Earth (*Parkinson et al. 2007*). This is a serious problem, because organisms on Earth that are able to survive in these energy poor environments are highly adapted to exploit them, and clearly evolved from more flexible ancestors. Hence, it is unlikely that they would be conducive to any scenario for the origin of life in the first place (*Kirschvink and Weiss 2002*).

Parkinson et al. (*2007*) note that the oxidant supply on Europa may pale in comparison with that of Enceladus. Although the production of oxidants per unit area on the surfaces of the two bodies should be roughly the same, the presence of the E-ring of Saturn may tip the balance in favor of Enceladus. Ice particles that are ejected in the plumes to form Saturn's E-ring act as a 'chemical processor' when exposed to energetic particles and UV radiation in the space environment. As it sweeps through its orbit, Enceladus will sweep up many of these particles again, adding them to the oxidants formed in situ. Coupled with the presence of an active ice cycle as indicated by the plumes themselves (*Hurford et al. 2007b; Nimmo et al. 2007*) this also argues for an enhanced biological potential for Enceladus in comparison with Europa. As discussed further in **Section 2.1.4.1**, particles in the E-ring are also responsible for reducing the background flux of lethal radiation in its portion of Saturn's ring system, which could well expand the habitable zone of surface-based life in extrasolar planetary systems with similar stressed moonlets.

Finally, and most importantly, the plumes of Enceladus simplify the problem of collecting samples from the ice-covered ocean. Although the plumes themselves may or may not be directly sampling the liquid water reservoir (*Nimmo et al. 2007*), the warm ice needed to support these plumes when tidal forces open cracks would most likely have risen from a deeper, liquid body near the heat source at depth. Under these circumstances it is quite plausible that bits of an oceanic biosphere (even intact microorganisms) could get trapped in these ice plumes as they rise, and be expelled into orbit around Saturn. Rather than searching the Jovian system for 'freeze-dried fish' ejected from the occasional massive impact on Europa, as suggested by *Dyson* (*1997*), detecting freeze-dried microbes around Enceladus might actually be possible.

Major Questions

Specific questions relevant to this science goal include: Is liquid water present on Enceladus, either in a subsurface ocean, in the plume vent regions, or elsewhere? How extensive and long-lived is the water, if present, and what is its chemistry? What energy sources are available for life? And on Enceladus, one may even be able to answer the most important question of all: is life present there now?

Measurement Requirements

Almost all measurement requirements considered here are important to this overarching science goal. Most critical are measurements that probe interior conditions, particularly measurements of the plume, its source region, and its fallout on Enceladus' surface, but also geophysical measurements that can establish the presence of a subsurface ocean and constrain the nature of the tidal heat engine. Some measurements in particular, however, hold the potential for direct detection of extant life. *In-situ* microscopic analysis of plume particles might be able to directly image biological structures frozen within the particles, if any existed, and a surface chemistry package with the ability to measure the chirality of organic compounds would be able to measure any enantiomeric excess (i.e., a preference for one chirality over the other), which would be a strong indicator of biotic origin.

2.1.3 Priority 2 Goals

2.1.3.1 Composition

Telescopic and recent spacecraft observations have provided most of what is known about the composition of Enceladus' surface. Composition is important to understanding the answers to several major questions regarding chemistry, surface processes, interactions with the rings, the formation and subsequent evolution of the Saturn system, and the evaluation of astrobiology potential. Strategies for answering these questions involve a combination of remote and *in-situ* approaches.

Current state of knowledge

The current state of knowledge is summarized in **Table 2.1.3-1**. Water ice occurs in both crystalline and amorphous forms over much of Enceladus' surface. CO_2 has been unambiguously detected by Cassini VIMS both as free ice and complexed with another material (*Brown et al. 2007*). This host may be water ice, a mineral, or another volatile ice. Clathrates have been suggested by several authors, e.g., *Kieffer et al.* (*2006*); *Brown et al.* (*2007*); *Kargel et al.* (*2007*). Evidence for low concentrations of short-chain organic molecules in the ice is strong, especially near the tiger stripes (**Figure 2.1.3-1**, *Brown et al. 2006*), and other absorption features have been observed that have yet to be identified. Curiously, carbon monoxide and ammonia have not yet been seen, though they are predicted by several lines of reasoning, including their possible role in producing the plume through melting point depression. Silicates also have not been identified, though Enceladus' high density of 1608 kg/m^3 suggests a high silicate/ice ratio.

Table 2.1.3-1: Molecules known or predicted to be on Enceladus. Entries in lower two rows of the table have been predicted on the basis of theoretical arguments but have not been observed.

	Surface	Plume
Observed	H_2O (crystalline, amorph.) CO_2 (free, trapped)	H_2O CO_2 CH_4 CO or N_2
Trace	Organics	NH_3 C_2H_2 C_3H_8 HCN
Expected	CO NH_3 or $NH_3 \bullet nH_2O$ Clathrates	CO OH O+
Theorized	Salts Acids Ammonium Methanol	

Plume material is likely to fall back to the surface on ballistic trajectories. A combination of mass spectrometry (**Figure 2.1.3-2**) and infrared spectroscopy reveals it to be dominated by H_2O, with from one to four percent of CO_2, CH_4 (*Waite et al. 2007*), and a molecule of mass 28. This molecule is believed to be either CO or N_2; most likely N_2, because of the absence of CO in the Cassini FUV spectra (*Waite et al. 2007*; *Hansen et* *al. 2007*). Additional materials observed in trace quantities include ammonia, acetylene, propane and HCN (*Waite et al. 2007*). Also expected, but not yet detected, are OH and O^+ (*Hansen et al. 2007*), which were previously observed to occupy a torus linked to Saturn's magnetosphere (*Shemansky et al. 1993*).

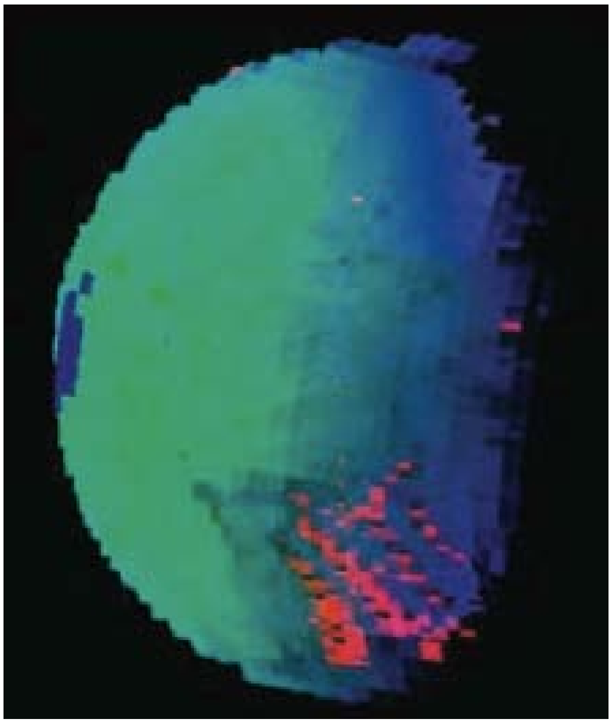

Figure 2.1.3-1: Near-infrared composite image of Enceladus showing the concentration of the 3.44 μm C-H stretch band (red) along the south polar tiger stripes. *Brown et al.* (*2006*).

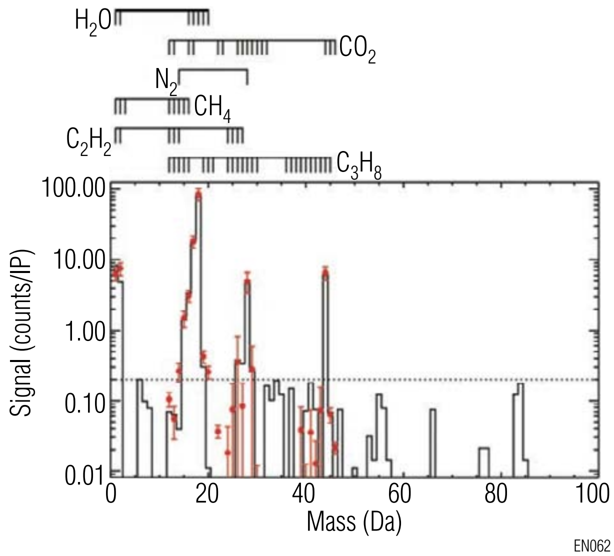

Figure 2.1.3-2: Cassini INMS mass spectrum of the Enceladus plume, taken in July 2004, showing mass peaks due to H_2O, CO_2, N_2, CH_4, and possibly C_2H_2 and C_3H_8. (*Waite et al. 2006*).

Major Questions

The presence, or absence, of various materials on the surface or in the plume is inextricably linked with several major issues. What chemical reactions are occurring in the plume, or in the subsurface, possibly in liquid H_2O? Aqueous chemistry in a subsurface liquid environment is expected to produce a number of compounds diagnostic of interior composition and circulation as well as low-temperature chemistry within the crust. Are biologically relevant materials being created? What are the physical conditions in the active regions? Is the plume composition the same everywhere, or are there variations in space and time? To what extent are materials transported to the surface altered through photolytic or radiolytic processing, or low-temperature chemistry at the surface? What are the details of the surface chemistry? How chemically heterogeneous is the surface? What are the timescales for cycling of crustal materials? Is there a chemical distinction between the materials of the optical surface layer and those below?

The composition of Enceladus should also be reflected in the composition of the plume and consequently of the E-ring as well. How does this affect the ring system? What are the rates and quantities of supplied materials, and the relative abundances of different components? What are the consequences for the rest of the ring system, or for the Saturn system?

The relative abundances of other materials within the ice can dramatically affect the appearance of surface features. What are the global distributions of chemical species? How do they affect the landscape? Are sublimation-degradation processes concentrating these materials? Are ammonia, methanol, chloride salts, or some other materials depressing the melting point and enabling cryovolcanism, or is it somehow occurring in their absence? Perhaps ammonia was present in the past but has been sequestered as ammonium minerals (*Kargel 2006*). Even small amounts of contaminants can change rheological properties by orders of magnitude, and would, for instance, affect our understanding of apparent viscous relaxation of craters seen on Enceladus. These effects of composition can be exploited to probe the formation history of Enceladus, the initial complements of planet-forming materials, and subsequent meteoritic and cometary infall, weathering and other processes.

And what is the impact of these processes on the astrobiology potential? Knowledge of the surface composition will enhance understanding of these processes and the ways in which they influence the creation and maintenance of viable habitats, production and transport of biogenic elements and compounds, and energy sources that could support biological processes.

Measurement Requirements

These questions are best addressed through a combination of remote and *in-situ* measurements that can detect both predicted and unknown compounds. From orbit, a multicolor visible imager can quantify changes in albedo, texture, coloration, and geomorphology, enabling interpretation of surface structures and inference of composition. The use of discrete filters can allow mapping of specific materials, such as CH_4 and H_2O. The real power of the remote sensing system for compositional analysis though is provided by near-IR spectroscopy, which will detect diagnostic absorption features for a number of compounds and map their abundances both locally and globally. Scientific return would be further enhanced by the addition of UV spectroscopy for surface and remote plume analysis (see Priority 2 goals).

Information about plume composition determined, for instance, by *in-situ* gas chromatography and mass spectroscopy (GCMS) can provide invaluable information on the nature of the plume source region. It can also provide valuable information for constraining interpretations of the remote sensing data, by providing detailed and broad (wide mass range) organic and molecular analysis of plume particles. Analysis of dust composition, density, and particle sizes will further enhance the scientific return. Knowledge of plume composition, knowledge of surface composition from landed instruments, which can provide precise quantitative information on major and minor constituents at a single location, and knowledge of surface composition from orbiting instruments can all serve to provide checks on results achieved by other methods, and ultimately feed into the other scientific objectives as well.

2.1.3.2 Cryovolcanism

The most remarkable known aspect of Enceladus is its south polar plume activity (**Figure 2.1.3-3**, *Hansen et al. 2006*; *Waite et al. 2006*; *Porco et al. 2006*; *Dougherty et al. 2006*; *Srama et al. 2006*). This is the only known example of active cryovolcanism in the solar system (the origin of Triton's very different plumes is unknown, but they are plausibly driven by seasonal N_2 frost sublimation rather than internal heat (*Brown et al. 1990*)). Understanding this remarkable phenomenon should thus be a major goal of future missions to Enceladus.

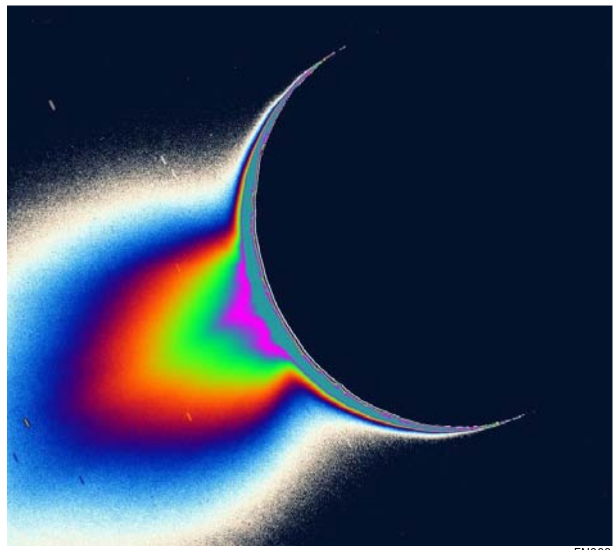

Figure 2.1.3-3: Cassini high phase angle false-color image of the Enceladus plume, showing forward-scattering by micron-sized plume particles. From *Porco et al.* (*2006*).

Current State of Knowledge

The plumes arise from warm surface fractures (*Spencer et al. 2006*), the "tiger stripes" (*Porco et al. 2006*). Sublimation of warm surface ice (*Spencer et al. 2006*), boiling of near-surface liquid water (*Porco et al. 2006*), decomposition of clathrates at depth (*Kieffer et al. 2006*), and sublimation at depth due to frictional heating (*Nimmo et al. 2007*) have all been proposed as plume generation mechanisms. The surface fractures radiate 6 GW (*Spencer et al. 2006*) and the plume latent heat carries away another ~1 GW, and this energy must be continually resupplied from the heat source at depth, by movement of gas or liquid water, or (less plausibly) by conduction through the ice.

The mass production rate of plume gas, crucial to understanding the plume source and Enceladus' effect on broader the Saturn system, is estimated to be ~150 kg/s from stellar occultation data (*Tian et al. 2006*). This value is surprisingly high, sufficient to remove a significant fraction of Enceladus' mass over the age of the solar system (*Kargel et al. 2006*). Plume ice particle production and escape rates are much more poorly constrained than the gas (*Porco et al. 2006*; *Spahn et al. 2006*), because of limited knowledge of plume particle sizes. A globally-distributed source of dust and gas is necessary to explain the Cassini *in-situ* data (*Waite et al. 2006*; *Spahn et al. 2006*) but whether this results entirely from sputtering and impacts or requires low-level non-polar plume activity is not yet established.

Major Questions

The plume generation mechanism, and how energy is delivered to the near-surface of Enceladus to supply the plumes, is not understood. Understanding this mechanism, and thus understanding the physical and chemical conditions in the plume sources, is of great importance.

Many uncertainties remain in understanding the plume gas and particle production, escape, and resurfacing rates. Particle masses and size distributions are an important constraint on plume mechanisms (*Porco et al. 2006*), and are crucial to understanding mass loss, and supply of material to the E-ring. Much of the dust, and probably some of the gas, falls back to the surface and is probably a major resurfacing mechanism, but rates and spatial distribution of this resurfacing are unknown. The detailed chemistry of the plumes is also not yet known.

The temporal variability of the plumes is unknown. There is a suggestion that they might be controlled by daily tidal changes (*Hurford et al. 2007b*), and longer-term variability is also likely. It is also unknown whether low-level plume or other cryovolcanic activity occurs at locations other than the south polar terrain. Other forms of cryovolcanism may occur on Enceladus, but details are unknown. For instance, the presence of large boulders near the tiger stripes (**Figure 2.1.4-3**) may imply occasional episodes of much more violent activity than have been seen by Cassini. It is also possible that extrusive cryovolcanism occurs on Enceladus, and might explain some of the more exotic landforms seen in the Cassini images (*Kargel et al. 2006*).

Measurement Requirements

Understanding Enceladus' plumes requires a combination of techniques. Remote sensing is necessary: high-resolution imaging of the plume vent morphology and the plumes themselves, detailed near-infrared mapping of the composition of the plume fallout and its spatial distribution, and thermal mapping of near-vent temperatures. Tidal flexing and radar sounding measurements will help to understand local heating and crustal structure near the vents. Measurements of plume chemistry and plume particle morphology will reveal much about the source region and will constrain resurfacing rates.

2.1.3.3 Tectonics

Understanding the complex tectonic evolution of Enceladus would be a primary goal of an Enceladus mission. Tectonic features dominate the surface, and have many intriguing similarities to, and differences from, tectonic features found on other icy satellites.

Current State of Knowledge

Cassini images have revolutionized the Voyager view of this satellite (cf., *Morrison et al. 1986*; *Kargel and Pozio, 1996*), demonstrating, for instance, that "smooth terrain" is pervasively tectonized (*Helfenstein et al. 2005*; *Rathbun et al. 2005*). **Figure 2.1.3-4** shows that diverse features crosscut the surface, revealing an intricate history. Several different tectonic processes seem to have been at work. The sinuous chain of scarps that bound the south polar terrain at a latitude of ~55 °S appear to have formed in response to compressional forces, while north-trending fracture zones that radiate from peculiar Y-shaped cusps and interrupt the chain of scarps appear to be extensional (*Helfenstein et al. 2006a*; *Porco et al. 2006*). Shear offsets along pre-existing rifts are also observed near the transition between these contractional and extensional features. The origin of "tiger stripes," a system of parallel rifts through which cryovolcanic plumes erupt, is currently unclear.

While the south polar terrain is a focus of pervasive active tectonism, other regions are less so (e.g., the cratered north polar region). Analysis of the relationship between impact craters and tectonic features (*Barnash et al. 2006*; *Bray et al. 2007*) indicates that the tectonism has persisted through time. Furthermore, fossil terrains elsewhere on Enceladus reminiscent of the south polar terrain suggest multiple resurfacing episodes throughout the satellite's history (*Helfenstein et al. 2006b*; *Schenk and Seddio, 2006*).

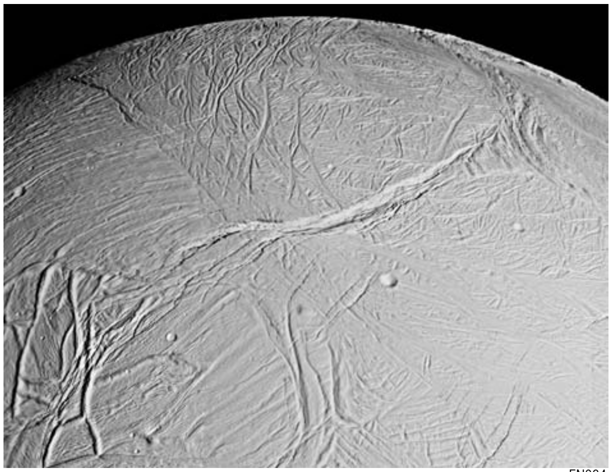

EN064

Figure 2.1.3-4: Mosaic of Cassini ISS images, displaying several different tectonic styles that indicate a complex tectonic history. South is towards the right. The radius of Enceladus is 251 km. Courtesy NASA/JPL-Caltech (image # PIA06191).

The chain of scarps bounding the south polar terrain, as well as the northward-radiating fracture zones, may be the product of a change in Enceladus's global figure, possibly associated with a wholesale reorientation of the satellite (i.e., polar wander). The correspondence of the south polar terrain with a rotational pole is not likely coincidental, and models that seek to explain the south polar activity (*Nimmo and Pappalardo, 2006*; *Collins and Goodman, 2007*) often incorporate a long-wavelength low in the equipotential surface of Enceladus that can drive polar wander. Last, the shape of the satellite is changed on a daily basis because of tidal working. The apparent morphology and orientation of at least one tiger stripe could be a result (*Hurford et al. 2007a*), and tidal flexing may play an important role in creating the vapor plumes issuing from the tiger stripes, in general (*Nimmo et al. 2007*; *Hurford et al. 2007b*).

Major Questions

Several questions motivate this science goal. A first question concerns the nature of the tectonic features, since whether they formed from horizontal extension, contraction, or shearing of the surface bears directly on the evolution of Enceladus. An Enceladus mission would also seek to resolve why tectonic patterns vary so widely across the surface and how tectonism has changed over time. It is also important to understand the stresses that have given rise to tectonic features, for instance convection within the icy mantle, possibly involving a regime similar to "plate tectonics" on Earth (e.g., *Helfenstein et al. 2006a*), can induce tractions on the surface; thus, unraveling the tectonics may illuminate these convective motions.

Finally, Enceladus may hold the key to understanding tectonic processes on other icy satellites. Indeed, many tectonic features on Enceladus may be analogous to features observed on other icy satellites such as Europa (**Figure 2.1.3-5**), Ganymede, and perhaps Titan. Thus, study of the tectonics of Enceladus, which is probably currently active, can be used as a natural laboratory to investigate the response to stresses of the other icy surfaces of the outer solar system.

Measurement Requirements

High-resolution images are vital for interpreting the individual features and the forces that led to their formation. Near-complete coverage of high-resolution (~10 m/pixel) imaging will provide a detailed tectonic framework, and morphology of individual features, that is essential for understanding Enceladus' tectonism. Stereo imaging of selected features will allow quantitative modeling of their evolution. Radar sounding can investigate the subsurface expressions of tectonic features, providing important constraints on their nature. Measurements of tidal flexing, and local gravity and topography, will aid understanding of the stresses driving tectonic activity. It is also possible that motions along active tectonic features could be detected by repeated very precise topographic measurements, for instance using laser altimetry, or by seismometry from the surface.

2.1.3.4 Tidal Heating and Interior Structure

Enceladus ranks alongside Io and possibly Triton as one of the few geodynamically active

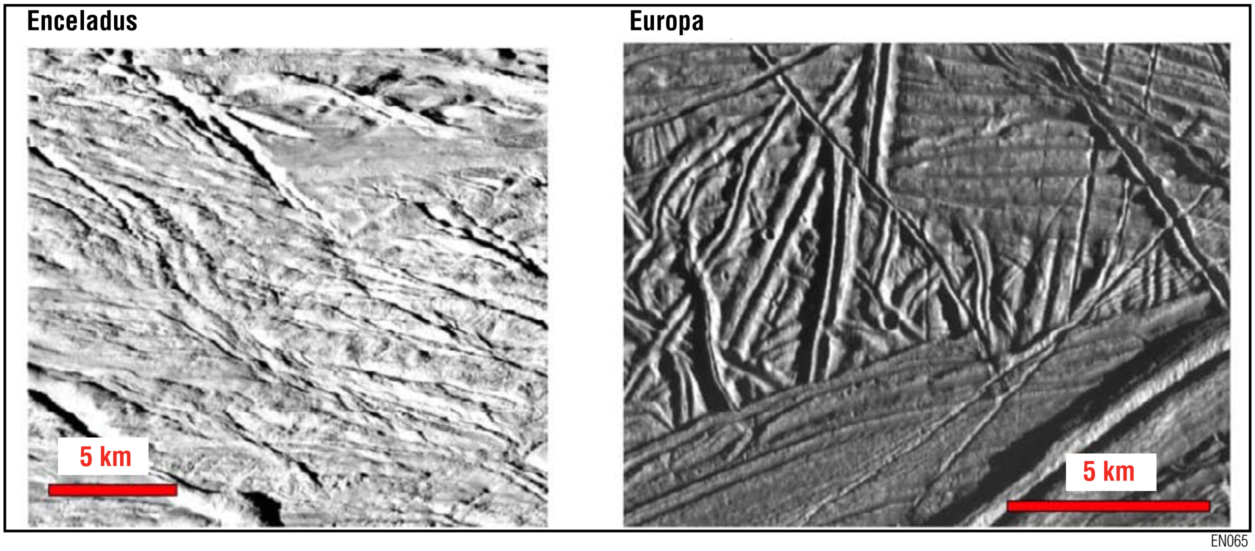

Figure 2.1.3-5: Comparison of tectonic features on Enceladus (left) and Europa (right) at similar scales. Credit: NASA/JPL/Space Science Institute/Arizona State University (PIA06251, PIA00849).

satellites in the solar system. Understanding the tidal heating engine that almost certainly drives this activity, and the interior structure that both controls and is controlled by the tidal heating, is vital to understanding Enceladus as a whole.

Current State of Knowledge

Enceladus' mean density is 1608.3 kg/m^3 and its mean radius 252.1 km (*Thomas et al. 2007*). The interior structure of Enceladus is not known, however, calculations suggest that it is likely differentiated with an icy shell ~90 km thick that surrounds a silicate core that could either be hydrated or dehydrated (**Figure 2.1.3-6**) (*Barr and McKinnon 2007*; *Schubert et al. 2007*).

It is not known whether Enceladus has a subsurface ocean. If a global ocean exists, it would decouple the ice shell from the underlying rocky core, permitting tidal dissipation and tidally driven tectonics similar to Europa. An ocean, or even isolated pockets of subsurface liquid water could conceivably provide a habitat for primitive life.

The heat flux from Enceladus' south polar region is between 3 to 7 GW based on CIRS observations (**Figure 2.1.3-7**, *Spencer et al. 2006*); the global heat flux could be ~10 times as high. Radiogenic heating from Enceladus' rocky component supplies only ~0.3 GW at present (*Schubert et al. 2007*), so tidal dissipation is likely supplying the rest of the heat. The exact mechanism by which tidal deformation in Enceladus results in

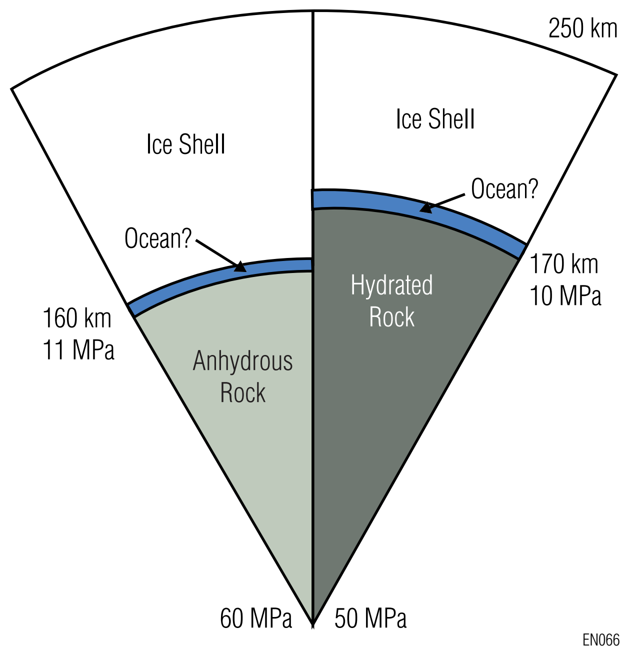

Figure 2.1.3-6: Interior structure of a differentiated Enceladus (*Barr and McKinnon 2007*), assuming solar-composition rock (*Mueller and McKinnon 1988*), a pure ice shell, and an updated iron abundance (*Lodders 2003*). An internal liquid layer may exist at the base of the ice shell.

internal heating is not known; it is possible that dissipation occurs within the deep interior of a warm convecting satellite (as envisioned by *Ross and Schubert* (*1989*)) but also plausible that dissipation occurs close to its surface on shallow fault zones (*Nimmo et al. 2007*). Regardless of the method of dissipation, Enceladus must be warm and/or partially molten to experience significant tidal flexing and dissipation – the mode of initial warming to "kick start" tidal heating is not known (though ^{26}Al heating has been suggested as one possible mechanism (*Castillo et al. 2006*)). If tidal dissipation is localized to the south pole, it could provide enough heat to maintain a local subsurface sea, topographic low, and to drive cryovolcanism (e.g., *Collins and Goodman 2007*).

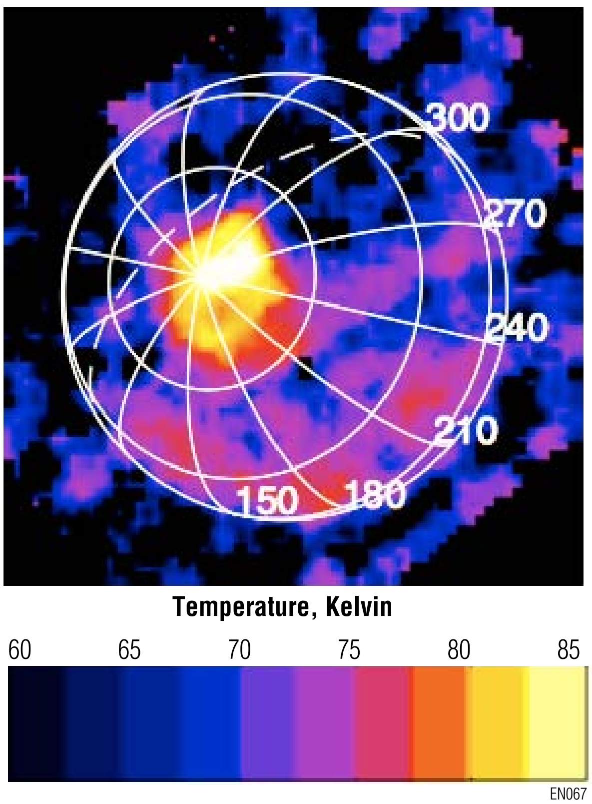

Figure 2.1.3-7: False-color image of 12-16 micron color temperatures on Enceladus, from the Cassini Composite Infrared Spectrometer (CIRS) showing the heat radiation from the warm tiger stripes in the south polar region. Peak temperatures are much warmer, at least 145 K, than the low-resolution averages shown here. The dashed line is the terminator. *(Spencer et al. 2006).*

Evidence that high heat flux has been present for long periods comes from the observations that many ancient impact craters on Enceladus show clear evidence of viscous relaxation due to locally elevated near-surface temperatures at some time in the body's past (*Passey 1983*; *Smith et al. 2007*; *Schenk and Moore 2007*).

To date, measurements of Enceladus' tidal heat flux are the only quantitative constraints on the amount of tidal dissipation and its spatial localization in any icy satellite. Tidal dissipation occurs in Enceladus because the satellite does mechanical work against its own internal rigidity. The amount of tidal dissipation therefore depends on the amount of deformation occurring within Enceladus over its daily orbital cycle.

Major Questions

Understanding the interior structure of Enceladus, and the heat engine that drives its activity, is a key goal of a flagship mission. It is important to constrain the extent of differentiation, the presence of an ocean, and the modes of heat transport and generation in the interior. For this it is necessary to understand the moon's heat flow, the internal density and thermal structure and ice shell thickness, and the location and distribution of liquid water.

Measurement Requirements

Determination of Enceladus' static gravity field to sufficient degree and order to look for subsurface density anomalies, and with proper geometry to independently measure J_2 and C_{22} (see *McKinnon 1997* for discussion); measurement of its magnetic field (both intrinsic and inductive); and seismic sounding, will provide essential constraints on interior structure. In addition, measurements of Enceladus' time-variable potential and surface deformation can provide estimates of its Love numbers, h_2 and k_2, which can be used to constrain its interior structure (for example to help determine the presence of an ocean), and, serve as first steps toward modeling tidal dissipation because they relate tidal deformation to the applied tidal potential. The determination of the subsurface thermal structure using some sort of sounding technique (such as seismology or ice-penetrating radar) would provide valuable information about the modes of tidal dissipation and hold the key to understanding tidal dissipation in other satellites, and thermal infrared measurements of surface temperature, coupled with bolometric albedo measurements to understand and remove the absorbed sunlight contribution, will constrain global and local heat flow. Such measurements would also provide valuable constraints on the thickness of Enceladus' lithosphere, which affects its modes of resurfacing and surface/subsurface material exchange. Measurements of the topography of viscously relaxed impact craters will provide important constraints on the time history and spatial distribution of heat flow throughout Enceladus' history.

2.1.4 Priority 3 Goals

2.1.4.1 Saturn System Interaction

In addition to Enceladus being an interesting body in its own right, it has a major influence on the rest of the Saturn system. In turn, the larger Saturn system influences Enceladus in many ways. The processes involved are particularly interesting because they may affect both Enceladus' ability to support life, and the habitability of hypothetical extrasolar planetary systems that may contain Enceladus-like worlds.

Current State of Knowledge

Since Enceladus orbits deep in Saturn's magnetosphere, the impact of energetic trapped particles on Enceladus' surface is an important process. Particle precipitation contributes to the aging and chemistry of Enceladus' surface layer through sputtering and radiolysis. While such processes are not unique to Enceladus, the interpretation of surface materials to determine the age of various surface regions on Enceladus depends on an understanding of such surface processes. For this reason, it is important to characterize the radiation environment of Enceladus in any mission that seeks to understand the resurfacing of the moon by its plume material. Micrometeorite gardening, either from interplanetary dust particles or returning E-ring particles, is also a potentially important process.

Of perhaps even broader interest, is the role Enceladus plays in modifying the inner magnetospheric environment of Saturn. Saturn's magnetosphere, although intermediate in size and field strength between the magnetospheres of Jupiter and Earth, traps much less intense energetic ion and electron populations than either Jupiter or Earth. Much of this difference can be attributed to Enceladus, and the relatively dense cold gas cloud it produces. This cloud of water products, ejected from Enceladus south polar rift features, is not gravitationally bound to Enceladus precisely because Enceladus is so small. Spreading out over the inner magnetosphere of Saturn, the gas removes essentially all of the energetic ions between six and three Saturn radii (R_s) via charge exchange, and degrades the energy of the energetic electron population throughout the same region through coulomb collisions. This results in a radiation environment three orders of magnitude less intense than that of Earth, and even weaker relative to Jupiter. And that relatively benign environment extends to the moons Mimas, Tethys, and Dione, and to a lesser degree, Rhea. Thus, Enceladus, at 500-km diameter, completely dominates the radiation environment throughout the inner Saturnian magnetosphere. If a process like this is at all common throughout the universe, it may be a significant factor in the probability of encountering habitable zones about giant planets such as Saturn where radiation might otherwise preclude life (at least at the surface of moon, as, for example, at Jupiter), or alternately, might provide energy for subsurface life (*Chyba 2000*). Investigation of Enceladus' interaction with the magnetosphere is, therefore, of interest to the entire question of the evolution of life throughout the universe.

In addition to gas, Enceladus' plumes also contain very fine dust particles. Many of these particles are ejected with sufficient velocity that they, too, escape Enceladus' weak gravity field and spread to form the tenuous E-ring about Saturn (**Figure 2.1.4-1**). The E-ring is dominated by ~1 micron ice particles, with some larger ones, though the size/frequency distribution is not well known. The E-ring is typically less than a Saturn radius in thickness, and extends from about three to ten R_s, with peak density near its source at the orbit of Enceladus. Particles in the E-ring are composed of ejecta from the plumes, either directly in solid state, or flash-frozen as they exit. In either case, they carry with them material from Enceladus interior in solid form, so their composition is of great scientific interest. These dust particles also deposit on the surfaces of the other icy moons, transferring mass from Enceladus to those moons, and modifying their surface albedo and texture.

Major Questions

Important questions that need to be addressed include the following. Has the influence of Enceladus on the magnetospheric environment been continuous over the evolution of the Saturn system, or is it relatively recent? Is the mechanism behind the plumes and the support of the cold gas cloud in the magnetosphere unique to Enceladus, or is it a mechanism that can be expected to recur

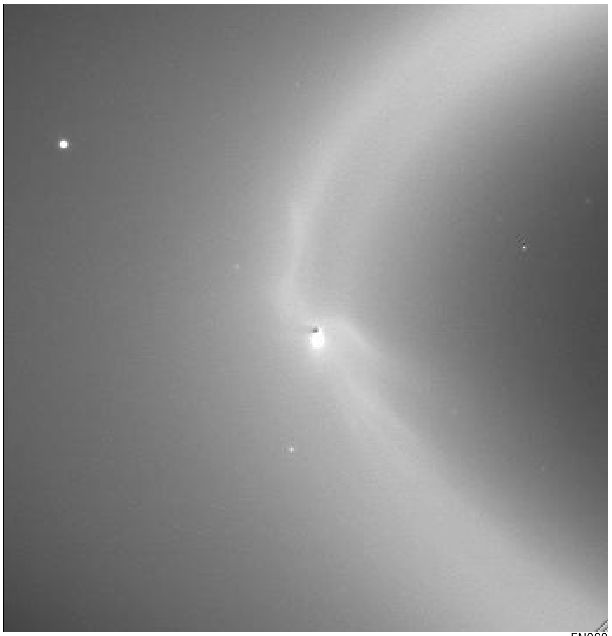

Figure 2.1.4-1: Very high phase angle Cassini image showing the complex interaction between Enceladus (the central black dot), its plume (the bright streak below Enceladus), and the E-ring (the diffuse arc). Credit: NASA/JPL/Space Science Institute (PIA08321).

regularly in other solar systems? What is the parametric dependence of the gas cloud on such variables as solar UV, plasma electron temperature, dipole tilt, solar cycle, etc.? What is the role of the E-ring dust in modifying the plasma and energetic particle environment of Enceladus and the other icy moons? What role does sputtering from satellite surfaces play in amplifying the density of the water products cloud? What controls the structure of the E-ring, and the dynamics, and lifetime of the particles that comprise it?

Measurement Requirements

Measurements needed to address these questions include magnetic field, energetic particles and plasma (electrons, ions, composition), and neutral gas density and composition. Measurements of the size and spatial distribution of E-ring particles, using *in-situ* or remote observations, are also important. These measurements are needed throughout the inner magnetosphere, both close to Enceladus and in the Enceladus to Titan magnetospheric regions. Measurements of the Enceladus plume itself, in particular the nature and fluxes of the escaping dust and gas, are also important for this goal.

2.1.4.2 Surface Processes

The term surface process as used here refers to any physical or geological mechanism that affects the composition, optical behavior, mechanical structure, morphology, or distribution of geological materials exposed at the surface of Enceladus. Both exogenic and endogenic processes shaped the visible surface of Enceladus, but this body is unique among the airless icy satellites because of the unusually strong role played by endogenic processes such as active cryovolcanism, widespread tectonism (see **Section 2.1.3.3**), and perhaps attendant seismic shaking.

Current State of Knowledge

Ballistic fallout from cryovolcanic plume eruptions at the south pole emplaces fresh new particulate materials on Enceladus' surface. Voyager and Cassini images, as well as VIMS multispectral data, show that the photometric and color properties of the south polar region are distinct from other regions of Enceladus (**Figure 2.1.4-2**, *Buratti et al. 1990*; *Brown et al. 2006*; *Porco et al. 2006*). Nearly all of the subtle color and albedo variations are believed to be the result of differences in the effective grain sizes of ice or micro-texture of icy surface deposits. It is possible that multiple episodes of volcanism extending to different locales have occurred throughout Enceladus' history (cf., *Helfenstein et al. 2007*; *Schenk and Seddio 2006*) and that accumulation of icy volcanic deposits has produced a layered near-surface structure.

It might be expected that particulate icy fallout should heavily mantle south polar terrains. However, the highest-resolution Cassini image obtained near the south pole (**Figure 2.1.4-3**) shows a bizarre terrain dissected by ubiquitous fractures and cracks and widespread cover by large rounded ice boulders. The boulders appear to be free of any particulate blanketing, and there are relatively few flat, topographically low, areas where smooth particulate materials have accumulated. Settling and downslope redistribution of particulates may be enhanced at the south pole due to intense seismic shaking associated with plume eruptions (cf., *Hurford et al. 2007b*; *Nimmo et al. 2007*).

The mechanical structure and optical properties of surface materials on Enceladus are likely altered by re-accretion of E-ring particles. On a

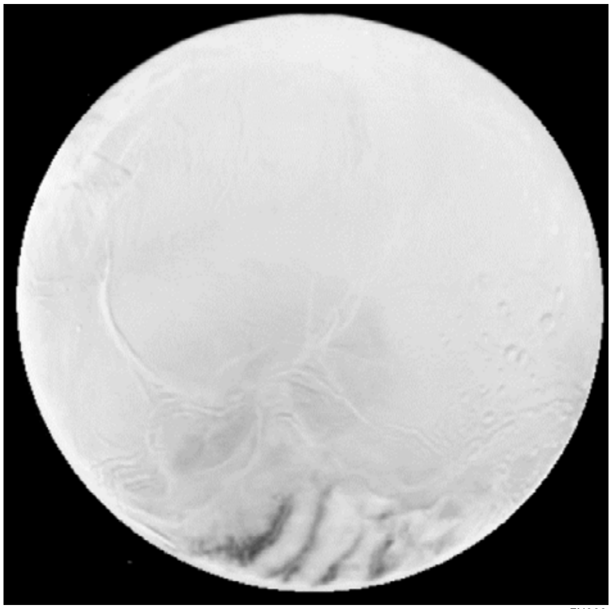

EN069

Figure 2.1.4-2: Low phase (12˚) clear-filter ISS Narrow Angle Camera image of Enceladus (adapted from *Porco et al. 2006*) showing photometric behavior differences between the south polar terrains (bottom of disk) where tiger stripes contrast with adjacent bright terrain, and other regions of Enceladus where regional photometric contrasts are muted. Differences in the optical and physical properties of surface materials are implied. Credit: NASA/JPL/Space Science Institute (PIA08980).

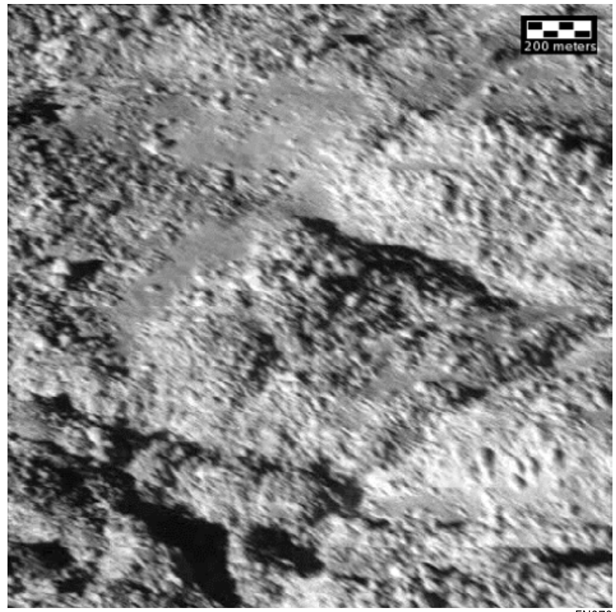

EN070

Figure 2.1.4-3: Highest resolution (4m/pixel) Cassini clear-filter NAC image ever obtained of Enceladus surface. The image was obtained adjacent to the tiger stripes at the south pole and exhibits dense cover by peculiar rounded ice boulders (from *Porco et al., 2006*).

microscopic scale, E-ring bombardment probably etches and ablates exposed surface materials, contributing to the extraordinarily high albedos and peculiar light-scattering behaviors of Enceladus and its neighboring satellites (*Buratti 1988*; *Verbiscer and Veverka 1994*; *Verbiscer et al. 2007*).

Surface sputtering and radiolysis from magnetospheric bombardment of Enceladus' surface is potentially important in modifying the surface chemistry and texture, and in providing a source of chemical energy for the interior.

Endogenic heat flow might also alter the lithology and structure of surface materials, by causing sintering at relatively shallow depths. In addition, processes more typical of those on other satellites, such as impact cratering, cosmic ray and micrometeorite bombardment must be occurring on Enceladus as it does other airless icy satellites throughout the Saturnian system and indeed throughout the solar system.

With the discovery of possible activity on Dione and Tethys (*Burch et al. 2007*), the activity on Enceladus can be seen as the best-developed example of a process that may not have reached full fruition on these other moons. Thus, understanding present-day surface processes on Enceladus is likely to prove key to understanding the evolution of surfaces elsewhere in the outer solar system.

Major Questions

It is important to understand the relative roles of plume and E-ring fallout, sputtering, micrometeorite bombardment, photolysis and radiolysis in determining the surface structure and chemistry of Enceladus.

Measurement Requirements

Surface processes can be understood partly by direct observations of the surface, including high-resolution (10 m/pixel or better) imaging from orbit (for instance it is important to understand the extent to which the bouldered terrain like that in **Figure 2.1.4-3** is distributed over the surface of Enceladus) and from the surface, and remote sensing of surface composition. Measurements of the impacting charged particle flux, and the characteristics of the plume particles and gas that impact the surface, are also important, as are *in-situ* measurements of surface chemistry from a lander.

2.1.5 Relationship to NASA Strategic Goals and Decadal Survey Goals

The most comprehensive recent articulation of the planetary community's scientific priorities is given in the Decadal Survey (NRC 2003). The Decadal Survey was written prior to the recent Cassini discoveries at Enceladus, and thus Enceladus is rarely mentioned. Now, with the discovery of geological activity, Enceladus can be seen as an ideal place to address a large fraction of the Decadal Survey's questions. The potential habitability of Enceladus, coupled with the ability to sample volatile and organic materials sourced from the sub-surface, make it particularly relevant to Decadal Survey goals. The four crosscutting themes of the Decadal Survey are: The first billion years of solar system history; volatiles and organics: the stuff of life; the origin and evolution of habitable worlds; and processes: how planetary systems work. A mission to Enceladus will address all these themes, in particular the second, third, and fourth, as summarized in **Table 2.1.5-1** and described in more detail below.

2.1.5.1 The First Billion Years of Solar System History

The present-day interior and thermal structure of Enceladus will help to decipher the processes controlling the initial stages of satellite formation. For instance, it is clear that live ^{26}Al, if present, will have had a significant effect on the initial thermal structure of the body (e.g., *Castillo-Rogez et al. 2007*). This structure, in turn, is likely to have controlled the subsequent orbital and thermal evolution of the satellite, which are coupled via the effects of tidal dissipation (cf., *Showman et al. 1997*).

2.1.5.2 Volatiles and Organics: The Stuff of Life

Enceladus is one of the very few places in the solar system where volatiles and organics from the interior can potentially be sampled by spacecraft. As such, it is of central importance to this particular theme. The *history of volatile compounds* may be investigated by direct measurement of isotopic ratios (e.g., D/H, N, C) of plume or surface volatile material. Such measurements provide strong constraints on these volatiles' provenance and mode of formation (e.g., *Niemann et al. 2005* for Titan). The nature and evolution of organic materials can be studied using similar techniques: acetylene and propane have already been detected in the vapor plume (*Waite et al. 2006*), but whether more complex molecules are present, and what processes may have affected them during their ascent from the interior, are currently unknown. Finally, Enceladus is a superb example of how global mechanisms affect volatile evolution. For example, the current plume mass flux, presumably tidally driven, would result in the loss of a 10-m thick shell of ice every million years. Similarly, it is possible that tidal heating in the silicate interior controls the composition of volatile materials seen in the plumes (*Matson et al. 2007*). There is, thus, a direct link between interior processes and structure, and volatile evolution.

2.1.5.3 The Origin and Evolution of Habitable Worlds

Enceladus has many of the requirements for habitability (*Mix et al. 2006*): simple organic compounds; an abundant energy source (tidal dissipation); and quite likely a subsurface ocean (*Porco et al. 2006*). It is thus an excellent place to determine what planetary processes are responsible for sustaining habitable worlds. In particular, determining the presence or absence of an ocean, either through magnetometry (e.g., *Zimmer et al. 2000*), seismometry (e.g., *Panning et al. 2006*), or tidal deformation studies (e.g., *Wahr et al. 2006*), is of fundamental importance for this science theme. As noted in **Section 2.1.4.1**, Enceladus' role in damping radiation in the Saturn system also demonstrates a process that may be an important influence on the habitability of other planetary systems. Perhaps even more exciting, Enceladus is perhaps one of only two places in the solar system (the other being Mars) where an answer can be given to the question: does (or did) life exist beyond Earth? Detection of, for instance, chiral molecules or pronounced isotopic anomalies in samples from the surface or the vapor plume would be strong evidence for life (e.g., *Mix et al. 2006*).

Table 2.1.5-1: Mapping of Science Goals to Decadal Survey Themes.

	Biological Potential	Tidal Heating & Internal Structure	Composition	Cryo volcanism	Tectonics	Surface Processes	Saturn System Interaction
The First Billion Years of Solar System History							
1. Initial processes		X	X				
Volatiles and Organics: The Stuff of Life							
4. History of volatiles	X	X	X	X		X	
5. Nature and evolution of organics	X					X	
6. Mechanisms of volatile evolution	X	X		X	X	X	X
The Origin and Evolution of Habitable Worlds							
7. Processes responsible for habitability	X	X		X	X	X	X
8. Life beyond Earth?	X	X		X	X		
Processes: How Planetary Systems Work							
11. Contemporary processes		X		X	X	X	X

2.1.5.4 Processes: How Planetary Systems Work

Enceladus is a particularly good example of how different planetary processes have operated and interacted to shape its present-day characteristics. For instance, as alluded to above, there is a complicated feedback between orbital, thermal and volatile evolution. Similarly, the magnetospheric and particle environment around Enceladus are both intimately affected by the behavior of the plumes (*Dougherty et al. 2006*). Cryovolcanism, and probably tectonism, important planetary processes, can be studied on Enceladus as they happen, and it is an excellent location for study of other important geological processes, such as viscous relaxation.

2.1.5.5 Relevance to Decadal Survey Large Satellites Sub-Panel Themes

In addition to the overarching themes of the Decadal Survey (NRC 2003), the Large Satellites sub-panel also identified four science themes and four high-priority scientific questions for satellite science. As shown in **Table 2.1.5-2**, these themes and questions can also be comprehensively addressed by an Enceladus mission.

A mission to Enceladus is thus capable of addressing all four themes identified by the 2003 Decadal Survey, with particular emphasis on those focusing on volatiles, organics and habitability. These latter topics in particular are also relevant to NASA's 2007 Science Plan, which among other questions seeks to answer:

Table 2.1.5-2: Relevance of Key Science Questions to the Decadal Survey Large Satellites Goals.

	Biological Potential	Tidal Heating and Internal Structure	Composition	Cryo volcanism	Tectonics	Surface processes	Saturn System Interaction
Themes							
Origin/evolution satellite systems		X	X				X
Origin/evolution water-rich environments	X	X	X	X			
Exploring organic-rich environments	X		X			X	X
Understanding dynamic planetary processes		X		X	X	X	
High-Priority Questions							
Is there extant life?	X	X	X	X		X	
Organic chemistry in extreme environments	X		X			X	
How common are liquid water layers?	X	X	X				
How does tidal heating affect satellite evolution?		X		X	X		X

- What are the characteristics of the solar system that led to the origin of life?
- Did life evolve elsewhere in the solar system than Earth?
- How did the solar system evolve to its current diverse state?

The 2006 Science Roadmap highlighted the discovery of water vapor plumes on Enceladus as a key development since the publication of the 2003 Decadal Survey. It noted that the discoveries at Enceladus are "pertinent to all four major science themes pertinent to large satellites, as recommended by the Decadal Survey" (p. 50) and stated that Enceladus is a "prime target for future solar system exploration." This document also identified a Titan/Enceladus explorer as one of the three highest-priority Flagship-class missions.

Finally, an Enceladus mission is consistent with NASA's highest-level goals as laid out in the 2004 Vision for Space Exploration. Such a mission will "explore . . . other bodies to search for evidence of life [and] to understand the history of the solar system."

In summary, a mission to Enceladus is fully consistent with NASA's current goals, addresses all four of the high-level questions posed by the 2003 Decadal Survey, and is targeted at a body that is not only potentially habitable but also provides readily accessible samples of the volatile and organic materials sourced from its interior.

2.2 Measurement Requirements Overview

The measurement requirements discussed for each science goal in **Section 2.1** can be addressed by specific instruments aboard specific types of mission, though many other types of instruments may also be used to meet those goals. **Table 2.2.1-1**, shows, in detail, the traceability from Enceladus science goals to measurements, suggested instrument types, and missions. There is much overlap between the measurements and instruments (for instance, understanding Enceladus' biological potential involves measuring the location and distribution of liquid water, which is also a requirement for understanding the tidal heating and interior structure), and cross-references are shown when possible, to avoid unnecessary duplication.

2.2.1 Traceability Matrix

The traceability matrix is shown in **Table 2.2.1-1**.

2.2.2 Cassini's Ability to Make These Measurements

Enceladus remains a major science target for the Cassini mission, and eight more flybys of Enceladus are planned before the end of the currently-planned extended mission in mid-2010 (**Table 2.2.2-1**).

Cassini carries a large suite of optical remote sensing and fields and particles instruments (see Cassini instrumentation articles in Space Science Reviews, 115, 2005). Those most relevant to Enceladus include UV, visible, near-IR and thermal IR remote sensing instruments, a mass spectrometer, dust analyzer, and plasma spectrometers, a magnetometer, and a radio science experiment. Much will be learned from these instruments about Enceladus during the remaining flybys. However, Cassini is limited in several important respects. First, the configuration of the spacecraft allows optimization of each flyby for only a few measurement goals, as shown in **Table 2.2.2-1**. If remote sensing instruments are pointed at Enceladus near closest approach, the dust analyzer, mass spectrometer, and plasma instruments obtain compromised data, and gravity measurements, which require pointing the high-gain antenna at Earth, are not generally compatible with either remote sensing or in-situ measurements. As a result, only two or three flybys are available for each type of measurement.

Another limitation is the lack of dust shielding on Cassini, which was not designed to fly through a dusty plume environment. Impact with a single particle larger than 1 mm in size could be fatal to the spacecraft, and the presence of such particles in the plume cannot yet be robustly ruled out. Though flybys at 21 km altitude are currently

Table 2.2.2-1: Cassini Enceladus flybys, 2008 onwards

Date	Orbit	Speed, km/s	Altitude, km	Orbit Inclination	Planned close encounter science emphasis
12-Mar-08	61	14.3	27	High	*In-situ* plume sampling
11-Aug-08	80	17.7	21	High	*In-situ* plume sampling or S. pole remote sensing
9-Oct-08	88	17.7	21	High	*In-situ* plume sampling or S. pole remote sensing or UV stellar occultation
31-Oct-08	91	17.7	196	High	S. pole remote sensing
2-Nov-09	120	7.7	96	Low	*In-situ* plume sampling
21-Nov-09	121	7.7	1560	Low	S. pole remote sensing
28-Apr-10	130	6.5	96	Low	S. pole gravity
18-May-10	131	7	246	Low	S. pole gravity or plume solar occultation

Table 2.2.1-1: Traceability Matrix

Science Objective	Measurement Objective(s)	Measurement Requirement	Mission Requirement	Suggested Instrument Type	Mission Type	Priority
Biological Potential	Location and distribution of liquid water	Magnetic field measurements to 0.1 nT	Polar orbits ideal	Magnetometer	Saturn or Enceladus Orbiter	1
		Surface magnetic field measurements to 0.1 nT	Lifetime of several Enceladus days, continuous operation.	Magnetometer	Hard or Soft Lander	2
		h_2 Love number to 0.1; tidal displacements to 1 m; Altimetry profiles with resolutions 10-m horizontal and 0.1-m vertical resolution	Enceladus orbital knowledge to 10-m precision; also possible with multiple (~10) flybys with range <1000 km. Simultaneous altimetry and gravity observations. Desire 10-m spot size; 100-m pointing accuracy, laser ranges to 1000 km; multi-beam for crossover analysis (require crossovers at different points in orbit relative to periapse). ~180 orbits required for global topography with 1° resolution.	Laser Altimeter	Saturn or Enceladus Orbiter	1
			Determine range to 1-2 transponders; for single transponder, orbital knowledge to 1-m precision required. Lifetime of several Enceladus days required.	Radio Science	Hard or Soft Lander + Orbiter	1
		k_2 Love number to 0.01; Degree-2 gravity coefficients to 10^{-3}. Lower priority: Gravity profiles to 1 mgal at surface, with ~20-40 km resolution	Multiple flybys w/ simultaneous altimetry and gravity measurements. Orbiter w/ both polar and equatorial passes.	Radio Science	Saturn or Enceladus Orbiter	1
		Seismic measurements with displacement sensitivity better than 1 mm at periods 0.001- 0.1 Hz. Short period sensitivity better than 0.1 micron/s at frequencies up to 100 Hz	Lifetime of several Enceladus days. One location is sufficient for normal mode measurement of shell thickness, two at different locations are preferred for more detailed interior structure determination	Seismometer	Hard or Soft Lander	1
	Physical conditions in the active regions	South polar surface temperature maps, 100-m spatial resolution, 0.5 K temperature sensitivity at 60 K	High inclination Enceladus orbits for polar passes, or multiple south polar flybys	Thermal Mapper	Saturn or Enceladus Orbiter	1
		South polar daytime imaging coverage, 4 wavelengths (0.35, 0.56, 0.8, 1.0 microns), 10-m spatial resolution. Plume imaging at phase angles from 130° to 175° with 100-m spatial resolution. Lower priority: Local stereo topography with 30-m horizontal and 10-m vertical resolution.	High inclination Enceladus orbits, or multiple south polar flybys. Variable altitude for very-high-resolution (2 m/pix) imaging of selected areas. Subsolar latitude < -10° during some of the prime mission, for south polar viewing. Lower priority: Multiple looks at same location from different angles required for stereo.	Visible Camera	Saturn or Enceladus Orbiter	1
		Image subsurface ice in vents to 250 K isotherm (~6 km) with 100-m vertical resolution	100-m pointing accuracy	Sounding Radar	Saturn or Enceladus Orbiter	2
		South polar daytime coverage, 1 - 5 microns, 0.002-micron spectral resolution, 100-m spatial resolution.	High inclination Enceladus orbits, or multiple south polar flybys. Subsolar latitude < -10° during some of the prime mission, for south polar viewing	Near Infrared Mapper	Saturn or Enceladus Orbiter	1
	Plume Chemistry	Plume stellar occultations probing water vapor abundance (and other species) to 1000 km altitude with multiple geometries. Spectral range 0.08 - 0.38 microns, 0.0002-micron spectral resolution at selected wavelengths	12 stellar occultations, pointing flexibility (i.e., not nadir pointed all the time)	FUV Spectrometer	Saturn or Enceladus Orbiter	2
		1 - 5 micron reflectance spectra of the plume	Pointing flexibility	Near Infrared Mapper	Saturn or Enceladus Orbiter	2
		Neutral gas composition (plus, isotopes), temperature, velocity distribution, density distribution	Polar Orbiter or multiple flybys through plume	Neutral Gas Spectrometer or GCMS	Saturn or Enceladus Orbiter	1
		Dust elemental and molecular composition	Polar Orbiter or multiple flybys through plume	Dust Analyzer (high-speed collection)	Saturn Orbiter	1
				Dust Analyzer (low-speed collection)	Enceladus Orbiter	1
	Global distribution of chemical species	Global daytime coverage at 1 - 5 microns, 0.002-micron spectral resolution, 100-m spatial resolution.	Orbiter allowing global coverage with some high inclination orbits, or 15 flybys at each of at least three different subsolar longitudes. Subsolar latitude < -10° during some of the prime mission for south polar viewing	Near Infrared Mapper	Saturn or Enceladus Orbiter	1
		Global daytime imaging coverage at 4 wavelengths (0.35, 0.56, 0.8, 1.0 microns) to map H_2O grain size and visible/NUV absorbers, 10-m resolution.	Orbiter allowing global coverage with some high inclination orbits, or 15 flybys at each of at least three different subsolar longitudes. Subsolar latitude < -10° during some of the prime mission for south polar viewing.	Visible Mapping Camera	Saturn or Enceladus Orbiter	1
	Detailed surface chemistry	1 - 5 micron mapping of landing site for context, ~.002-micron spectral resolution, 10-mrad angular resolution	At least 1 meter above the surface	Near-IR Spectrometer	Hard or Soft Lander	2
		Distribution and abundance of primary amines, including amino acids, nucleobases, amino sugars, to sub part-per-billion detection limits, mass up to 550 a.m.u., enantiomeric abundances to 5%	Soft lander with solid ice sample acquisition capability	Micro-capillary electrophoresis with laser induced fluorescence detection and ToF-MS	Soft Lander	1
		Carbon, hydrogen isotope measurements	Soft lander with solid ice sample acquisition capability	Tunable Laser Spectrometer	Soft Lander	1
		Identify oxidants in surface ice (e.g., H_2O_2, superoxide, etc.)	Soft lander with solid ice sample acquisition capability	Surface Ice Oxidant detector	Soft Lander	1
		Refractory organic component (e.g., PAHs)	Soft lander with solid ice sample acquisition capability	Laser Desorption Mass Spectrometer	Soft Lander	2
	Biogenic structures in the plume particles?	Plume grain morphology with 0.1-micron spatial resolution	Low-speed data collection or surface sampling	Dust Micro-analyzer	Enceladus Orbiter or Soft Lander	1
Composition	Plume Chemistry	Same measurements as for "Biological Potential/Plume chemistry" science goal				
	Global distribution of chemical species	Same measurements as for "Biological Potential/Global distribution of chemical species" science goal				
	Detailed surface chemistry	Same measurements as for "Biological Potential/Detailed surface chemistry" science goal				
Cryovolcanism	Global distribution of active cryovolcanism	Global surface temperature maps, both day and night, 100-m spatial resolution, temperature sensitivity 0.5 K at 60 K	Orbiter allowing global coverage with some high inclination orbits, or 10 flybys at each of at least three different subsolar longitudes	Thermal Mapper	Saturn or Enceladus Orbiter	1
		Global search for plume activity	High phase angle global imaging at a large range of geometries	Visible Camera	Saturn or Enceladus Orbiter	2
	Nature of the Plume Source	Same measurements as "Biological potential/Physical conditions in the active regions" science goals				
	Plume physical characteristics	Plume imaging at 3 wavelengths (0.35, 0.55, 0.9 microns), up to 165° phase.	Need to be able to point at Enceladus from most locations in the spacecraft orbit, at phase angles up to 165°.	Visible Camera	Saturn or Enceladus Orbiter	2
		Plume grain morphology with 0.1 micron spatial resolution	Low-speed data collection	Dust Micro-analyzer	Enceladus Orbiter	1
		Dust size and spatial distribution over 0.1 - 100 micron, dust velocity distribution	Polar Orbiter or multiple flybys through plume	Dust Analyzer	Saturn or Enceladus Orbiter	1
		Neutral gas temperature, velocity distribution, density distribution	Polar Orbiter or multiple flybys through plume	Neutral Gas Spectrometer or GCMS	Saturn or Enceladus Orbiter	1
		Plume stellar occultations probing water vapor abundance and spatial distribution to 1000 km altitude with multiple geometries.	12 stellar occultations, pointing flexibility (i.e., not nadir pointed all the time)	FUV Spectrometer	Saturn or Enceladus Orbiter	2
	Plume Chemistry	Same measurements as for "Biological Potential/Plume chemistry" science goal				

Table 2.2.1-1: Traceability Matrix (Continued)

Science Objective	Measurement Objective(s)	Measurement Requirement	Mission Requirement	Suggested Instrument Type	Mission Type	Priority
Tectonics	Morphology and distribution of tectonic features	Global daytime imaging coverage, 10-m spatial resolution. Lower priority: Local stereo topography with 30-m horizontal and 10-m vertical resolution.	Orbiter allowing global coverage with some high inclination orbits, or 15 flybys at each of at least three different subsolar longitudes. Variable altitude for very-high-resolution (2 m/pix) imaging of selected areas. Subsolar latitude < -10° during some of the prime mission for south polar viewing. Lower priority: Multiple looks at same location from different angles required for stereo. Plume imaging over several orbital cycles	Visible Mapping Camera	Saturn or Enceladus Orbiter	1
		Global and regional topography	Desire 10-m spot size at ranges < 1000 km; 100-m pointing accuracy, multi-beam for crossover analysis. ~180 orbits required for global topography with 1° resolution.	Laser Altimeter	Saturn or Enceladus Orbiter	1
		Subsurface expression of tectonic features, with 100-m vertical resolution	100-m pointing accuracy	Radar Sounder	Saturn or Enceladus Orbiter	2
	Tectonic stresses	h_2 Love number (same measurements as for "Biological potential/Location and distribution of liquid water"" h_2 requirement)				
		k_2 Love number (same measurements as for "Biological potential/Location and distribution of liquid water"" k_2 requirement)				
		Static Gravity field and regional gravity anomalies with resolution better than 1 mGal	Orbiter with polar and low inclination orbits, or multiple close flybys	USO, part of communication subsystem	Saturn or Enceladus Orbiter	1
		Topography with 30-m horizontal resolution and 10-m vertical resolution	Desire 10-m spot size at ranges < 1000 km; 100-m pointing accuracy, multi-beam for crossover analysis. ~180 orbits required for global topography with 1° resolution.	Laser Altimeter	Saturn or Enceladus Orbiter	1
			Orbiter allowing global coverage with some high inclination orbits, or 15 flybys at each of at least three different subsolar longitudes. Variable altitude for very-high-resolution (2 m/pix) imaging of selected areas. Subsolar latitude < -10° during some of the prime mission for south polar viewing. Multiple looks at same location from different angles required for stereo.	Visible Mapping Camera	Saturn or Enceladus Orbiter	1
	Motion of individual tectonic features	Altimetry profiles with 10-m horizontal and 0.1-m vertical resolution	Desire 10-m spot size, 100-m pointing accuracy. Multiple altimetry profiles of the same features at different orbital positions relative to periapse, to look for motion	Laser Altimeter	Saturn or Enceladus Orbiter	1
		Characterize and locate sources of seismic activity	Lifetime of several Enceladus days. One location is sufficient for characterizing level and style of activity, two or more locations are preferred for more detailed analysis including source determination	Seismometer	Hard or Soft Lander	1
Tidal Heating and Interior Structure	Heat flow and thermal structure	Global surface temperature maps, both day and night, 100-m spatial resolution, temperature sensitivity 0.5 K at 60 K	Orbiter allowing global coverage with some high inclination orbits, or 10 flybys at each of at least three different subsolar longitudes	Thermal Mapper	Saturn or Enceladus Orbiter	1
		Bolometric albedo maps to 5% precision	Wide range of viewing and illumination geometries	Visible camera	Saturn or Enceladus Orbiter	2
		Subsurface thermal profile, penetrate ice to depth of 250 K isotherm (~6 km), 100-m vertical resolution.	100-m pointing accuracy	Radar Sounder	Saturn or Enceladus Orbiter	2
	Internal density structure and ice shell thickness	h and k Love numbers (same requirements as for "Biological potential/Location and distribution of liquid water" measurements above)				
		Static Gravity Field (same measurements as for "Tectonics/Tectonic Stresses" static gravity field requirement)				
		Topography (same measurements as for "Tectonics/Tectonic Stresses" topography requirement)				
		Image subsurface ice structure to 250 K (~6 km) with 100-m vertical resolution.	100-m pointing accuracy	Radar Sounder	Saturn or Enceladus Orbiter	2
		Seismic measurements with displacement sensitivity better than 1 mm at periods 0.001- 0.1 Hz. Short period sensitivity better than 0.1 micron/s at frequencies up to 100 Hz	Lifetime of several Enceladus days. One location is sufficient for normal mode measurement of shell thickness, two at different locations are preferred for more detailed interior structure determination	Seismometer	Hard or Soft Lander	1
	Location and distribution of liquid water	Magnetic field measurements to 0.1 nT	Polar orbits ideal	Magnetometer	Saturn or Enceladus Orbiter	1
		Surface magnetic field measurements to 0.1 nT	Lifetime of several Enceladus days, continuous operation.	Magnetometer	Hard or Soft Lander	2
		h and k Love numbers (same requirements as for "Biological potential/Location and distribution of liquid water"" measurements above)				
		Seismic measurements with displacement sensitivity better than 1 mm at periods 0.001- 0.1 Hz. Short period sensitivity better than 0.1 micron/s at frequencies up to 100 Hz	Lifetime of several Enceladus days. One location is sufficient for normal mode measurement of shell thickness, two at different locations are preferred for more detailed interior structure determination	Seismometer	Hard or Soft Lander	1
Saturn System Interactions	Plume physical characteristics	Same measurements as "Cryovolcanism/Plume physical characteristics" science goal				
	Plume chemistry	Same measurements as for "Biological potential/Plume chemistry" science goal				
	Interaction of gas plume with magnetospheric plasma and neutrals	Magnetic field measurements to 0.1 nT	Polar orbits ideal	Magnetometer	Saturn or Enceladus Orbiter	1
		Energetic ions, electrons, 20 keV to 10 MeV	Polar Orbiter or multiple flybys with variable geometry	Energetic ion and electron spectrometer	Saturn or Enceladus Orbiter	2
		3-D plasma distribution function, composition, from 1 eV to 50 keV, 40% energy resolution, 20° angular resolution	Polar Orbiter or multiple flybys through plume	Low Energy Plasma Analyzer	Saturn or Enceladus Orbiter	2
		Map O, OH, other species, in the neutral torus. Spectral range of 0.08 - 0.38 micron, 0.0002-micron spectral resolution at selected wavelengths	Pointing flexibility	FUV Spectrometer	Saturn or Enceladus Orbiter	2
	E-ring structure and dynamics	0.1-micron spatial resolution, elemental resolution down to carbon	Low-speed data collection	Dust Micro-analyzer	Enceladus Orbiter prior to Enceladus orbit insertion	1
		Visible imaging of E-ring with 10-km spatial resolution, 3 wavelengths (0.35, 0.55, 0.9 micron).	Flexible pointing including high phase angles, observations outside the Saturn ring plane are valuable	Visible camera	Saturn or Enceladus orbiter	1
		Dust size distribution over 0.1 - 100 micron, dust velocity distribution, composition (ice, silicon, organics)	Polar Orbiter or multiple flybys through plume	Dust Analyzer, with ion and neutral mass spectrometer, pyrolizer (in orbit)	Saturn or Enceladus Orbiter	1
Surface Processes	Sputtering and Radiolysis	Energetic ions, electrons, 20 keV to 10 MeV	Polar Orbiter or multiple flybys with variable geometry	Energetic ion and electron spectrometer	Saturn or Enceladus Orbiter	2
		3-D plasma distribution function, composition, from 1 eV to 50 keV, 40% energy resolution, 20° angular resolution	Polar Orbiter or multiple flybys with variable geometry	Low Energy Plasma Analyzer	Saturn or Enceladus Orbiter	2
	Surface physical processes: impact, plume deposition, mass wasting	Dust size distribution over 0.1 - 100 micron, dust velocity distribution, composition (ice, silicon, organics)	Polar Orbiter or multiple flybys through plume	Dust Analyzer, with ion and neutral mass spectrometer, pyrolizer (in orbit)	Saturn or Enceladus Orbiter	1
		Global daytime imaging (same measurements as for "Tectonics/Morphology and distribution of tectonic features" global daytime imaging requirement)				
		Visible imaging, 0.3 mrad angular resolution, 4 wavelengths (0.3 - 1.0 micron), steerable	At least 1 meter above the surface	Panoramic Lander Camera(s)	Hard or soft Lander	1
	Surface Chemistry	Same measurements as for "Biological potential/Global distribution of chemical species" and "Biological potential/Detailed surface chemistry" science goals				

planned, these are not over the south pole, and the closest planned approach to the plume sources is 100 km. Even this altitude may be determined to be too hazardous, and may be increased. Cassini is thus limited in its ability to investigate near-vent conditions that may reveal crucial information on the nature of the plume source, and more distan flybys reduce gas density, limiting sensitivity to potentially critical trace species in the plume.

Cassini's instrumentation also has importan limitations. The remote sensing instruments are not designed for rapid coverage of large areas during close flybys, allowing only "postage stamp" coverage at maximum resolution (**Figure 2.2.2-1**) Wide-field push-broom sensors, such as those carried on many recent spacecraft (e.g., MOC on Mars Global Surveyor, Ralph on New Horizons and HiRISE on Mars Reconnaissance Orbiter on the missions studied here can make much better use of precious time near closest approach.

The mass-to-charge (m/z) ranges of the mas spectrometers in the INMS (range 1-99 atomic mass units (amu), *Waite et al. 2004*) and CDA instruments (*Srama et al. 2004*) are insufficien to detect complex organic molecules directly tha might be critical in determining the biological potential of Enceladus. A wider m/z range for analyses of plume ions, neutral gas, and ice particles would significantly improve science return, even at flythrough speeds comparable to Cassini (several km/s). Moreover, the opportunity to sample plume material relatively undisturbed, at the low velocities associated with an Enceladus orbiter, does not exist on Cassini. This improvement would additionally allow the analysis of more fragile organic compounds that could not survive the encounter at much higher speeds in any recognizable form (i.e., only as small fragments).

Cassini also does not carry instrumentation, such as ground-penetrating radar, that can provide direct information about the subsurface structure, and presence of liquid water, near the plume source. Cassini also has no ability to directly measure tidal flexing (e.g., using a laser altimeter), which would provide unique information on the possible presence of an ocean and the nature of the tidal heat source. Furthermore, Cassini has no ability to do the bulk surface chemical analysis or seismic measurements that can only be performed by a lander.

The mission concepts studied in this report alleviate most of the above limitations on Cassini's ability to address Enceladus science goals, using a combination of improved instrumentation, and mission designs better suited to Enceladus

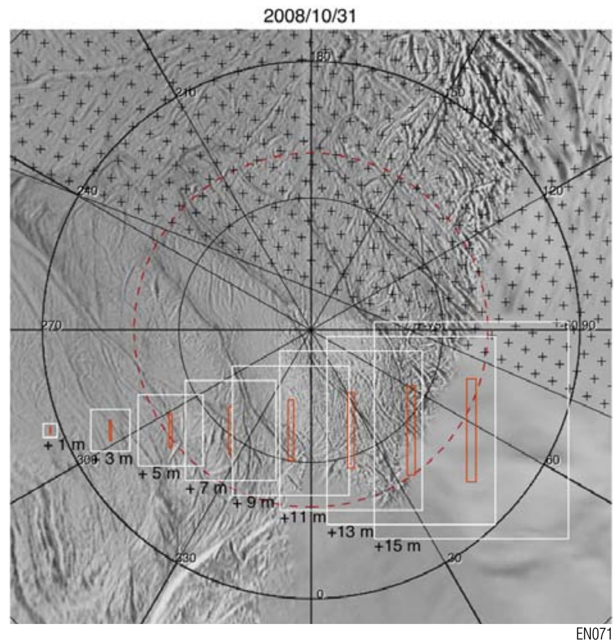

Figure 2.2.2-1: Expected Cassini remote sensing coverage of the south polar region of Enceladus on Rev. 91, the only encounter currently guaranteed to be dedicated to remote sensing before the sun sets for the south pole in August 2009. Images and other data are taken as the spacecraft speeds away from Enceladus. The stippled region is in darkness. White squares show the fields of view of the narrow-angle camera (1024x1024 pixels) and the near-infrared instrument (VIMS, 12 x 24 pixels), and the red rectangle shows the size of the thermal-IR instrument (CIRS) field of view (1 x 10 pixels). Fields of view are shown every 2 minutes, because VIMS requires 2 minutes to scan each field of view shown. The field of view at +1 minute has an imaging resolution of 6 meters. Field of view placement is arbitrary. In contrast, *the missions proposed here would image most of Enceladus with a spatial resolution of 10 meters, almost as good as the single highest-resolution Cassini image shown here.*

2.3 Instrument Types

The follow sections outline the details of various instrument types considered for orbiter and lander missions. Category 1 instruments were included in the mission designs, while Category 2 instruments were omitted because they were judged to have somewhat lower science value (**Tables 2.3.7-1** and **2.3.7-2**) and because resources were not available to support them. It should be noted that these are discussed only as example strawman payload possibilities. This list is not intended to be exhaustive, nor is it intended to imply that this the exact payload that should be chosen. Rather, this list was chosen to provide a balanced complement of instruments representative of a payload that could meet the science goals and measurement objectives and to provide scoping information for the detailed mission designs discussed in **Section 3**.

2.3.1 Orbiter Remote Sensing Instruments

2.3.1.1 Thermal Mapper (Category 1)

The thermal mapper is used to determine passive surface temperatures with a typical diurnal range of 50 to 75 K (*Spencer et al. 2006*) and temperatures along the tiger stripes and other active endogenic features, which reach at least 150 K and probably much warmer. Science goals include understanding the geophysics and thermodynamics of the plume source regions, and determination of local and global heat flow. The design concept is again a push-broom design similar to the Thermal Emission Imaging System (THEMIS, *Christensen et al. 2004*), the thermal mapper aboard Mars Odyssey, and uses a microbolometer array to obtain images at three broadband wavelengths (centered near 5, 15, and 30 microns). To improve signal-to-noise, multiple images are shifted and added together as the scene moves across the focal plane. The use of multiple wavelengths allows determination of the temperature and area of small (sub-pixel) regions at temperatures much higher than the background temperature, as are likely near the tiger stripes. The sensitivity of commercial microbolometer arrays at wavelengths beyond 20 microns is not well characterized, and here an extrapolation of short-wavelength behavior is assumed in calculating sensitivities. With the long exposures per resolution element possible in Enceladus orbit in push-broom mode (~100 seconds), and a THEMIS-like design, with a 20-40 micron filter, a sensitivity of better than +/-1 K is expected down to 65 K at 100 m/pixel spatial resolution, or down to 50 K when binned to 1 km resolution. For the Saturn orbiter, with 4 km/second flyby speeds and thus much shorter effective exposure times of 2.5 seconds, sensitivity of better than +/- 1 K is expected down to 63 K at 1 km resolution, or 84 K at 100 meter resolution. This compromises mapping of nighttime temperatures but still provides good sensitivity to daytime temperatures at reduced spatial resolution, and excellent science at the warm tiger stripes. Sensitivity could be improved in this case by the use of longer wavelengths, if long-wavelength detector sensitivity could be improved.

Resource Estimates

Mass (11 kg), power (14 W), and volume (55x29x37 cm) are assumed to be similar to THEMIS.

2.3.1.2 Near-IR Mapper (Category 1)

The Near-Infrared (NIR) Mapping Spectrometer is based on heritage from the Cassini VIMS (Visible and Infrared Mapping Spectrometer), the Moon Mineralogy Mapper (M^3) and the New Horizons Ralph/MVIC-LEISA instrument (*Brown et al. 2005*; *Reuter et al. 2005*; *Green et al. 2007*). For the Saturn orbiter it is combined with the push-broom visible mapper behind a single telescope, as in the New Horizons Ralph instrument, resulting in significant reductions in mass, power and volume requirements. The use of a push-broom imaging spectrometer design eliminates the need for moving parts while enabling high signal-to-noise observations. In order to achieve 100 m NIR spatial resolution from a 200 km orbit, the instantaneous field-of-view (IFOV) is 0.5 mrad/pixel and the swath width, assuming a 256-pixel array in the spatial direction like LEISA, is 25 km. The instrument covers the spectral range from 1 to 5 μm at a spectral resolution of 4 nm, requiring 1000 spectral pixels, and uses 12-bit precision. This is sufficient to uniquely identify most of the volatile, clathrate, and hydrate compounds predicted to exist at the surface. This instrument generates data at a high rate (6 Mbits/s in Enceladus orbit), and to intelligent onboard compression (e.g., spatial and/or spectral averaging in relatively featureless parts of the spectrum) would be used to enable large, but flexible, reductions in the data volume.

Resource Estimates

For the Enceladus orbiter, mass (10 kg), power (6 W), and volume (50x50x30 cm) are assumed similar to Ralph when combined with the push-broom visible imager. For the Saturn orbiter, because of the requirement for shorter exposures and faster readouts discussed below in the visible mapper section, these parameters are assumed for the near-IR mapper alone.

2.3.1.3 Visible Mapper (Category 1)

The visible mapper considered for these mission concepts is a push-broom instrument based on the Multicolor Visible Imaging Camera (MVIC) carried by New Horizons, part of the Ralph instrument (*Reuter et al. 2007*). MVIC has four 32x5000 pixel CCD arrays, each overlain with a separate color filter, plus a panchromatic channel. The CCDs are operated in Time Delay Integration (TDI) mode, can cover a swath 5000 pixels wide and an arbitrary number of pixels long. Many other modern planetary imagers, for instance HiRISE on Mars Reconnaissance Orbiter operate on a similar principle. These imagers are well suited for covering large areas in a short period of time without the time-consuming mosaicing required by a traditional framing camera. Four broadband color filters, probably centered near 0.35, 0.55, 0.80, and 0.95 microns, would provide the ability to map dark surface contaminants and coarse-grained water ice at very high spatial resolution. In the Saturn orbiter mission, with MVIC's optics (field of view 0.1 radians), this instrument could cover a 200 x 40 km swath at 10 m/pixel from 500 km range on each flyby, greatly improving on Cassini's resolution and coverage over the course of the mission (Cassini has so far taken only a single image at comparable resolution, covering 2 x 2 km). On the Enceladus orbiter, with a nominal altitude of 200 km, wider optics than MVIC (field of view 0.2 radians) would be used in order to image a 40 - 50 km swath from this altitude.

Resource Estimates

In Enceladus orbit when nadir pointing, exposure times are long (4 seconds per pixel, compared to typical exposures of ~1 second for MVIC), so telescope size could possibly be reduced compared to MVIC, resulting in mass savings, but the MVIC mass is assumed here to be conservative. On New Horizons MVIC is combined with the near-infrared mapper (the Linear Etalon Imaging Spectral Array, LEISA), into a single instrument called Ralph, and here a similar configuration is assumed, with the same combined mass (10 kg), power (6 W), and volume (50x50x30 cm) as Ralph. For the high flyby speeds of the Saturn orbiter ~4 km/sec, TDI exposure times are much shorter (~0.08 seconds for a 32-pixel wide array like MVIC), requiring much faster readout electronics and perhaps a larger telescope than MVIC for adequate signal-to-noise. To accommodate these enhancements, for the Saturn orbiter the full Ralph mass and power is allocated to the visible mapper and a similar mass and power to the near-IR mapper, doubling the mass and power of the combined package.

2.3.1.4 Framing Camera (Category 2)

For the Saturn orbiter, a framing camera was considered as a Category 2 instrument. The purpose of this camera, which would have a narrower field of view and higher resolution than the pushbroom camera, would be to image Enceladus, its plumes, and the E-ring (and other targets of opportunity in the Saturn system) during the times when the spacecraft is not close to the moon. The nominal design is based on the New Horizons Long-Range Reconnaissance Imager (LORRI, *Cheng et al. 2007*), which has a 5-mrad field of view and a 5-microrad pixel size. A filter wheel would be added to this design.

Resource Estimates

LORRI mass, power, and volume is 9 kg, 5 W, and approximately 25 x 25 x 50 cm. With the addition of the filter wheel, 11 kg, 7 W, and 25 x 25 x 60 cm are estimated for the Enceladus instrument.

2.3.1.5 UV Spectrometer (Category 2)

An ultraviolet spectrometer could be used for remote characterization of the Enceladus plume and the neutral torus that it creates around Saturn. It is a Category 2 instrument, because one can obtain more detailed information about the plume from direct *in-situ* sampling and because the neutral torus is part of the "Saturn system interaction" Priority 3 science goal, and thus it is not included in the mission concept payloads. However, it would be a valuable addition if resources were available. For instance it would allow more frequent characterization of the plume from the Enceladus orbiter, which spends most of its time in a medium-inclination orbit which does not intersect the plume, than would be possible from *in-situ* instruments. The density of H_2O and probably additional gases could be determined, as with Cassini (*Hansen et al. 2006*), using stellar occultations in the 1200–1800 Å range, and

N_2 could be mapped using solar occultations at 800–900 Å. In addition, the neutral torus could be mapped using line emission from neutral O (1304 Å), (*Esposito et al. 2005*), and, if the instrument had sufficient wavelength coverage, from OH at 3090 Å (*Shemansky et al. 1993*).

Resource Estimates

Mass (4.4 kg), power (4 W), and volume (30x20x15 cm) are assumed to be the same as the New Horizons Alice instrument (*Stern et al. 2007*), which covers the wavelength range 520 to 1800 Å and has a solar occultation port and photon-counting "time-tag" mode for occultations, and thus could accomplish all these science goals without modification (except for the low-priority 3090 Å OH torus mapping).

2.3.2 Orbiter Geophysics Instruments

2.3.2.1 Laser Altimeter (Category 1)

The example laser altimeter is a multi-beam instrument similar to the LOLA altimeter on the Lunar Reconnaissance Orbiter (*Smith et al. 2006*). Its primary objectives are: to determine the time-variable long-wavelength (tidal) topography of Enceladus (cf., *Wahr et al. 2006*); to determine the global, static short-wavelength topography (cf., Smith et al. 2001); and to improve knowledge of spacecraft position using crossover analysis (cf., *Neumann et al. 2001*). For an orbiter these requirements are relatively straightforward, and would in many ways resemble those met by Mars Global Surveyor (*Smith et al. 2001*). The requirements are more difficult to satisfy with a series of flybys, and require periapses and ground tracks distributed across the satellite, and varying approach directions, to ensure sufficient longitudinal coverage and crossovers. The nominal flyby frequency of once per 8.22 days over > 400 days ensures that observations will be made at various points in the tidal cycle of Enceladus (precession period 1.31 years). It is estimated that 45 well-distributed flybys are sufficient to satisfy the requirements (Neumann, personal communication).

The principal modification to the original LOLA design is the use of a pulse-pumped fiber laser amplifier, rather than a single-stage laser. This modification entails lower pulse energies (1 mJ). For an Enceladus orbiter at 200 km altitude, the reduced power and the lower spacecraft velocity compared with the Moon increases the spot size compared with LOLA (to 20 m) and decreases the sampling rate (to 7 Hz). The original five-spot configuration is retained, with the spots contained within a 200 m diameter circle. Pointing knowledge of 10 arcsec is set by the spot size and assumed spacecraft altitude (200 km). The vertical precision is 0.1m and the maximum range 1000 km. For a flyby mission, the spacecraft velocity is much greater (4 km/s), resulting in a greater spot spacing (130 m) even with a higher (30 Hz) sampling rate, and thus degrading the vertical precision.

Resource Estimates

The reduced pulse energy requires a larger (30 cm) telescope compared with LOLA. The mass (10 kg) and dimensions (42x45x36 cm for the optics; 21x29x12 cm for the electronics) are assumed to be similar to LOLA; the power requirements (10 W) are reduced due to the different laser employed. Although a pulse-pumped laser has not been employed before as an altimeter, such lasers build on extensive flight experience and form a central part of the Mars Laser Communication Demonstration system (*Townes et al. 2004*).

2.3.2.2 Radio Science (Category 1)

Although not involving a dedicated science instrument, spacecraft tracking (and specifically, the Doppler-derived line-of-sight velocity) allows determination of the satellite's internal structure and whether it possesses an ocean. The main objectives of the radio science investigation are to determine the tidal response of the satellite (that is, its k_2 Love number), and to determine the low-order harmonics of the gravity field.

A satellite's Love number depends on its internal structure, and in particular whether an ocean decouples the ice shell from the subsurface (*Moore and Schubert 2000*; *Wahr et al. 2006*). Degree-2 gravity harmonics allow the moment of inertia of the body, and hence its internal structure, to be constrained (e.g., *Anderson et al. 1998*). Higher-order harmonics, coupled with topography, may allow the rigidity of the ice shell to be determined.

Even with the relatively frequent orbital corrections required at Enceladus, determination of the low-order gravity harmonics via observations of the line-of-sight velocity of an orbiter is straightforward. Individual flybys can in general only constrain some lumped combination of the degree-2 gravity harmonics; multiple flybys at different inclinations are required to determine them independently.

Resource Estimates

A standard Ultra-Stable Oscillator (USO), with a mass of 1 kg and power of 1.5 W, was included in the example payload to meet this measurement objective.

2.3.2.3 Magnetometer (Category 1)

The strawman magnetometer is essentially identical to the instrument currently being flown on the MESSENGER mission to Mercury (*Anderson et al. in press*). Its primary scientific aims are to search for an induction signature due to a putative subsurface ocean on Enceladus (cf., *Zimmer et al. 2000*), and to characterize the magnetic and plasma environment surrounding the satellite.

The primary induction signature arises because of the periodically varying Enceladus-Saturn distance. The expected induction amplitude is 2-3 nT, comparable to time-variable Alfven currents that arise due to the interaction of Saturn's magnetosphere with the tenuous atmosphere generated by Enceladus' plumes (*Dougherty et al. 2006*). Distinguishing between these competing effects using spacecraft flybys alone is challenging and likely to require at least 50 passes within one satellite radius (Khurana, personal comm.). Simultaneous measurements with a lander magnetometer (here assumed to have the same characteristics as the spacecraft version, minus the boom) allow the internal and external field harmonics to be separated and thus greatly simplify matters. Detecting an induction signature with an orbiter, as opposed to multiple flybys, is more straightforward because it allows a much better characterization of the time-variable magnetospheric environment surrounding the satellite.

The instrument consists of a boom-mounted three-axis ring-core fluxgate magnetometer, with an operating range of +/- 1530 nT, with a resolution of 0.047 nT and a maximum sampling frequency of 40 Hz.

Resource Estimates

The mass (4 kg), power (1W) power and volume (10x10x15 cm, plus a 10m boom which is deployed after launch) are similar to the MESSENGER specifications; the data rate is increased slightly to account for the higher time-resolution needed to separate short-period plasma fluctuations from the longer-period induction signature.

2.3.2.4 Radar Sounder (Category 1 or 2)

Only the Enceladus-O mission concept is assumed to include a radar sounder as Category 1, though it would be a valuable addition, as a Category 2 instrument, on the other concepts' orbiters. The design for the strawman radar sounder is based on the extensive study by the Europa Radar Sounder Instrument Definition Team (IDT) (*Blankenship et al. 1999*). The main aim of this instrument is to characterize the subsurface structure of the ice shell on Enceladus, and potentially to detect an ice-ocean interface. Penetration depths of tens of kilometers are possible, depending on the thermal structure of the ice shell. A secondary data set will be surface altimetry, though this will have lower spatial resolution than that obtained from the laser altimeter.

The basic design consists of a deployable 10m x 2.6m Yagi antenna, a 20-W transmitter, and a receiver. The transmitting frequency is 50 MHz, resulting in vertical and lateral resolution of ~100m and ~2 km, respectively, from a nominal orbital altitude of 200 km. The data transmission rate has been increased by a factor of five relative to the planned Europa Mode 1 rate because a higher overall downlink bandwidth is anticipated. This increase will allow data to be transmitted with less onboard pre-processing. The 25% duty cycle arises primarily from the competing data transmission requirements of the other remote sensing instruments.

Resource Estimates

Mass (9 kg) power (20 W), and volume (10m x 2.6m for the antenna, 10x15x10 cm for the electronics) are based on the Europa IDT report. The basic design would perform significantly better at Enceladus than Europa, due to the lower orbital velocity and the much-reduced background noise of Saturn compared to Jupiter. Thus, the current mass and power estimates are highly conservative.

2.3.3 Saturn Orbiter *In-Situ* Instruments

2.3.3.1 Ion and Neutral Gas Mass Spectrometer (Category 1)

The ion and neutral gas mass spectrometer (INGMS) instrument provides a means to measure chemical composition in the vicinity of Enceladus, as encountered during flybys by the spacecraft. The primary interest is in obtaining a broad composition of the plume emanating from the south polar region, during fly-through trajectories of various altitudes. As such the experimental scenario for INGMS is similar to that of the ion and neutral mass spectrometer (INMS) on Cassini (*Waite et al. 2004*), with new capabilities optimized for Enceladus science.

In the Saturn-OL (Enceladus flyby) mission concept, encounter speeds are expected to be ~4 km/s. This is half the speed of the recent Enceladus flyby by Cassini/INMS, but still high enough that the open and closed source-type analysis of neutrals and ions with ram enhancement can be accomplished as in INMS. An appropriate recent proxy for INGMS is the version of the Neutral Gas and Ion Mass Spectrometer (NGIMS) that was developed for CONTOUR. The CONTOUR NGIMS is a modern derivative of INMS and earlier NGIMS designs, with increased sensitivity and mass range. The objective mass range for INGMS is 300 amu, which could permit detection of any free (and likely neutral) complex aromatics that might be entrained in the plume. Unit mass resolution across the mass range (m/Δm approaching 300 defined at the 10% peak height positions) is considered sufficient to provide identification of the majority of peaks based on nominal mass and isotope patterns. The absolute quantities of N and O are important for understanding the potential for liquid water on Enceladus. INMS has detected a significant signal at m/z 28, presumed to be mostly N_2 (*Waite et al. 2006*). Resolving CO and N_2 directly would require a mass resolution at least ten times this level. While desirable in principle and certainly possible with various mass analyzer types, such performance should not come at the cost of low sensitivity to complex trace organic species or poor precision in isotope ratios. These isobars could be resolved indirectly with multiple electron ionization energies. Through a combination of higher sensitivity, reduced detector/background noise, and careful preflight calibration using Cassini INMS and other data, INGMS is expected to measure directly the concentrations of NH_3, HCN, C_2H_2, C_2H_6, C_3H_8, CH_3CN, C_6H_6 and multi-ring compounds, etc. (or provide upper bounds) to mixing ratios of 10-100 parts per million (ppm) by volume, with statistical errors (relative standard deviations) of ~ 10%-20%. The instrument will also measure noble gas abundances and isotopes at Enceladus as well as other key isotope ratios such as D/H and $d^{15}N$.

Resource Estimates

Mass (10 kg), power (25 W), and volume (25x25x20 cm) are derived from the Contour NGIMS instrument.

2.3.3.2 Dust Analyzer (Category 1)

The Enceladus dust analyzer instrument provides a means to measure chemical composition of dust particles in the vicinity of Enceladus, as encountered during flybys of the Saturn orbiter in the Saturn-OL mission concept. The primary interest is in analyzing the icy particulate component of the plume emanating from the south polar region, during fly-through trajectories of various altitudes. As such, the experimental scenario for the dust analyzer is similar to that of the Cosmic Dust Analyzer (CDA) on Cassini (*Spahn et al. 2006*), with new capabilities optimized for Enceladus science.

The vast majority of icy particles emanating from the Enceladus south polar vents return to the surface ("snow out") in the same region (VIMS data indicate typical grain sizes of several hundred mm between tiger stripes). Even so, escaping dust (v > 235 m/s) dominates the flux experienced by CDA by a factor of ten or more over other sources (E-ring or interplanetary). For such escaping particles, the inferred total mass escape rate is 0.04 kg/s. These particles are primarily water ice grains, with a minority population of silicate+H_2O grains, and contain minor or trace levels of other compounds including organic molecules. CDA has obtained dust flux data (Spahn et al. 2006) and some compositional data using TOF-MS out to m/z 150 (*Srama et al. 2006*). The Enceladus dust analyzer instrument will take advantage of updated technology, such as developed for the Cometary Impact Dust Analyzer (CIDA) on Stardust, to improve the sensitivity and m/z range for mass analysis of these species.

Dust analyzer data out to at least m/z 300 amu/e$^-$ with unit mass resolution will be compared directly with the INGMS data over the same m/z range, to help determine (1) if ice particle, neutral gas, and ions sample the same subsurface material, and if it is liquid; (2) if trace organic compounds (either volatile or non-volatile) are associated with the minor silicate phase or water ice in the particles; and (3) if there is evidence of liquid-phase prebiotic synthesis drawing chemical precursors from or involving surface reactions with bounding silicate-matrix walls. The dust analyzer will also be used to more fully analyze the distribution and composition of dust particles in the E ring.

Resource Estimates

Mass (5 kg), power (5 W), and volume (10x10x10 cm) are derived from the Cassini CDA and Stardust CIDA instruments.

2.3.3.3 Low Energy Plasma Analyzer (Category 2)

The ion portion of this example instrument is based directly on the Mercury MESSENGER Fast Imaging Plasma Spectrometer (FIPS, *Gold et al. 2001*). It will characterize the plasma ion environment of Enceladus, so that both sputtering and plasma-plume interactions may be measured and modeled quantitatively.

The design of the FIPS sensor is predicated on the following goals:

1. Low mass, volume, and power
2. Suppression of ultraviolet (UV) to permit operation in full sunlight near Mercury
3. Wide field of view
4. Large dynamic range
5. Good mass resolution
6. High voltages required for the electrostatic analyzer, and for post-acceleration, which enables low-energy ions to penetrate the carbon foil
7. Good dynamic range for energy-per-charge, fast transitions between steps
8. Fast time-resolution capability
9. Low data rate

Particles that pass through the electrostatic analyzer have a known E/Q, proportional to the stepped deflection voltage. They are then post-accelerated by a fixed voltage, before passing through a very thin carbon foil. The ions travel a known distance and hit the stop micro-channel plate (MCP), while forward-scattered electrons from the carbon foil are focused onto the start MCP. Position sensing with a wedge-and-strip anode in the start MCP assembly determines the initial incidence angle. The mass-per-charge (M/Q) of a given ion follows from the known E/Q and the measured time of flight, allowing reconstruction of distribution functions for different M/Q species. In its Normal (nominal) scan mode, the electrostatic analyzer system covers the E/Q range in 64 logarithmically spaced steps every 65 s. It can also run in a fast “Burst mode” that allows highly focused sweeps in only 2 s.

In addition to the FIPS, an electron spectrometer would also be desirable. This could be based on the FIPS design, but would eliminate the time of flight section of the FIPS sensor. The additional resources for the electron spectrometer would then be ~1.0 W power, 0.5 kg mass, and approximately half the volume of the FIPS head.

Resource Estimates

Mass (1.4 kg), power (2.1 W), and volume (17x21x19 cm), without the electron spectrometer, are derived from the Messenger FIPS instrument.

2.3.3.4 Energetic Particle Spectrometer (Category 2)

This strawman instrument is based directly on the New Horizons Pluto Energetic Particle Spectrometer Science Investigation (PEPSSI) sensor and the Mercury MESSENGER Energetic Particles Spectrometer (EPS, *Gold et al. 2001*). It will characterize the energetic ion and electron environment of Enceladus, so that surface processes such as sputtering and radiolysis can be modeled quantitatively.

The EPS head is a compact particle telescope with a time-of-flight (TOF) section 6 cm long and a solid-state detector (SSD) array. A mechanical collimator defines the acceptance angles for the incoming ions and electrons. The collimator together with the internal geometry defines the acceptance angles. The FOV is 160° by 12° with six segments of 25° each; the total geometric factor is ~0.1 cm^2 str.

Energetic ions from ~ 5 keV/nucleon to 1 MeV total energy are binned in energy and species using TOF only at lower energies, TOF x E at higher energies. Energetic electrons are measured simultaneously in the dedicated electron pixels from ~20 to 700 keV. Only protons with energies >300 keV (and water-group ions with higher energies,) can penetrate the Al absorber on these pixels. Most such high-energy penetrators are eliminated by onboard coincidence with MCP events; the rest can be removed by ground analysis of the data containing the simultaneous ion flux (*Williams et al. 1994*).

Resource Estimates

The EPS sensor has a mass of ~2.5 kg, power 2 W, and dimensions ~10 x 10 x 15 cm. Further efficiencies in mass, power, and volume can be realized by building common electronics elements for FIPS, e-FIPS, and EPS, similar to what was done on MESSENGER.

2.3.4 Enceladus Orbiter *In-Situ* Instruments

2.3.4.1 Gas Chromatograph Mass Spectrometer (Category 1)

The Gas Chromatograph Mass Spectrometer (GCMS) instrument is based on heritage from the Cassini-Huygens Titan Probe GCMS and the Sample Analysis at Mars (SAM) GCMS on the Mars Science Laboratory (MSL). Enceladus ice and dust particles collected during plume passage can be heated by vacuum pyrolysis and the evolved gases then separated by gas chromatography. Both simple and complex hydrocarbons with molecular weights up to 535 amu can be detected at the part per billion by quadrupole mass spectrometry (QMS) or time of flight mass spectrometry. Carbon isotopic measurements ($^{13}C/^{12}C$) of carbon dioxide released from the plume particles can be measured to 3 per mil with the QMS. In addition, reduced inorganic gases such as ammonia can be measured at < 100 ppb. The QMS operates in two modes: (1) dynamic, or continuous gas inlet and pumping, or high throughput and sub-picomole (< 10^{-12} mol) sensitivities; or (2) static, or batch gas inlet and no active pumping, for high-precision isotope measurements. The QMS ion source is identical to the NGIMS closed source which is ten times more sensitive than that of the Cassini INMS.

A sample collection funnel would be used to collect ice and dust particles in the Enceladus plume during low speed flybys. The captured material could then be analyzed by the *in-situ* instruments including pyrolysis GCMS and the Dust Micro-Analyzer (below). Assuming a 1:1 solid/gas mass ratio and the UVIS-derived near-surface gas column density of 1.6 x 10^{16} molecules of H_2O per cm^2, a column density of 5 x 10^{-7} g/cm^2 of gas is calculated (**Section 2.5**). Using a 100 cm^2 surface area collection funnel, approximately 50μg of dust could be collected for analysis during a single plume passage. GCMS has a limit of sensitivity for amino acids at the 10^{-12} mol range. If one assumes part per million levels (μg amino acid per g ice/dust) of amino acids in the Enceladus plume, then one could collect 5 x 10^{-13} mol of amino acids in each plume passage. Therefore, sample from at least two plume passages would be required to detect amino acids if present at the part per million level.

Resource Estimates

The mass (15 kg), power (20 W, on average) and volume (25x25x20 cm) are derived from the Cassini Huygens Probe GCMS (*Niemann et al. 2002*) and the SAM GCMS instrument on the 2009 Mars Science Laboratory (MSL). Reduced mass, power, and volume could be achieved if a miniature time of flight mass spectrometer was used instead of a QMS.

2.3.4.2 Dust Micro-Analyzer (Category 1)

As noted above, the low relative speed from Enceladus orbit makes it possible to catch plume particles and get them affixed to the surface of a known substrate for some form of imaging. The proposed instrument is based on MEMSA (Micro Electron Microprobe with Sample Analyzer, *Manohara et al. 2005*), which is a form of scanning electron microscope that will have high spatial resolution (<40 nm) and perform energy dispersive X-ray (EDX) analyses, and is well-suited to this purpose. The targeted energy range for EDX is from 100 eV to 20 keV, which covers low-Z elements of biological interest such as carbon to high-Z trace elements of mineralogical interest. This technology builds on the SEMPA instrument that had been approved for the (cancelled) Rosetta mission. MEMSA achieves significant weight reduction by using high-current carbon nanotube bundle arrays developed at JPL that accelerate electrons using only 8-10 V/μm, and can yield a spot resolution of ~ 40 nm (*Manohara et al. 2005*). In addition, MEMSA uniquely avoids the energy-consuming and massive beam scanning technology in electron microscopy by simply stepping the sample across a stationary electron beam with piezoelectric transducers. This instrument would also be fed by the sample collection funnel described in the GCMS section above.

A Dust Micro-Analyzer is considered Category 1 because scanning electron microscopy with an analytical capability is one of the most powerful techniques available for the initial characterization of novel or unknown materials in both the biological and geological sciences. It is even conceivable that biological structures ejected from the plume vents could be imaged by such an instrument, something that would be the discovery of the century.

Resource Estimates

These are derived from the proposed MEMSA instrument. The simplified principle of operation of MEMSA translates to lighter weight (10 kg including sample collection system, compared to 13 kg), lower power (5 W vs. 25-30 W), and smaller dimensions (5×20×10 cm vs. 50×25×18 cm) compared to its SEMPA predecessor.

2.3.5 Enceladus Soft Lander Instruments

2.3.5.1 Lander Camera (Category 1)

The soft lander would include a pair of cameras to provide context for the material that is sampled for onboard analysis, to investigate surface processes, and for serendipitous science. Use of two cameras would provide stereo coverage. Cameras similar to the Mars Exploration Rover Pancam system (*Bell et al. 2003*), which has a 0.27 mrad/pixel resolution and eight filters per camera, would be very suitable. The camera would be mounted on an articulating mast to enable construction of full panoramas of the scene near the lander. Images of the south polar plume, which would be visible above the horizon from the proposed south polar landing site, would also be valuable.

Resource Estimates

Mass (0.6 kg for the pair), power (5 W for the pair), and volume (roughly 8x8x8 cm each) are derived from the MER Pancam cameras. A mast roughly 1-m high is also required to support the cameras.

2.3.5.2 Seismometer (Category 1)

The seismometer is part of the landed package that derives its design from the proposed NetLander SEIS experiment (*Lognonne et al. 2000*). Its primary objectives are to detect long-period normal-mode oscillations (to determine the bulk interior structure of Enceladus; cf. *Panning et al. 2006*), and to detect shorter-period body and surface waves to infer the local ice-shell properties (cf., *Lee et al. 2003*, *Kovach and Chyba, 2001*).

For moderately-sized (M_w~5; Nimmo and Schenk 2006) seismic events exciting regional or global surface waves, the required displacement sensitivity in the long-period (0.001-0.1 Hz) range is 1 mm (cf., *Panning et al. 2006*). In the short-period range (0.1-100 Hz), the velocity sensitivity required is better than 0.1 μm/s to resolve the main P- and S-wave arrivals (*Lee et al. 2003*). The estimated sensitivity of the NetLander instrument of 10^{-10} m s^{-2} Hz$^{-1/2}$ easily meets these requirements.

Long-period (1 Hz) data require a continuous transmission rate of ~0.03 kbps; these records will be used to identify potential records of interest in the high-frequency data, which will be subsequently transmitted (or this process could be automated on board the lander). *In-situ* storage of 24 hours of the high-frequency data requires 250 Mb.

Although a network of at least three seismometers is require to accurately locate seismic events, *Kovach and Chyba* (*2001*) and *Lee et al.* (*2003*) showed that a single seismometer suffices to infer ice shell thicknesses, using moderate period (2-10 s) surface waves and direct P- and S-wave reflections, respectively. A single seismometer also provides the frequency-amplitude relationship for longer period normal mode oscillations, which is sufficient to infer the deep interior structure of a satellite (*Panning et al. 2006*). The primary value of adding a second or third seismometer would be to accurately locate local events, potentially allowing correlation with individual surface features.

Resource Estimates

Mass (2.3 kg) and power (1 W) are assumed to be identical to those of the NetLander SEIS instrument.

2.3.5.3 Radio Science (Category 1)

The Enceladus soft lander would also be capable of precise Doppler tracking from the orbiter, both to pinpoint its location and, in the Enceladus-OL concept, to potentially provide additional precise measurements of tidal flexing at one point on the surface. Tidal flexing measurements would not be possible using Doppler tracking from the lander in the Saturn-OL concept, because only two brief tracking opportunities exist (after landing and during relay eight days later), and both will occur at essentially the same point in Enceladus' tidal cycle.

Resource Estimates

The transponder is assumed to be integral to the communications system and no additional mass and power allocation is assumed.

2.3.5.4 Surface Chemistry Package and Oxidant Detector (Category 1)

The surface chemistry package includes a micro capillary electrophoresis analyzer with laser induced fluorescence (μCE-LIF) and electrospray ionization time of flight mass spectrometer (ESI-TOF-MS) for the detection of amino acids, amines, amino sugars, and nucleobases, and a chemometric sensor array for the detection of oxidants such as hydrogen peroxide and oxidizing acids. These instruments are similar to the Urey: Mars Organic and Oxidant Detector that was selected for the Pasteur Payload on the 2013 ESA ExoMars rover mission (*Bada et al. 2005*, *Skelley et al. 2006*). The μCE-LIF instrument is used to determine the composition of target organic compounds of biological significance (such as amino acids), and if detected, are analyzed further to determine their chirality. Samples of Enceladus surface ice would be introduced into a μCE chip and the organic species labeled with a fluorescent tag with microfluidics technology. Derivatized amines are then separated along tiny capillary channels filled with a chiral resin by applying an electric potential across the channel. Eluting compounds are then detected by laser induced fluorescence at part per trillion sensitivities. In addition, the μCE system is used to transfer key molecular species in solution for direct analysis by ESI-TOF-MS. Electrospray efficiently forms singly or multiply-charged ions of large parent molecules for MS analysis, including amino acids/peptides, carboxylic acids/lipids, purines, pyrimidines, and other compounds of biochemical interest. The analysis of these ions by TOF-MS assures that the higher m/z "parent" compounds may be detected directly (m/z range of several thousand amu), thus complementing the more focused LIF method with a broad assay. Using the composition and chirality characteristics of amino acids, along with characterization of a host of other key organics, the source (biologic or non-biologic, e.g., meteoritic organics) of these compounds can be determined.

The chemometric sensor array measures the reaction rates of films that have different sensitivities to particular types of oxidants expected to be present in the Enceladus surface environment. The detection of oxidants and a determination of their concentration with depth in the surface ice is important for understanding redox gradients that may serve as an energy source for a potential subsurface biosphere on Enceladus. These measurements are important for determining the chemical composition of the surface and determine what energy sources might be available to support life.

Resource Estimates

The mass (3 kg), power (maximum 25 W) and volume (21x17x20 cm) are derived from the Mars Organic and Oxidant Detector instrument for the ESA ExoMars mission.

2.3.5.5 Laser Desorption Mass Spectrometer (Category 1)

The laser desorption mass spectrometer (LDMS) instrument provides a means to measure the composition of Enceladus surface materials with no sample contact or preparation. A pulsed laser is focused onto a sample, causing chemical species to enter the gas phase directly, which are then analyzed by a mass spectrometer. The instrument can be operated in the hard vacuum conditions at Enceladus – no pumps are needed. Both ice and rock samples of any type may be studied, including the fine, frozen plume-derived particulate that likely coats much of the surface. Chemical species ionized by the laser are directly detected with a miniature time-of-flight mass spectrometer (TOF-MS). The short, intense laser pulse coupled with the high mass-to-charge (m/z) range of the TOF-MS (up to ~10^4 amu/e^-) permits the characterization of complex non-volatile organics including polycyclic aromatic hydrocarbons (PAHs), polymeric compounds, and macromolecular hydrocarbons, which can have molecular weights from hundreds to thousands of amu. The particular abundance distributions and branching (heterosubstitution) patterns of these compounds, as a function of molecular weight, can aid in understanding the carbon inventory and cycle of Enceladus, and to distinguish between endogenous and exogenous (meteoritic) organics. The laser also volatilizes neutral atoms and molecules that can be independently sampled with the GCMS, providing that instrument with species that may be more difficult to sample with pyrolysis and electron ionization (EI) alone. Neutral species include those mentioned above as well as semi-volatile compounds (e.g., certain heavier carboxylic acids such as lipids) that could reveal complex organic synthesis at Enceladus, but which are challenging to ionize intact by EI. By controlling the laser intensity, elemental and molecular/organic composition may be obtained with LDMS. Both positive and negative ions may be analyzed, an important feature to characterize composition broadly.

A possible implementation of LDMS on Enceladus involves direct analysis of solid samples after collection by an arm-based ice scraper or a scoop, as part of the whole sample analysis chain. Only a tiny amount of material, in the form of a thin layer of particles or an ice film, is required for laser sampling. Each analysis would involve approximately 10^3 laser pulses, at ~1 Hz, of increasing intensity. Neutral gas generated by laser desorption would be collected for GCMS simultaneously with the TOF-MS analysis of laser-induced ions. LDMS can additionally be used at high intensity to remove sample residue from the sample holder, detect and characterize any adsorbed contamination, and provide *in-situ* calibration using delivered solid-phase targets.

Resource Estimates

Mass (1.9 kg), power (5 W maximum) and volume (36x7.6x7.6 cm) are derived from the ExoMars MOMA instrument.

2.3.5.6 Magnetometer (Category 2)

A magnetometer would be a useful addition to the lander science package: a combination of magnetic field measurements from a surface magnetometer and an orbital magnetometer would make it easier to separate the magnetic effects of induction within Enceladus, a valuable probe of the interior, from the effects of Enceladus' interaction with the Saturnian magnetosphere. Magnetometer design would be very similar to that carried on the orbiter spacecraft previously described, though techniques other than a boom (e.g., ejection onto the surface) might be used to separate the magnetometer from the magnetic fields generated by the lander. This instrument is lower priority because the short lifetime of the battery-powered landers included in these studies would prevent useful synergism with a Saturn orbiter, and the Enceladus orbiter should provide adequate magnetic sounding even without the addition of a lander magnetometer.

Resource Estimates

Mass (4 kg) power (1 W), and volume (10x10x15 cm) are assumed similar to the MESSENGER magnetometer.

2.3.5.7 Tunable Laser Spectrometer (Category 2)

The Tunable Laser Spectrometer (TLS) is a key instrument in the SAM suite on MSL. The TLS provides for high sensitivity, unambiguous detection of targeted species of biological relevance (e.g., methane to 0.1 ppb, water and hydrogen peroxide to 1 ppb) and isotope ratios (e.g., $^{13}C/^{12}C$, D/H, $^{17,18}O/^{16}O$) to typically 1 per mil or below (*Webster et al. 1990*). The TLS is essential to carrying out measurements of trace species and precision isotope measurements for those frequent cases expected in an unknown chemical environment where spectral overlaps in the QMS during evolved gas analyses might limit precision or accuracy. High precision isotope measurements of evolved gases are important for understanding past and present habitability of Enceladus.

The TLS is a six-channel tunable laser absorption spectrometer. TLS comprises three main parts: the laser-detector assemblies, the multipass sample cell, and the electronics. TLS can incorporate both near-IR tunable diode laser and quantum cascade laser sources operating continuous-wave. The multipass sample cell is an all-aluminum structure with gold-on-chromium-on-nickel aluminum mirrors in an athermal design configuration. Mirrors will be used in a Herriott cell configuration with a 10.2-m path length.

Resource Estimates

Mass (1.9 kg), power (5 W max) and volume (36x8x8 cm) are derived from the TLS in the SAM instrument suite on MSL.

2.3.6 Hard Lander Instruments (Category 2)

Hard lander instruments were considered briefly. These could provide valuable additional science if resources permitted. The most important role of hard landers would be to establish a seismic network, either with multiple hard landers or in conjunction with the seismometer on a soft lander. Seismometers would be similar to those carried on the soft lander. The presence of two or three seismometers on the surface simultaneously would greatly enhance the ability to probe crustal structure and locate and characterize individual seismic events (see the discussion of the soft lander seismometer in **Section 2.3.5.2**). Doppler tracking of multiple hard landers from an Enceladus orbiter would also provide precise constraints on tidal flexing amplitudes at those locations, though this would not be possible from a Saturn orbiter because there would be only two tracking opportunities, eight days apart, each at the same point in the tidal cycle. A penetrator camera would also be valuable for understanding surface processes in the vicinity of the penetrator.

Resource Estimates

Seismometer mass (2.3 kg) and power (1 W) are assumed to be identical to that on the soft lander, derived from the Netlander SEIS instrument. Camera mass (1.2 kg) and power (2 W) are derived from the camera on the Russian Mars 96 penetrators. The transponder needed for Doppler tracking was assumed to be part of the communications system, with no additional mass and power allocation.

2.3.7 Matrices Relating Instruments to Science Goals

The following tables describe the value of each proposed instrument for addressing the science goals. The value of each instrument for each goal is qualitatively scored from 1 to 10, with color coding (darker colors indicating greater value) to enhance readability. A weighted mean score for each instrument is also given, with weights of 4, 2, and 1 for Priority 1, 2, and 3 science goals, respectively. Category 2 instruments, discussed above, are included in these tables: they are of potential value but were not included in the final strawman payloads due to mass, power, or other engineering constraints.

The tables show that most broad science goals are addressed by multiple instruments, though the roles of individual instruments are generally unique. For instance the thermal mapper and visible mapper both are very valuable for addressing the goal of understanding cryovolcanism on Enceladus, but they address very different aspects of the phenomenon (surface morphology and plumes from the visible mapper vs. temperatures and heat flow from the thermal mapper).

2.4 Science Evaluation of Architecture Trade Space

Table 2.4-1 lists all the possible mission configurations considered in this trade space study, with a brief assessment of science value. Orbiters, as well as a single flyby spacecraft, were considered, with the added possibility for sample return, and various lander-type options. The subsections below outline the reasons why some of this trade space was removed from further consideration by the Science Definition Team, because of low science value, high risk, expected high cost, or other reasons. Missions removed from consideration are shaded, leaving the remaining trade space in white.

2.4.1 Mission Configurations Not Chosen for Detailed Study

2.4.1.1 Sample Return

Sample return offers the possibility for high science return, enabling sophisticated analysis in Earth laboratories that is not possible onboard a robotic spacecraft. However, there are many risks and complications associated with sample return.

Table 2.3.7-1: Instruments considered for the Enceladus-O and Enceladus-OL mission concepts. The Enceladus orbiter instruments were identical for both of these studies except for the radar sounder, thus the two Enceladus orbiters are not listed separately.

Instrument Value Matrix for Enceladus Orbiter + Enceladus Lander (Enceladus O, Enceladus OL										
Instrument	Mission Element	Included in Strawman Payload?	Biological Potential (Priority 1)	Composition (Priority 2)	Cryovolcanism (Priority 2)	Tectonics (Priority 2)	Tidal Heating and Interior Structure (Priority 2)	Saturn System Interaction (Priority 3)	Surface Processes (Priority 3)	Weighted Mean Score
Thermal Mapper	Enc. Orbiter	Y	8	2	9	5	9	0	2	6.0
Near-IR Mapper	Enc. Orbiter	Y	7	7	5	3	3	5	5	5.3
Visible Mapper	Enc. Orbiter	Y	6	4	8	9	7	6	8	6.7
Laser Altimeter	Enc. Orbiter	Y	8	2	5	7	9	0	4	5.9
Radio Science	Enc. Orbiter	Y	8	2	4	6	9	0	1	5.4
Magnetometer	Enc. Orbiter	Y	7	2	3	2	8	6	1	4.6
GCMS	Enc. Orbiter	Y	8	8	7	2	3	8	5	6.1
Dust Micro-Analyzer	Enc. Orbiter	Y	8	8	8	1	3	6	4	5.9
RADAR Sounder	Enc. Orbiter	Y/N*	6	4	7	6	8	0	5	5.6
UV Spectrometer	Enc. Orbiter	N	3	5	6	0	2	7	3	3.4
Low Energy Plasma Analyzer	Enc. Orbiter	N	2	6	5	0	0	9	4	3.1
Energetic Particle Spectrometer	Enc. Orbiter	N	2	6	5	0	0	9	6	3.2
Lander Camera (two)	Soft Lander	Y	4	5	5	4	4	1	8	4.4
Seismometer	Soft Lander	Y	5	3	6	8	9	0	4	5.4
Radio Science	Soft Lander	Y	5	2	4	5	5	0	1	3.8
Surface Chemistry Package	Soft Lander	Y	9	9	6	2	2	7	7	6.3
Surface Ice Oxidant Detector	Soft Lander	Y	8	7	5	0	0	7	7	5.0
LDMS	Soft Lander	Y	9	8	5	0	0	7	7	5.4
Lander Magnetometer	Soft Lander	N	6	3	3	4	7	3	0	4.4
Tuneable Laser Spectrometer	Soft Lander	N	7	6	4	0	0	5	6	4.2
Penetrator Camera	Hard Lander	N	4	5	5	4	4	1	6	4.2
Radio Science	Hard Lander	N	5	2	4	5	5	0	1	3.8
Seismometer	Hard Lander	N	5	3	6	8	9	0	4	5.4
*Included on Enceladus Orbiter mission, not on Orbiter+Lander mission										

Table 2.3.7-2: Instruments considered for the Saturn-OL mission concept.

Instrument Value Matrix for Saturn Orbiter + Enceladus Lander (Saturn OL)										
Instrument	Mission Element	Included in Strawman Payload?	Biological Potential (Priority 1)	Composition (Priority 2)	Cryovolcanism Priority 2)	Tectonics (Priority 2)	Tidal Heating and Interior Structure (Priority 2)	Saturn System Interaction (Priority 3)	Surface Processes (Priority 3)	Weighted Mean Score
Thermal Mapper	Saturn Orbiter	Y	7	2	7	5	8	0	2	5.3
Near-IR Mapper	Saturn Orbiter	Y	7	9	5	3	3	5	5	5.6
Visible Mapper	Saturn Orbiter	Y	6	4	7	7	7	6	9	6.4
Laser Altimeter	Saturn Orbiter	Y	7	2	5	7	7	0	4	5.3
Radio Science	Saturn Orbiter	Y	7	2	4	6	7	0	1	4.8
Magnetometer	Saturn Orbiter	Y	7	2	3	2	6	6	1	4.4
INGMS	Saturn Orbiter	Y	7	7	7	2	3	7	5	5.6
Dust Analyzer	Saturn Orbiter	Y	7	7	7	2	3	7	5	5.6
Framing Camera	Saturn Orbiter	N	3	2	6	5	5	4	3	3.9
UV Spectrometer	Saturn Orbiter	N	3	5	6	0	2	7	3	3.4
RADAR Sounder	Saturn Orbiter	N	6	4	7	6	7	0	5	5.5
Low Energy Plasma Analyzer	Saturn Orbiter	N	2	6	5	0	0	9	4	3.1
Energetic Particle Spectrometer	Saturn Orbiter	N	2	6	5	0	0	9	6	3.2
Lander Camera (two)	Soft Lander	Y	4	5	5	4	4	1	8	4.4
Seismometer	Soft Lander	Y	5	3	6	8	9	0	4	5.4
Radio Science	Soft Lander	Y	5	2	4	5	5	0	1	3.8
Surface Chemistry Package	Soft Lander	Y	9	9	6	2	2	7	7	6.3
Surface Ice Oxidant Detector	Soft Lander	Y	8	7	5	0	0	7	7	5.0
LDMS	Soft Lander	Y	9	8	5	0	0	7	7	5.4
Tuneable Laser Spectrometer	Soft Lander	N	7	6	4	0	0	5	6	4.2
Penetrator Camera	Hard Lander	N	4	5	5	4	4	1	8	4.4
Radio Science	Hard Lander	N	3	1	2	3	3	0	1	2.2
Seismometer	Hard Lander	N	5	3	6	8	9	0	4	5.4

In its simplest form, a sample could be obtained during a single spacecraft flyby on a free return trajectory (i.e., one requiring no additional propulsive maneuvers to return to Earth). As detailed in **Section 3**, a free return trajectory takes approximately 13 years to reach Saturn and encounters

Table 2.4-1: Configuration Trade Space (Rejected Options Grayed Out)

Configuration	Only	Base Configuration + Soft Lander	Base configuration + Hard Lander(s)	Base Configuration + Dumb Impactor	Base Configuration + Plume Sample Return
Saturn Orbiter	Incremental science return	High science return	Seismic network adds value	Modest science return	High potential science return
Enceladus Orbiter	High science return	Highest science return	Seismic network adds value	Modest science return	High potential science return
Single Flyby	Low science return	Low science return	No way to return data	Modest science return	High potential science return
Lander Only	Low science return	N/A	No way to return data	Low science return	High potential science return

Enceladus with a relative velocity of ~7 km/s. This flyby speed would enable robust sample collection, comparable to the Stardust flyby velocity of ~6 km/s, well within the realm of current aerogel capture technology. However, the mission would require longevity of at least 26 years, and is high risk, with only one opportunity for a successful sample collection, and a relatively small amount of additional data obtained about Enceladus during the single flyby. Sample collection and return from Saturn orbit would be an option worth further investigation, and might possibly allow a faster flight time while keeping collection speed acceptable, though with greatly increased mission complexity.

For any type of sample return, Earth return velocities are high unless more time-consuming inner solar system flybys are used to lower the velocity, and capture techniques would require further investigation. In addition, planetary protection must be carefully considered, because while cryogenic, preserved, samples would provide the best science return, they would also require guaranteed containment on landing/capture, quarantine and special precautions and handling on Earth (Planetary Protection Level V and Class IV Biohazard containment and quarantine). Thus, the overall risk, complexity and lifetime of sample return missions were deemed unacceptable for a Flagship-class mission at this time, despite their potential for high scientific return.

2.4.1.2 Dumb Impactors

Kinetic or “dumb” impactors offer the opportunity to create a “control plume” away from the south pole, for investigating compositional differences at various locations on the surface, for example. They can also be useful for seismic sounding in conjunction with surface seismometers. However, large compositional differences are not expected elsewhere on the surface (which is coated with plume fallout and processed E-ring particles), and tidal flexing should generate sufficient seismic signals for internal sounding. Thus, this option was considered to be of low to modest scientific value. As dumb impactors require only basic technology, they do not require further investigation at this time and could be included if mass were available and if future scientific evaluation warranted their use.

2.4.1.3 Saturn Orbiter Only (no landers)

A well-equipped Saturn orbiter has scientific value, but does not meet the full science goals of an Enceladus-focused Flagship-class mission, particularly after the current Cassini mission. In particular, a Flagship-class mission should substantially increase our scientific knowledge of Enceladus, achieving all of the top priority science goals. A single Saturn orbiter, with advanced instrumentation would provide multiple fast passes of Enceladus, but would have difficulty providing sufficient knowledge of surface chemistry and interior structure to be deemed worthwhile as a Flagship mission. Results of the JPL-led study documented in Titan and Enceladus $1B Mission Feasibility Report, JPL D-37401 (*Reh et al. 2007*) can be used to evaluate the value of such a mission for a New Frontiers-class mission. The addition of a soft lander or a seismic network is sufficient to create a scientifically attractive mission, however, and was considered.

2.4.1.4 Single Flyby Missions

A single flyby mission, one where the spacecraft never enters Saturn orbit, but simply flies through the system and passes Enceladus once, has the advantage of being a relatively inexpensive and simple mission. However, it offers only one opportunity to observe Enceladus, while passing at high relative velocity. Even with the addition of landers or impactors, it would not allow sufficient science return for a Flagship-class mission, given that little of the surface could be mapped in a single fast flyby. Adding a lander or impactors increases the knowledge that can be obtained through *in-situ* sampling and seismometry, however, the need for direct-to-earth communication with the lander after the flyby would be a further complication.

2.4.1.5 Lander-Only Missions

In this configuration, there is no orbital component, only a limited-life surface mission. While the surface science would be very compelling, particularly for a long-lived surface station, the lander would need to communicate directly with Earth, requiring substantial power and a large antenna. In addition, a single lander is high risk, given the difficulty of landing on unknown terrain, implying a significant chance of no science return; this is unacceptable for a Flagship-class mission. The science lost, such as surface mapping, by not having an orbital component also gives this mission lower value, and reduces the value of the lander science due to the lack of context. Additional hard impactors have no simple way to return data to the lander and offer no additional value. A more scientifically valuable subset of this mission type is an Enceladus orbiter that lands after the end of an orbital phase. That mission would be of high scientific value and is considered under the Enceladus orbiter case.

2.4.6 Missions Chosen for Detailed Study

The science rationale for the three missions chosen for detailed study: Enceladus Orbiter plus Lander, Enceladus Orbiter only; and Saturn Orbiter plus Lander, are given in detail in **Sections 3.3 to 3.5** of this report. **Table 2.4.6-1** summarizes the science value of each of these missions and compares them to the science value of the Cassini extended mission.

2.5 Plume Particle Sizes and Abundances: Potential Hazards and Sampling Opportunities

For Enceladus missions, the cryovolcanic south polar plume is both a golden opportunity for easy collection of interior samples, and a potential spacecraft hazard. Cassini data can be used to estimate the size of the hazard and the number of particles available for sampling, though uncertainties are large. Note that this analysis was done after the dust shielding design discussed in **Section 3**, so assumptions and results may differ in detail.

The Cassini Cosmic Dust Analyzer (CDA) measured 10^{-7} particles/cm^3 larger than 4-micron diameter in July 2005 passage through the edge of the plume (*Spahn et al. 2006*). This provides a strong lower limit to expected small particle fluxes in the interior of the plume. Much higher densities are expected near the plume source, where Cassini visible and near-IR images show abundant forward-scattering particles, but particle sizes and densities are difficult to determine uniquely from the remote sensing data, and analysis is still in progress. Neither the CDA, nor remote sensing instruments, are sensitive to large, potentially hazardous, particles (D > ~1mm); the abundance of such particles must be inferred indirectly.

This analysis follows the approach developed by Dr. Larry Esposito (personal communication) for consideration of hazards to the Cassini spacecraft during future plume passages. He proposed that for theoretical reasons, total mass of plume particles (which are dominantly water ice) is unlikely to exceed the mass of the water vapor in the plume, the column density of which has been measured quite accurately by the Cassini Ultraviolet Imaging Spectrograph (UVIS) instrument, as 7×10^{15} molecules/cm^2, or 2×10^{-7} g/cm^2, in a tangent column at 100 km minimum altitude, comparable to likely spacecraft plume passages. The number of particles of a given diameter then depends on the assumed size/frequency distribution (a power law with differential exponent q is assumed), the ice/gas ratio, and the total range of particle sizes, which is determined by the physics of the particle production process. A q of 3 was measured by CDA in the few micron size range, though larger values (implying more small particles and fewer large ones) was inferred from the

Table 2.4.6-1: This table summarizes the ability of the various mission options, including the extended Cassini mission, to address the science objectives. The relative ability of each mission to address each science objective is graded by a numerical score from 1-10, with 10 being best, and the reasoning behind the score is summarized in the associated text. The estimated overall science value of each mission option is also given. Individual and overall scores are necessarily subjective, but summarize the best judgment of the science definition team. Color-coding is used to enhance readability, with dark colors indicating higher scores.

Science Value of Various Enceladus Mission Options				
Science Objectives	Enceladus-OL	Enceladus-O	Saturn-OL	Cassini Extended Mission
Level 1: Biological Potential	10: Excellent probling of interior and plume source region: excellent bulk analysis of surface materials	7: Excellent probing of interior and plume source region, plume characterization	8: Adequate probing of interior and plume, excellent bulk analysis of surface materials	3: Improved plume analysis, and understanding of the plume source region from remote sensing
Level 2: Composition	9: good plume chemistry, excellent surface chemistry of bulk samples	6: good plume chemistry, lack of bulk samples limits quality of analysis	8: Excellent surface chemistry of bulk samples	4 Improved plume sampling , limited by instrumentation
Level 2: Cryovolcanism	9 Low-speed plume sampling, extensive surface mapping and radar sounding (though limited in polar regions)	9 Low-speed plume sampling, extensive surface mapping and radar sounding (though limited in polar regions)	6: High-speed plume sampling and polar surface mapping	4: Improved remote sensing and *in-situ* sampling, limited by instrumentation and small number of flybys
Level 2: Tectonics	9: global mapping, tidal flexing, altimetry, surface seismometry	8: global mapping, tidal flexing, altimetry, radar sounding	7: Orbital mapping with some limitations, surface seismometry	3: limited hi-res coverage, little geophysics
Level 2: Tidal Heating and Interior Structure	10: Excellent on tidal deformation, gravity, topography, magnetic sounding, excellent seismic sounding	8: Excellent on tidal deformation, gravity, topography, magnetic sounding	7: Adequate on tidal deformation, gravity, topograpy, poor on magnetic sounding, excellent seismic sounding	2: Some improved knowledge of the gravity field and heat flow
Level 3: Saturn system interaction	5: Good plume characterization, but no plasma instruments carried	5: Good plume characterization, but no plasma instruments carried	4: Good plume characterization (limited by high speed), but no plasma instruments carried	4: Multiple passes with good plasma instumentation
Level 3: Surface Processes	9: Close-up imaging and direct surface sampling	7: Global hi-res mapping and composition	9: Close-up imaging and direct surface sampling	2: Very limited hi-res remote sensing, improved knowledge of plume resurfacing
Relative Science Value (subjective rating based on the above matrix)	10	8	7	3

plasma signature of particle impacts. **Figure 2.5-1** shows the fluence of particles larger than a given size from a single plume passage at 100 km altitude, assuming a dust/gas ratio of 1.0 and a particle radius range or 0.1 – 1000 microns. For a 100 cm^2 collection area, in this example, between one and several thousand plume particles larger than 10-micron diameter would be collected in one plume passage. The largest particle hitting a 10 m^2 spacecraft could be larger than 1-mm diameter, depending on the dust power law index, so shielding would be necessary if such particles were dangerous to the spacecraft.

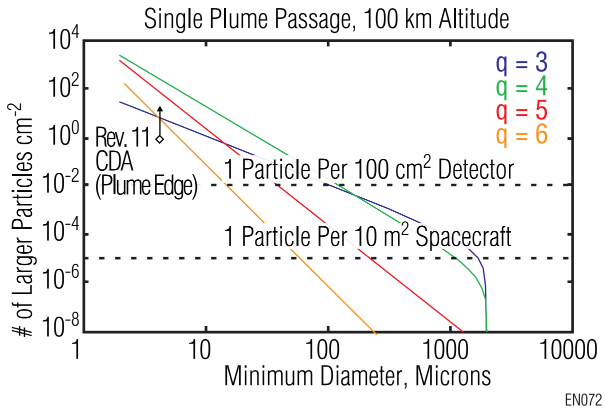

Figure 2.5-1: Expected fluence of plume particles from a single plume passage, assuming a particle diameter range between 0.2 and 2 microns and a dust/gas ratio of 1.0. Curves are shown for various plausible values of the differential size/frequency distribution power law index, *q*. The particle fluence measured by the Cassini CDA instrument on its single plume passage so far, on Rev. 11, is also shown: this is a strong lower limit to the expected fluence within the plume as the Rev. 11 flyby only skirted the edge of the plume.

2.6 References

1. Anderson, B.J., Acuna M.H., Lohr, D.A., Scheifele, J., Raval, A., Korth, H., Slavin J.A., 2007, The magnetometer instrument on MESSENGER, Space. Sci. Rev., in press.

2. Anderson, J.D., Schubert G., Jacobson R.A., Lau E.L., Moore W.B., Sjogren W.L. 1998. Europa's differentiated internal structure: Inferences from four Galileo encounters. Science 281, 2019-2022.

3. Bada, J.L., Sephton, M.A., Ehrenfreund, P., Mathies, R.A., Skelley, A.M., Grunthaner, F.J., Zent, A.P., Quinn, R.C., Josset, J.L., Robert, F., Botta, O., and Glavin, D.P. 2005. New strategies to detect life on Mars. Astron. Geophys. 46, 26-27.

4. Barnash, A.N., Rathbun, J.A., Turtle, E.P., Squyres, S.W., 2006. Interactions between impact craters and tectonic fractures on Enceladus. Am. Astron. Soc. Bull. 38, Abstract 24.06.

5. Barr, A. C. and W. B. McKinnon 2007. Convection in Enceladus' ice shell: Conditions for initiation. Geophys. Res. Lett. 34, L09202, doi:10.1029/2006GL028799.

6. Bell, J.F. et al. 1993. Mars Exploration Rover Athena Panoramic Camera (Pancam) investigation. J. Geophys. Res. 108, DOI 10.1029/2003JE002070.

7. Blankenship, D.D. et al. 1999. Feasibility study and design concept for an orbiting ice-penetrating radar sounder to characterize in three-dimensions the Europan ice mantle down to (and including) any ice/ocean interface, Jet Propulsion Lab. Tech Report.

8. Bray, V. J., Smith, D.E., Turtle, E.P., Perry, J.E., Rathbun, J.A., Barnash, A.N., Helfenstein, P., Porco, C.C., 2007. Impact crater morphology variations on Enceladus. Lunar Planet. Sci. XXXVIII, Abstract 1873.

9. Brown, R. H. et al. 2005. The Cassini Visual and Infrared Mapping Spectrometer (VIMS) Investigation. Space Sci. Rev. 115, 111.

10. Brown, R. H., R. L. Kirk, T. V. Johnson, L. A. Soderblom 1990. Energy sources for Triton's geyser-like plumes, Science 250, 431.

11. Brown, R. H.; Clark, R. N.; Buratti, B. J.; Cruikshank, D. P.; Barnes, J. W.; Mastrapa, R. M. E.; Bauer, J.; Newman, S.; Momary, T.; Baines, K. H.; Bellucci, G.; Capaccioni, F.; Cerroni, P.; Combes, M.; Coradini, A.; Drossart, P.; Formisano, V.; Jaumann, R.; Langevin, Y.; Matson, D. L.; McCord, T. B.; Nelson, R. M.; Nicholson, P. D.; Sicardy, B.; Sotin, C. 2006. Composition and Physical Properties of Enceladus' Surface. Science 311, 1425-1428.

12. Buratti, B.J.; Mosher, J.A.; Johnson, T.V.; 1990. Albedo and color maps of the Saturnian satellites. Icarus 87, 339-357.

13. Buratti,, B.J., 1988. Enceladus - Implications of its unusual photometric properties. Icarus 75, 113-126.

14. Burch, J. L., Goldstein, J. Lewis, W.S., Young, D. T., Coates, A., Doughterty, M., Andre, N.; 2007. Tethys and Dione as sources of outward-flowing plasma in Saturn's magnetosphere. Nature 447, 833-835.

15. Castillo, J. C., Matson, D. L., T. V. Johnson, J. Lunine 2006. Enceladus' geysers – A clue to hydrothermal activity at the surface of Enceladus. Astrobiology 6, 158.

16. Castillo-Rogez J.C., Matson D.L., Johnson T.V., Lunine J.I., Thomas P.C. 2007. Iapetus' geophysics: rotation rate, shape and equatorial ridge Icarus, in press.

17. Cheng, A.F. et al. 2007. Long-range reconnaissance imager on New Horizons. Space Science Reviews, in press.

18. Christensen, P.R., 11 colleagues, 2004. The Thermal Emission Imaging System (THEMIS) for the Mars 2001 Odyssey Mission. Space Sci. Rev. 110, 85–130.

19. Chyba C. 2000. Energy for microbial life on Europa 2000. Nature 406, 368-381?

20. Collins GC, Goodman JC. 2007. Enceladus' south polar sea. Icarus 189, 72-82.

21. Dougherty, M.K., Khurana K.K., Neubauer, F.M., Russell, C.T., Saur, J., Leisner, J.S., Burton, M.E., 2006. Identification of a dynamic atmosphere at Enceladus with the Cassini magnetometer. Science 311, 1406-1409.

22. Dyson FJ. 1997. Warm-Blooded Plants and Freeze-Dried Fish. The Atlantic Monthly 280, 71-80.

23. Esposito, L.W. et al. 2005. Ultraviolet Imaging Spectroscopy Shows an Active Saturnian System. Science 307, 1251.

24. Gaidos EJ, Nealson KH, Kirschvink JL. 1999. Biogeochemistry - Life in ice-covered oceans. Science 284, 1631-3.

25. Gold, R. E., S. C. Solomon,R. L. McNutt, Jr., A. G. Santo, J. B.Abshire, M. H. Acuña, R. S.Afzal, B. J. Anderson, G. B. Andrews, P. D. Bedini, J. Cain, A. F. Cheng, L. G. Evans, R. B. Follas, G. Gloeckler, J. O. Goldsten, S. E. Hawkins III, N. R. Izenberg, S. E. Jaskulek, E. A. Ketchum, M. R. Lankton, D. A. Lohr, B. H. Mauk, W. E. McClintock, S. L. Murchie, C. E. Schlemm II, D. E. Smith, R. D. Starr, and T. H. Zurbuchen, 2000. The MESSENGER mission to Mercury: Scientific payload, Planet. Sp. Sci.

26. Green, R.O., Pieters, C., Mouroulis, P., Sellars, G., Eastwood, M., Geier, S., Shea, J. 2007. The Moon Mineralogy Mapper: Characteristics and Early Laboratory Calibration Results, Proc. Lunar Planet. Sc. XXXVIII, March 12-16, League City, Texas, 1338.

27. Haff, P.K., G. L. Siscoe, and A. Eviatar 1983. Ring and plasma - The enigmae of Enceladus. Icarus 56, 426-438.

28. Hand KP, Chyba CF, Carlson RW, Cooper JF. 2006. Clathrate hydrates of oxidants in the ice shell of Europa. Astrobiology 6, 463-82.

29. Hansen, C.J., Esposito, L., Stewart, A.I.F., Colwell, J., Hendrix, A., Pryor, W., Shemansky, D., West, R., 2006. Enceladus' water vapor plume. Science 311, 1422-1425.

30. Helfenstein, P., P.C. Thomas, J. Veverka, J.A. Burns, T. Roatsch, B. Giese, R. Wagner, T. Denk, G. Neukum, E. Turtle, V. Bray, J. Perry, J. Rathbun, C.C. Porco, 2007. Patterns of Tectonism and Polar Wander on Enceladus, Icarus, submitted.

31. Helfenstein, P., Thomas, P.C., Veverka, J., Rathbun, J., Perry, J., Turtle, E., Denk, T., Neukum, G., Roatsch, T., Wagner, R., Giese, B., Squyres, S., Burns, J., McEwen, A., Porco, C., Johnson, T.V., ISS Science Team, 2006a. Patterns of fracture and tectonic convergence near the south pole of Enceladus. Lunar Planet. Sci. XXXVII. Abstract 2182.

32. Helfenstein, P., Thomas, P.C., Veverka, J., Porco, C., Giese, B., Wagner, R., Roatsch, T., Denk, T., Neukum, G., Turtle, E., 2006b. Surface geology and tectonism on Enceladus. Eos Trans. AGU 87(52), Fall Meet. Suppl., Abstract P22b-02.

33. Helfenstein, P., Thomas, P.C., Veverka, J., Squyres, S., Rathbun, J.A., Denk, T., Neukum, G., Roatsch, T., Wagner, R., Perry, J., Turtle, E., McEwen, A.S., Johnson, T.V., Porco, C., Cassini ISS Team, 2005. Geological features and terrains on Enceladus as seen by Cassini ISS. Am. Astron. Soc. Bull. 37. Abstract 36.01.

34. Hurford, T.A., Helfenstein, P., Greenberg, R., Hoppa, G.V., 2007a. A cycloid-like rift near Enceladus' South Pole: Europa-style production by tidal stress. Lunar Planet. Sci. XXXVIII. Abstract 1844.

35. Hurford TA, Helfenstein P, Hoppa GV, Greenberg R, Bills BG. 2007b. Eruptions arising from tidally controlled periodic openings of rifts on Enceladus. Nature 447: 292-4.

36. Kargel, J., Enceladus: Cosmic gymnast, volatile miniworld. Science 311, 1389-1391, 2006.

37. Kargel, J.S., Pozio, S., 1996. The volcanic and tectonic history of Enceladus. Icarus 119, 385-404.

38. Kieffer, S. W.; Lu, X.; Bethke, C. M.; Spencer, J.R.; Marshak, S.; Navrotsky, A.; 2006. A Clathrate Reservoir Hypothesis for Enceladus' South Polar Plume, Science 314, 1764.

39. Kirschvink JL, Weiss BP. 2002. Mars, panspermia, and the origin of life: Where did it all begin? Palaeontologia Electronica 4: editorial 2: 8p.

40. Kovach, R.L., Chyba C.F. 2001. Seismic detectability of a subsurface ocean on Europa, Icarus 150, 279-287.

41. Lee, S.W., Zanolin, M., Thode, A.M., Pappalardo, R.T., Makris N.C. 2003. Probing Europa's interior with natural sound sources. Icarus 165, 144-167.

42. Lodders, K. 2003. Solar system abundances and condensation temperatures of the elements, Astrophys. J. 591, 1220-1247.

43. Lognonne, P. et al. 2000. The NetLander very broad band seismometer, Planet, Space Sci. 48, 1289-1302.

44. Manohara, H.M., M.J. Bronikowski, M. Hoenk, B.D. Hunt, P.H. Siegel 2005. High-current-density field emitters based on arrays of carbon nanotube bundles, Journal of Vacuum Science and Technology B 23, 157-161.

45. Matson DL, Castillo JC, Lunine J, Johnson TV. 2007. Enceladus' plume: Compositional evidence for a hot interior, Icarus 187, 569-73.

46. McKinnon, W. B. Mystery of Callisto: Is it undifferentiated? Icarus 130, 540-543, 1997.

47. Mix, L.J. et al. 2006. The Astrobiology primer: an outline of general knowledge, Astrobiology 6, 735-813.

48. Moore, W.B., Schubert G., 2000. The tidal response of Europa, Icarus 147, 317-319.

49. Morrison, D., Owen, T., Soderblom, L.A., 1986. The satellites of Saturn. In: Burns, J.A., Matthews, M.S. (Eds.), Satellites, Univ. of Arizona Press, Tucson, pp. 764-801.

50. Mouroulis P, Green RO, Chrien TG 2000. Design of push-broom imaging spectrometers for optimum recovery of spectroscopic and spatial information, Applied Opt. 39,13).

51. Mueller, S. and W. B. McKinnon 1988. Three-layered models of Ganymede and Callisto – Compositions, structures, and aspects of evolution, Icarus 76 437-464.

52. Neumann, G.A., Rowlands, D.D., Lemoine, F.G., Smith, D.E., Zuber, M.T. 2001. Crossover analysis of Mars Orbiter Laser Altimeter data, J. Geophys. Res. 106, 23753-23768.

53. Newman, Sarah; Buratti, B. J.; Brown, R. H.; Jaumann, R.; Bauer, J.; Momary, T. 2007. Photometric and spectral analysis of the distribution of crystalline and amorphous ices on Enceladus as seen by Cassini, Icarus, accepted.

54. Niemann, H.B. and 17 co-authors, 2005. The abundance of constituents of Titan's atmosphere from the GCMS instrument on the Huygens probe, Nature 438, 779-784.

55. Niemann, H.B., Atreya, S.K., Bauer, S.J., Biemann, K., Block, B., Carignan, G.R., Donahue, T.M., Frost, R.L., Gautier, D., Haberman, J.A., Harpold, D., Hunten, D.M., Israel, G., Lunine, J.I., Mauersberger, K., Owen, T.C., Raulin, F., Richards, J.E., and Way, S.H. 2002. The Gas Chromatograph Mass Spectrometer for the Huygens Probe, Space Sci. Rev. 104, 553-591.

56. Nimmo F, Spencer JR, Pappalardo RT, Mullen ME. 2007. Shear heating as the origin of the plumes and heat flux on Enceladus, Nature 447, 289-91.

57. Nimmo, F. and Pappalardo, R.T. 2006. Diapir-induced reorientation of Saturn's moon Enceladus, Nature 441, 614-616.

58. Nimmo, F., Schenk, P., 2006. Normal faulting on Europa: Implications for ice shell properties, J. Struct. Geol. 28, 2194-2203.

59. NRC 2003. New frontiers in the solar system: an integrated exploration strategy. Technical report, Space studies board, National Research Council, Washington DC.

60. Panning, M., Lekic, V., Manga, M., Cammarano, F., Romanowicz, B., Long-period seismology on Europa: 2. Predicted seismic response, J. Geophys. Res. 111, E12008.

61. Parkinson CD, Liang MC, Hartman H, Hansen CJ, Tinetti G, et al. 2007. Enceladus: Cassini observations and implications for the search for life. Astronomy & Astrophysics 463: 353-7.

62. Passey, Q. 1983. Viscosity of the lithosphere of Enceladus. Icarus 53, 105-120.

63. Porco, C. C. Helfenstein, P.; Thomas, P. C.; Ingersoll, A. P.; Wisdom, J.; West, R.; Neukum, G.; Denk, T.; Wagner, R.; Roatsch, T.; Kieffer, S.; Turtle, E.; McEwen, A.; Johnson, T. V.; Rathbun, J.; Veverka, J.; Wilson, D.; Perry, J.; Spitale, J.; Brahic, A.; Burns, J. A.; DelGenio, A. D.; Dones, L.; Murray, C. D.; Squyres, S., 2006. Cassini observes the active South Pole of Enceladus. Science 311, 1393-1401.

64. Rathbun, J.A., Turtle, E.P., Helfenstein, P., Squyres, S.W., Thomas, P., Veverka, J., Denk, T., Neukum, G., Roatsch, T., Wagner, R., Perry, J., Smith, D., Johnson, T.V., Porco, C.C., 2005. Enceladus' global geology as seen by Cassini ISS. Eos Trans. AGU 86(52), Fall Meet. Suppl., Abstract P32A-03.

65. Reh, K., J. Elliot, T. Spilker, E. Jorgensen, J. Spencer, and R. Lorenz 2007. Titan and Enceladus $1B Mission Feasibility Study Report. JPL D-37401B.

66. Reuter, D.C., Stern, S.A., Scherrer, J., Jennings, D.E., Baer, J., Hanley, J., Hardaway, L., A. Lunsford, S. McMuldroch, J, Moore, C. Olkin, R. Parizek, H. Reitsma, D. Sabatke, J. Spencer, J. Stone, H. Throop, J. Van Cleve, G. E. Weigle and L. A.Young, Ralph: A Visible/Infrared Imager for the New Horizons Pluto/Kuiper Belt Mission, Astrobiology and Planetary Missions. Edited by Hoover, Richard B.; Levin, Gilbert V.; Rozanov, Alexei Y.; Gladstone, G. Randall 2005. Proc. of the SPIE, 5906, pp. 433-443.

67. Ross, M. N. and G. Schubert 1989, Viscoelastic Models of Tidal Heating in Enceladus. Icarus 78, 90-101.

68. Schenk, P. M. and Moore, J. M. 2007, Impact Crater Topography and Morphology on Saturnian Mid-Sized Satellites. Lunar and Planetary Science XXXVIII, Contribution No. 1338, p.2305.

69. Schenk, P., Seddio, S., 2006. Geologic and cratering history of Enceladus. Am. Astron. Soc. Bull. 38. Abstract 18.01.

70. Schubert, G., J. D. Anderson, B. T. Travis, J. Palguta 2007. Enceladus: Present internal structure and differentiation by early and long-term radiogenic heating. Icarus 188, 345-355.

71. Shemansky, D.E., Matherson, P., Hall, D.T., and Tripp, T.M. 1993. Nature 363, 329.

72. Showman, A.P., Stevenson D.J., Malhotra R. 1997. Coupled orbital and thermal evolution of Ganymede. Icarus 129, 367-383.

73. Skelley, A.M., Cleaves, H.J., Jayarajah, C.N., Bada, J.L., and Mathies, R.A. 2006, Application of the Mars Organic Analyzer to nucleobase and amine biomarker detection. Astrobiology 6, 824-837.

74. Smith, B. A. et al. 1986. Voyager 2 in the Uranian system: Imaging Science Results, Science 233, 43-64.

75. Smith, B.A. et al. 1982. A new look at the Saturn system: The Voyager 2 images, Science 215, 504-537.

76. Smith, D. E.; Turtle, E. P.; Melosh, H. J.; Bray, V. J. 2007. Viscous Relaxation of Craters on Enceladus, Lunar and Planet, Science XXXVIII, 2237.

77. Smith, D.E. et al. 2001, Mars Orbiter Laser Altimeter: Experiment summary after the first year of global mapping of Mars, J. Geophys. Res. 106, 23689-23722.

78. Smith, D.E., Zuber, M.T., Neumann, G.A., Lemoine, F.G., Robinson, M.S., Aharonson, O., Head, J.W., Sun, X., Cavanaugh, J.F., Jackson, G.B., 2006. The Lunar Orbiter Laser Altimeter (LOLA) on the Lunar Reconnaissance Orbiter. EOS Trans. AGU, U41C-0826.

79. Spahn et al. 2006, Cassini dust measurements at Enceladus and Implications for the origin of the E-ring. Science 311, 1416-1418.

80. Spencer, J. R., J. C. Pearl, M. Segura, F. M. Flasar, A. Mamoutkine, P. Romani, B. J. Buratti, A. R. Hendrix, L. J. Spilker, R. M. C. Lopes 2006. Cassini Encounters Enceladus: Background and the Discovery of a South Polar Hot Spot. Science 311, 1401-1405.

81. Squyres SW, Reynolds RT, Cassen PM, Peale SJ. 1983. Liquid Water and Active Resurfacing on Europa Nature 301, 225-6.

82. Srama R. et al. 2006. Planet, Space Science 54,967-987.

83. Stephan, K.; Jaumann, R.; Hansen, G. B.; Clark, R. N.; Buratti, B. J.; Brown, R. H.; Baines, K. H.; Bellucci, G.; Coradini, A.; Cruikshank, D. P.; Griffiths, C. A.; Hibbitts, C. A.; McCord, T. B.; Nelson, R. M.; Nicholson, P. D.; Sotin, C.; Wagner, R. 2007. Distribution of Icy Particles Across Enceladus' Surface as Derived from Cassini-VIMS Measurements. Lunar and Planetary Science XXXVIII), Contribution No. 1338, p.1747.

84. Stern, S. A. et al. 2007. ALICE: The Ultraviolet Imaging Spectrograph aboard the New Horizons Pluto-Kuiper Belt Mission, Space Science Reviews, in press.

85. Thomas, P. C., J. Burns, P. Helfenstein, S. Squyres, J. Veverka, C. Porco, E. P. Turtle, A. McEwen, T. Denk, B. Giese, T. Roatsch, T. V. Johnson, R. A. Jacobson 2007, Shapes of the saturnian icy satellites and their significance. Icarus, in press.

86. Tian, F., A.I.F. Stewart, O.B. Toon, K.M. Larsen, L.W. Esposito 2006, Monte Carlo simulations of the water vapor plumes on Enceladus, Icarus 188, 154-161.

87. Townes, S.A. and 19 co-authors, 2004. The Mars Laser Communication Demonstration, IEEE Aerospace Conference Proceedings, vol. 2, pp. 1180-1195.

88. Verbiscer, A. J.; Veverka, J. 1994. A photometric study of Enceladus. Icarus 110, 155-164.

89. Verbiscer, A. J.; Peterson, Dawn E.; Skrutskie, Michael F.; Cushing, Michael; Helfenstein, Paul; Nelson, Matthew J.; Smith, J. D.; Wilson, John C. 2006. Near-infrared spectra of the leading and trailing hemispheres of Enceladus, Icarus 182, 211-223.

90. Verbiscer, A.; French, R.; Showalter, M.; Helfenstein, P.; 2007. Enceladus: Cosmic Graffiti Artist Caught in the Act, Science 315, 815.

91. Wahr, J.M., Zuber, M.T., Smith, D.E., Lunine, J.I., 2006. Tides on Europa and the thickness of Europa's icy shell, J. Geophys. Res. 111, doi:10.1029/2006JE002729.

92. Waite JH et al. 2004. Space Science Rev. 114, 113-231.

93. Waite, J.H., Combi, M.R., Ip, W-H., Cravens, T.E., McNutt, R.E., Kasprzak, W., Yelle, R., Luhmann, J., Niemann, H., Gell, D., Magee, B., Fletcher, G., Lunine J., and Tseng,W-L. 2006. Cassini Ion and neutral gas mass spectrometer: Enceladus plume composition and structure, Science 311, 1419-1422.

94. Webster, C.R., Sander, S.P., Beer, R., May, R.D., Knollenberg, R.G., Hunten, D.M., and Ballard, J. 1990. Tunable diode laser infrared spectrometer for *in-situ* measurements of the gas phase composition and particle size distribution of Titan's atmosphere, Appl. Opt. 29, 907-917.

95. Williams, D. J., R. W. McEntire, C. Schlemm II, A. T. Y. Lui, G. Gloeckler, S. P. Christon, and F. Gliem, Geotail energetic particles and ion composition instrument, J. Geomag. Geoelect., 46, 39-57, 1994.

96. Zimmer, C., Khurana, K.K., Kivelson, M.G., 2000. Subsurface oceans on Europa and Callisto: Constraints from Galileo magnetometer observations, Icarus 147, 329-347, 2000.

3.0 MISSION ARCHITECTURE ASSESSMENT

3.1 Technical Approach

As this is the first flagship mission architecture design study to evaluate methods for conducting scientific investigations at Enceladus, the solution space is quite broad and includes a number of candidate approaches. The approach used in this study was to conduct mission architecture designs on a few key points in that solution space and then to apply the knowledge gained to provide insight into some of the remaining points. This approach is consistent with remaining in Phase I, and at the architecture level of detail, under the Study Groundrules and was selected to maximize coverage across the solution space rather than to identify a single preferred mission concept for detailed investigation.

Before commencing mission concept design work, the mission design team performed risk reduction and fact finding studies. These studies are described in **Section 3.1.1**, and focused principally on the flight dynamics of getting to Saturn and orbiting Enceladus for a range of flight segment mass constraints. The team also consulted with experts from other NASA centers and the Department of Energy (DOE) to examine the use of:

- solar electric and chemical propulsion trajectories
- aerocapture to reduce ΔV requirements
- debris shielding
- radioisotope power systems

The team then conducted three mission point design studies (see **Section 3.2**), using the NASA/GSFC Integrated Mission Design Center (IMDC). The IMDC provides specific engineering analyses and services for mission design and provides end-to-end mission design products and parametric cost estimates. A reserve of 30% on mass, power, and data volume was held for each mission architecture concept. Propellant requirements were determined based on a dry mass that includes 30% reserve and on a ΔV that includes 10% reserve on maneuvers. An additional ΔV reserve of 500 m/s was held for Enceladus-OL and Enceladus-O concepts. With the exception of the Saturn-OL lander, all flight segment elements are designed to be single fault tolerant to credible failures. The selection of launch vehicles was limited by study Study Groundrules to Delta IV Heavy (4050H) or Atlas V 501 - 551 vehicles.

3.1.1 Risk Reduction / Fact Finding Activities

3.1.1.1 Key Challenges to Studying Enceladus

Missions to study Enceladus present some key challenges. Some are common to any mission to Saturn, and others are unique to the study of Enceladus. Those common to any mission to Saturn include designing a trajectory that will deliver the spacecraft to the Saturn system in a reasonable amount of time and with a reasonable amount of payload. Those unique to Enceladus include the large ΔV required once in the Saturn system to either orbit or land on Enceladus. Alternatively, they include methods to mitigate that large ΔV at the expense of adding to mission duration and life cycle cost. They also include methods to protect the spacecraft while it samples the plume near the Enceladus south pole. Additionally, planetary protection considerations become important not only for disposal of landers left on Enceladus, but also for orbiters which may impact Enceladus. The same is potentially true for boosters which separate between Titan and Enceladus and which may impact other icy moons within the Saturn system.

Risk reduction analyses were conducted prior to initiating mission architecture design studies to help address some of these challenges. These analyses included: a) evaluation of inner planet gravity assists enroute to Saturn, b) the use of Solar Electric Propulsion (SEP) as well as chemical propulsion trajectories, c) the use of Saturn moons between Titan and Enceladus and aerocapture to reduce the ΔV required to either orbit or land on Enceladus, d) the viability of a free-return trajectory for a sample return mission, and e) requirements for debris shielding.

The evaluation of these risks identified further considerations. The use of gravity assists at Venus drives the spacecraft thermal system, and the use of gravity assists at Earth with a spacecraft that uses a radioisotope power supply imposes special safety constraints. Also, the extended duration between launch and the start of science operations resulting from the use of multiple gravity assists drives mission reliability. Additionally, for architectures that include orbiting Enceladus (a small moon), the characterization of the gravitational field of Enceladus is a challenge as many of the orbits about Enceladus are significantly perturbed by the size and proximity of Saturn. The internal density variations of Enceladus and their impact on orbit stability will not be well understood until an orbiter arrives at Enceladus. And, a landing on Enceladus must be able to be conducted in a fully autonomous manner, which means the lander must be able to identify and react to surface hazards as it approaches the surface.

3.1.1.2 Trajectory Work

A direct trajectory from Earth to Saturn (about 1.4 billion km, or 9.6 AU, from the Sun) requires a C_3 from the launch vehicle of 105.9 km^2/s^2. The total lift capability of the largest launch vehicles identified in the study Study Groundrules to this C_3 is under 500 kg. As this capability is well below that required for this mission, other techniques are required to define a trajectory that can deliver a capable mission to Enceladus. Basic planetary and natural satellite data are shown in **Appendix C**.

3.1.1.2.1 Gravity Assists to Saturn

Gravity assists using other planets can be used to provide the needed velocity to get to Saturn at the cost of additional mission time. Two approaches for gravity assists to Saturn were selected for this study. The first uses a single Earth flyby in conjunction with SEP. The second uses a much lengthier Venus-to-Venus-to-Earth-to-Earth-to-Saturn (VVEES) trajectory in conjunction with chemical propulsion.

3.1.1.2.1.1 SEP Trajectories

With assistance from NASA Glenn Research Center (GRC), the team considered a number of SEP parameters when evaluating candidate trajectories, including the number of operating ion engines (1, 2, or 3) + 1 redundant engine, the solar array power available (20, 25, 30, and 35 kW), the desired transit time to Saturn (6.5, 7.0, and 7.5 years), the Earth flyby altitude (1000 km or 2000 km), the net mass delivered to the vicinity of Saturn (not into Saturn orbit), and the system size. The configuration selected for study was the 3+1, 25 kW SEP module with a 7.5 year transit time and a 1000 km Earth flyby.

In this trajectory, the spacecraft departs Earth in March 2018 into a heliocentric orbit as shown in **Figure 3.1.1-1**. The SEP module thrusts almost continuously to increase the apoapsis of this heliocentric orbit beyond the radius of the Mars orbit. Approximately two years after launch, the spacecraft executes a single flyby of Earth with the SEP module still providing thrust. The amount of thrust varies, as solar power varies with distance from the Sun. Once power drops below the point where the SEP is effective (occurs in early 2021, 1024 days after launch), the SEP module is jettisoned.

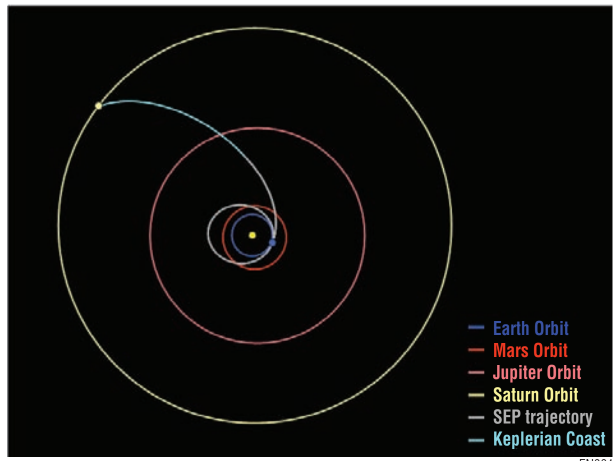

Figure 3.1.1-1: Solar Electric Propulsion Trajectory with Earth Gravity Assist

3.1.1.2.1.2 Chemical Propulsion Trajectories

The most promising trajectories for this study for designs using all-chemical propulsion involve VVEES cases in 2018, 2020, 2021 and 2023 and VEES cases in 2015, 2016, 2018, 2019, 2022, and 2023. VEES trajectories were discounted due to their higher C_3 requirements. **Figure 3.1.1-2** depicts the VVEES trajectory used for the two all-chemical propulsion mission design cases studied. The intermediate period between consecutive Earth flybys is about four years, and the period between consecutive Venus flybys is about one year. It is worth noting that while a Venus-to-Earth-to-Earth-to-Jupiter-to-Saturn (VEEJS) trajectory becomes available in 2015, it was not used for this study as there was no practical backup launch opportunity. With the synodic period between Jupiter and Saturn being 19.8 years, the next launch opportunity for this trajectory occurs in 2035. Gravity assist trajectories that end at Jupiter (e.g,. VEEJ) were discounted due to the high ΔV required from a deep space maneuver to continue on to Saturn.

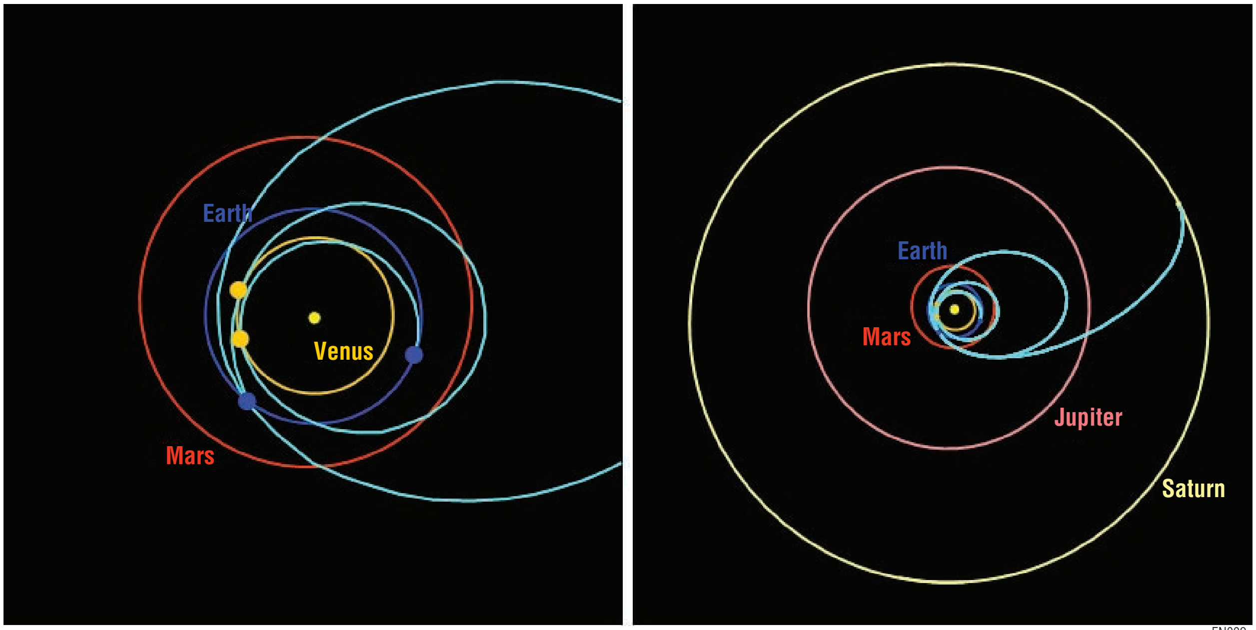

Figure 3.1.1-2: Chemical Propulsion Trajectory with Multiple Venus and Earth Gravity Assists

Specific altitudes and timing of the inner planet flybys along with the launch window considerations are discussed in **Section 3.3.3.1.1**.

3.1.1.2.2 Saturn Orbit Insertion and Gravity Assists within the Saturn System

For this study, a Saturn capture approach similar to that of the Cassini mission was employed, i.e., to approach Saturn as closely as possible from the interplanetary trajectory for maximum gravity assist. In general, the most efficient capture scenario involves applying a deceleration at periapsis to capture to as high an apoapsis as is practical (see **Figure 3.1.1-3**). Often a modest acceleration is applied at apoapsis to raise periapsis to some convenient distance. In support of the navigation, the mission uses ranging on all DSN contacts. Delta Differenced One-Way Ranging (DDOR) and optical navigation using the science instruments (not used during propulsive events) are used to refine the targeting maneuvers for the gravity assists. Updated spacecraft and natural satellite ephemerides will be uploaded as needed, based on new solutions propagated on the ground to reduce targeting uncertainties.

In general, this approach tends to optimize efficiency by minimizing the capture ΔV needed at both periapsis and apoapsis. For the Cassini mission, this approach was employed with the addi-

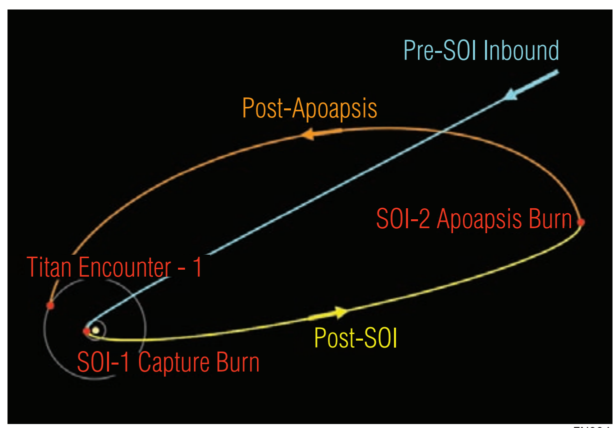

Figure 3.1.1-3: Approach and Saturn Capture Sequence for Enceladus Mission

tion of a few small burns to target an encounter with the moon Titan, the destination of the sequence.

A similar approach is used for the Enceladus mission. Further, since the only moon of any appreciable size in the Saturn system is Titan, Titan is the destination of the capture sequence. The differences for the Enceladus mission lie in the small interim maneuvers used to target the Titan encounter.

The Enceladus-O and Enceladus-OL mission designs used an approach radius of 82,000 km (very similar to Cassini) to reduce the ΔV required for Saturn orbit insertion (SOI). The Saturn-OL mission design used a more conservative approach radius of 210,000 km. In each case, the spacecraft coasts to apoapsis and performs a second maneuver to raise periapsis to target Titan and to settle the spacecraft into the plane of the Saturn system. Allowance is made in the ΔV budget for the likelihood of a small targeting burn after this second maneuver to insure the desired encounter with Titan occurs.

From there, a series of four gravity assist passes (see **Figure 3.1.1-4**) at Titan reduce the apoapsis of the Saturn orbit from about 204 Saturn radii to an orbit with a 16:31 resonance with Titan; that is to say the spacecraft orbital period is 16/31 of the Titan orbital period (or alternatively, for every 31 spacecraft orbits there are 16 Titan orbits). In this way, over the time the spacecraft has executed one complete orbit of Saturn, Titan will have completed two orbits and be back in position for the next gravity assist. This process is repeated from the 2:1 resonance to a 1:1 resonance to a 2:3 resonance down to a 16:31 resonance with the periods shown below.

This last orbit is important since it is not only in a 16:31 resonance with Titan, but also is in very nearly a 6:1 resonance with Enceladus. Setting apoapsis outside the Titan orbit radius and periapsis slightly outside the Enceladus orbit radius in this resonance means that both Titan and Enceladus are accessible during subsequent orbits; Titan for gravity assists and Enceladus for scientific observations.

At this point, the spacecraft is in a 1.31×10^6 km x 257×10^3 km orbit about Saturn with a period of 8.22 days. This places periapsis higher than the Enceladus orbit radius of 238×10^3 km. In this orbit, the relative locations of Enceladus and the spacecraft remain constant, but Enceladus is not yet in the vicinity of the spacecraft at spacecraft periapsis. Next, a small burn is performed which reduces periapsis and causes the orbit to lose resonance with both Enceladus and Titan. Being slightly out of resonance, the relative position of Enceladus at spacecraft periapsis begins to drift. This condition is maintained until Enceladus 'moves' into a position where it can be targeted. Another small burn is then performed to put the spacecraft on a path that will encounter Enceladus at an altitude of approximately 200 km for the start of the mapping flybys. At that time, apoapsis is raised to approximately 1.33×10^6 km, which restores resonance between the spacecraft and both Enceladus and Titan, and the mapping

02:01 orbit	Period = 31.89 days
01:01 orbit	Period = 15.94 days
02:03 orbit	Period = 10.63 days
16:31 orbit	Period = 8.22 days

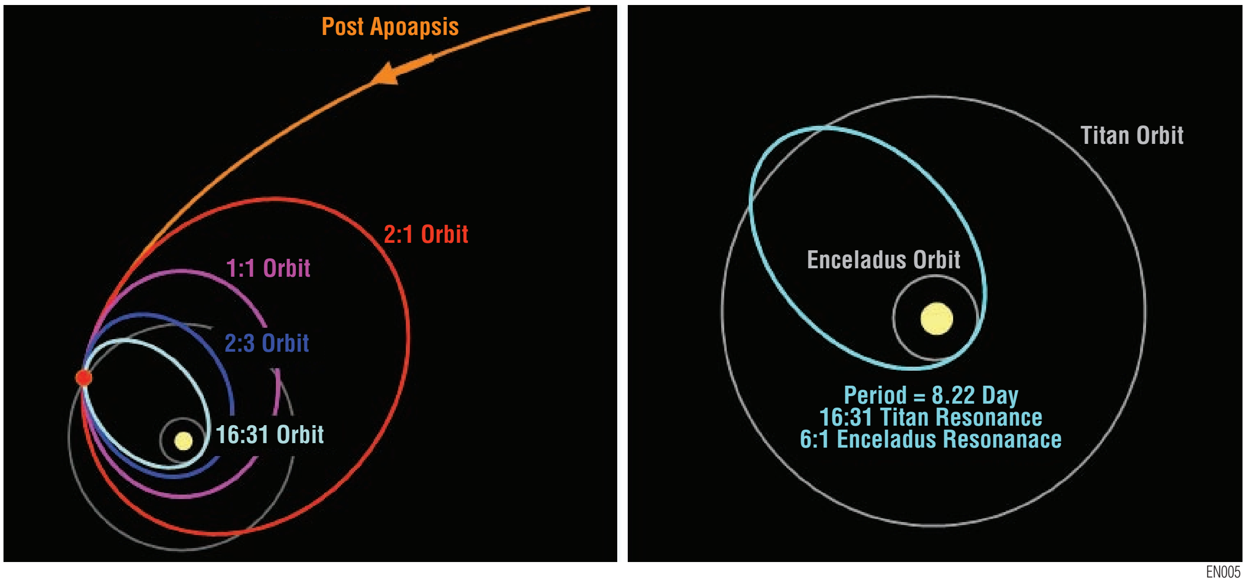

Figure 3.1.1-4: Multiple Resonant Orbits for Titan and Titan/Enceladus

flybys are initiated. The velocity at periapsis in this 8.22 day mapping orbit is ~16.4 km/s, which means the velocity relative to the Enceladus circular orbit velocity (~12.6 km/s) is about 3.8 km/s.

In order to orbit Enceladus (or to land), this relative velocity must be cancelled. With chemical propulsion, this requires significant propellant mass. Another method exists, however, in using Saturn's lesser moons (Rhea, Dione, Tethys) between Titan and Enceladus to reduce orbit energy. **Figure 3.1.1-5** shows these moons within the Saturn system. The Enceladus-O mission design uses a gravity assist from Rhea, and the Enceladus-OL mission design uses gravity assists from both Rhea and Dione.

In both the Enceladus-O and Enceladus-OL missions, Titan flybys lower periapsis to Rhea, instead of to Enceladus. Flybys of Rhea lower the apoapsis (initially at Titan) such that it becomes periapsis at either Enceladus (for Enceladus-O) or Dione (for Enceladus-OL). **Figures 3.1.1-6A** and **3.1.1-6B** depict this sequence for Enceladus-OL. In the former case (Enceladus-O), circularizing at Enceladus from the Rhea/Enceladus elliptical orbit saves a ΔV of ~1.6 km/s at a cost of 2.5 additional years of mission time. In the latter case (Enceladus-OL), the 'walkdown' is continued as flybys at Dione lower apoapsis (initially at Rhea) to become periapsis at Enceladus. Circularizing at Enceladus from the Dione/Enceladus elliptical orbit saves a total ΔV of ~2.1 km/s at a cost of adding one additional year (relative to the 2.5 years added by using Rhea). Alternatively, when in the Rhea/Dione elliptical orbit, the walkdown could be continued using Tethys before circularizing at Enceladus to save another ~0.4 km/s at a cost of an additional 1.5 years. In **Figures 3.1.1-6A** and **3.1.1.6B**, the color coding is as indicated in **Figure 3.1.1-5**.

3.1.1.2.3 Free Return Trajectories

A sample return mission that used a "free return" to Earth was evaluated. It included one pass by Saturn and through the Enceladus plume in such a way that the spacecraft is put on a path that

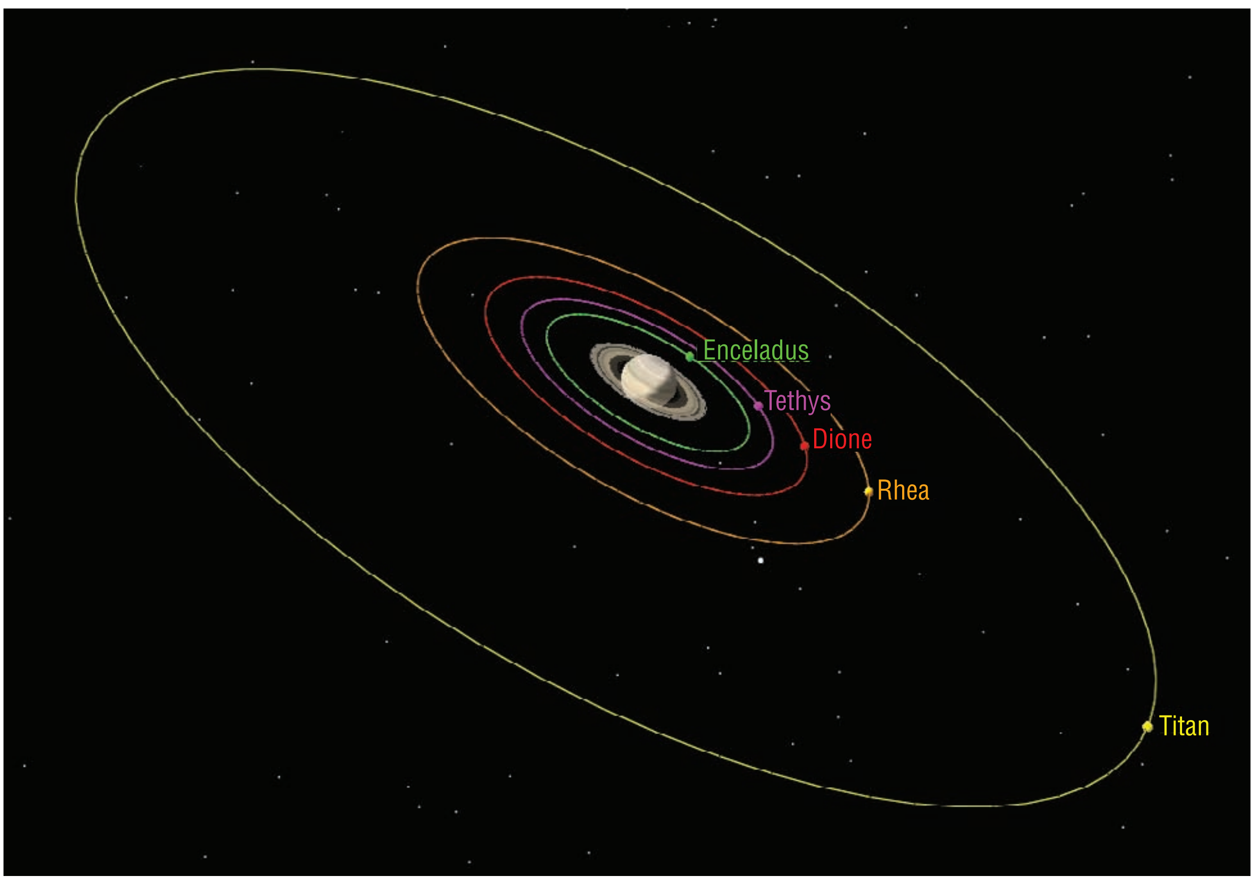

Figure 3.1.1-5: Key Moons in the Saturn System between Titan and Enceladus

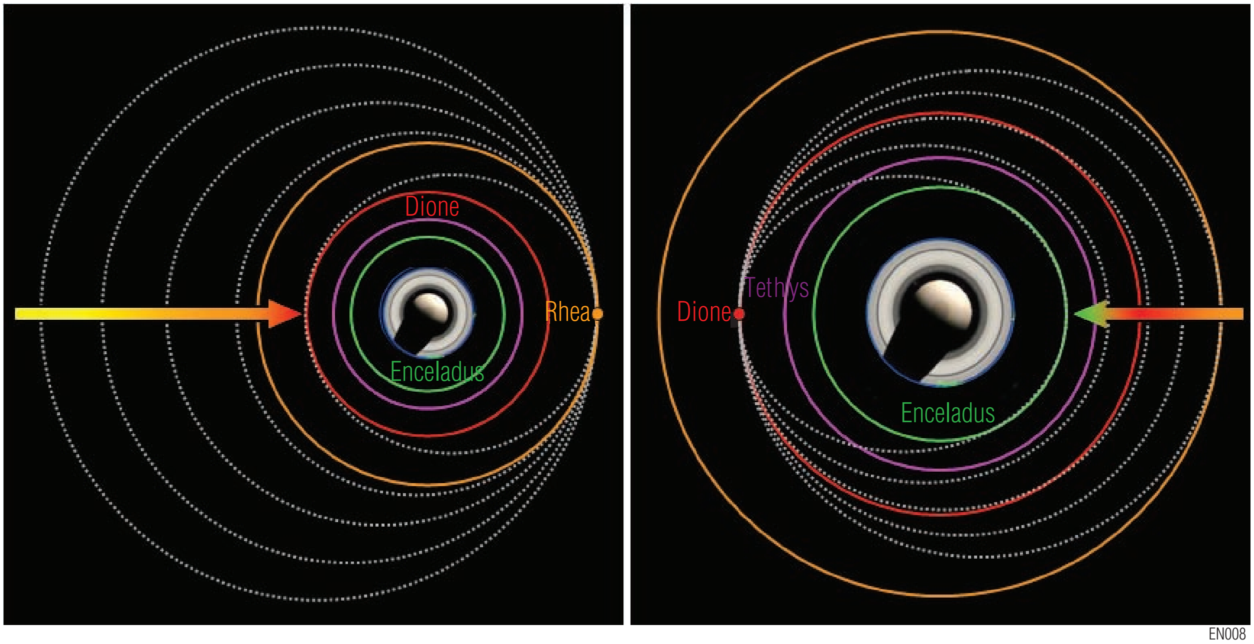

Figure 3.1.1-6A: Using Gravity Assist at Rhea to Set Periapsis at Dione
Figure 3.1.1-6B: Using Gravity Assist at Dione to Set Periapsis at Enceladus

returns it directly to Earth. Assuming apoapsis of the transfer ellipse out to Saturn is further from the Sun than Saturn, there are four possible encounter strategies (for the Hohmann transfer case, this reduces to two). For Type I encounters, where the spacecraft encounters the planet before it reaches heliocentric apoapsis, the spacecraft can pass either in front of or behind the planet. The same two options exist for the Type II encounter, where the spacecraft encounters the planet after it reaches heliocentric apoapsis. Of these four possibilities, only two provide a possible free return to Earth.

The only realistic possibility of a free return mission (the third of four cases) is depicted in **Figures 3.1.1-7A and B**, but it takes approximately 25.4 years which is likely to be unacceptably long. The Enceladus encounter happens in the same direction as Enceladus' orbital motion, resulting in an acceptable relative velocity of 6.86 km/s. The trajectory takes as long to return to the vicinity of Earth as it took to travel to Saturn, approximately 12.7 years. Upon arrival at Earth, the V_{hp} (the hyperbolic excess velocity on arrival at the planet, in this case Earth) is about 10.7 km/s, which translates to a velocity of about 15.4 km/s (neglecting the relative velocity of the atmosphere due to the Earth's rotation) if an Earth periapsis radius of 190 km altitude were targeted. As a point of reference, the Stardust sample return capsule entered Earth's atmosphere at 12.9 km/s. Analysis to optimize the entry trajectory was not performed.

The other possible free return trajectory requires the spacecraft to encounter Enceladus in the opposite direction from Enceladus' orbit. This results in an encounter speed of over 32 km/s, far above the maximum of 10 km/s set by the anticipated capability of the aerogel that would be used to capture plume particles from Enceladus.

Sample return missions were not investigated further. The long mission lifetime and the single opportunity for sample collection were the principal reasons making this option significantly less attractive than others.

3.1.1.3 Aerocapture

With assistance from NASA Langley Research Center (LaRC), the Enceladus team evaluated aerocapture as a method to achieve some of the ΔV reduction needed in approaching Enceladus from an orbit about Saturn. The team evaluated what orbital ΔV's could be affected by aerocapture, how aerocapture compared to using chemical propulsion to reduce ΔV, and other considerations involved.

Case 3: Type II Transfer, Pass in Front Saturn

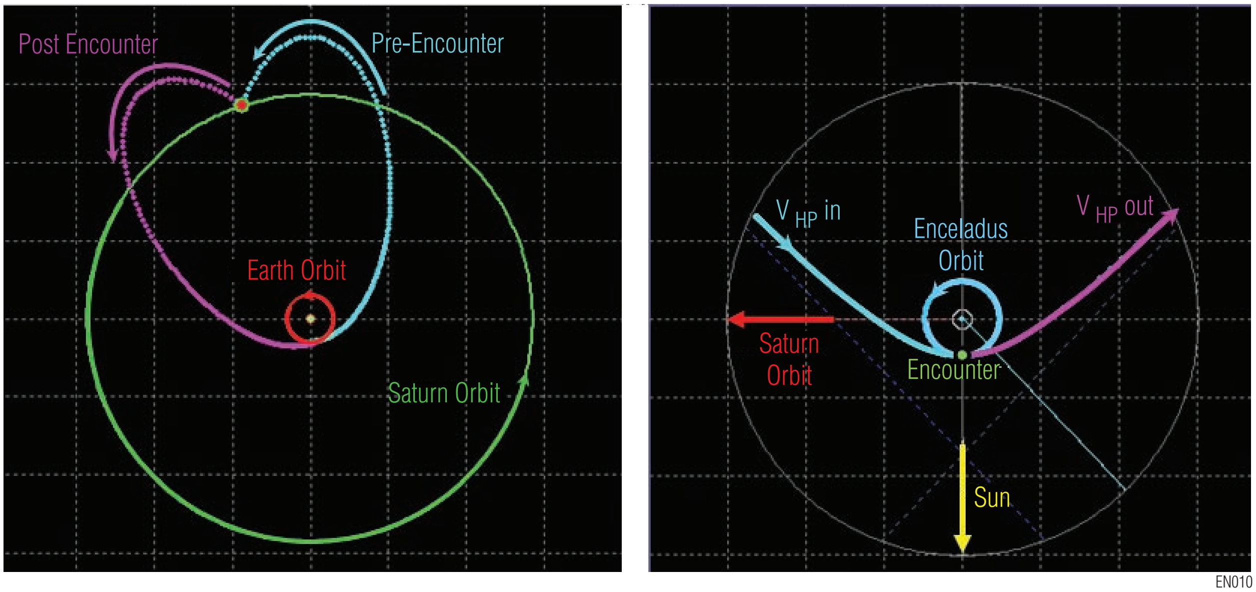

Figure 3.1.1-7A: Case 3 Trajectory in the Heliocentric Frame
Figure 3.1.1-7B: Case 3 Encounter in the Saturn Centered Frame

There are two bodies in the Saturn system with enough atmosphere to permit aerocapture. One of these is Saturn itself and the other is Titan.

Using Saturn on arrival (Options I and II in **Figures 3.1.1-8A** and **3.1.1-8B**, respectively) requires entering the atmosphere to slow the spacecraft down enough to enter into orbit about Saturn. If the spacecraft is to enter into a Saturn orbit with a high apoapsis (Option I), which minimizes the ΔV required to raise periapsis to Enceladus, aerocapture (denoted by yellow dot) using Saturn must reduce spacecraft velocity by about 1 km/s. A single Saturn flyby is used to avoid hazards associated with multiple ring plane crossings. A ΔV burn (denoted by a red dot) at apoapsis would be needed to raise periapsis to the Enceladus radius. An additional ΔV burn to reduce apoapsis would be needed to circularize at the Enceladus radius. If instead, an apoapsis near Titan is desired (Option II), which makes Titan available for subsequent gravity assists or aerocapture, a velocity reduction of 1.7 km/s is needed from Saturn. A ΔV burn would be needed to raise periapsis to the Enceladus radius. Additionally, a ΔV burn would be needed to circularize at Enceladus.

Figures 3.1.1-9A and **3.1.1-9B** illustrate the use of Titan's atmosphere for aerocapture upon arrival. Option III shows an approach that targets periapsis at Enceladus. A ΔV burn would be needed to lower apoapsis from the Titan radius to circularize at the Enceladus radius. Option IV shows an approach that targets periapsis at Saturn, and then uses Saturn aerocapture to target apoapsis at Enceladus. A ΔV burn would be needed to raise periapsis to circularize at the Enceladus radius.

The results of this study show using aerocapture at either Saturn or Titan can potentially save from 1 - 1.7 km/s. The orbits that could be achieved either have apoapsis near Titan and periapsis near Enceladus, or apoapsis near Enceladus and periapsis near Saturn. The additional ΔV required for each of these cases is on the order of 4 km/s to either orbit or land on Enceladus. Previous studies (ref. (a)) have shown an aeroshell can add about 40% to the dry mass of the vehicle. Since the aeroshell would be jettisoned prior to conducting any large ΔV burns, use of an aeroshell could provide an overall mass savings through reducing required propellant. This savings diminishes as the remaining ΔV required from the propulsion system decreases. Based on discussions with NASA/LaRC, these mass benefits are balanced by increases in design and operational complexity, as spacecraft equipment (communications, power, thermal, etc.) must operate while packaged within an aeroshell for the duration of the mission up through the aerocapture maneuver. From a risk

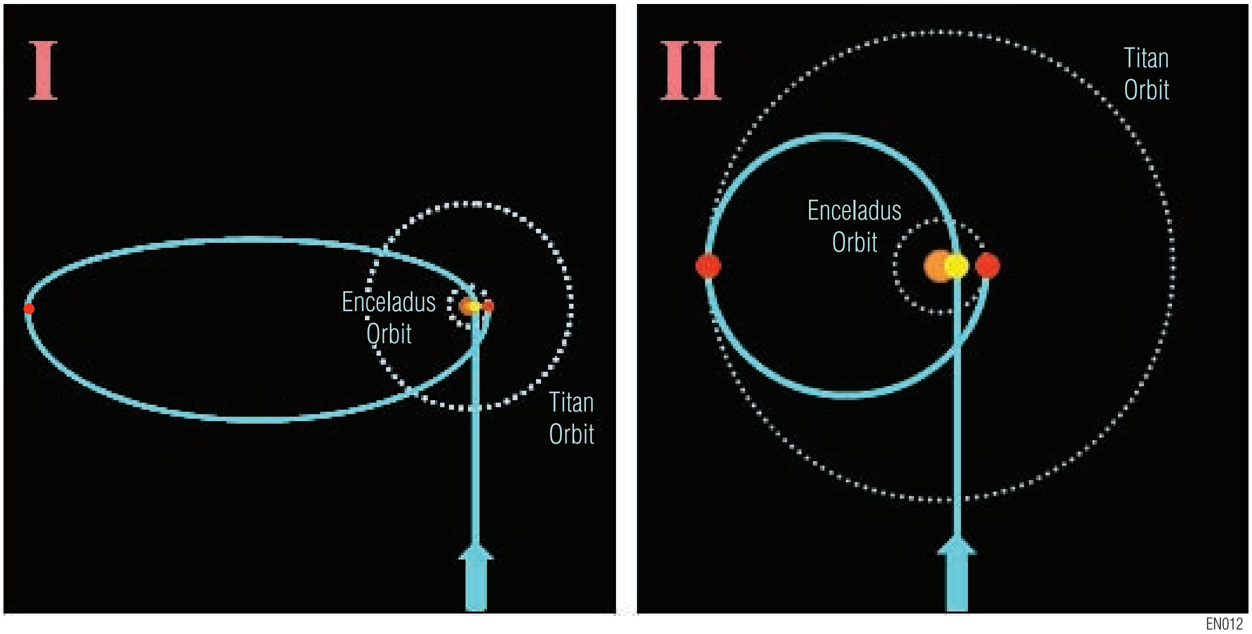

Figure 3.1.1-8A: Saturn Aerocapture to High Apoapsis
Figure 3.1.1-8B: Saturn Aerocapture to Titan Apoapsis

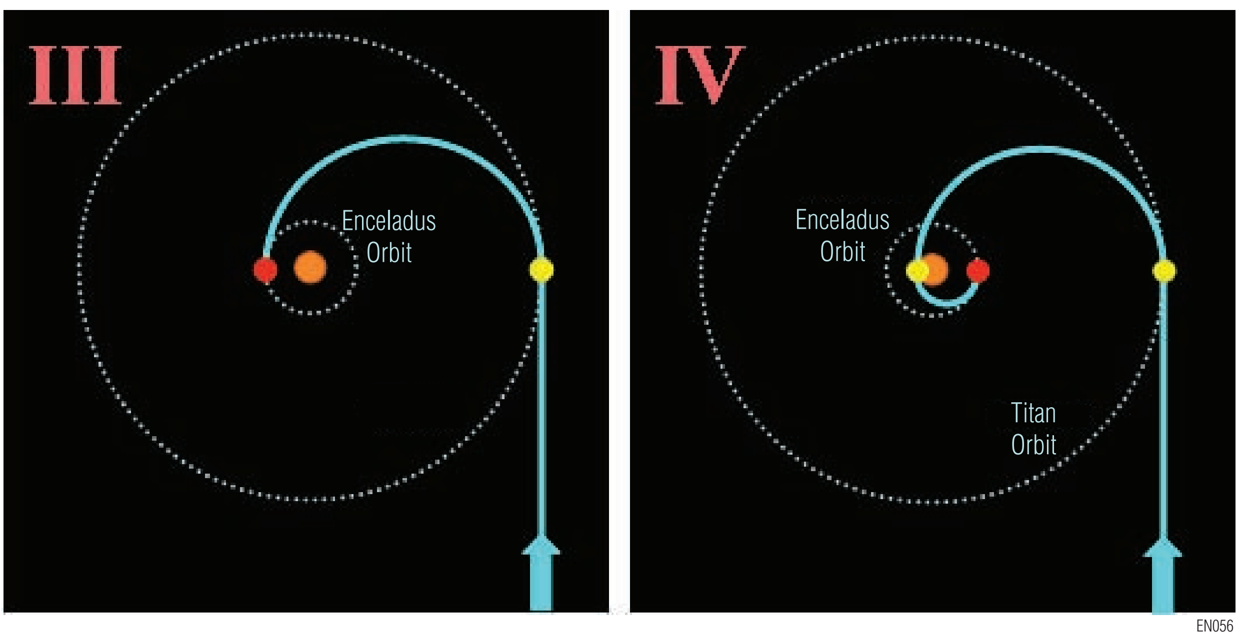

Figure 3.1.1-9A: Titan Aerocapture to Enceladus Periapsis
Figure 3.1.1-9B: Titan Aerocapture to Saturn Periapsis

perspective, since Enceladus has no atmosphere and aerocapture is not central to the mission at Enceladus, it is not evident that adding a unique and critical aerocapture maneuver along with the attendant design complexities is warranted. Gravity assists with a moderate increase in mission duration can provide an equivalent benefit.

3.1.1.4 Particle Shielding

One of the goals of this mission is to perform *in-situ* sampling of the plume arising from the south polar region of Enceladus. The particles in this plume represent a risk to the spacecraft and instruments, and these components will need to

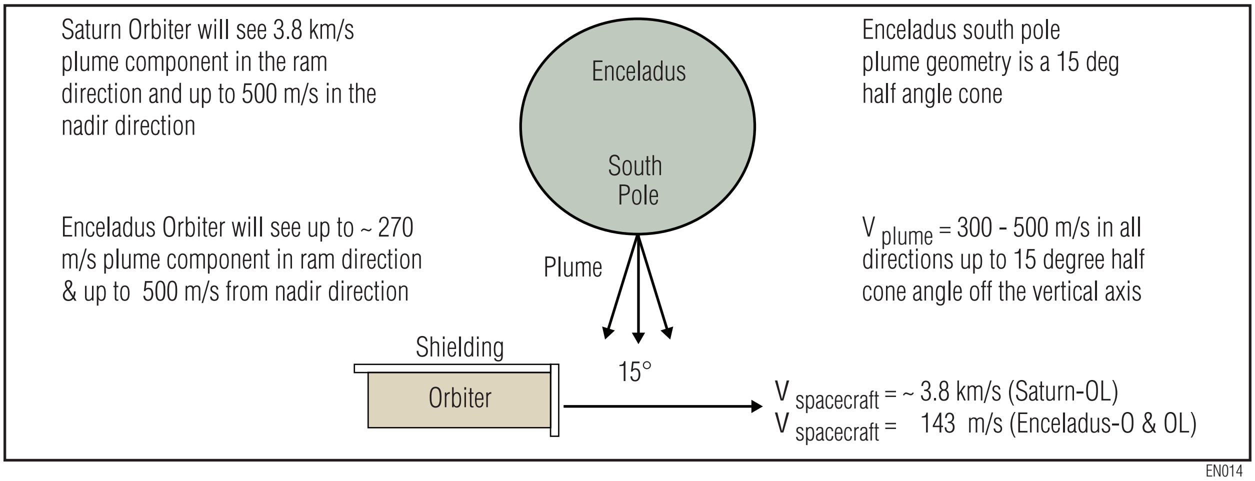

Figure 3.1.1-10: Enceladus Plume Geometry and Impact Velocity

be protected. A representation of the plume is shown in **Figure 3.1.1-10**.

The current characterization of the plume is based on a few Cassini flybys; subsequent observations should provide better estimates of the plume parameters (see **Section 2.5**). The plume is assumed to be made up of primarily water ice particles. Extrapolation based on Cassini results indicates particles may be as large as 2 mm in diameter. The velocity of some of the particles exceeds the Enceladus escape velocity of 241 m/s.

The Saturn orbiter velocity of 3.8 km/s through the plume results in a plume transit time of just under 30 seconds at an altitude of 200 km. The Saturn orbiter makes 50 flybys of Enceladus, but only 12 are assumed to go through the plume. For the Enceladus orbiting concepts, the spacecraft orbits Enceladus and passes through the plume at a much slower speed of 143 m/s giving a plume transit time of about six minutes at an altitude of 100 km. The Enceladus orbiters only go through the plume during the two 24-hour polar orbit campaigns. For the shielding analysis, a total of 10 plume passages was assumed (subsequent mission design work discussed in **Sections 3.3** and **3.4** resulted in 12 plume passages).

The particle shielding analysis was performed by the NASA Johnson Space Center (JSC) lead for hypervelocity impact shielding, ref. (b). Plume characteristics were used to estimate the particle hazard and to recommend protection methods. For the Saturn orbiter, a Whipple shield (composed of two layers of material separated by a gap) was recommended. Per ref. (b), Whipple shields can be effective for particles with relative velocities above 2 km/s. The particle hits the first layer at high velocity and shatters, and the second layer protects the spacecraft from the particle's debris. For the Saturn orbiter, the recommended Whipple shield protects against particles up to 0.65 mm in diameter. The shields used have 0.15 mm Kevlar-epoxy facesheets with a 6.4 mm aluminum honeycomb core for a 97% probability of survival (which is defined as no penetration of the shield). The mass per unit area is ~1.3 kg/m^2, including the support structure.

The relative velocity for the particles encountered by the Enceladus orbiter concepts is too low to shatter the particles, so a Whipple shield is not appropriate. Instead a single layer shield of 0.74 mm Kevlar-epoxy is used to protect from particles up to 2.0 mm in diameter. Kevlar-epoxy shielding was selected for a 97% probability of survival. The mass per unit area is ~1.3 kg/m^2, including the support structure.

Although particle impact velocities are much less for the Enceladus orbiter than for the Saturn orbiter, the particle fluence per plume passage is much larger since the Enceladus orbiter velocity is smaller than the particle velocity. For a power-law particle size distribution (a relationship quantifying that there are significantly more small particles than large particles), this results in the largest particle likely to impact the Enceladus orbiter being larger than that for the Saturn orbiter. This analysis did not account for altitude differences between the two concepts.

In each of the three concept designs, shielding was included to protect the spacecraft and instrument components, and the mass of the shielding was included in the thermal mass estimates. The shielding for the Saturn orbiter is on components that face in the velocity direction; for the Enceladus orbiter, the shielding is also on the side (nadir) of the orbiter that faces the plume.

3.2 Architecture Trade Space

The trade space for this architecture study is notionally depicted in **Figure 3.2-1**.

It includes candidate architectures such as:

1. Enceladus orbiter with soft lander with chemical propulsion (Enceladus-OL)
2. Enceladus orbiter with chemical propulsion (Enceladus-O)
3. Saturn orbiter with soft lander with SEP (Saturn-OL)
4. Enceladus orbiter that lands with chemical propulsion
5. Enceladus orbiter using SEP
6. Enceladus orbiter with hard impactor(s)
7. Saturn orbiter with soft lander using chemical propulsion and gravity assists
8. Saturn orbiter with soft lander using SEP and more Saturnian moon flybys
9. Saturn orbiter with hard impactor(s)
10. Sample return with or without orbiter
11. Dual launch vehicle – loosely coupled orbiter/lander
12. Dual launch vehicle – Low Earth Orbit (LEO) assembly

The first three concepts above were selected for initial concept development for their high science value (see **Table 2.4.6-1**) and for their ability to provide the most insight into the remaining architectures identified. A summary of these architectures is provided in **Appendix E (Table E-1)**. Results suggest these architectures merit additional investigation. Some of the remaining architectures (e.g., single flybys) in the solution space were considered to be of lower scientific value and were not considered further.

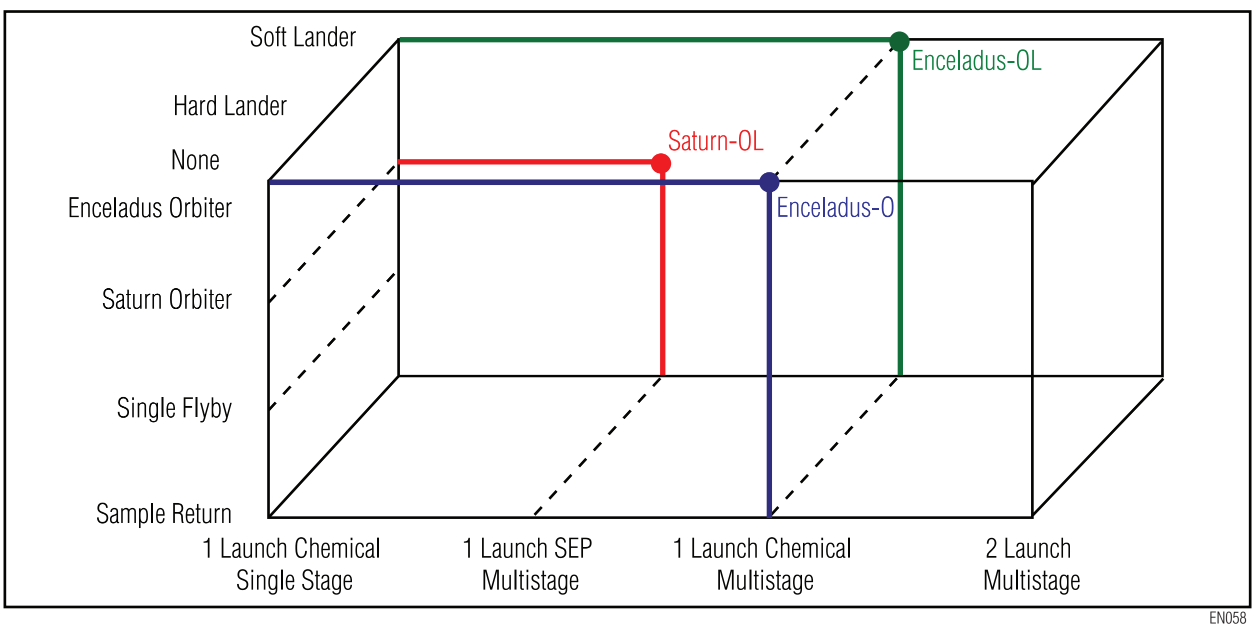

Figure 3.2-1: Enceladus Flagship Study Architecture Trade Space

3.3 Enceladus Orbiter with Soft Lander (Enceladus-OL)

3.3.1 Enceladus-OL Architecture Overview

The Enceladus-OL mission includes an Enceladus orbiter and soft lander and its purpose is to provide for more in-depth mapping of the Enceladus surface and for more encounters with the south polar plume than are possible with the Saturn orbiter concept evaluated in the Saturn-OL mission design discussed in **Section 3.5**.

Relative to the Saturn-OL orbiter's orbit, an orbit about Enceladus requires a reduction in orbital velocity of 4.0 km/s (~3.8 km/s plus associated targeting maneuvers). This velocity reduction is associated with the difference in the periapsis velocity of the spacecraft in its elliptical orbit around Saturn and the velocity of Enceladus in its circular orbit around Saturn. The orbit of the spacecraft around Saturn in the Saturn-OL mission design is highly elliptical with apoapsis radius (~1.33 x 10^6 km) just beyond Titan radius and periapsis radius (~238 x 10^3 km) about 200 km inside Enceladus's radius. As discussed in **Section 3.1.1.2.2**, the velocity at periapsis in this orbit is approximately 16.4 km/s, which is 3.8 km/s faster than the 12.6 km/s velocity of Enceladus in its circular orbit around Saturn. Once the spacecraft velocity is matched with that of Enceladus (i.e., not moving with respect to Enceladus), a small additional ΔV of about 0.2 km/s is needed to match the required velocity of the spacecraft at the desired orbit altitude and achieve the desired inclination.

The Enceladus-OL concept includes a three stage flight segment, a ground segment for communications and mission and science operations and data archival, and a launch segment. The flight segment is described in **Section 3.3.3**. Chemical propulsion is used for the entire flight segment with dual mode bi-propellant N_2O_4 / hydrazine in the booster and orbiter, and monopropellant hydrazine in the lander. The ground segment consists of the NASA Deep Space Network (DSN) 70-m equivalent X/Ka band communications ground station (as allowed in the Study Groundrules), a flight dynamics and navigation facility, a mission operations center, a science operations center, and a science products storage facility as shown in **Figure 3.3.3-1**.

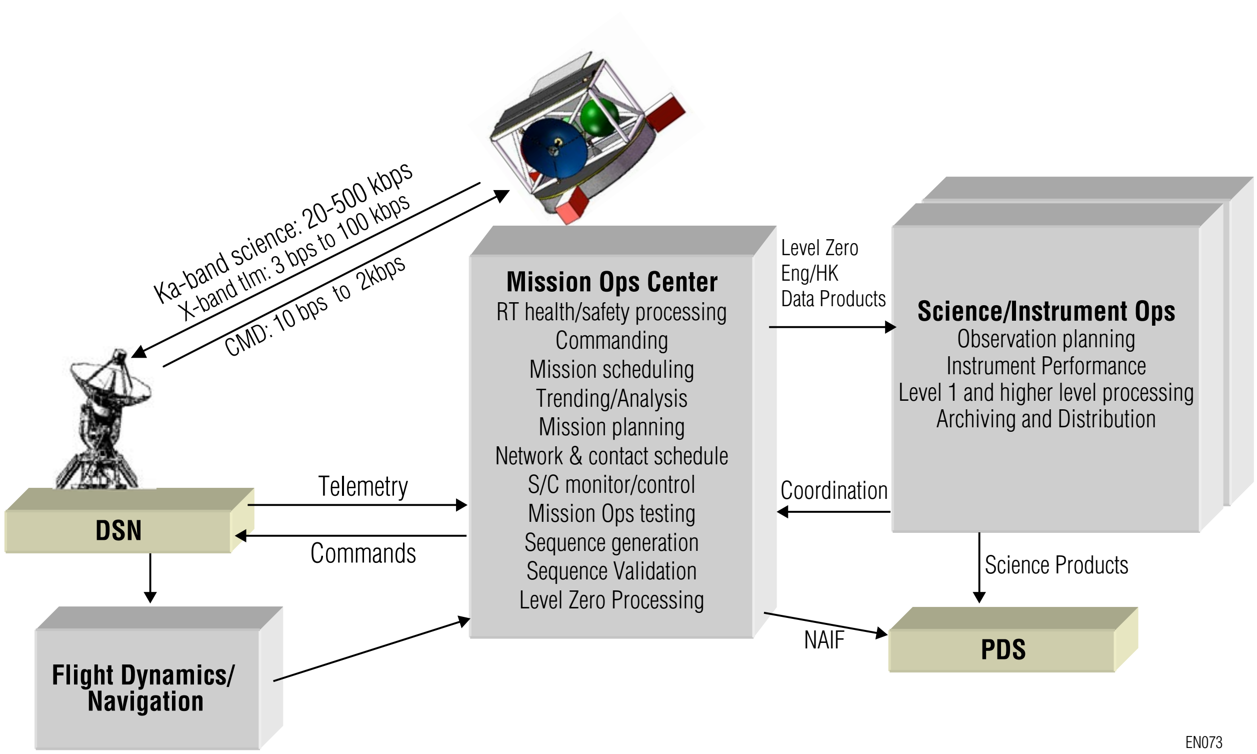

Figure 3.3.3-1: Ground Segment Functional Architecture

The launch segment consists of a single Delta IV Heavy (4050H-19) vehicle (see **Figure 3.3.3-2**), and associated launch and range facilities supporting operations at space launch complex 37 (SLC-37) at Cape Canaveral Air Force Station. Interfaces with the launch segment are defined in ref. (c), and launch vehicle performance with launch date specific declinations was provided by ref. (d). The Delta 4050H-19 is used for this mission concept since it is the only launch vehicle of those identified by the Study Groundrules that has sufficient lift capability for Enceladus-OL.


EN015

Figure 3.3.3-2: Delta IV Heavy Launch Vehicle at SLC-37

3.3.2 Enceladus-OL Science Investigation

All of the science goals shown in **Table 2.1.1-1** can be fully addressed by combining an Enceladus orbiter with a robust surface package, with the exception of Saturn System Interactions (a third priority goal), as shown in **Table 2.4.6-1**. The close altitude and slow velocity of the orbiter relative to the surface allow for intact capture and analysis of plume particles and gases, complete global mapping, detailed gravity and magnetic field measurements, and tidal flexing measurements that can be indicative of interior structure. The landed package allows for seismometry and detailed *in-situ* surface chemistry analyses. The science drivers listed below are met by the strawman payload. A lander seismometer would need a method of surface coupling (in this case, by placement on a lander foot), and anchoring might be required to prevent the surface sampler from pushing the lander off of the surface, given Enceladus' weak gravity. **Tables 3.3.2-1** and **3.3.2-2** show the Enceladus-OL orbiter and lander strawman payload suites.

Orbiter Science Drivers:

- Global mapping visible, near-IR and thermal IR
  - Understand tectonics, cryovolcanism, surface processes
- Determine Love numbers with laser altimetry and Doppler tracking, and determine interior conductivity with magnetic sounding
  - Constrain interior structure, and presence or absence of a global ocean
- *In-situ* analysis of plume gas and dust components
  - Understand cryovolcanic processes, organic chemistry
- Enceladus orbit enables:
  - Precise measurements of gravity field and tidal deformation
  - Robust magnetic sounding for a subsurface ocean
  - Complete and consistent global morphological, compositional, and thermal mapping
  - Low-speed plume sampling opportunities for more detailed analysis of more pristine plume samples
  - Good communication relay for more detailed and robust surface observations

Lander Science Drivers:

- Detailed *in-situ* analysis of surface chemistry (esp. organic)
  - Composition, cryovolcanism, habitability, presence of key amino acids and biotic compounds?

Table 3.3.2-1: Enceladus-OL Strawman Orbiter Payload

Instrument	Mass (kg)	Power (W)	Duty Cycle (in Enceladus Orbit)	Dimensions L x W x H (or L x dia.) (cm)	Data Rate (kbps)	Notes on Downlink	Preferred Location and Aperture Pointing Direction	Req'd Pointing Accuracy (arc sec)	% New Development Req'd	Precursor Instrument
Thermal Mapper	11	14	80%	55x29x37	5		Nadir		~50% (longer wavelength capability)	THEMIS
Visible/Near IR Mapper	10	6	50% (dayside only)	50x50x30	2338	10:1 compression (to be done by C&DH)	Nadir, radiator with sky view		~30% (longer wavelength capability)	New Horizons Ralph
Laser Altimeter	10	10	100%	42x45x36 (optics; 21x29x12 electronics)	0.5		Nadir-pointing (off-nadir by 25^{o} to fill in poles)	100	~50% new development	LRO LOLA
Radio Science	1	1.5	100% during tracking	10x10x10	0		N/A	N/A	0% new	
Magnetometer	4	1	100%	10x10x15 plus 10m boom	0.05		N/A	N/A	0% new	Messenger heritage
GCMS	10	20 W average	100% operation mode desired		35		Nadir, in direction of plume material		~30-50% (pyrolysis heater unit, sample collector interface, miniature mass spec, wet chemistry?)	NGIMS, MSL SAM
Dust Micro Analyzer	10	5	20%	10x20x15	0.87		Nadir, in direction of plume material. Simple funnel to channel particles onto plate	N/A	~60%	MEMSA

Table 3.3.2-2: Enceladus-OL Strawman Lander Payload

Instrument	Mass (kg)	Power (W)	Duty Cycle	Dimensions L x W x H (or L x dia.) (cm)	Data Volume (kb/day)	Notes on Downlink	Preferred Location and Aperture Pointing Direction	Req'd Pointing Accuracy (arc sec)	% New Development Req'd	Precursor Instrument
Lander Camera (two)	0.6	5	Panorama followed by staggered plume monitoring		144	includes 5:1 compression, handled by C&DH	1 meter above surface, panoramic	N/A	0%	MER PANCAM
Radio Science	part of comm system	part of comm system	100% during comm. passes		N/A			N/A	0%	
Seismometer	2.3	1	100%	2.5x2x7.5	2.24		coupled to surface	N/A	0%	Netlander SEIS
Surface Chemistry Package	3	25	Alternates w/ other chemistry experiments	15x19x11	28			N/A	TBD	Part of ExoMars Urey
LDMS	4	5	Alternates w/ other chemistry experiments		120	includes 2:1 compression, handled by C&DH		N/A	TBD	ExoMars MOMA
Sampling Arm	3	1			N/A			N/A	TBD	
Piezoelectric Corer	1.3	5			N/A			N/A	TBD	Europa Lander
Surface Ice Oxidant Detector	0.3	1	Alternates w/ other chemistry experiments	2.9x2.5x.89	150	includes 2:1 compression, handled by C&DH		N/A	TBD	Part of ExoMars Urey

- High-frequency and low-frequency seismometry
  - Ice shell thickness, structure, cryovolcanism

- Imaging
  - Surface processes

- Radio Science
  - Tidal flexing

3.3.3 Enceladus-OL Mission Design

The following sections focus principally on the flight segment. Interfaces with the ground and launch segments will be summarized only, as the configuration of these segments was given in the Study Groundrules.

3.3.3.1 Enceladus-OL Flight Dynamics

3.3.3.1.1 Enceladus-OL Launch Window

The trajectory, time of flight, and launch capability are defined using the 20-day launch window shown in **Table 3.3.3-1**. This table shows the earliest launch date (19 September 2018) in the window results in the lowest required C_3 and the longest time of flight to Saturn. Conversely, the latest launch date (9 October 2018) in the window results in the highest required C_3 and the shortest time of flight to Saturn. The trajectory initially modeled for Enceladus-OL corresponds to the center of the window (29 September 2018). Since the ΔV required from the spacecraft varies across the launch window only on the order of tens of meters per second, the team continued to use the 29 September 2018 trajectory as the reference condition. However, two additional constraints were imposed to allow the flight segment to accommodate any launch date in the window. The first was the launch vehicle capability was limited to 6300 kg by the C_3 associated with the 9 October 2018 launch date. The second was the maximum time of flight was determined by the 19 September 2018 launch date. Launch dates earlier than 19 September 2018 were evaluated but required inner planet flyby altitudes were lower than considered safe (in some cases, the trajectories intercepted the planet).

The target plane of the final trajectory (in this case, the interplanetary trajectory) sets the inclination needed at the time of launch, which in turn sets the declination of the launch asymptote (DLA), a measure of the difference between the required launch direction and the launch location. Per ref. (d), the reduction in performance for using a DLA other than 28.5° (the minimum for a Cape Canaveral launch) is 6.1% for DLA = -39.6°, 4.6% for DLA = -34.0°, and 4.0% for DLA = -31.1°. These reductions are reflected in the Delta 4050H lift masses shown in **Table 3.3.3-1**. While shortening the launch window would have increased available launch mass, a 20-day window was believed to be the shortest practical window for a mission with a launch opportunity every 18 months considering constraints and uncertainties in weather, range operations, and launch vehicle readiness once the launch window opens.

The trajectory begins with Earth departure on 29 September 2018 with a C_3 of 14.87 km^2/s^2, a DLA of -33.96°, and an orbit geometry of 0.648 x 1.016 AU. A VVEES sequence of gravity assists increases orbit periapsis and apoapsis to arrive at Saturn as shown in **Figure 3.1.1-2**. Design parameters for the trajectory are shown in **Table 3.3.3-2**. The closest flyby of Earth is at an altitude of 1558 km (for reference, the Cassini mission used 1171 km Earth flyby altitude). The altitude for Earth flyby is above 1000 km throughout the launch window. A similar launch opportunity exists every 18 months (i.e., the synodic period of Venus), when Venus is in the correct position relative to Earth. Saturn's orbital position will change only a small amount every 18 months, as its orbit period is about 29.5 years.

Table 3.3.3-1: Launch Energy and Trip Time for 20-Day Launch Window

Launch Date	C_3 (km^2/s^2)	DLA (deg)	V_{hp} Earth (km/s)	V_{hp} Saturn (km/s)	Saturn Arrive Date	Trip Time (yrs)	Delta 4050H Lift Mass (0% Margin) (kg)
19 Sep 2018	13.25	- 39.6	12.47	5.92	26 Dec 2030	~ 12.25	6915
29 Sep 2018	14.87	- 34.0	12.92	5.79	25 May 2030	~ 11.75	6805
9 Oct 2018	19.05	- 31.1	13.56	5.92	7 Jul 2029	~ 10.75	6300

Table 3.3.3-2: Enceladus-OL Design Parameters for Trajectory to Saturn

Event	Date	V_{hp} (km/s)	Flyby Altitude (km)	Post Fly by Orbit Geometry (AU)
Flyby Venus	Feb 27, 2019	7.19	4520	0.706 x 1.574 AU
Flyby Venus	Apr 22, 2020	7.17	1545	0.717 x 1.858 AU
Flyby Earth	Jun 15, 2020	12.88	1558	0.893 x 4.149 AU
Flyby Earth	Jun 15, 2024	12.99	5450	0.962 x 9.118 AU
Arrive Saturn	May 4, 2030	5.79		0.962 x 9.118 AU

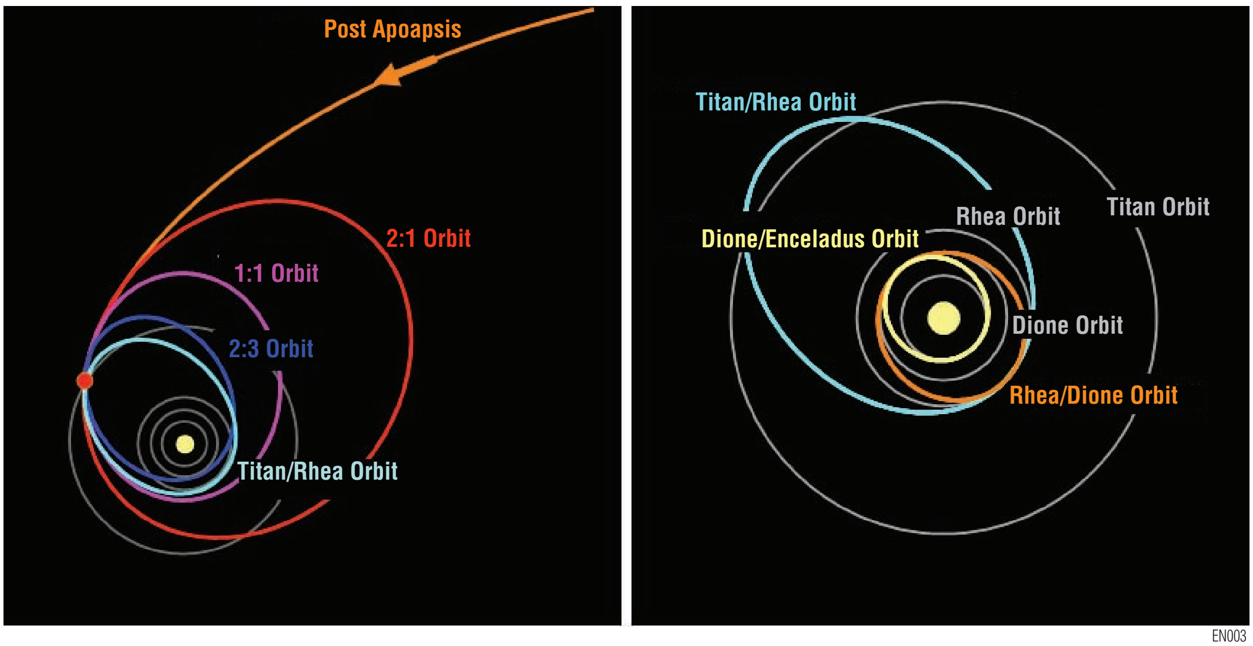

Figure 3.3.3-3A: Multiple Titan Resonant Orbits
Figure 3.3.3-3B: Titan/Rhea/Dione/Enceladus Resonant Orbits

3.3.3.1.2 Enceladus-OL Capture at Saturn and Rhea/Dione Walkdown

The handoff between the interplanetary trajectory and the planetary capture sequence into a Titan/Rhea resonant orbit is executed using an approach similar to that discussed in **Section 3.1.1.2.2** where the magnitude and direction of the arrival V_{hp} and the allowable closest approach radius sets the placement and targeting of the inbound hyperbolic asymptote. A higher V_{hp} may result from a trajectory with a different trip time, but will require a larger braking ΔV to settle into Saturn orbit. Since the only moon of any appreciable size is Titan, the destination of the capture sequence is as discussed in **Section 3.1.1.2.2**. For Enceladus-OL, the closest approach to Saturn is 82,000 km radius to provide maximum benefit of the Saturn gravity assist, and hence minimize the ΔV required from the orbiter.

There are two key enablers for the Enceladus-OL mission. The first is staging, discussed in **Section 3.3.3.2.2**, and the second is the use of Rhea and Dione flybys, discussed in **Section 3.1.1.2.2** and depicted in **Figures 3.3.3-3A** and **3.3.3-3B**, to scrub orbital energy before conducting the Enceladus orbit insertion (EOI) burn. A total of 30 Rhea flybys is used to reduce ΔV by 1650 m/s. This is followed by a total of 13 Dione flybys to reduce ΔV by another 480 m/s. The flyby frequency averages about once per month, starting off less frequent and becoming more frequent as the orbital period decreases. The combined ΔV reduction of 2130 m/s for these flybys greatly reduces requirements for propulsion and enables the mission to fit on a Delta 4050H launch vehicle.

The cost of adding these 43 flybys is an additional 3.5 years in mission lifetime as discussed in **Section 3.1.1.2.2**. Prior to conducting the Rhea flybys, four flybys of Titan are conducted over a period of about nine months following the SOI burn. These flybys reduce the orbit periapsis to the radius of the Rhea orbit and set apoapsis near the radius of the Titan orbit.

3.3.3.1.3 Enceladus-OL Orbit Design

The primary mapping orbit around Enceladus is circular, with a 45° inclination and a 200 km altitude (period 6.26 hrs, orbiter velocity 126 m/s). Analysis shows this orbit appears stable for over 2.7 years to the level of fidelity available with the gravitational models used (the gravity model is based on a uniform density triaxial ellipsoid model of Enceladus with Saturn as point source disturbance). The gravitational model of Enceladus will not be well defined until Enceladus is orbited, and this improved definition may result in a less stable orbit. This was one of the principal reasons for carrying a 500 m/s ΔV reserve (the other being the uncertainty in the assumptions, such as finite burn losses, used for the Saturn capture sequence).

The reference concept of operations (ConOps) uses 12 months of operation at 45°, followed by a plane change and altitude reduction to polar orbit at 100 km (orbiter period 4.30 hrs, orbiter velocity 143 m/s) for 24 hours, followed by a plane change back to 45° at 200 km. The cycle is repeated one year later. To provide margin on orbit stability, mapping operations are limited to 24 hours, enough time for six south pole passes and five north pole passes. Transit time through the plume is about six minutes, assuming the plume is a 15° half angle cone (*Spahn et al. 2006*) at 100 km altitude. The polar orbit is oriented such that right ascension maintains an equivalent mean local time of the ascending node at 3:00 pm. This orbit was selected as a compromise between a noon/midnight orbit, which yields good signal to noise for composition and thermal inertia measurements, and a low Sun angle dawn/dusk orbit that induces shadows needed for topography measurements. The lander deploys from the 45° orbit, so as not to divert the limited time available in polar orbit to functions associated with monitoring lander descent, landing, and checkout.

The visible mapping instrument was assumed sized to allow a 50-km wide swath of surface to be observed at an altitude of 200 km. This set the angular field of view for the nadir pointing instrument at 14.03°. To cover as much of the scientific region of interest on the southern surface of Enceladus as possible, the spacecraft attitude (instrument boresight) is offset. Science constraints limit the incidence angle of surface observations to no greater than 50°. This results in a 200 km, 45° orbit with a maximum attitude offset of about 18.35° (see **Figure 3.3.3-4**). In this orbit, all of the surface ranging in latitudes from about 35° north to about 70° south can be imaged. While this gives significant coverage, it leaves a portion of the southern hemisphere unmapped as shown in **Figure 3.3.3-5** (since the orbiter has the ability to slew the boresight, the option exists to image up to about 70° north latitude from the 45° orbit, though this scenario has not been evaluated). This level of coverage could be accomplished in as few as 15 days, if the spacecraft were collecting image data 100% of the time. However, the data collection rate is constrained to a 1.85% duty cycle by the communication link to Earth, so the required mapping time increases to 2.4 years.

Two campaigns designed to cover the south pole fill in the gaps in the mapping. Combining the results of the two polar campaigns with the long term data from the 45° orbit almost completely maps the southern hemisphere of Enceladus (see **Figure 3.3.3-6**).

Polar orbit stability introduces significant mission constraints. If a major scientific goal were to map the entire surface of Enceladus, it would be desirable to enter into a near polar orbit of the moon. Being inertially fixed, the ground track of a 100-km circular polar orbit about the tidally locked moon could completely cover of the surface in about a month when the gravitational field of Enceladus is based on a point source model. But when the simple triaxial uniform density model is used, the 100-km polar orbit is stable for just under three days before impact occurs. Increasing the altitude to 200 km causes the orbit to become more eccentric until eventually periapsis is reduced to the point where the orbit intersects the surface. Starting in an eccentric polar orbit (e.g., 100 km x 200 km) is even more unstable, as though the spacecraft were further along in the circular orbit's tendency to become more eccentric. The twice daily orbit maneuvers required to maintain any polar orbit call for intense ground operations (including a significant amount of expensive orbit determination activity) and a ΔV

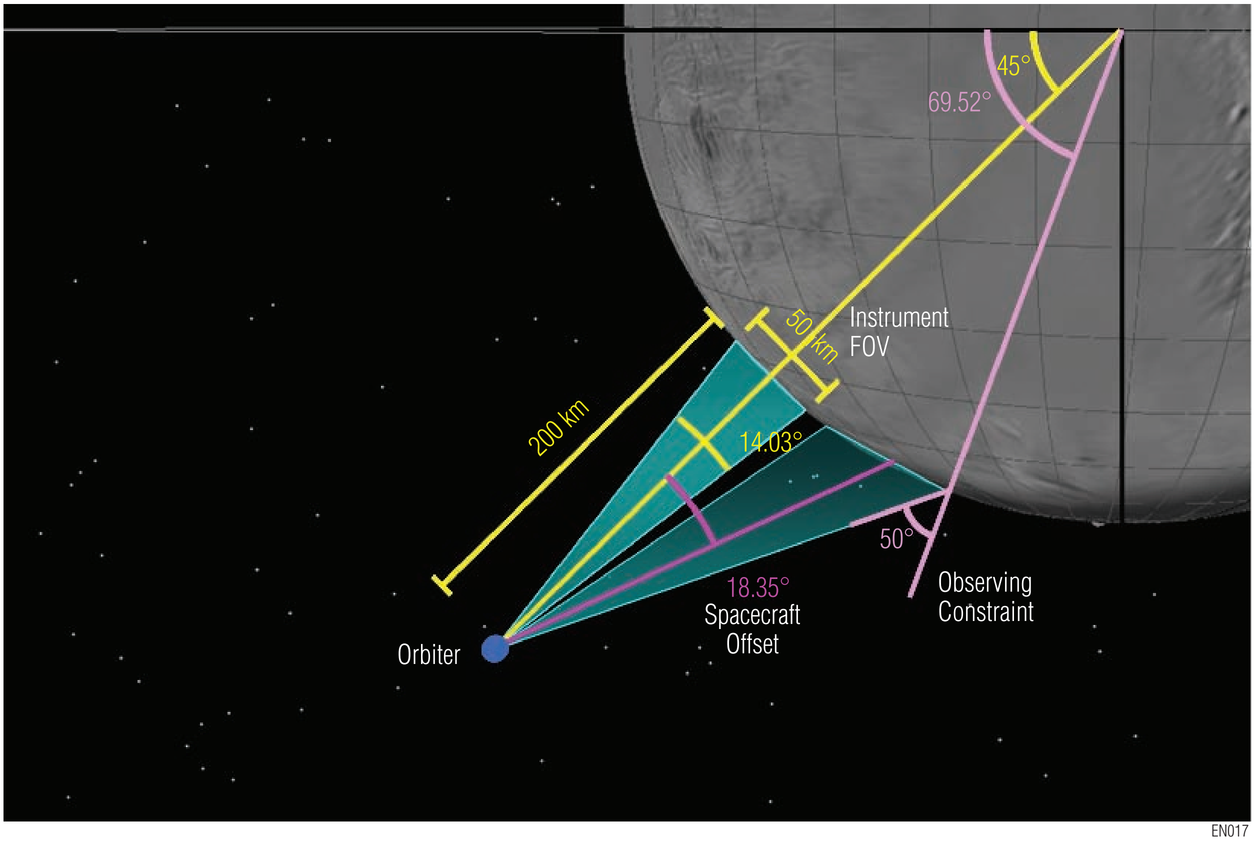

Figure 3.3.3-4: Enceladus-OL Relationship between Orbital Altitude, Instrument FOV and Spacecraft Offset Angle

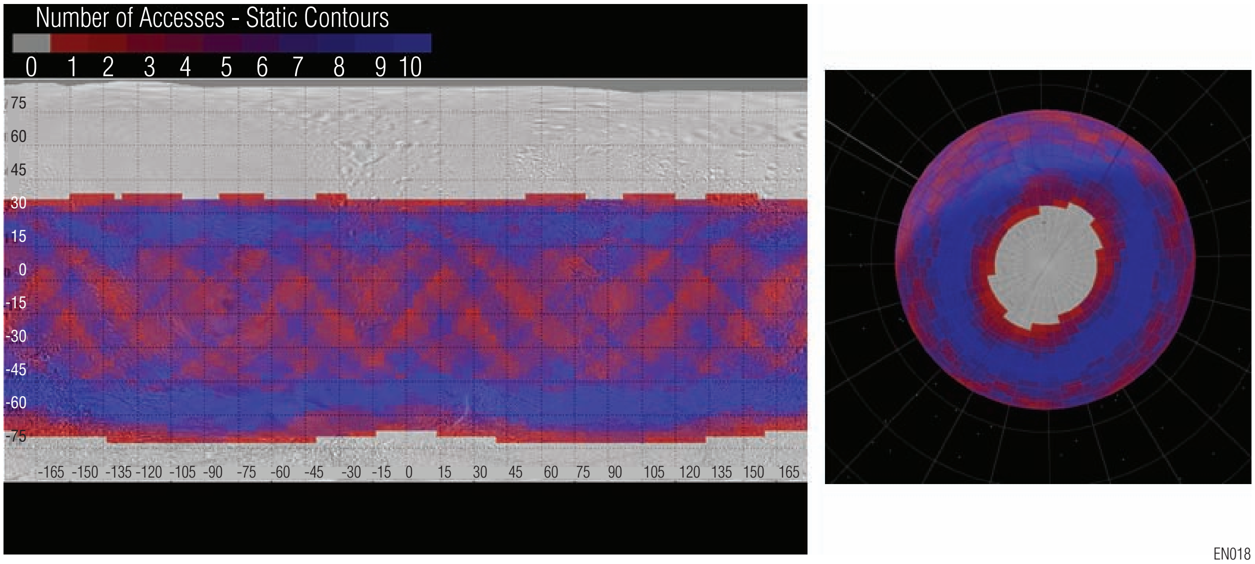

Figure 3.3.3-5: Enceladus-OL Mapping Coverage for Spacecraft with Offset Biased Toward the South

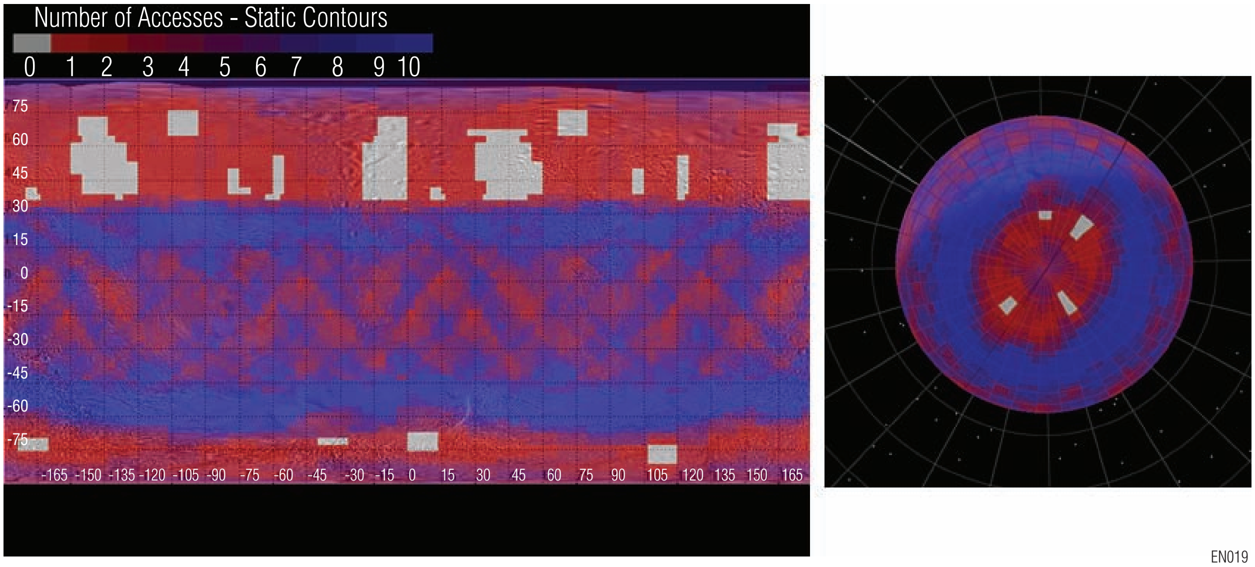

EN019

Figure 3.3.3-6: Enceladus-OL Combined Mapping Coverage for 2.4-Year 45° Orbit (with Offset Biased Toward the South) and Two 24-Hour Polar Orbit Campaigns

of up to 10 m/s per day. Even if the navigation and orbital operations could be made autonomous and orbit corrections were possible after an anomaly event, the unstable nature of the polar orbit would call for more fuel mass than appeared feasible for the mapping mission.

A range of orbital inclinations was examined. At inclinations above about 50°, instabilities caused orbit eccentricity to increase, in some cases causing the spacecraft to impact the surface within a few days. However, a 45° orbit (**Figure 3.3.3-7**) allowed the spacecraft to remain in orbit for an extended period (analysis showed no impact on the surface in a 1000-day scenario, though the altitude of the orbit showed some periodic variation). The stability noted for the 45° orbit is likely an artifact of the symmetries inherent in the uniform density, elliptical spheroid assumption used to build the gravity potential model. The actual stability is likely to deviate from this, but without more knowledge of the Enceladus shape and mass distribution, it is not possible to render a high fidelity model. Since the current model is believed to be a reasonable first order approximation, maneuvers required to maintain this orbit could be expected to be relatively small and to be accommodated by the ΔV reserve discussed above.

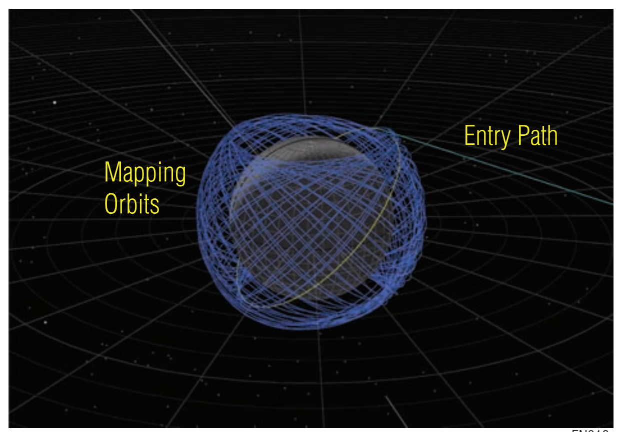

EN016

Figure 3.3.3-7: Enceladus-OL Enters into a 45° Inclination Orbit from Saturn Orbit

3.3.3.1.4 Enceladus-OL Landing Approach

An analysis was conducted to determine what it would take to land on Enceladus from an Enceladus orbit. In that analysis, the lander was deployed from the 45°, 200-km mapping orbit and executed a periapsis lowering maneuver and an inclination change with a single burn (see **Figure 3.3.3-8**). A ΔV of about 90 m/s is needed to execute a combined plane change and retroburn to get to the south pole, and another 180 m/s is needed to null the resulting impact velocity at the south pole. Once at the pole, another 90 m/s is allocated for landing site hazard avoidance and landing site selection. These ΔV values exclude ACS tax and reserve. The lander is in communication with the orbiter from deployment through landing.

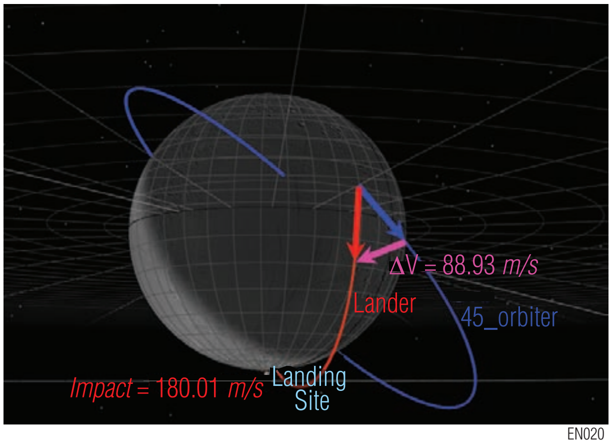

Figure 3.3.3-8: ΔV Required to Alter 45° Orbit to Impact at South Pole

3.3.3.1.5 Enceladus-OL Timeline of Key Events

Figures 3.3.3-9, **3.3.3-10**, and **Table 3.3.3-3** give high level descriptions of the trajectory phases and the corresponding timeline of key events in the 18.3-year mission.

3.3.3.1.6 Enceladus-OL Mission ΔV Budget

The total ΔV for the Enceladus-OL trajectory, including maneuvers required to enter orbit about Enceladus and conduct 2.4 years of mapping operations, is 4497 m/s as shown in **Table 3.3.3-4**. This ΔV is used to size the booster and orbiter propulsion systems and includes the ΔV required to accomplish two round-trip plane changes from the 45° mapping orbit to the polar mapping orbit. It also includes a reserve of 10% plus the additional reserve of 500 m/s noted in **Section 3.3.3.1.3**. The ΔV required for lander operations is 415 m/s. In the Enceladus-OL study, the 5% tax to account for propellant used in non-ΔV attitude control maneuvers for the booster and orbiter is accounted for as a propellant tax (not shown here), rather than as a ΔV tax.

3.3.3.2 Enceladus-OL Flight Segment Design

The flight segment configuration, mass, and subsystem design approach is described in the following sections.

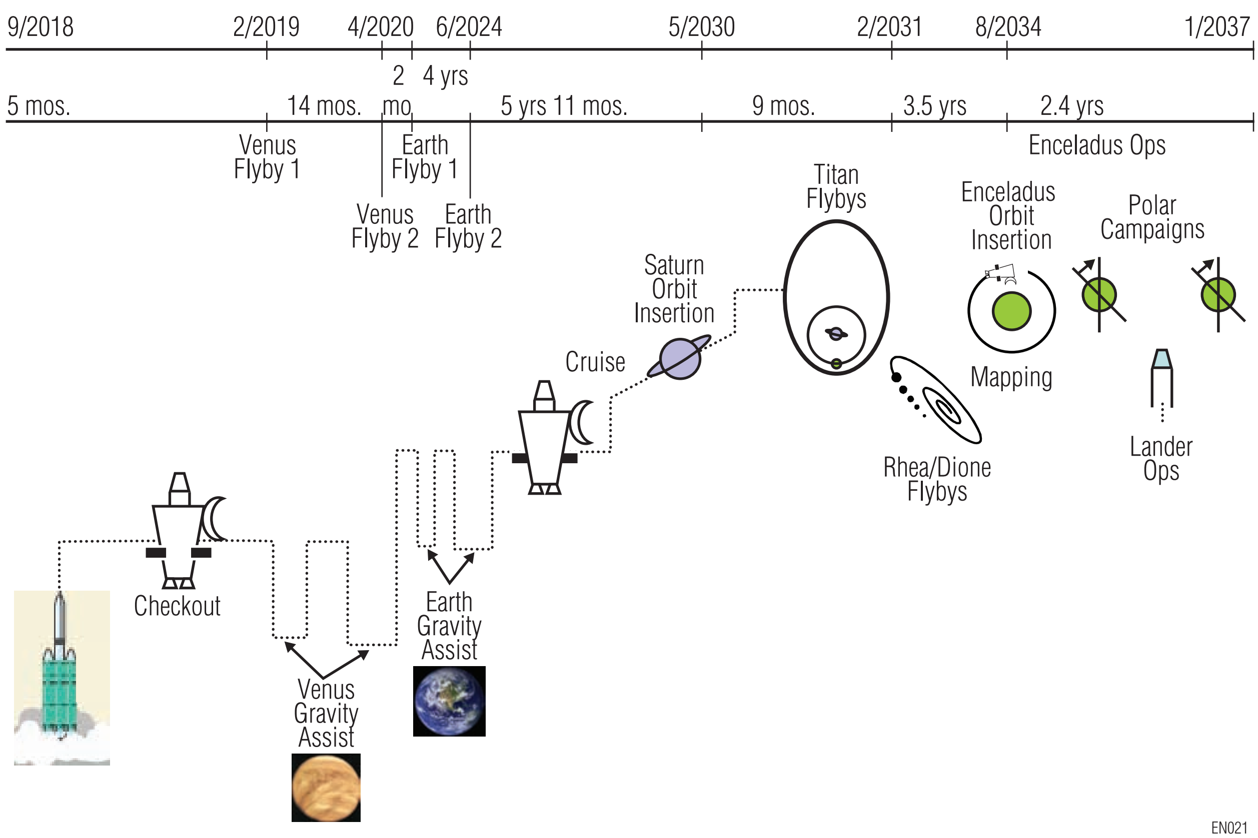

Figure 3.3.3-9: Enceladus-OL Mission Key Events

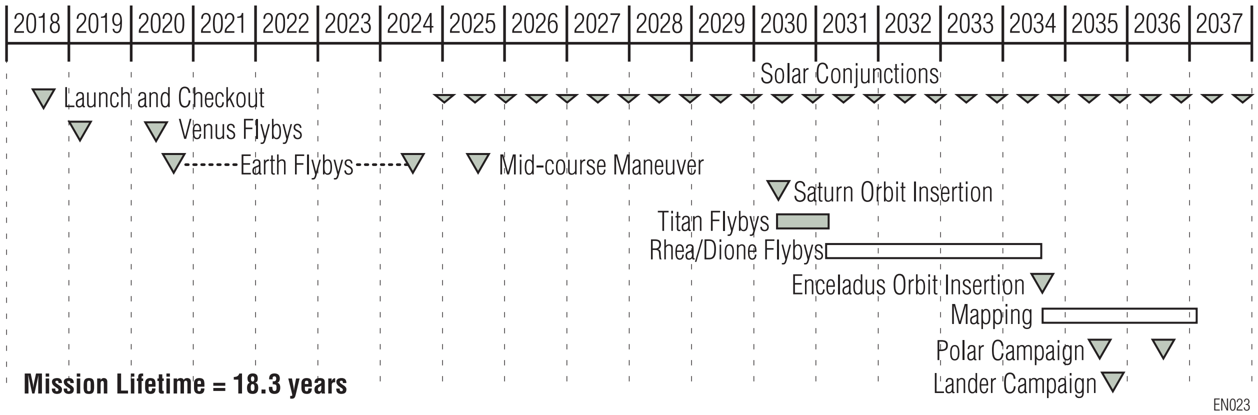

Figure 3.3.3-10: Enceladus-OL Mission Timeline

Table 3.3.3-3: Key Events in 18.3-Year Enceladus-OL Mission Timeline

Date	Year	Event
September 29	2018	Launch/Checkout
February 27	2019	Venus Flyby 1
April 22	2020	Venus Flyby 2
June 15	2020	Earth Flyby 1
June 15	2024	Earth Flyby 2
June 10	2025	Mid course trajectory maneuver
May 4	2030	Saturn Orbit Insertion
August 8	2034	Enceladus Orbit Insertion
August	2035	Polar Campaign (24 hours)
October	2035	Landing
August	2036	Polar Campaign (24 hours)
January	2037	End of Mission

3.3.3.2.1 Enceladus-OL Configuration

Figures 3.3.3-11 through **3.3.3-16** show the general arrangement of the flight segment. The flight segment consists of the booster (also referred to as Step 1, using MIL-STD-176A nomenclature for multi-stage systems), the orbiter (referred to as Step 2), and the lander (referred to as Step 3). The lander is also referred to as Stage 3, whereas the orbiter + lander configuration is referred to as Stage 2, and the booster + orbiter + lander is referred to as Stage 1. In most instances, the stage is the more relevant entity, since a stage represents the incremental configuration of the flight segment during mission operations. Steps 1, 2, and 3 as entities are used principally to account for mass that separates from the vehicle during staging events.

3.3.3.2.2 Enceladus-OL Mass Properties

Table 3.3.3-5 gives a top level summary of flight segment mass by stage, including mass contingency (B = Booster, O= Orbiter, L = Lander). The Stage 1 gross mass is 6320 kg, including the instrument suite (shown in **Tables 3.3.2-1** and **3.3.2-2**) and propellant. This leaves slightly negative (-0.3%) lift margin on the Delta 4050H lift capability of 6300 kg.

Approximate sensitivities of Stage 1 gross mass to changes in the masses of each step be determined using the rocket equation, $m_p = m_f [e^{(\Delta V / I_{sp}\, g\, \eta)} -1]$, where m_p is propellant mass, m_f is the final mass, I_{sp} is the effective specific impulse, g is the Earth gravitational acceleration, and η is an efficiency term (η = 1.00 was used in this analysis). Noting that $m_i = m_f + m_p$, where m_i is the initial stage mass, the ratio of initial to final stage mass follows.

$$m_i/m_f = 1 + m_p/m_f = e^{(\Delta V / I_{sp}\, g\, \eta)}$$

Applying this equation to the Stage 1, 2, and 3 masses in **Table 3.3.3-5**, gives m_i/m_f = 1.63, 2.83, and 1.21, respectively. Values for m_i/m_f depend only on ΔV and effective I_{sp}, with g and η being constant. Compounding the effect of these changes, the resulting values for the change in Stage 1 initial mass with changes in Step 1, 2, and 3 masses are shown below.

Table 3.3.3-4: Enceladus-OL Mission ΔV Budget

Maneuver	ΔV (m/s)	ACS Tax (%)	ΔV (m/s) with ACS Tax	ΔV Margin (%)	Effective ΔV (m/s)
Booster & Orbiter ΔV Budget					
Launch	0.0	0.0	0.0	0.0	0.0
TCM 1: Target Venus 1	10.0	0.0	10.0	10.0	11.0
TCM 2: Target Venus 2	10.0	0.0	10.0	10.0	11.0
TCM 3: Target Earth 1	10.0	0.0	10.0	10.0	11.0
TCM 4: Target Earth 2	10.0	0.0	10.0	10.0	11.0
Mid Course Correction	10.0	0.0	10.0	10.0	11.0
Saturn Orbit Injection (SOI)	650.0	0.0	650.0	10.0	715.0
Post SOI TCM's	10.0	0.0	10.0	10.0	11.0
Apoapsis Burn	350.0	0.0	350.0	10.0	385.0
Titan Resonant TCM's (as needed)	10.0	0.0	10.0	10.0	11.0
Target Titan 2:1 Orbit	10.0	0.0	10.0	10.0	11.0
Target Titan 1:1 Orbit	10.0	0.0	10.0	10.0	11.0
Target Titan 2:3 Orbit	10.0	0.0	10.0	10.0	11.0
Target Titan 16:31 Orbit	10.0	0.0	10.0	10.0	11.0
Target Enceladus	10.0	0.0	10.0	10.0	11.0
Sub Total Transit to Saturn	**1120.0**		**1120.0**		**1232.0**
Enceladus Orbit Insertion, Ops & Maint					
Match Enceladus	3780.0	0.0	3780.0	10.0	4158.0
Orbit Enceladus	220.0	0.0	220.0	10.0	242.0
Plane Changes (4)	400.0	0.0	400.0	10.0	440.0
Orbit Maintenance (2.4 years)	50.0	0.0	50.0	10.0	55.0
Sub Total Enceladus (no Rhea/Dione Flybys)	**4450.0**		**4450.0**		**4895.0**
Total (no Rhea/Dione Flybys)	**5570.0**		**5570.0**		**6127.0**
Add 3.5 years & 43 Rhea/Dione Flybys					
ΔV Reduction*	2130.0	0.0	2130.0	0.0	2130.0
Sub Total Enceladus (with Rhea/Dione Flybys)	**2320.0**		**2320.0**		**2765.0**
Total (with Rhea/Dione Flybys)	**3440.0**		**3440.0**		**3997.0**
ΔV Reserve (Held for Modeling Uncertainty)	500.0			0.0	500.0
Total Booster & Orbiter ΔV with Reserve	**3940.0**				**4497.0**
Lander ΔV Budget					
Separation From Orbiter	0.0	0.0	0.0	0.0	0.0
Plane Change to South Region & Retroburn	88.9	5.0	93.3	10.0	102.7
Null Impact Velocity	180.0	5.0	189.0	10.0	207.9
Hazard Avoidance	90.0	5.0	94.5	10.0	104.0
Total Lander ΔV with Reserve	**358.9**		**376.8**		**414.5**
*Relative to an approach which enters a Titan - Enceladus elliptical orbit prior to circularizing at Enceladus					

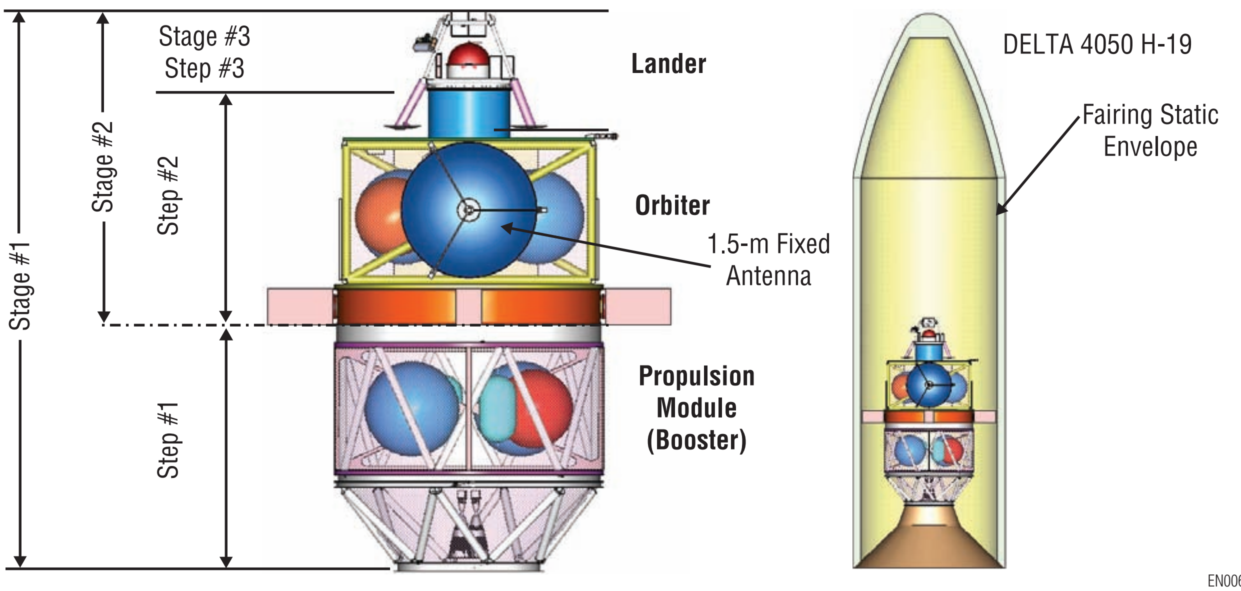

Figure 3.3.3-11: View Looking at Enceladus-OL +Z Face and Showing Compatibility with Delta 4050H Fairing Static Envelope

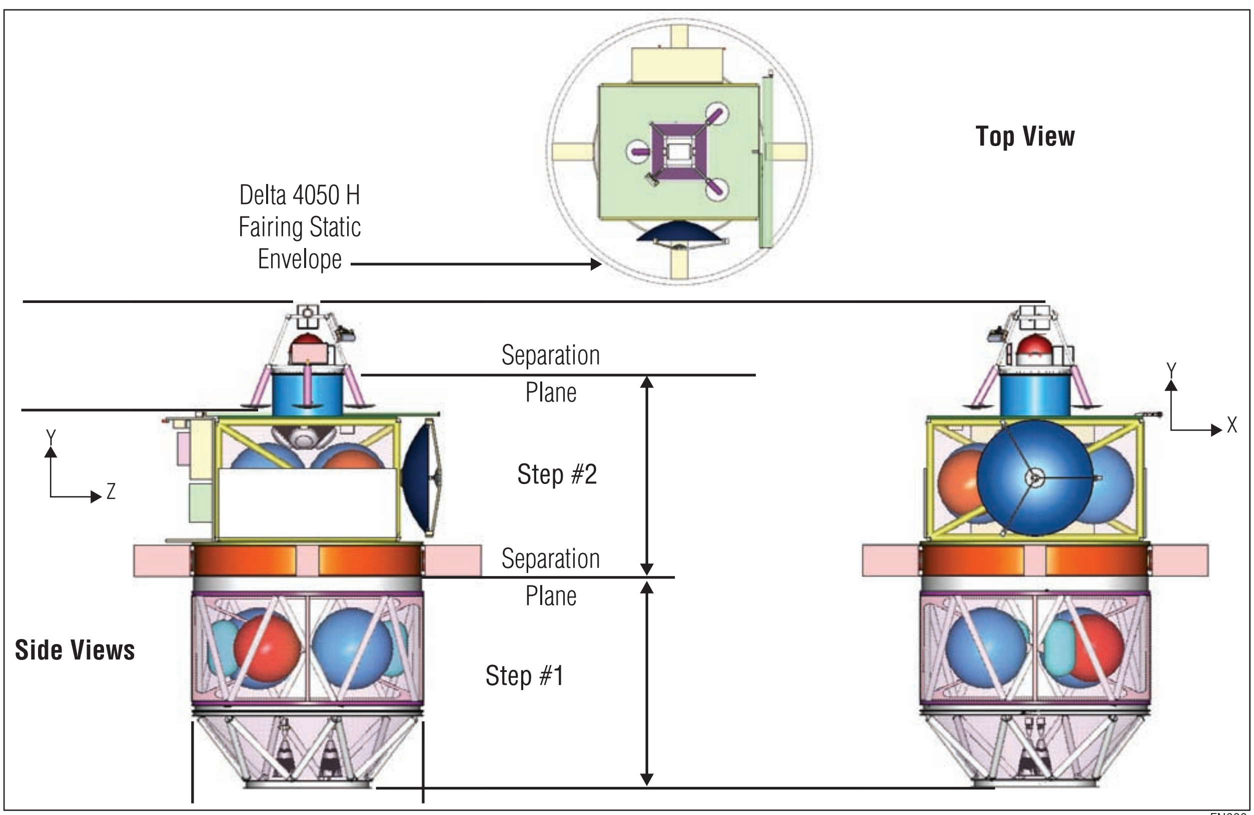

Figure 3.3.3-12: Three View of Enceladus-OL

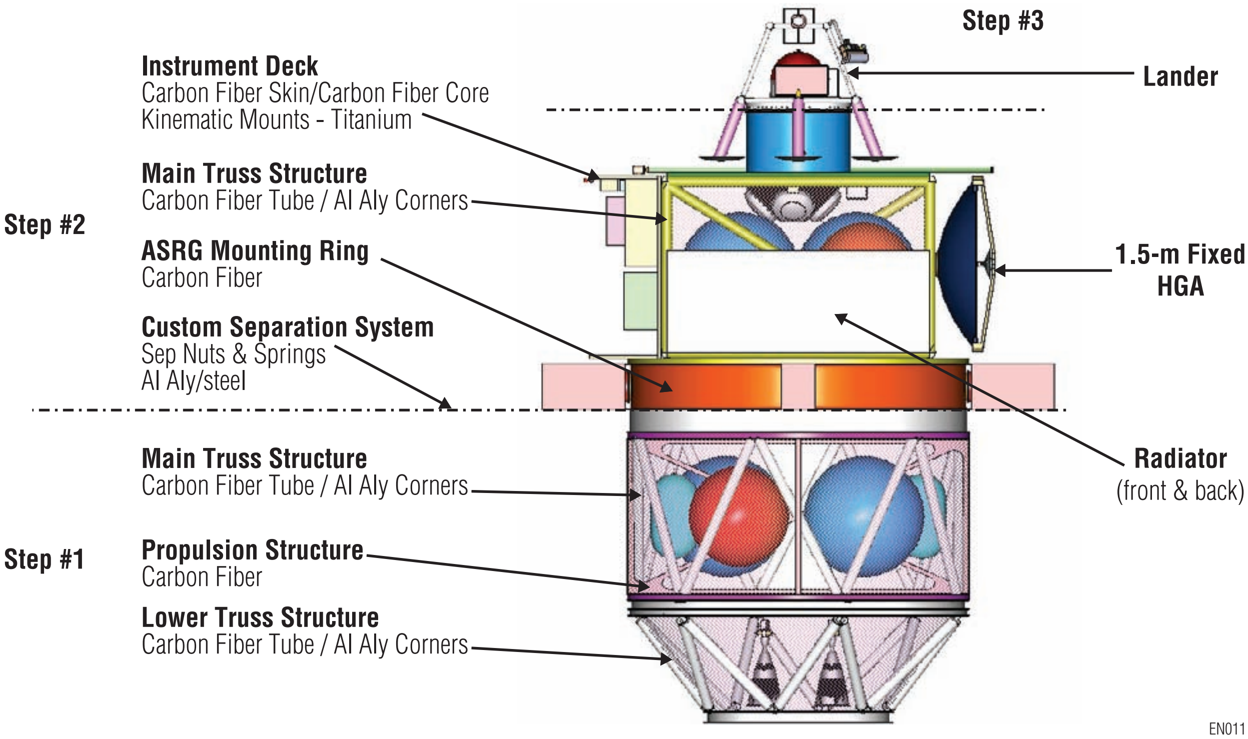

Figure 3.3.3-13: Major Components of Enceladus-OL (View Looking at –X Face)

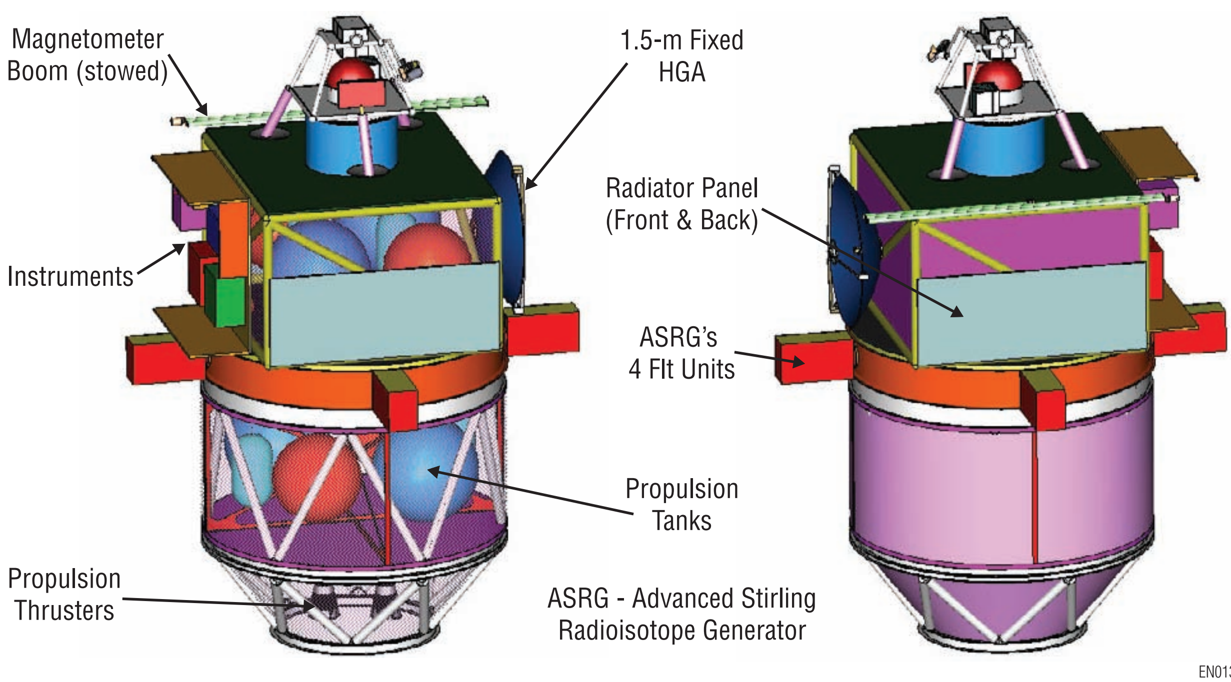

Figure 3.3.3-14: Enceladus-OL Perspective View and Closeout Configuration

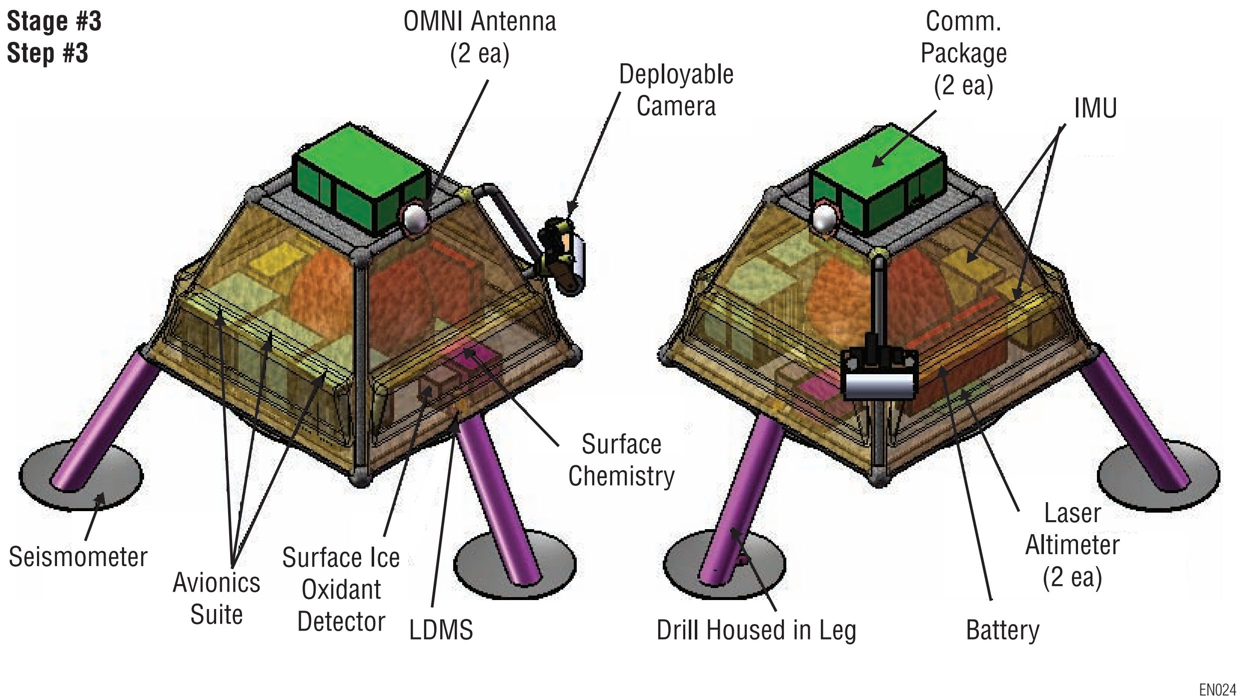

Figure 3.3.3-15: Enceladus-OL Lander Instrument Locations

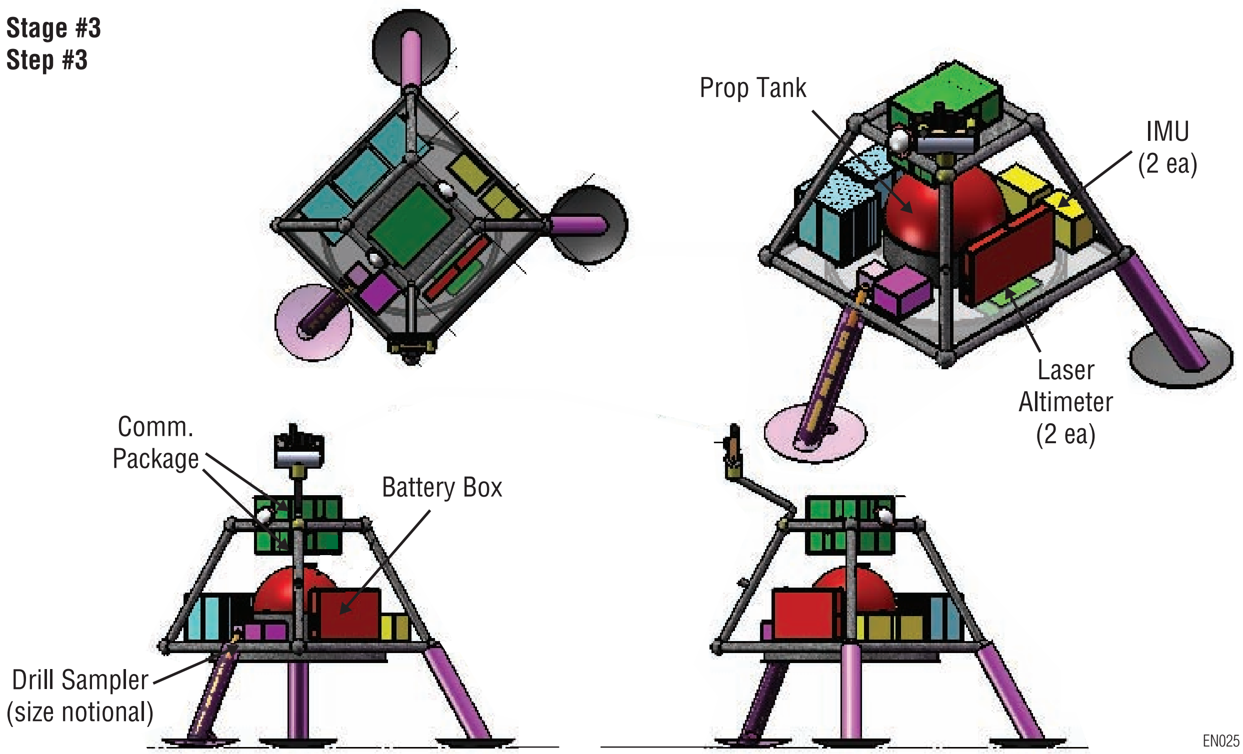

Figure 3.3.3-16: Enceladus-OL Lander Configuration

Table 3.3.3-5: Enceladus-OL Mission Level Summary Mass Statement

	Enceladus OL
Launch Vehicle Margin (%)	**-0.3**
Launch Vehicle Capability (kg)	**6300**
	Mass (kg)
Stage 1 (B+O+L) Initial	6320
- Stage 1 Propellant*	2450
Stage 1 Dry	3870
- Step 1 (Booster) Dry	489
Stage 2 (O+L) Initial	3381
- Stage 2 Propellant*	2186
Stage 2 Dry w/instruments	1196
- Step 2 (Orbiter) Dry	968
Stage 3 (Lander) Initial	228
- Stage 3 Propellant*	42
Stage 3 Dry w/instruments	186
* Includes residuals and loading uncertainty	

Δ Stage 1_i / Δ Step 1_{Dry} $= (m_i/m_f)_1 = 1.63$

Δ Stage 1_i / Δ Step 2_{Dry} $= (m_i/m_f)_2\ (m_i/m_f)_1 = 4.62$

Δ Stage 1_i / Δ Step 3_{Dry} $= (m_i/m_f)_3\ (m_i/m_f)_2\ (m_i/m_f)_1 = 5.59$

Scaling using this approach gives only a first-order approximation and should be used with caution. For example, while it accounts for the additional propellant required for an increase in dry mass, it excludes the corresponding increase in propellant tank size and supporting structure. The increase in propellant tank dry mass is about 6.5% of the increase in propellant mass for both the Stage 1 and Stage 2 propulsion systems. The increase in propulsion system supporting structure mass is about 8% of the increase in propulsion system dry mass (which, to the first approximation, is the same as the increase in propellant tank mass). Combining these factors, propellant tank dry mass plus supporting structure is about 7% of propellant mass. Also, when an existing solid motor is used for one of the stages, scaling only applies within the limits of the size of that motor. The supporting structure factor of 8% is usable for scaling propellant mass changes of about +/- 150 kg. Beyond that, structure growth (not included in the 8% factor) can become significant, particularly when changes in structural length accompany propellant increases.

A further breakout of mass by subsystem for each step is provided in **Tables 3.3.3-6** through **3.3.3-8**. Propellant was computed on the basis of mass with contingency, i.e., the "allocation" mass.

3.3.3.2.3 Enceladus-OL Booster and Orbiter (B & O) Description

All booster and orbiter subsystems are designed to be 1-fault tolerant for credible failures, consistent with NPR 8705.4 guidance for Class A missions. A brief summary of orbiter design approach is provided below.

3.3.3.2.3.1 Enceladus-OL (B & O) Mechanical Subsystem

The orbiter mechanical system uses carbon fiber composite for the Step 1 and Step 2 propulsion structure and truss members and for the Step 2 ring housing the Advanced Stirling Radioisotope Generators (ASRGs). Aluminum alloy is used at both sides of the interface between Step 1 and Step 2 and at the separation interface with the launch vehicle. Step 2 top, bottom, experiment deck, and antenna deck panels are carbon fiber with an aluminum honeycomb core. Examples of spacecraft and instruments that have flown using graphite reinforced epoxy composite structural elements include SWIFT, FUSE, WMAP, and GLAS (an instrument which flew on the ICESAT spacecraft). In addition, composite material systems are being used for other missions currently in development, including SDO, GLAST, and JWST. The magnetometer is deployed on a 10-meter boom during the post-launch checkout.

3.3.3.2.3.2 Enceladus-OL (B & O) Power Subsystem

Power for the booster and orbiter is provided by four 143 W beginning of life (BOL) ASRGs and a rechargeable lithium ion battery. The power system, located in the orbiter, provides 28V DC power to subsystems and instruments on the orbiter and heater power to the booster. To conserve lander battery power, the orbiter also provides power to the lander for pre-separation checkout and thermal conditioning of the propulsion system as well as for uploading terrain map scenes taken during orbiter mapping passes. At the end

Table 3.3.3-6: Enceladus-OL Step 1 (Propulsion Module) Mass Statement

Step 1 (Propulsion Module) Dry Mass				
	Estimate (Kg)	% Total Dry Mass	% Contingency	Allocation (Kg)
Mechanical	196	52	30	255
Attitude Control	0	0	30	0
Thermal	18	5	30	23
Propulsion	157	42	30	203
Power	0	0	30	0
C&DH	0	0	30	0
Communications	0	0	30	0
Propulsion Module Harness	6	1	30	7
Propulsion Module Total Dry Mass	**376**	**100**	**30**	**489**
Step 1 (Propulsion Module) Wet Mass				
	Estimate (Kg)	% Total Wet Mass	% Contingency	Allocation (Kg)
Propulsion Module Dry Mass	376	13	30	489
Propellant Mass (Incl. Residuals)	2450	87	0	2450
Propulsion Module Wet Mass	**2826**	**100**		**2939**

of the 18.8 year (worst case) mission life, each ASRG provides 124 W. The maximum steady state load of 362 W includes 30% contingency and occurs during the normal science mapping mode (in both the 45° and polar orbits). **Table 3.3.3-9**, provided by ref. (e), shows using three ASRG units will meet this load requirement, but unlike the RTG, the ASRG is not considered internally redundant, so a fourth ASRG is carried as an operating spare. Mass being a critical parameter, it was of interest to know how four ASRG units, one of which is assumed to have failed, compared with three operating RTG units. **Table 3.3.3-9** shows flying three RTG units results in higher mass and insufficient power compared with flying four ASRG units under these conditions. Additionally, thermal rejection requirements are significantly higher with the RTG units.

Occasionally during the mission, the orbiter power system will see loads significantly higher than the 372 W available for transient periods. For example, a load of 746 W occurs during SOI and EOI maneuvers, during which the omni antennas are concurrently transmitting telemetry. The battery must have sufficient capacity to provide the transient load under the worst case single failure condition, which corresponds to the loss of one main engine for an EOI maneuver (all four ASRGs operating). In this case, the two engine EOI burn time of 1.55 hrs nominally doubles to 3.10 hours. Since the EOI maneuver occurs at 16.5 years, the power available from four ASRGs is 505 W. Assuming a battery charge discharge efficiency of 0.813, this requires a battery capacity of 32.7 Ahr and results in a battery depth of discharge (DoD) of about 82% relative to the baselined 40 Ahr internally redundant battery. This DoD is relatively high and indicates the battery size should be re-evaluated in future studies, given the battery is needed for routine communications during Enceladus mapping operations. Other failure cases; including pre-SOI engine failure, or pre-SOI or pre-EOI ASRG failure; resulted in depth of discharge levels no higher than 66%.

3.3.3.2.3.3 Enceladus-OL (B & O) Thermal Control Subsystem

The Enceladus-OL thermal design (see **Figure 3.3.3-17)** maintains spacecraft component temperatures within -10°C to +40°C (operating) and -20°C to +50°C (non-operating). This is done in part through the use of a combination of coatings and multi-layer insulation (MLI). Additionally, variable conductance heat pipes (VCHPs) transport heat from bus components to two aluminium honeycomb bus radiator panels with embedded VCHPs. Orbiter instruments are thermally isolated from the bus and maintain temperatures within -10°C to +40°C operating and -20°C to +50°C non-operating with a combination of MLI and heaters. Heaters and thermistors are also used to control temperatures of orbiter

Table 3.3.3-7: Enceladus-OL Step 2 (Orbiter) Mass Statement

Step 2 (Orbiter) Science Payload				
	Estimate (Kg)	% Total Dry Mass	% Contingency	Allocation (Kg)
Thermal Mapper	11	1	30	14
VIS/NIR Mapper	10	1	30	13
Laser Altimeter	10	1	30	13
Radio Science	1	0	30	1
Magnetometer	4	1	30	5
GCMS	10	1	30	13
Dust Micro Analyzer	10	1	30	13
Sounding Radar	0	0	30	0
Payload Total	**56**	**8**	**30**	**73**
Step 2 (Orbiter) Spacecraft Bus				
	Estimate (Kg)	% Total Dry Mass	% Contingency	Allocation (Kg)
Mechanical	236	32	30	306
Attitude Control	27	4	30	35
Thermal	36	5	30	47
Propulsion	154	21	30	200
Power	94	13	30	122
C&DH	46	6	30	59
Communications	55	7	30	72
Spacecraft Harness	42	6	30	55
Bus Total	**688**	**92**	**30**	**895**
Step 2 (Orbiter) Dry Mass				
	Estimate (Kg)	% Total Dry Mass	% Contingency	Allocation (Kg)
Science Payload Total	56	8	30	73
Bus Total	688	92	30	895
Orbiter Dry Mass	**744**	**100**	**30**	**968**
Step 2 (Orbiter) Wet Mass				
	Estimate (Kg)	% Total Wet Mass	% Contingency	Allocation (Kg)
Orbiter Dry Mass	744	25	30	968
Propellant Mass (Incl. Residuals)	2186	75	0	2186
Orbiter Wet Mass	**2930**	**100**		**3153**

and booster components; where the largest share of heater power goes to propulsion. The thermal mapper has a dedicated passive radiator to maintain an operating temperature of 60 K, and the lithium ion battery is maintained at an operating temperature between 0°C and +30°C. Shields on the +Y side of the ASRGs serve to protect the instruments from ASRG thermal radiation as well as to shield the ASRGs from particle impact from the Enceladus plume. A sunshade made of heat resistant ceramic cloth is located on the booster -Y face, and the booster main engines have a heat shield to minimize heat transfer to the orbiter and to the booster propellant tanks during engine firing.

3.3.3.2.3.4 Enceladus-OL (B & O) Propulsion Subsystem

A three-stage design is used to maximize mass delivered to Enceladus orbit and to the Enceladus surface relative to that achievable with two stage (i.e., orbiter and lander) design. The booster and orbiter contain dual-mode nitrogen tetroxide (N_2O_4)/hydrazine propulsion systems. The booster provides the required ΔV in bi-propellant mode for SOI through targeting the Titan/Rhea elliptical orbit, with monopropellant for ACS control (see **Table 3.3.3-4**). Up until the main engines are needed for SOI, however, it operates in monopropellant blowdown mode for

Table 3.3.3-8: Enceladus-OL Step 3 (Lander) Mass Statement

Step 3 (Lander) Science Payload				
	Estimate (Kg)	% Total Dry Mass	% Contingency	Allocation (Kg)
Lander Camera (2 Flt. Units)	0.6	0.4	30	0.8
Radio Science (In Comm.)	0.0	0.0	30	0.0
Seismometer	2.3	1.6	30	3.0
Surface Chemistry Package	3.0	2.1	30	3.9
LDMS	4.0	2.8	30	5.2
Piezoelectric Corer	1.3	0.9	30	1.7
Surface Ice Oxidant Detector	0.3	0.2	30	0.4
Sample Arm Mechanism	3.0	2.1	30	3.9
Payload Total	**14.5**	**10.2**	**30**	**18.9**
Step 3 (Lander) Spacecraft Bus				
	Estimate (Kg)	% Total Dry Mass	% Contingency	Allocation (Kg)
Mechanical	37.8	26.5	30	49.1
Attitude Control	9.8	6.9	30	12.7
Thermal	7.8	5.4	30	10.1
Propulsion	13.9	9.7	30	18.1
Power (Includes S/C Harness)	16.2	11.4	30	21.1
C&DH	33.7	23.6	30	43.8
Communications	9.1	6.4	30	11.8
Bus Total	**128.3**	**89.8**	**30**	**166.7**
Step 3 (Lander) Dry Mass				
	Estimate (Kg)	% Total Dry Mass	% Contingency	Allocation (Kg)
Science Payload Total	14.5	10.2	30	18.9
Bus Total	128.3	89.8	30	166.7
Lander Dry Mass	**142.8**	**100.0**	**30**	**185.6**
Step 3 (Lander) Wet Mass				
	Estimate (Kg)	% Total Wet Mass	% Contingency	Allocation (Kg)
Lander Dry Mass	142.8	77	30	185.6
Propellant Mass	42.4	23	0	42.4
Lander Wet Mass	**185.1**	**100**		**227.9**

Table 3.3.3-9: Characteristics of Radioisotope Power Supply Units

No.	Type	Unit Mass (kg)	Unit Power BOL (W)	Power Loss (%/Year)	Unit Power 18.8 year EOL (W)	Total Power EOL (W)	Total Mass (kg)
3	RTG	44	125	1.6	96	288	132
4	ASRG	20.2	143	0.8	124	372*	80.8
* assumes one of four ASRG units has failed							

pitch and yaw control as well as for trajectory correction maneuvers. The monopropellant thrusters are used for both ACS control and ΔV to avoid exposing the stainless steel oxidizer thruster valves to N_2O_4 and to avoid the potential for iron nitrate contamination during the 11.7-year cruise to Saturn. Following SOI, all thrusters operate in pressure regulated mode. The orbiter provides the ΔV in bi-propellant mode (with monopropellant for ACS control) for EOI and for maneuvers required while in Enceladus orbit. Orbiter maneuvers occur frequently enough to the purge the

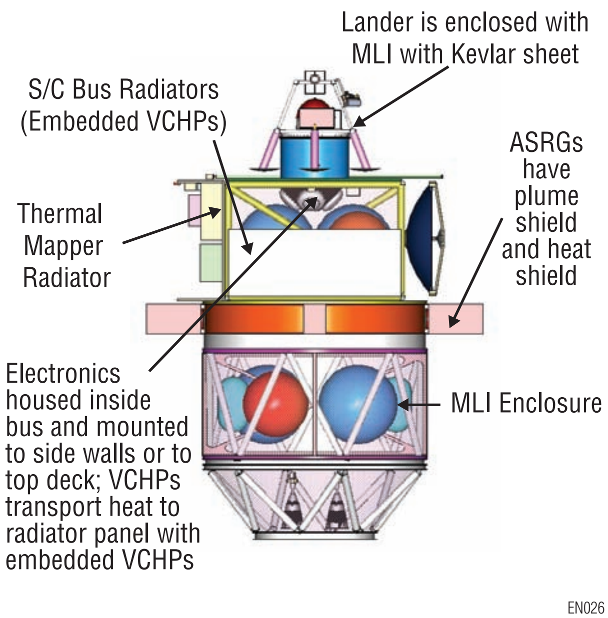

Figure 3.3.3-17: Enceladus-OL Stage 1 Thermal Configuration

anticipated build up of iron nitrate. The orbiter also operates in monopropellant blowdown mode for Stage 2 pitch, roll, and yaw control, as well as for roll control of Stage 1 prior to EOI. Following EOI, all thrusters operate in pressure regulated mode. Titanium is used for booster and orbiter tanks, components, and lines up to the thruster valves.

Both the booster and orbiter propulsion systems contain two 445 N bi-propellant main engine thrusters. The booster step has eight monopropellant 22 N thrusters for pitch/yaw control and ΔV, and the orbiter has 16 monopropellant 22 N thrusters for pitch/yaw control and ΔV and eight monopropellant 4 N thrusters for roll control. These thrusters, which include redundant thrusters, are existing hardware. Each system contains two hydrazine, two N_2O_4, and two helium (pressurant) tanks. Customized tank volumes are used to limit the mass of the propellant tanks on both the booster and the orbiter. This may result in the need for re-qualification. The propellant distribution between the booster and orbiter resulted from an optimization study that maximized mass available for the lander. The combination of maneuvers conducted in bi-propellant and monopropellant mode over the total propellant expended results in an effective I_{sp} for the booster and orbiter of 293 s and 303 s, respectively. The propellant quantities in Tables 3.3.3-6 and 3.3.3-7 include a 5% tax for attitude control maneuvers.

3.3.3.2.3.5 Enceladus-OL (B & O) Attitude Control Subsystem

Three axis attitude control is provided by four 4 Nms reaction wheels mounted on the orbiter and by thrusters mounted on both the orbiter and the booster. The wheels are oriented such that any three suffice to meet control requirements and such that momentum unloading (not done when communicating or taking science data) can be done with pure torques. Attitude knowledge is provided by a combination of two star trackers, eight coarse Sun sensors, and two inertial reference units. The orbiter attitude control requirement of .028 deg is driven by the laser altimeter instrument.

During the inner planet flybys and up to about 1.5 AU, Stage 1 is oriented with the booster engine pointed toward the Sun to minimize the thermal load from absorbed solar flux. In most cases, Stage 1 slews away from this orientation for communication events using the HGA. Beyond about 1.5 AU, it is no longer necessary to orient the booster engine toward the Sun for thermal reasons. During the SOI burn and EOI burns, the Stage 1 and Stage 2 engines, respectively, orient along the velocity vector.

Orbiter slew times meet communication line of sight requirements between the lander and the orbiter, which is in the 45° inclination, 200 km orbit (even with the altitude variations observed in this orbit, the slant range will be always be greater than 200 km). They also suffice to slew the instrument boresight 30° off nadir (about the longitudinal axis) prior to plume passage in the polar orbit to help protect the optical instruments and to orient the GCMS into the nadir position. The use of larger wheels could reduce the boresight slew time and increase the time available for mapping. Thrusters could also be used to do this, but the weak orbit stability may be incompatible with the use of thrusters. The wheels will be maintained above a threshold speed to prevent lubricant deterioration.

3.3.3.2.3.6 Enceladus-OL (B & O) Avionics and Flight Software Subsystem

The avionics system is fully block redundant, and its components are located on the orbiter and principally in the ring housing the ASRGs. The system uses an architecture based on a PowerPC class single board computer, MIL-STD-1553 for command and telemetry, RS-422 for science data acquisition and Spacewire or cPCI for internal high speed communications, and I2C for internal low speed communications. Autonomous, on-board fault detection and correction and safe mode capability is implemented due to the ~80 minute communication delay between the DSN and the orbiter. Flight software margins for the central processor and memory exceed 50%. Three test strings are used, one for each of the C&DH and ACS testbeds and one for the system level / maintenance testbed (the latter being the highest fidelity).

Avionics boxes are shielded with 2.54 mm aluminum. With this thickness of shielding, radiation models predict a total absorbed dose of 10 krad prior to SOI. The SATRAD model used to estimate Total Ionizing Dose (TID) once within the Saturn system estimated a TID as high as 2 krad/week for trapped particles or 250 krad for the 2.4 year mapping mission. Applying a (customary) factor of two for design margin, the TID becomes 500 krad. The TID for the 3.5 years spent in Rhea and Dione flybys is anticipated to be an order of magnitude lower than for the mapping phase. That gives a mission TID of ~560 krad with 2.54 mm shielding, which is well above an acceptable (< 100 krad) level. An increase in shield thickness (approximately double, with an attendant increase in mass) will be required to decrease the TID to an acceptable level of about 50 krad. It should be noted that: a) the SATRAD model has not been validated for TID estimation, and b) this analysis accounts for no reduction in the radiation environment due to the presence of the neutral gas torus in the vicinity of the Enceladus orbit, since that reduction has not been validated.

3.3.3.2.3.7 Enceladus-OL (B & O) Communications Subsystem

The communications system consists of a fixed 1.5 m diameter high gain antenna (HGA) system and a nadir and zenith mounted omni antenna system on the orbiter. The capabilities of the systems are summarized in **Table 3.3.3-10**. When the HGA is needed, the orbiter will slew to point the HGA. Ranging can be done using the HGA with X-band uplink and Ka-band downlink or can be done with X-band uplink and downlink on either the HGA or the omni system. Ranging can be performed simultaneously with telemetry transmission. Telemetry coverage is provided by the omni antennas for ΔV burns for critical events such as SOI, EOI, and Enceladus orbit plane changes, which require a specific thruster orientation. Upon completion of the event, the orbiter slews quickly using thrusters to point the HGA toward Earth to dump the full telemetry stream from the event. Communications coverage during the SOI burn will be interrupted when Stage 1 is eclipsed by Saturn (as a point of reference, Cassini was out contact for about 65 minutes during the SOI burn). The balance of critical event burns can be accomplished within communications contact of DSN. Margins of 3 dB or better exist on all links with the exception of the omni antenna uplink and downlink link between the orbiter and the DSN. Given the transmit power for the omni is relatively high and the data rate is about as low as practical for this stage of design, the addition of a medium gain antenna may be a better option for improving link margin than increasing power or reducing data rate.

Table 3.3.3-10: Enceladus-OL Orbiter Communication Capability at Enceladus

	HGA Ka Band	HGA X Band	OMNI
Orbiter			
Transmit to Earth	40 kbps	8 kbps	3 bps*
Receive From Earth		2 kbps	10 bps*
Transmit to Lander		~ 2 kbps	
Receive from Lander		500 kbps	
Lander			
Transmit to Orbiter			500 kbps
Receive from Orbiter			~ 2 kbps
* Link margin is less than 3 dB			

The total data volumes stored for the polar orbit, the 45° mapping orbit, and for the lander are summarized in **Table 3.3.3-11**. These volumes assume 10:1 compression on the visible/near infared mapper, 5:1 compression on the lander cameras, and include instrument and spacecraft housekeeping along with 30% contingency. Data storage volume differs from downlink data volume in that it includes 7-bit Hamming code error detection whereas the downlink data volume excludes Hamming code error detection and includes Reed Solomon coding overhead. Both storage and downlink include CCSDS overhead. Orbiter instruments (aside from dust micro-analyzer and magnetometer) collect data for 25% of the 4.3 hour orbit on south pole passes and 25% of the orbit on north pole passes. The magnetometer collects data continuously, and the dust micro-analyzer collects data selectively.

Table 3.3.3-11: Enceladus-OL Data Stored and Transmitted

	Total Data Stored (Gb)	Total Data Transmitted (Gb)
Orbiter 90 deg orbit	19.17	18.12
Orbiter 45 deg orbit	1.17	1.10
Lander	0.803	0.651

As discussed in **Section 3.3.3.1.3**, the daily data collection in the 45° orbit is limited by the orbiter downlink rate and by a communication window of 9.0 hours per day, per the study Study Groundrules. A period of 7.64 hours is required to downlink 1.10 Gb at 40 kbps, and Enceladus eclipses the orbiter line of sight to Earth for about 1.25 hour. Data taken during each polar campaign will be stored for transmission once back in the 45° orbit to avoid time lost to slewing. Transmitting about 18.1 Gb of polar orbit data requires 16 passes of just under eight hours each to the DSN at 40 kbps. Lander data will be transmitted to the orbiter while in the 45° orbit. About 22 minutes per day is required to transmit lander data to the orbiter. With the lander located exactly at the south pole (worst case) and a 5° elevation angle, the minimum contact time available is 94 minutes per 24 hour Earth day (the orbiter would be above 10° elevation for at least 24 minutes per day if the lander were located exactly at the south pole). The contact time increases rapidly as the location moves away from pole and/or the elevation constraint is relaxed. Over six hours per day is available at a latitude of -70°. Mapping operations will be suspended for the brief time it takes to collect and downlink the lander data.

3.3.3.2.4 Enceladus-OL Lander Description

The lander design and operation is described in the following section. All lander subsystems are single fault tolerant for credible failures.

3.3.3.2.4.1 Enceladus-OL Lander Descent, Landing, and Surface Operations

The lander delivers the instruments listed in **Table 3.3.2-2** to the surface of Enceladus to operate for eight days. The lander is off for most of the time between launch and its deployment, about 17 years later. It is turned on periodically to checkout the lander components. While attached to the orbiter, the lander uses power from the orbiter.

The target landing site is between 70° S and the south pole. It is selected after analysis of images from the first polar orbit campaign. The landing site needs to be smooth, flat, and have evidence of relatively fresh material. The hazard avoidance algorithms will be tailored based on the features that surround the targeted site. The images gathered in the first polar campaign are converted on the ground into targeting maps that the lander uses during the automated landing. These maps are tested using the ground simulators and then uploaded to the lander via the orbiter. The landing time is selected so that the lighting conditions are similar to that of the targeting maps.

The lander is deployed from the orbiter using a clampband separation system and springs. The landing profile is shown in **Figure 3.3.3-18**. At the equator, the lander performs a major propulsion burn to change its inclination and lower its periapsis. The lander continues on this trajectory using the Inertial Measurement Unit (IMU) until it is 20 km from the surface. At that point, it uses its imager and the onboard maps to determine its position. It uses the propulsion system to slow its descent and to translate to a position above the landing target. At a 5-km height, the hazard avoidance software uses the data from the imager and the range finder to identify and avoid hazards, such as ice blocks that are larger than ~25 cm that could cause the lander to overturn. The lander turns off the thrusters at a height of 20 meters and the lander descends gently to the surface. The lander retains a small residual horizontal velocity when the thrusters are turned off so that the thrusters' plumes do not contaminate the landing site. The lander has sufficient propellant to allow for the identification and avoidance of hazards. The landing trajectory is designed so the lander can communicate with the orbiter from deployment through landing.

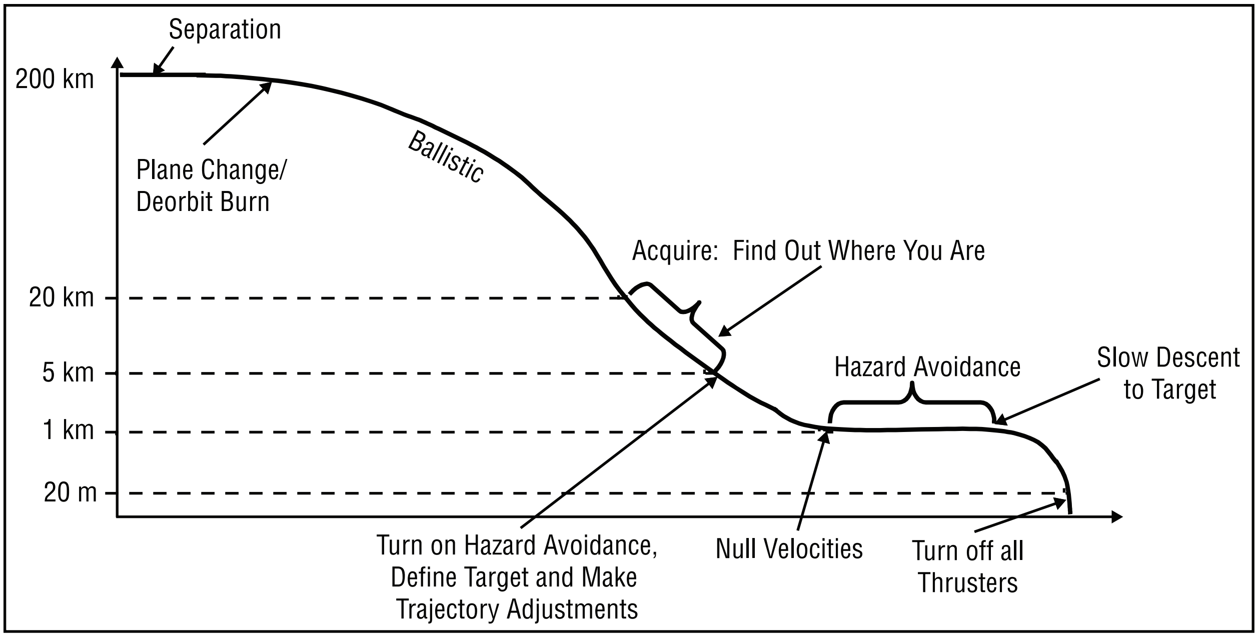

Figure 3.3.3-18: Enceladus-OL Landing Profile

The instruments start operating immediately upon landing (landing is indicated by the accelerometer) and are turned off once they have completed their observations in order to conserve power. Operations for the sample analysis instruments are complete after 24 hours. Operations for the imagers are complete after 36 hours. The seismometer (incorporated within the lander footpad) remains operating for eight days. The imagers take a panoramic picture every two hours over one Enceladus day. The imagers also observe the plumes, with onboard change detection software processing this data to reduce its volume. The sample collection device collects *in-situ* samples and distributes them to the three sample analysis instruments. The lander's avionics collects the instrument data and sends it back to the orbiter once per day. The lander communications approach is discussed in **Section 3.3.3.2.3.7**. The lander transmitter will be turned off between communication events, by stored command, to conserve power and will be turned on by stored command. The orbiter has additional capability to command the transmitter on and off, also by stored command.

3.3.3.2.4.2 Enceladus-OL Lander Mechanical Subsystem

The lander structure uses carbon fiber composite and aluminum alloy in the feet and on the lander side of the separation structure. The lander legs use a sleeve within a cylinder arrangement to absorb the shock of landing. A pan and tilt mechanism is provided for the camera instruments. **Figures 3.3.3-15** and **3.3.3-16** show the lander and its components.

3.3.3.2.4.3 Enceladus-OL Lander Power Subsystem

Power for the lander is provided by a 5000 Whr lithium ion non-rechargable battery. The lander operating life is eight days. Prior to separation, the lander uses the orbiter power as needed to maintain temperatures within limits and to perform periodic checkouts and engineering functions.

3.3.3.2.4.4 Enceladus-OL Lander Avionics and Flight Software Subsystems

The avionics subsystem is 1-fault tolerant and the lander can autonomously switch to the redundant avionics string if it detects a problem. The avionics includes the lander processor, a communications card, data compression for the imagers, propulsion electronics, power supply electronics, and electronics for the thermal system. The processor is a PowerPC class unit that provides 240 MIPS at a clock speed of 132 MHz. The avionics uses RS-422 connections to the science instrument for science data and a 1553 bus for command and telemetry communication. Storage for 803 Mbits of science and housekeeping data is provided.

The lander flight software processes the imager, laser altimeter, and other ACS sensor data to provide for a safe landing. It uses the onboard maps and the imager data to locate itself, then drives the lander to the target while avoiding hazards. Once on the ground, the flight software processes the plume images to detect changes in order to reduce the volume of the data. Flight software margins for the central processor and memory exceed 50%.

3.3.3.2.4.5 Enceladus-OL Lander Propulsion Subsystem

The lander propulsion system is a monopropellant blowdown design, using a single hydrazine tank, one 22 N main thruster, and redundant strings of eight 4 N attitude control system thrusters. The propulsion system is single fault tolerant to credible failures; the ACS thrusters can be used in the event of a main engine failure. The propulsion system is sized to provide 415 m/s of ΔV (including ACS tax and reserve) to accomplish the plane change and retroburn and to null the impact velocity. This ΔV includes an allocation for hazard avoidance as described in **Section 3.3.3.1.4**. An area that merits future study is the use of a pressure regulated system that maintains a constant level of thrust.

3.3.3.2.4.6 Enceladus-OL Lander Attitude Control Subsystem

The lander attitude control system consists of redundant IMUs (gyro and accelerometer), laser rangefinders, and the imaging instruments. The lander uses the IMU for navigation from separation from the orbiter until the lander is about 20 km from the surface. At that point, the navigation transitions to use of the imager and the laser rangefinder to complete the landing. The redundant attitude control thruster strings mounted on the top and bottom decks provide six degree-of-freedom control. The IMU is calibrated prior to release from the orbiter.

3.3.3.2.4.7 Enceladus-OL Lander Thermal Control Subsystem

The thermal system maintains the temperature of the instruments, battery, electronics, and propulsion systems within operating limits. The lander is covered with 18 layers of MLI including a layer of Kevlar. The lander propulsion module is thermally conditioned prior to separation to minimize the amount of lander battery power required for heaters. A combination of electrical heaters (primarily for the propulsion module) and radioisotope heater units (RHUs) are used to maintain temperatures within operating limits. The thermal system uses RHUs to heat the interior cavity of the lander. Electrical heaters are used for the sampling mechanism. Propulsion system heaters are turned off after landing.

3.3.3.2.4.8 Enceladus-OL Lander Communications Subsystem

The lander communicates with the orbiter in X-band. The lander's frequencies are reversed from the orbiter, with the lander's transmitter using the same frequency as the orbiter's receiver and vice versa. The lander uses a one Watt transmitter and two cross dipole omni antennas that are positioned 180° apart and pointed 60° from zenith. The orbiter uses its high gain antenna to communicate with the lander, and the link margin is 4 dB. The data rate from the lander to the orbiter is up to 500 kbps. The telemetry data is convolutionally encoded.

3.3.3.2.4.9 Enceladus-OL Lander Integration and Test (I&T)

The lander is integrated and tested as a unit, in parallel with the orbiter (see **Section 3.3.3.2.7**). The lander I&T process is designed for planetary protection class IV, including cleaning at the launch site.

The lander requires unique I&T facilities. A drop test facility is required to verify some of the landing techniques, including target acquisition, hazard avoidance, and correct responses to contingencies. A hybrid simulator is used to test and verify those functions that cannot be completely tested by the drop test facility. A subset of the lander test equipment is maintained through the actual landing, so landing can be tested using the targeting maps acquired during the first polar campaign.

3.3.3.2.5 Enceladus-OL Mission Reliability

Even with single fault tolerant design, the mission level Enceladus-OL reliability (a total of

18.3 years was used for this analysis) is low. The probability of mission success for the entire flight segment is 0.595, estimated at the 95% confidence level (i.e., in at least 95% of 1000 random cases evaluated by a Monte-Carlo model the reliability was at or above 0.595). Propulsion, thermal, and attitude control systems are the mission reliability drivers, and the effect is most pronounced on the orbiter and booster, which have significantly longer operating lives than the lander. Instrument and launch vehicle reliability were not addressed in this model, i.e., they were assumed 100% reliable. It is noted that the absolute values associated with this type of very early reliability estimate typically are considered to be less meaningful than the relative values among estimates (i.e., between the Enceladus-OL, Enceladus-O, and Saturn-OL estimates) and also tend to be conservative. However, these initial reliability results clearly indicate the need for special attention in future studies.

3.3.3.2.6 Enceladus-OL Orbital Debris Protection

A 1.0 mm Kevlar sheet is used to reinforce MLI on the lander and to shield the lander from plume particles during pre-lander separation, and during polar campaign operations. As discussed in **Section 3.1.1.4**, a maximum particle diameter of 2.0 mm and a maximum particle relative velocity of 500 m/s have been assumed. The 1.0 mm Kevlar sheet provides some margin against the 0.74 mm required facesheet thickness. Propellant tanks are also protected from micrometeorid impact during Earth flybys by a combination of external MLI over a 1.0 mm Kevlar panel, and internal MLI is offset sufficiently from the propellant tanks to act as a Whipple shield. This separation distance is 0.44 cm, or five times the particle diameter of 0.087 cm needed to penetrate the critical surface. The probability of collision with small objects during two Earth flybys is .001, an order of magnitude below the maximum permitted probability of .01, due mainly to the short amount of time the spacecraft spends near Earth.

3.3.3.2.7 Enceladus-OL Mission Level I&T

Parallel fabrication and component test of the booster, orbiter bus, orbiter instruments, lander bus, and lander instruments starts in January 2015. This is followed by parallel I&T for the same hardware elements starting in March 2016 (this phase includes lander drop testing). Instruments are then integrated with the orbiter bus and lander bus starting in January 2017, fit checks are conducted with the booster, and parallel orbiter and lander I&T is conducted. In November 2017, the orbiter and lander are mated for I&T as a combined unit. In March 2018, the booster is integrated with the orbiter and lander and combined booster/orbiter/lander I&T is conducted. The flight segment is ready for shipment to the launch site in June 2018 for a September 2018 launch.

3.3.4 Enceladus-OL Operational Scenarios

Table 3.3.4-1 identifies the driving operational scenarios for this mission concept.

Table 3.3.4-1: Enceladus-OL Driving Operations Scenarios

Scenario	Driver
Venus Flyby	Thermal
Earth Flyby	Safety
Enceladus Orbit Insertion	Power
Titan/Rhea/Dione Flybys	Navigation
Enceladus Mapping	Data Volume
Polar Campaign	Data Storage
Landing	Lander Design

The thermal environment drives the operations early in the mission during Venus and Earth flybys when the spacecraft is close to the Sun. During most of this time, and roughly inside of the Mars orbit radius, the bottom of Stage 1 is pointed to the Sun. This surface is covered with heat resistant ceramic cloth, similar to that used by Messenger, except for the thruster nozzles. Variable conductance radiators on the spacecraft provide for maximum radiating area during this phase, whereas radiator area can be closed down later in the mission when the solar environment is reduced. As this thermal pointing constraint restricts the ability to point HGA, X-band omni antennas are used for communications during most of this time. Using the omni antennas (data rate as low as 60 bps at maximum range during this phase) does not permit returning all the spacecraft housekeeping data except when the spacecraft is in the vicinity of the Earth. Instead, the flight software provides event messages and snapshots of the status of the spacecraft subsystems during the regularly scheduled DSN contacts. If a problem is detected, the spacecraft can be oriented briefly to use the HGA to dump the full set of housekeeping data.

The plutonium in the ASRGs would be a potential health hazard if the spacecraft were to enter the atmosphere during the Earth flybys. This mission uses techniques that were used on Cassini to mitigate this risk. These techniques include additional micrometeoroid protection for the propellant tanks, biasing the trajectory away from the Earth until 7-10 days before the flyby, and using special policies regarding uplinking real time commands during parts of the flyby.

The booster provides the ΔV for the SOI burn and for targeting the Titan/Rhea elliptical orbit. The Titan/Rhea/Dione flyby phase uses gravity assists from Rhea and Dione to reduce the ΔV required to get into orbit around Enceladus. This phase takes 4.25 years and includes 47 flybys of these moons. This phase drives the navigation support for the mission. The ground navigation team plans the maneuvers required to target the flybys, monitors the maneuvers and flybys, and adjusts the subsequent plans as necessary. This phase begins after the apoapsis maneuver and includes four flybys of Titan to reduce the periapsis to Rhea, 30 flybys of Rhea to lower the orbit from Titan/Rhea to Rhea/Dione, and 13 flybys of Dione that result in a Dione/Enceladus orbit. At the end of this process, the orbit is about two days long. The number of navigation operations requires a navigation process that has the staff to respond promptly with orbit solutions and maneuvers plans to safely operate the mission in this phase.

The orbiter propulsion system provides the ΔV for the EOI maneuver and for small targeting maneuvers needed for the Rhea/Dione walkdown. Once in orbit around Enceladus, mapping and communication operations are conducted as discussed in **Sections 3.3.3.1.3** and **3.3.3.2.3.7**. **Figure 3.3.4-1** shows the timeline during the mapping phase. The magnetometer is taking data all of the time, but the other instruments only take data infrequently. The instruments are powered on all of the time to maintain their stability.

The orbiter has two polar campaigns, each 24 hours long. These polar campaigns drive the orbiter data storage as discussed in **Section 3.3.3.2.3.7**. The instruments generate data over both the north and south poles from 65° and poleward, the areas not well covered in the mapping orbit. **Figure 3.3.4-2** shows the timeline for the instrument data taking in this phase. During the polar campaign, the orbiter passes through the plume on every orbit. The side of the orbiter with the thrusters and selected points on the nadir pointing side of the orbiter have blankets to protect from plume particles.

The lander timeline is shown in **Figure 3.3.4-3**. The instruments are on until they have completed their objectives, and then they are turned off to save power. The seismometer is on the longest, with a science requirement to be on for at least 5 days. Over the nominal eight-day lifetime, the lander generates 5.22 Gbits of data. This data is transferred at least once per day to the orbiter as described in **Section 3.3.3.2.3.7**.

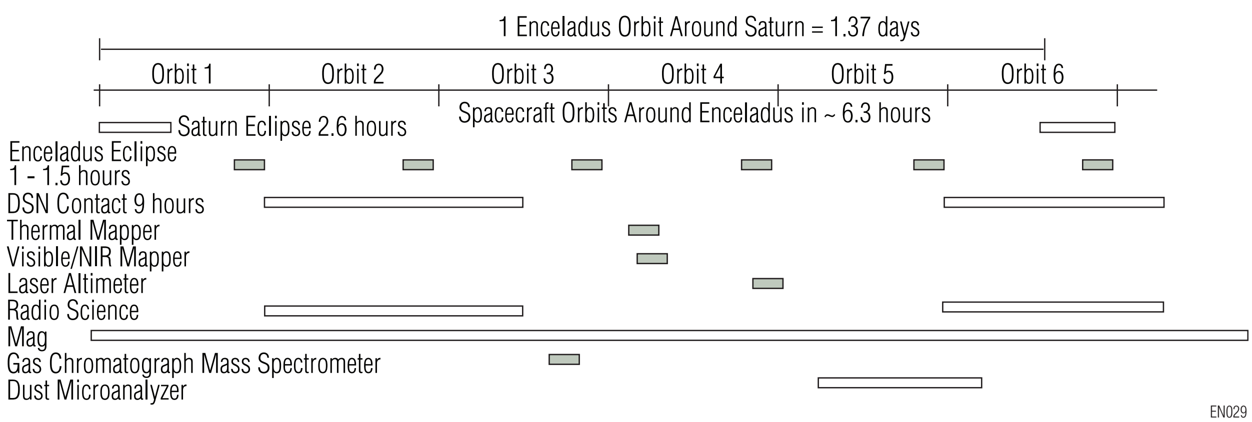

Figure 3.3.4-1: Enceladus-OL Mapping Phase Timeline

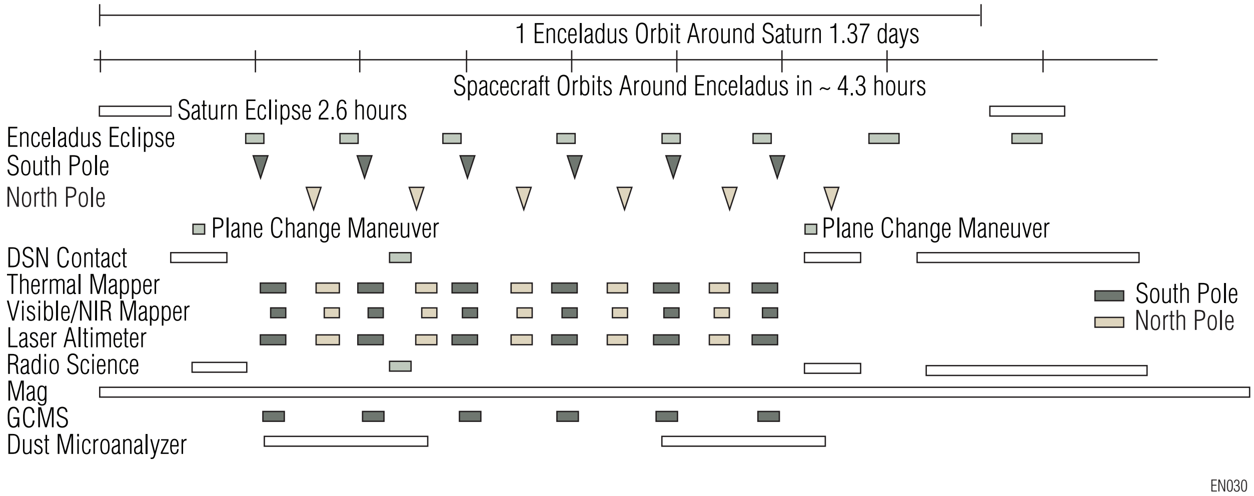

Figure 3.3.4-2: Enceladus-OL Polar Campaign Timeline

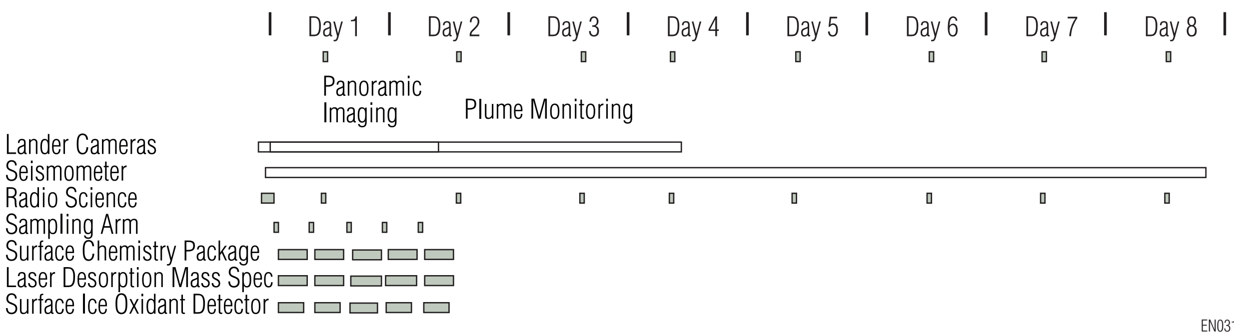

Figure 3.3.4-3: Enceladus-OL Lander Instrument Timeline

3.3.5 Enceladus-OL Planetary Protection Approach

The lander is designed and cleaned to planetary protection level IV. Additionally, it is assumed the booster will separate after insertion into the Titan/Rhea elliptical orbit. Analysis that demonstrates the booster will have less than a $1x10^{-4}$ probability of inadvertently contaminating any icy moon inside of Titan's radius has not been done, and is a recommended future study. For the purposes of this study, it was presumed the booster would need to be cleaned to planetary protection level IV.

3.3.6 Enceladus-OL Major Open Issues and Trades

3.3.6.1 Flight Dynamics and ΔV Reserve

A ΔV reserve of 500 m/s has been held to account for uncertainties in the trajectory modeling up through Saturn capture and for uncertainties in Enceladus orbit stability. Further study is required to optimize the trajectory assumptions used, as well as to explore other possible paths to Enceladus that might be shorter or less expensive. Further study is also required to investigate the stability of the Enceladus orbit.

3.3.6.2 Radiation Environment

The discussion in **Section 3.3.3.2.3.6** indicates radiation shielding for electrical components needs to be doubled from 2.54 mm to 5.08 mm to assure TID levels below 100 krad, if results from SATRAD are to be used and if no reduction in the radiation environment due to the presence of the neutral gas torus in the vicinity of Enceladus is assumed. Additionally, the Saturn radiation models should be updated based on Cassini experience.

3.3.6.3 Reliability

3.3.6.3.1 Mission Reliability Estimate

The overall mission reliability estimate (59.5% at 95% confidence level) discussed in **Section 3.3.3.2.5** indicates the need to conduct an early probabilistic risk assessment to identify design or operations changes that could improve reliability for the most likely failure modes.

3.3.6.3.2 Hibernation Mode

The cruise phase, from the last Earth flyby until SOI, is almost six years long. The use of Hibernation mode, soon to be used on New Horizons, should be investigated. In Hibernation mode, the spacecraft spins for stability, some spacecraft subsystems are turned off, and communication is limited to once per week via beacons that indicate whether the spacecraft is either in a safe state or whether it needs ground intervention. Hibernation mode could save operations costs, as operations staff is reduced. It could also increase overall mission reliability as a result of reducing the operating lifetime of some of the spacecraft components.

3.3.6.4 Landing Operations

Further trade studies are needed on the attitude sensors. Additional sensors, such as a star tracker, could provide a more robust landing design that would better protect from unexpected deviations from the nominal landing trajectory. The thrusters induce variation in the images used to locate the landing site. Work is required to understand how to compensate for this motion, and understand the implications on the image processing speed.

A trade study to evaluate the use of a pressure regulated (constant thrust) propulsion system vs. a blowdown (non-constant thrust) system, including requirements for software, is also recommended.

3.3.6.5 Fault Detection and Correction

The fault detection and correction approach for the critical burns needs to be better defined to enable a better understanding of how a failure in one of the redundant booster or orbiter main thrusters affects achieving orbit insertion and attitude stability for the remainder of the burn.

3.3.6.6 Mapping Duty Cycle

The mapping orbit lifetime was determined by the mapping time (12 days) divided by the communication bandwidth limited duty cycle of 1.85%. In the 12-day mapping time, all areas are imaged once; however some areas are imaged multiple times. The science objective is to image the area once, so the mission lifetime could be reduced after the analysis of the duration required to image everything once is performed.

3.3.6.7 Communications

3.3.6.7.1 Science Downlink

Evaluate reducing the data quantity (e.g., via compression or editing) or increasing the transmitted data rate (e.g., via a larger HGA or increased power) to reduce the time required to complete the primary mission. This would reduce both the cost (this phase has the highest Phase E staffing) and the risk of a failure prior to completing the primary science phase.

3.3.6.7.2 Medium Gain Antenna

Evaluate use of a medium gain antenna to increase the link margin for command uplink and for telemetry downlink link between the orbiter and the DSN when the HGA is unavailable.

3.3.6.8 Staging and Booster Disposal Strategy

Determine the optimal strategy for staging with respect to delivered mass, cost, and complexity. The study also should assess the optimal location for booster separation and should define trajectories that assure the booster will have a less than 1×10^{-4} probability of inadvertently contaminating an icy moon.

3.3.7 Enceladus-OL Technology Needs

The Enceladus-OL mission uses existing technology with the single exception of the hazard avoidance system for the lander. This system is required to autonomously identify landing hazards such as steep slopes or rough terrain and guide the lander to a safe landing site. NASA is currently investigating hazard avoidance sensors and algorithms for landing on the Moon and Mars. The Autonomous Landing and Hazard Avoidance Technology (ALHAT) is one of several technology initiatives in this area. ALHAT is currently at

TRL 4 and is expected to be at TRL 6 in FY 2011, prior to the need date for the Enceladus-OL mission. An Enceladus-OL mission should be able to adapt these techniques rather than have to design entirely new techniques.

If the technology were not mature enough to use on this mission, the alternative would be to add the capability to image potential landing sites at higher resolution and identify sites without hazards. In addition, the lander could be made more robust to hazards – for example, the ability to operate successfully on steeper slopes or to land safely amid larger rocks/ice chunks.

3.3.8 Enceladus-OL Technical Risk Assessment

3.3.8.1 Mission Lifetime

The 18.3-year mission life poses inherent design risks. Several components are not qualified for this lifetime. For example, the ASRG is rated for 14 years of operation and the booster and orbiter pyrovalves have been qualified for 10 years.

The long mission duration is also an operational risk, in maintaining expertise that is developed in phase C/D until it is needed, potentially 20 years later. The development effort includes knowledge capture, to document the designs and any insights that result from the integration and test of the instruments. The mission maintains the high fidelity simulator for the orbiter and lander, to test new operations sequences and any flight software changes before their use onboard. The mission also maintains the unique landing test facility, so that the landing can be simulated before it is actually done, using the maps that are generated from the orbiter observations.

3.3.8.2 Enceladus Gravity Model

The current Enceladus triaxial gravity model provides for a 45° orbit that is stable for long periods of time and permits a 24-hour polar orbit. The model can get minor adjustments based on future Cassini flybys, but won't be significantly improved until an orbiter reaches Enceladus. The Encleadus-OL orbiter has some fuel allocated for maintenance in the 45° orbit. If the gravity field is found significantly different in ways that decrease the stability of the orbits, it may compromise the science goals for the polar orbits, for *in-situ* plume sampling, and possibly for the mission duration required to completely map the lower latitudes. This risk can be mitigated by developing contingency plans using a variety of plausible gravitational models and understanding where the stable orbits are for each one.

3.3.9 Schedule

The Enceladus-OL design uses a development schedule of 72 months from the start of Phase B to launch. The durations of Phase B, C, and D are 12 months, 15 months, and 49 months, respectively. The length of Phase D is driven principally by the length of time need to fabricate, integrate and test the booster, orbiter, and lander systems both separately and in combined configurations, and includes the four month period immediately following launch (i.e., the duration of Phase D up until launch is 45 months).

3.4 Enceladus Orbiter (Enceladus-O)

3.4.1 Enceladus-O Architecture Overview

The Enceladus-O mission concept includes an Enceladus orbiter without a lander. As Enceladus-O shares many design and operating characteristics with Enceladus-OL, only a discussion of the aspects that differ is provided in this section, along with significant study results. References to **Section 3.3.3** are given where design and operating characteristics are shared with Enceladus-OL. Enceladus-O uses dual mode bi-propellant N_2O_4 / hydrazine propulsion in the booster and in the orbiter. The orbiter instrument suite is the same as that in the Enceladus-OL design with the exception that a sounding radar is included. The launch and ground segments are identical to that described in **Section 3.3.1**.

3.4.2 Enceladus-O Science Investigation

With an Enceladus orbiter alone, most of the science goals in **Table 2.1.1-1** can be met with the addition of a radar sounder to the strawman payload, though Composition and Tectonics, etc., are better addressed with a landed package, as shown in **Table 2.4.6-1**. The goals are identical to those for the Enceladus-OL concept discussed in **Section 3.3.2**, with the exception that the Enceladus-O concept adds:

Orbiter Science Drivers:

- radar subsurface sounding
  - Ice shell thickness, structure

The incremental (relative to **Table 3.3.2-1**) strawman orbiter payload for Enceladus-O is shown in **Table 3.4.2-1**.

3.4.3 Enceladus-O Mission Design

The following sections focus principally on the flight segment. Interfaces with the ground and launch segments will be summarized only, as the configuration of these segments was given in the Study Groundrules.

3.4.3.1 Enceladus-O Flight Dynamics

3.4.3.1.1 Enceladus-O Launch Window

The time of flight and launch capability are defined using the same 20-day launch window and constraints as used for Enceladus-OL and shown in **Table 3.3.3-1**, and the VVEES trajectory is the same as used for Enceladus-OL and shown in **Table 3.3.3-2**.

3.4.3.1.2 Enceladus-O Capture at Saturn and Rhea Walkdown

As for Enceladus-OL, there are two key enablers for the Enceladus-O mission. The first is staging, discussed in **Section 3.3.3.2**, and the second is the use of Rhea flybys discussed in **Section 3.1.1.2.2** and in **Figures 3.4.3-1A** and **3.4.3-1B**, to scrub orbital energy prior to conducting the EOI burn. A total of 30 Rhea flybys is used to reduce ΔV by 1650 m/s. The cost of adding these 30 flybys is an additional 2.5 years in mission lifetime. The trajectory up to the point of initiating the Rhea flybys is identical to that for Enceladus-OL, and orbital operations at Enceladus are the same as described in **Section 3.3.3.1.3** for Enceladus-OL, with the exception that there is no lander to deploy or operate.

Table 3.4.2-1: Enceladus-O Incremental Strawman Orbiter Payload

Instrument	Mass (kg)	Power (W)	Duty Cycle (in Enceladus Orbit)	Dimensions L x W x H (or L x dia.) (cm)	Data Rate (kbps)	Notes on Downlink	Preferred Location and Aperture Pointing Direction	Req'd Pointing Accuracy (arc sec)	% New Development Req'd	Precursor Instrument
Sounding RADAR	9	20	25%	Antenna 10mx2.6m Electronics 10x15x10	30		Nadir-pointing	3600	~70% new	Europa IDT report

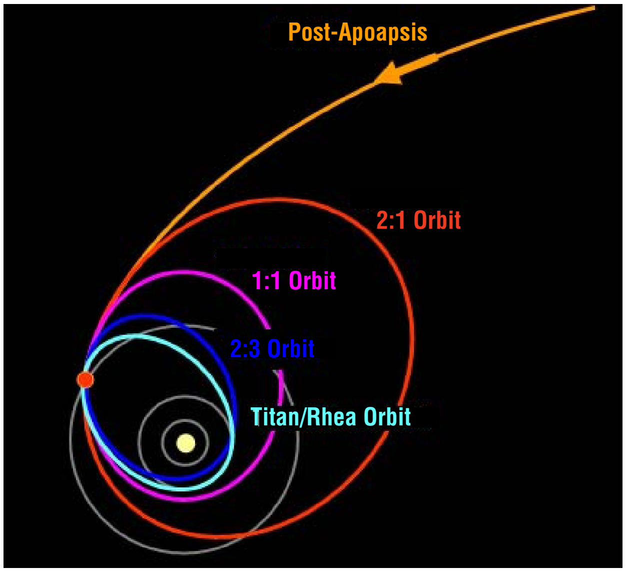

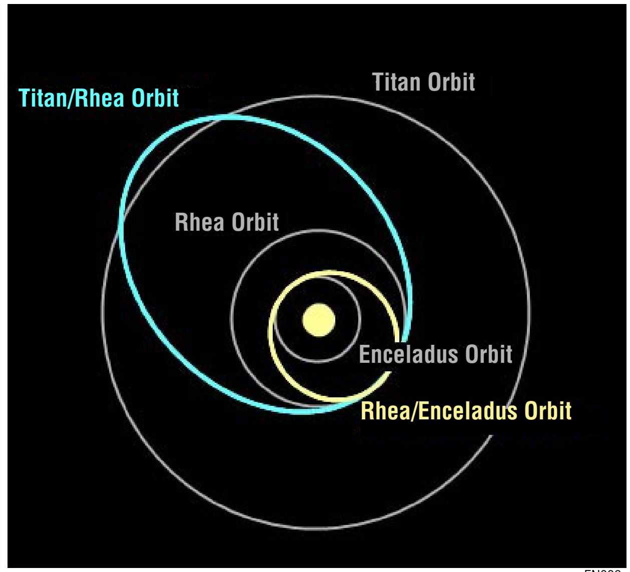

Figure 3.4.3-1A: Multiple Titan Resonant Orbits
Figure 3.4.3-1B: Titan/Rhea/Enceladus Resonant Orbits

3.4.3.1.3 Enceladus-O Orbit Design

The orbit design for Enceladus-O is as discussed in **Section 3.3.3.1.3**, with the exception that the Enceladus-O concept has no lander.

3.4.3.1.4 Enceladus-O Timeline of Key Events

Table 3.4.3-1 gives a high level description timeline of key events in the 17.3 year mission. With the exception that 1.0 year for Dione fly-bys is excluded in the Enceladus-O mission design, the trajectory phases are similar to those in **Figures 3.3.3-9** and **3.3.3-10**.

3.4.3.1.5 Enceladus-O Mission ΔV Budget

The total ΔV for the Enceladus-O trajectory, including maneuvers required to enter orbit about Enceladus and conduct 2.4 years of mapping operations, is 4977 m/s as shown in **Table 3.4.3-2**. This ΔV is used to size the booster and orbiter propulsion systems and includes the ΔV required to accomplish two round-trip plane changes from the 45° mapping orbit to the polar mapping orbit. It also includes a reserve of 10% plus an additional reserve of 500 m/s. In the Enceladus-O study, the 5% tax to account for propellant used in non-ΔV attitude control maneuvers is accounted for as a propellant tax (not shown here), rather than as a ΔV tax.

Table 3.4.3-1: Key Events in 17.3-Year Enceladus-O Mission Timeline

Date	Year	Event
September 29	2018	Launch/Checkout
February 27	2019	Venus Flyby 1
April 22	2020	Venus Flyby 2
June 15	2020	Earth Flyby 1
June 15	2024	Earth Flyby 2
June 10	2025	Mid course trajectory maneuver
May 4	2030	Saturn Orbit Insertion
August 8	2033	Enceladus Orbit Insertion
August	2034	Polar Campaign (24 hours)
August	2035	Polar Campaign (24 hours)
January	2036	End of Mission

3.4.3.2 Enceladus-O Flight Segment Design

The flight segment configuration, mass, and subsystem design approach is discussed in the following sections.

Table 3.4.3-2: Enceladus-O Mission ΔV Budget

Maneuver	ΔV (m/s)	ACS Tax (%)	ΔV (m/s) with ACS Tax	ΔV Reserve (%)	Effective ΔV (m/s)
Launch	0.0	0.0	0.0	0.0	0.0
TCM 1: Target Venus 1	10.0	0.0	10.0	10.0	11.0
TCM 2: Target Venus 2	10.0	0.0	10.0	10.0	11.0
TCM 3: Target Earth 1	10.0	0.0	10.0	10.0	11.0
TCM 4: Target Earth 2	10.0	0.0	10.0	10.0	11.0
Mid Course Correction	10.0	0.0	10.0	10.0	11.0
Saturn Orbit Injection (SOI)	650.0	0.0	650.0	10.0	715.0
Post SOI TCM's	10.0	0.0	10.0	10.0	11.0
Apoapsis Burn	350.0	0.0	350.0	10.0	385.0
Titan Resonant TCM's (as needed)	10.0	0.0	10.0	10.0	11.0
Target Titan 2:1 Orbit	10.0	0.0	10.0	10.0	11.0
Target Titan 1:1 Orbit	10.0	0.0	10.0	10.0	11.0
Target Titan 2:3 Orbit	10.0	0.0	10.0	10.0	11.0
Target Titan 16:31 Orbit	10.0	0.0	10.0	10.0	11.0
Target Enceladus	10.0	0.0	10.0	10.0	11.0
Sub Total Transit to Saturn	**1120.0**		**1120.0**		**1232.0**
Enceladus Orbit Insertion, Ops & Maint					
Match Enceladus	3780.0	0.0	3780.0	10.0	4158.0
Orbit Enceladus	220.0	0.0	220.0	10.0	242.0
Plane Changes (4)	400.0	0.0	400.0	10.0	440.0
Orbit Maintenance (2.4 years)	50.0	0.0	50.0	10.0	55.0
Sub Total Enceladus (no Rhea Flybys)	**4450.0**		**4450.0**		**4895.0**
Total (no Rhea Flybys)	**5570.0**		**5570.0**		**6127.0**
Add 2.5 years & 30 Rhea Flybys					
ΔV Reduction*	1650.0	0.0	1650.0		1650.0
Sub Total Enceladus (with Rhea Flybys)	**2800.0**		**2800.0**		**3245.0**
Total (with Rhea Flybys)	**3920.0**		**3920.0**		**4477.0**
ΔV **Reserve (Held for Modeling Uncertainty)**	500.0				500.0
Total ΔV **with Reserve**	**4420.0**				**4977.0**
* Relative to an approach which enters a Titan-Enceladus elliptical orbit prior to circularizing at Enceladus					

3.4.3.2.1 Enceladus-O Configuration

Figures 3.4.3-2 through 3.4.3-4 shows the general arrangement of the flight segment. The flight segment consists of the booster (also referred to as Step 1) and the orbiter (referred to as Step 2). The orbiter configuration is also referred to as Stage 2, where the booster + orbiter configuration is referred to as Stage 1.

3.4.3.2.2 Enceladus-O Mass Properties

Table 3.4.3-3 gives a top level summary of flight segment mass by stage, including mass contingency. The Stage 1 gross mass is 5810 kg, including the instrument suite shown in Table 3.4.3-5 and propellant. This leaves an 8.4% lift margin on the Delta 4050H lift capability of 6300 kg.

Table 3.4.3-3: Enceladus-O Mission Level Summary Mass Statement

	Enceladus O
Launch Vehicle Margin (%)	**8.4**
Launch Vehicle Capability (kg)	**6300**
	Mass (kg)
Stage 1 (B+O) Initial	5810
- Stage 1 Propellant*	3343
Stage 1 Dry	2466
- Step 1 (Booster) Dry	576
Stage 2 (Orbiter) Initial	1890
- Stage 2 Propellant*	1048
Stage 2 Dry w/instruments	842
* Includes residuals and loading uncertainty	

Approximate sensitivities of Stage 1 gross mass to changes in the masses of each step can be determined as in Section 3.3.3.2.2. Values for m_i/m_f = 2.36, and 2.24 for Stages 1 and 2, respectively. Values for m_i/m_f depend only on ΔV and effective I_{sp}, with g and η being constant, and can vary slightly depending on how propellant residuals are book kept. Compounding the effect of these changes, the resulting values for the change in Stage 1 initial mass with changes in Step 1 and 2 masses are shown below.

Δ Stage 1_i / Δ Step 1_{Dry} = $(m_i/m_f)_1$ = 2.36

Δ Stage 1_i / Δ Step 2_{Dry} = $(m_i/m_f)_2$ $(m_i/m_f)_1$ = 5.29

Scaling using this approach gives only a first order approximation and should be used with caution as discussed in Section 3.3.3.2.2. A further breakout of mass by subsystem for each step is provided in Tables 3.4.3-4 and 3.4.3-5. Propellant was computed on the basis of mass with contingency (i.e., the allocation mass).

3.4.3.2.3 Enceladus-O Booster and Orbiter (B&O) Description

Booster and orbiter subsystems are similar in many cases (e.g., Mechanical, Avionics, Flight Software, and Attitude Control) to those discussed for Enceladus-OL design and will not be discussed here except where significant differences exist or an item warrants specific attention. Note that the sounding radar is similar in size, shape, and deployment approach to the magnetometer boom. Interfaces that existed with the lander in the Enceladus-OL design do not exist in the Enceladus-O design. Subsystems are 1-fault tolerant for credible failures, consistent with NPR 8705.4 guidance for Class A missions.

3.4.3.2.3.1 Enceladus-O (B&O) Power Subsystem

Power for the booster and orbiter is provided by three ASRGs and a 40 Ahr rechargeable lithium ion battery located on the orbiter. The sizing conditions associated with the ASRGs and battery are the same as used in the Enceladus-OL design with the exception of having one year less degradation on the ASRGs (the sounding radar operates selectively and is duty cycled such that it doesn't increase the total instrument power required). After completing the Enceladus-O study, it was determined (per ref. (f)) that an individual ASRG could not be considered single fault tolerant and a redundant ASRG would be required. This means a fourth ASRG would have to be added to the Enceladus-O design. The discussion of battery DoD in Section 3.3.3.2.3.2 applies equally to Enceladus-O.

3.4.3.2.3.2 Enceladus-O (B&O) Propulsion Subsystem

The Enceladus-O booster and orbiter dual mode N_2O_4 / hydrazine propulsion systems are similar to those for the Enceladus-OL design with two exceptions. The first difference is in the number and size of the propellant and pressurant tanks. The Enceladus-O design booster and orbiter have single N_2O_4 and hydrazine tanks. The booster has

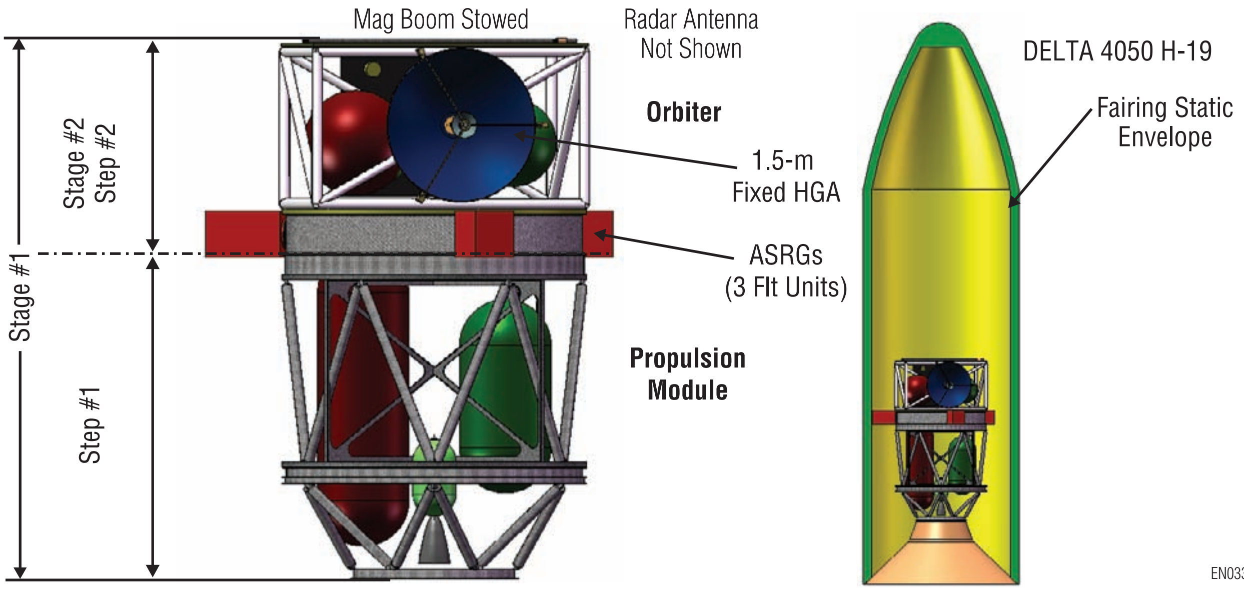

Figure 3.4.3-2: View Looking at Enceladus-O +Z Face and Showing Compatibility with Delta 4050H Fairing Static Envelope

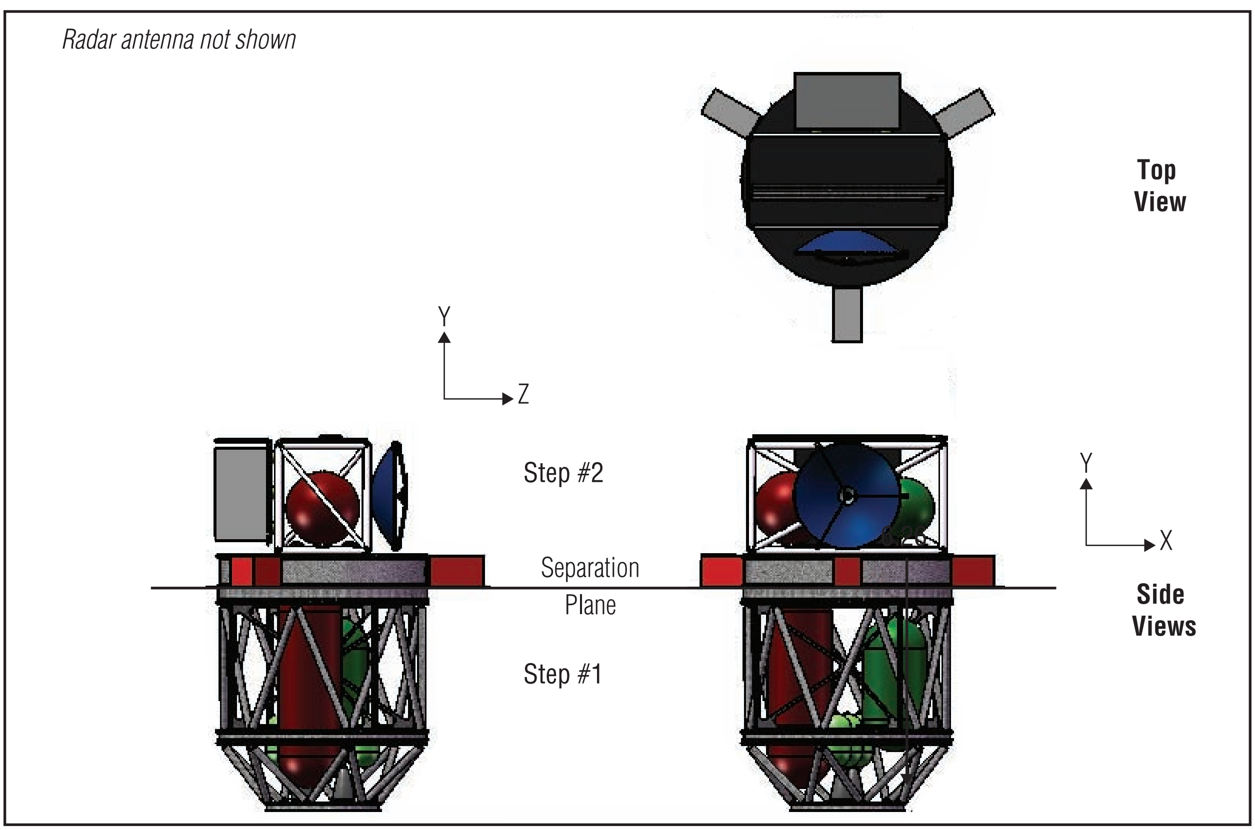

Figure 3.4.3-3: Three View of Enceladus-O

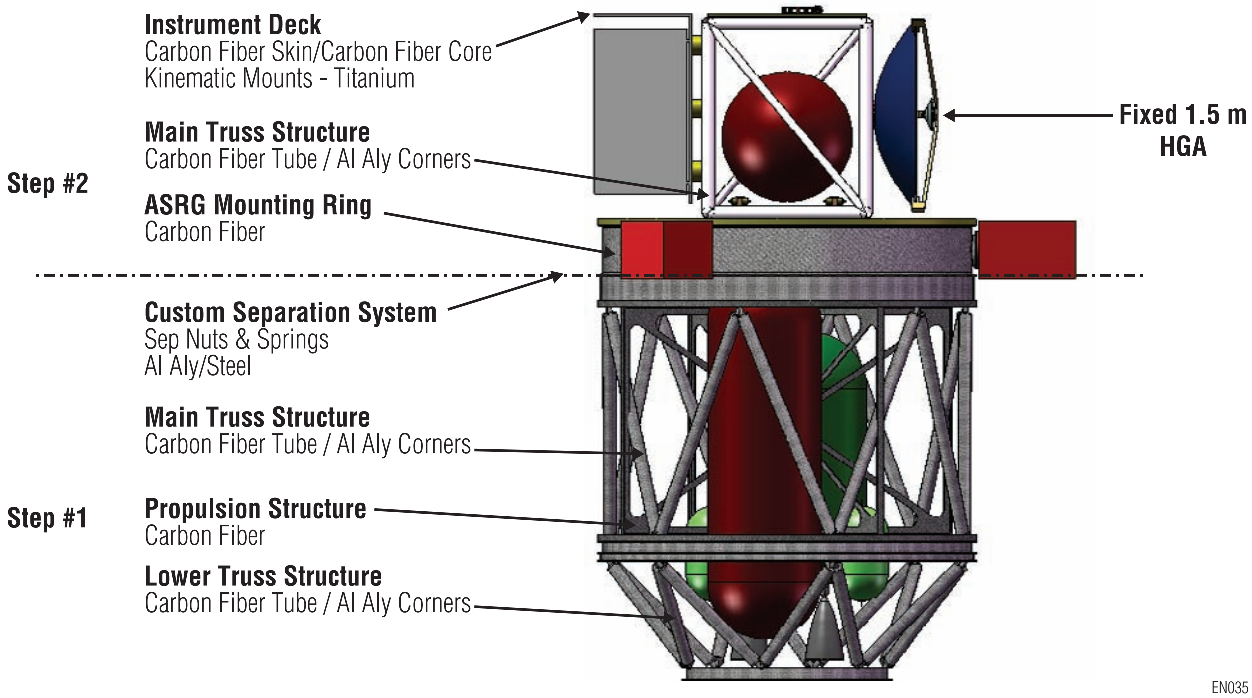

Figure 3.4.3-4: Major Components of Enceladus-O (View Looking at –X Face)

Table 3.4.3-4: Enceladus-O Step 1 (Propulsion Module) Mass Statement

Step 1 (Propulsion Module) Dry Mass				
	Estimate (Kg)	% Total Dry Mass	% Contingency	Allocation (Kg)
Mechanical	211	48	30	274
Attitude Control	0	0	30	0
Thermal	12	3	30	15
Propulsion	219	49	30	284
Power	0	0	30	0
C&DH	0	0	30	0
Communications	0	0	30	0
Propulsion Module Harness	2	0	30	3
Propulsion Module Total Dry Mass	**443**	**100**	**30**	**576**
Step 1 (Propulsion Module) Wet Mass				
	Estimate (Kg)	% Total Wet Mass	% Contingency	Allocation (Kg)
Propulsion Module Dry Mass	443	12	30	576
Propellant Mass*	3343	88	0	3343
Propulsion Module Wet Mass	**3787**	**100**		**3920**
* Includes residuals and loading uncertainty				

Table 3.4.3-5: Enceladus-O Step 2 (Orbiter) Mass Statement

Step 2 (Orbiter) Science Payload				
	Estimate (Kg)	% Total Dry Mass	% Contingency	Allocation (Kg)
Thermal Mapper	11	2	30	14
VIS/NIR Mapper	10	2	30	13
Laser Altimeter	10	2	30	13
Radio Science	1	0	30	1
Magnetometer	4	1	30	5
GCMS	10	2	30	13
Dust Micro Analyzer	10	2	30	13
Sounding Radar	9	1	30	12
Payload Total	**65**	**10**	**30**	**85**
Step 2 (Orbiter) Spacecraft Bus				
	Estimate (Kg)	% Total Dry Mass	% Contingency	Allocation (Kg)
Mechanical	223	34	30	290
Attitude Control	26	4	30	34
Thermal	27	4	30	35
Propulsion	104	16	30	135
Power	73	11	30	95
C&DH	39	6	30	51
Communications	55	9	30	72
Spacecraft Harness	35	5	30	46
Bus Total	**583**	**90**	**30**	**758**
Step 2 (Orbiter) Dry Mass				
	Estimate (Kg)	% Total Dry Mass	% Contingency	Allocation (Kg)
Science Payload Total	65	10	30	85
Bus Total	583	90	30	758
Orbiter Dry Mass	**648**	**100**	**30**	**842**
Step 2 (Orbiter) Wet Mass				
	Estimate (Kg)	% Total Wet Mass	% Contingency	Allocation (Kg)
Orbiter Dry Mass	648	38	30	842
Propellant Mass*	1048	62	0	1048
Orbiter Wet Mass	**1696**	**100**		**1890**
* Includes residuals & loading uncertainty				

three helium pressurant tanks, where the orbiter has one. The second difference is the system is operated in bi-propellant mode during cruise prior to SOI. This results in a higher booster effective I_{sp} than attained for Enceladus-OL. This has the disadvantage of exposing the oxidizer thruster valves to N_2O_4 during the 11.7-year cruise to Saturn. Periodic flushing burns would likely be required to limit the potential for iron nitrate contamination. The propellant distribution between the booster and orbiter resulted from an optimization study that maximized mass available for the orbiter. The combination of maneuvers conducted in bi-propellant and monopropellant mode over the total propellant expended results in an effective I_{sp} for the booster and orbiter of 306 s and 303 s, respectively.

3.4.3.2.3.3 Enceladus-O (B&O) Thermal Control Subsystem

The Enceladus-O thermal design is similar to that for Enceladus-OL except in the design of the radiators. Where the Enceladus-OL design uses radiator panels with embedded VCHPs facing in the -X and +X direction, the Enceladus-O radiator use louvered radiators facing in the +Y direction as shown in **Figure 3.4.3-5**. The Enceladus-OL radiator configuration is expected to have performance advantages relative to the Enceladus-O configuration.

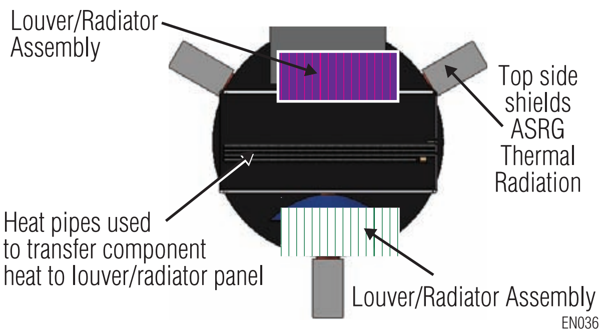

Figure 3.4.3-5: Enceladus-O Orbiter Radiator Configuration (View Looking at +Y Face)

3.4.3.2.3.4 Enceladus-O (B&O) Communications Subsystem

The communications system design is similar to that for Enceladus-OL. However, the total data volumes differ slightly. They are summarized for the polar orbit and the 45° mapping orbit in **Table 3.4.3-6**. These volumes assume 10:1 compression on the visible/near infared mapper and include instrument and spacecraft housekeeping along with 30% contingency. Daily data collection in the 45° orbit is limited by the orbiter downlink rate and by a communication window of 9.0 hours per day, per the study Study Groundrules. A period of 8.14 hours is required to downlink 1.17 Gb at 40 kbps, and Enceladus eclipses the orbiter line of sight to Earth for about 1.25 hour per communication pass. This results in a total communication pass time of about 9.4 hours, which exceeds the 9.0 hour/day allocation. The orbiter will not transmit to Earth during the polar orbit to avoid time lost to slewing. Instead, the polar orbit data will be stored for transmission once back in the 45° orbit. This transmission will require about 18 passes of about eight hours each at the DSN at 40 kbps for each day of the 90 deg orbit. The discussion of the omni antenna link margin in **Section 3.3.3.2.3.7** applies to the Enceladus-O configuration.

Table 3.4.3-6: Enceladus-O Data Stored and Transmitted

	Total Data Stored (Gb)	Total Data Transmitted (Gb)
Orbiter 90 deg orbit	21.20	20.03
Orbiter 45 deg orbit	1.24	1.17

3.4.3.2.4 Enceladus-O Mission Reliability

Even with single fault tolerant design, overall reliability for this mission lifetime (a total of 17.3 years was used for this analysis) is low. The probability of mission success of .604 is estimated at the 95% confidence level (see **Section 3.3.3.2.5**). Propulsion, thermal, and attitude control systems are the mission reliability drivers. This configuration had no redundancy in ASRGs. But due to the lack of reliability information available for ASRGs that operate beyond 14 years, this did not significantly affect the results relative to those for Enceladus-OL.

3.4.3.2.5 Enceladus-O Mission Level I&T

Parallel fabrication and component test of the booster, orbiter bus, and the orbiter instruments starts in April 2015. This is followed by parallel I&T for the same hardware elements starting in June 2016. Instruments are then integrated with the orbiter bus starting in April 2017, fit checks are conducted with the booster, and orbiter I&T is conducted. In February 2018, the orbiter and booster are mated for I&T as a combined unit. The flight segment is ready for shipment to the launch site in June 2018 for a September 2018 launch.

3.4.4 Enceladus-O Operational Scenarios

Table 3.4.4-1 identifies the driving operational scenarios for this mission concept.

Table 3.4.4-1: Enceladus-O Driving Operations Scenarios

Scenario	Driver
Venus Flyby	Thermal
Earth Flyby	Safety
Enceladus Orbit Insertion	Power
Titan/Rhea	Navigation
Enceladus Mapping	Data Volume
Polar Campaign	Data Storage

These are a subset of the scenarios for the Enceladus-OL mission, without the landing. The only significant difference is that Dione is not used during the gravity assist phase at Saturn. The other differences were minor, such as slightly different data volumes due to the slightly different instrument complement.

3.4.5 Enceladus-O Planetary Protection (& Disposal)

The booster separates after conducting part of the EOI burn (after completing the Rhea flybys) and will be in an orbit with periapsis at Enceladus and apoapsis below Rhea. Analysis that demonstrates the booster will have less than a $1x10^{-4}$ probability of inadvertently contaminating any icy moon inside of Rhea's radius has not been done, and is the subject of a recommended future study. For the purposes of this study, it was presumed the booster would need to be cleaned to planetary protection level IV.

3.4.6 Enceladus-O Major Open Issues and Trades

With the exception of the lander element, the major open issues and trades are similar to those discussed in Section 3.3.6. Additional trades to consider for this concept include:

3.4.6.1 Single vs. Two Stage Vehicle / Booster Disposal Strategy

While this mission concept baselined a two stage propulsion system, if may be of interest to investigate whether the launch margin available will permit use of a single stage system. A trade study is required to determine the benefits of optimal staging with respect to cost and complexity. The study also should define trajectories that assure the booster will have less than a $1x10^{-4}$ probability of inadvertently contaminating any icy moon to enable cleaning the booster to planetary protection level III rather than to level IV.

3.4.6.2 Reduction in Communication Time

In addition to the trade discussed in Section 3.3.6, evaluate solutions to reduce contact time between the orbiter and the ground station from 9.4 hours/day to the allocated 9.0 hours/day. Include potential reduction in instrument complement (e.g., the sounding radar was removed for Enceladus-OL design).

3.4.6.3 Additional ASRG

Add a fourth ASRG to make the power system 1-fault tolerant.

3.4.6.4 Use of ACS Thrusters Prior to SOI

The approach used for the Enceladus-OL concept (uses only ACS thrusters prior to SOI) is recommended for Enceladus-O. A study to determine the reduction in effective I_{sp} and the corresponding increase in launch mass should be conducted. Using only monopropellant up to SOI will inhibit formation of iron nitrates on the main engine oxidizer valves.

3.4.6.5 Radiator Configuration

Evaluate Enceladus-OL radiator design and location for use on Enceladus-O.

3.4.7 Enceladus-O Technology Needs

The Enceladus-O mission uses existing technology. No new technology was identified.

3.4.8 Enceladus-O Technical Risks

The Enceladus-O design risks are a subset of the Enceladus-OL mission risks – mission lifetime and its impact on component qualification and knowledge retention, and the Enceladus gravity model.

3.4.9 Enceladus-O Schedule

The Enceladus-O design uses a development schedule of 66 months from the start of Phase B to launch. The durations of Phase B, C, and D are 12 months, 12 months, and 46 months, respectively. The length of Phase D is driven principally by the length of time need to fabricate, integrate and test the booster and orbiter systems both separately and in combined configurations, and includes the four month period immediately following launch (i.e., the duration of Phase D up until launch is 42 months).

3.5 Saturn Orbiter with Soft Lander (Saturn-OL)

3.5.1 Saturn-OL Architecture Overview

The Saturn-OL mission includes a Saturn orbiter with a soft lander package. Relative to the Enceladus-O and Enceladus-OL designs, it features modest ΔV requirements and overall mission duration. In exchange, it provides less complete mapping of the Enceladus surface and higher-speed plume flybys. It includes a three stage flight segment with xenon ion propulsion for the SEP module, dual mode bi-propellant N_2O_4 / hydrazine chemical propulsion for the orbiter and bi-propellant chemical propulsion for the lander. The launch and ground segments are identical to that described in **Section 3.3.1**.

3.5.2 Saturn-OL Science Investigation

All of the science goals in **Table 2.1.1-1** can be met by a properly instrumented Saturn orbiter and lander, as shown in **Table 2.4.6-1**, but with much less surface coverage and higher flyby velocities than from an Enceladus orbiter. Thus, Surface Processes, Tectonics and Tidal Heating are not addressed as well from Saturn orbit. Saturn System Interactions goals are met, but with higher flyby velocities of the plume material; intact plume particles cannot be examined, but a high velocity dust impact experiment can be used (similar to, but more capable than that on Cassini) to obtain some information about the plume particles. In addition, laser altimetry will require much more careful design to provide adequate cross over tracks, and precision of the gravity coefficients and shape and gravity Love numbers, and magnetic sounding data, will be lower. The soft lander package will provide seismometry and detailed chemistry, but will only have a single chance to communicate data to the orbiter, unless redesigned for a longer life. The lander entry, landing and descent sequence will also be further complicated by the high flyby velocities, and the same difficulties with surface coupling and anchoring apply as in the Enceladus-OL case. **Tables 3.5.2-1** and **3.5.2-2** show the Saturn-OL orbiter and lander strawman payload suites.

Orbiter Science Drivers:

- Surface mapping in visible, near-IR and thermal IR
  - Understand tectonics, cryovolcanism, surface processes
- Determine Love numbers with laser altimetry and Doppler tracking, and determine interior conductivity with magnetic sounding
  - Constrain interior structure, and presence or absence of a global ocean
- *In-situ* analysis of plume gas and dust components
  - Understand cryovolcanic processes, organic chemistry

Lander Science Drivers:

- Detailed *in-situ* analysis of surface chemistry (esp. organic)
  - Composition, cryovolcanism, habitability, presence of key amino acids and biotic compounds?
- High-frequency and low-frequency seismometry
  - Ice shell thickness, structure, cryovolcanism
- Imaging
  - Surface processes

3.5.3 Saturn-OL Mission Design

The following sections focus principally on the flight segment. Interfaces with the ground and launch segments will be summarized only, as the configuration of these segments was given in the Study Groundrules.

3.5.3.1 Saturn-OL Flight Dynamics

3.5.3.1.1 Launch Window

The Saturn-OL trajectory combines SEP and chemical propulsion to achieve orbit around Saturn and is designed as described in **Sections 3.1.1.2.1.1** and **3.1.1.2.2**. The launch date for the 7.5 year cruise to Saturn is 25 March 2018 and was selected to enable Enceladus mapping to start after sunrise at the Enceladus south pole (occurs in ~mid 2025). The SEP stage operates for 1024 days. During that time it enters a phasing orbit (see **Figure 3.1.1-1**), which extends beyond the orbit of Mars, and conducts a single Earth flyby at 688 days (~1.9 years) at an altitude of 1000 km. The SEP system is sized to be consistent with an initial mass of 6525 kg and a maximum C_3 of 19.2 km^2/s^2 over a 20 day launch window. The corresponding V_{hp} at Saturn arrival is

Table 3.5.2-1: Saturn-OL Strawman Orbiter Payload

Instrument	Mass (kg)	Power (W)	Duty Cycle	Dimensions L x W x H (or L x dia.) (cm)	Data Volume per Encounter (Gb)	Notes on Downlink	Preferred Location and Aperture Pointing Direction	Req'd Pointing Accuracy (arc sec)	% New Development Req'd	Precursor Instrument
Thermal Mapper	11	14	100% within +/- 500 km of Enceladus c/a, 20% duty cycle (alternating with cameras) within +/- 5000 km.	55x29x37	0.032		Nadir, radiator with sky view		~50% (longer wavelength capability)	THEMIS
Visible Mapper	10	6	100% within +/- 500 km of Enceladus c/a, 20% duty cycle (alternating with Thermal IR and NIR cameras) within +/- 5000 km.	50x50x30	0.308	includes 10:1 compression, handled by C&DH			0% new	New Horizons MVIC
Near IR Mapper	10	6	100% within +/- 500 km of Enceladus c/a, 20% duty cycle (alternating with Thermal IR and vis cameras) within +/- 5000 km.	50x50x30	2.4	includes 10:1 compression, handled by C&DH	Nadir, radiator with sky view		~30% (longer wavelength capability)	New Horizons LEISA
Laser Altimeter	11.7	33	100% within +/- 500 km of Enceladus c/a	42x45x36 (optics; 21x29x12 electronics)	0.001		Nadir	360	~50% new development	LRO LOLA
Radio Science	1	1.5	100% within +/- 5000 km of Enceladus c/a	10x10x10	0		N/A	N/A	0% new	
Magnetometer	4	1	100%	10x10x15 plus 10m boom	0		N/A	N/A	0% new	Messenger heritage
INGMS	10	25	100% within +/- 10000 km of Enceladus		0		Ram direction		~30-50% (pyrolysis heater unit, sample collector interface, miniature mass spec, wet chemistry?)	NGIMS, MSL SAM
Dust Analyzer	5	5	100% within +/- 10000 km of Enceladus, 20% rest of the orbit.	10x10x10	0		Ram direction	N/A	~60%	Cassini CDA, Stardust CIDA

Note: c/a denotes "closest approach"

Table 3.5.2-2: Saturn-OL Strawman Lander Payload

Instrument	Mass (kg)	Power (W)	Duty Cycle	Dimensions L x W x H (or L x dia.) (cm)	Data Volume (kb/day)	Notes on Downlink	Preferred Location and Aperture Pointing Direction	Req'd Pointing Accuracy (arc sec)	% New Development Req'd	Precursor Instrument
Lander camera (two)	0.6	5	Panorama followed by staggered plume monitoring		144	includes 5:1 compression, handled by C&DH	1 meter above surface, panoramic	N/A	0%	MER PANCAM
Radio Science	part of comm system	part of comm system	100% during comm. passes		N/A			N/A	0%	
Seismometer	2.3	1	100%	2.5x2x7.5	2.24		coupled to surface	N/A	0%	Netlander SEIS
Surface chemistry package	3	25	Alternates w/ other chemistry experiments	15x19x11	28			N/A	TBD	Part of ExoMars Urey
LDMS	4	5	Alternates w/ other chemistry experiments		120	includes 2:1 compression, handled by C&DH		N/A	TBD	ExoMars MOMA
Sampling Arm	3	1			N/A			N/A	TBD	
Piezoelectric Corer	1.3	5			N/A			N/A	TBD	Europa Lander
Surface Ice Oxidant Detector	0.3	1	Alternates w/ other chemistry experiments	2.9x2.5x.89	150	includes 2:1 compression, handled by C&DH		N/A	TBD	Part of ExoMars Urey

5.57 km/s. A similar launch opportunity exists every 12 months.

3.5.3.1.2 Multiple Passes of Enceladus

In the mapping orbit, the spacecraft will pass by Enceladus every 8.22 days as depicted in **Figure 3.5.3-1**.

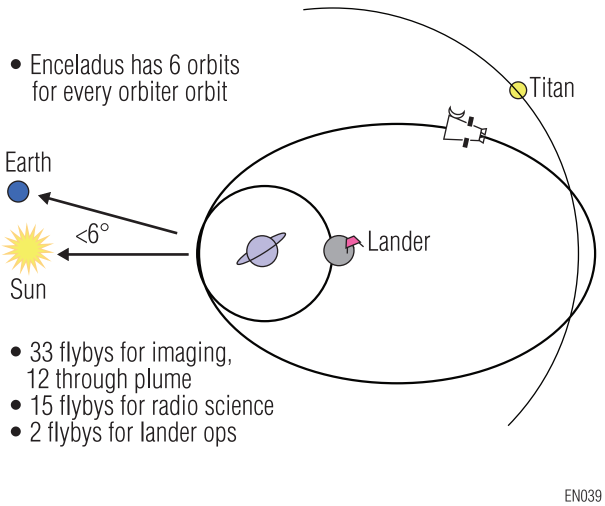

Figure 3.5.3-1: Saturn-OL Enceladus Flyby Orbit Geometry

Small targeting maneuvers assure the spacecraft passes Enceladus to within a desired altitude over a range of latitudes with emphasis on the south pole. Precession of Enceladus' orbit (precession period 1.31 years) provides flybys of Enceladus and different positions relative to periapsis, as required for geophysical measurements. Periodic adjustments to the spacecraft orbit would be required for global mapping, but are not considered here. When the lander (targeting Enceladus' south pole) is deployed from this orbit, the slight inclination of the orbit provides for an extended contact time (visibility) after the point of closest approach as shown in **Figures 3.5.3-2A** and **3.5.3-2B**.

3.5.3.1.3 Landing on Enceladus

A landing attempt from the Saturn centered, 6:1 resonant orbit with Enceladus requires the lander to null the relative velocity of 3.8 km/s in order to execute a soft landing on the surface. The lander for this mission concept requires significantly more ΔV than required for the Enceladus-OL concept, and the communications visibility is more constrained.

3.5.3.1.4 Saturn-OL Timeline of Key Events

Figures 3.5.3-3, **3.5.3-4**, and **Table 3.5.3-1** give high level descriptions of the trajectory phases and corresponding timeline of key events in the 9.5 year mission.

Table 3.5.3-1: Key Events in 9.5 Year Saturn-OL Mission Timeline

Date	Year	Event
March 25	2018	Launch
~ February 15	2020	Earth Flyby
January 19	2021	Jettison SEP Module
September 6	2025	Saturn Orbit Insertion
July 21	2026	Start Enceladus Flyby's
~ August 31	2026	Lander Separation
~ September 8	2026	Complete Lander Ops
~ September 5	2027	Disposal

Table 3.5.3-2 shows the ΔV budget used to design the orbiter and lander. As noted in **Section 3.1.1.2.2**, the assumptions for Saturn capture were more conservative than used for the Enceladus-O and Enceladus-OL mission designs, and the Saturn-OL design has no Enceladus orbiter. Accordingly, the ΔV reserve of 500 m/s held for the Enceladus-O and Enceladus-OL mission designs was not held for Saturn-OL. In the Saturn-OL study (the first of the three studies conducted), the 5% tax to account for propellant used in non-ΔV attitude control maneuvers was accounted for as a tax on ΔV, rather than directly on propellant.

3.5.3.2 Saturn-OL Flight Segment Design

3.5.3.2.1 Saturn-OL Configuration

Figures 3.5.3-5 through **3.5.3-8** show the general arrangement of the flight segment.

3.5.3.2.2 Saturn-OL Mass Properties

Tables 3.5.3-3 and **3.5.3-4** respectively, give top level mass sensitivities and a top level

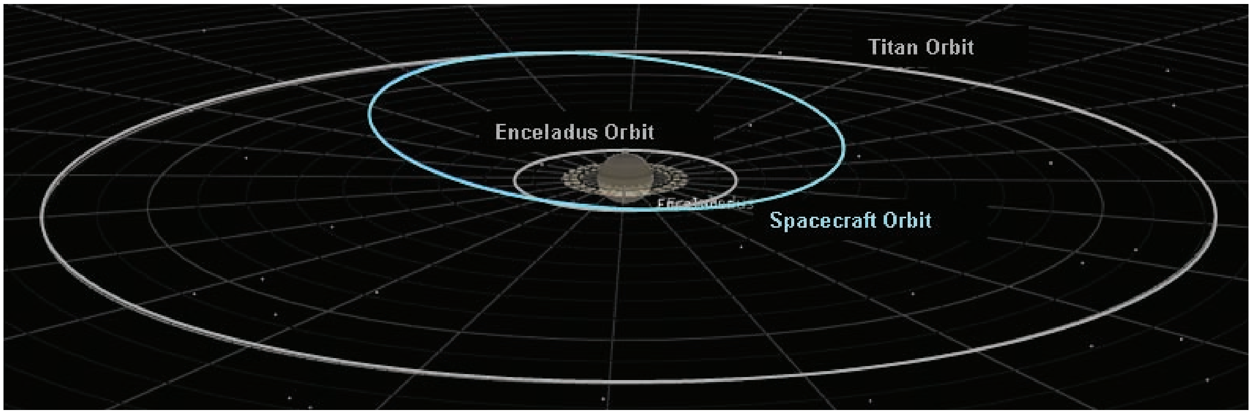

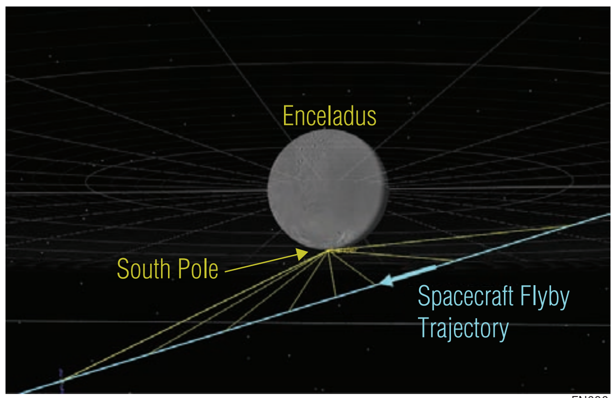

EN038

Figure 3.5.3-2A: Saturn-OL 8.22 Day Enceladus/Titan Mapping Orbit
Figure 3.5.3-2B: Sample Pass of Enceladus' South Pole by Saturn-OL

summary of flight segment mass by stage, including mass contingency (O= Orbiter, L = Lander). The Stage 1 gross mass is 6196 kg. This leaves a 5.3% lift margin on the Delta 4050H lift capability of 6525 kg. The approximate sensitivities of Stage 1 gross mass to changes in the masses of each step were determined as discussed in **Section 3.3.3.2.2**.

Stages 1, 2, and 3 have values for m_i/m_f = 1.13, 1.92, and 4.17, respectively. However, as a practical matter, the mass of Step 1 (the xenon ion propulsion module), was held fixed during the design trades, since it had been provided as an input to the design study by NASA/GRC and since the SEP module was designed to accommodate a launch mass of up to 6525 kg. This means the scaling actually observed for Stage 1 corresponded to m_i/m_f =1.00.

Additionally, the Stage 2 m_i/m_f of 1.92 applies when dry mass is added to the third stage (where the third stage mass impacts Stage 2 propellant only for the duration of the flybys for which it remains attached to the orbiter). When dry mass is added just to the orbiter, the Stage 2 m_i/m_f = 2.54. Values for m_i/m_f depend only on ΔV and effective I_{sp}, with g and η being constant, and can vary slightly depending on how propellant residuals are book kept. Compounding the effect of these changes, the resulting values for the change in Stage 1 initial mass with changes in Step 1, 2, and 3 masses are shown in **Table 3.5.3-3**.

Scaling using this approach gives only a first order approximation and should be used with caution as discussed in **Section 3.3.3.2.2**.

The value of Δ Stage 1_i / Δ Step 2_{dry} consists of two discrete values for m_i/m_f, as the Stage 2 burn is conducted in two parts to enable deploying the lander early during orbiter operations. The first part, with lander attached, includes the ΔV (a total of 2052 m/s) for SOI and five of the 50 planned Enceladus flybys. The second part, after lander separation, includes the ΔV (a total of 745 m/s)

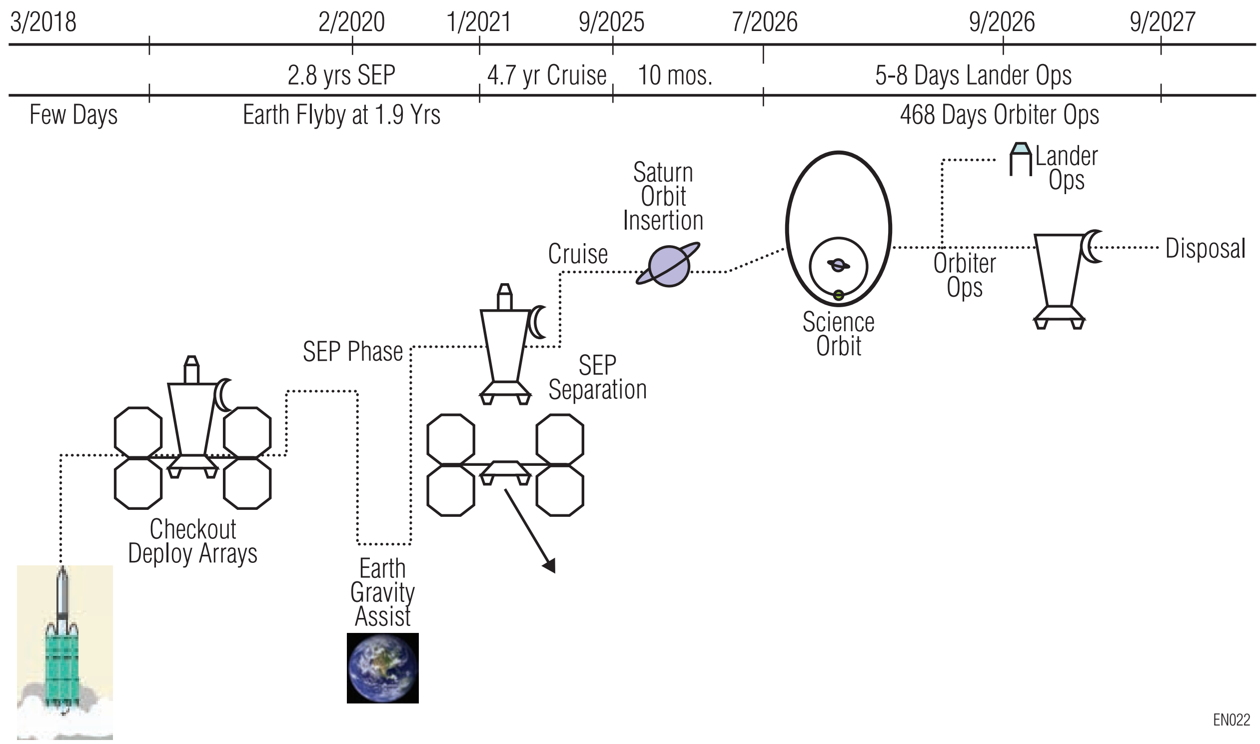

Figure 3.5.3-3: Saturn-OL Mission Phases and Key Events

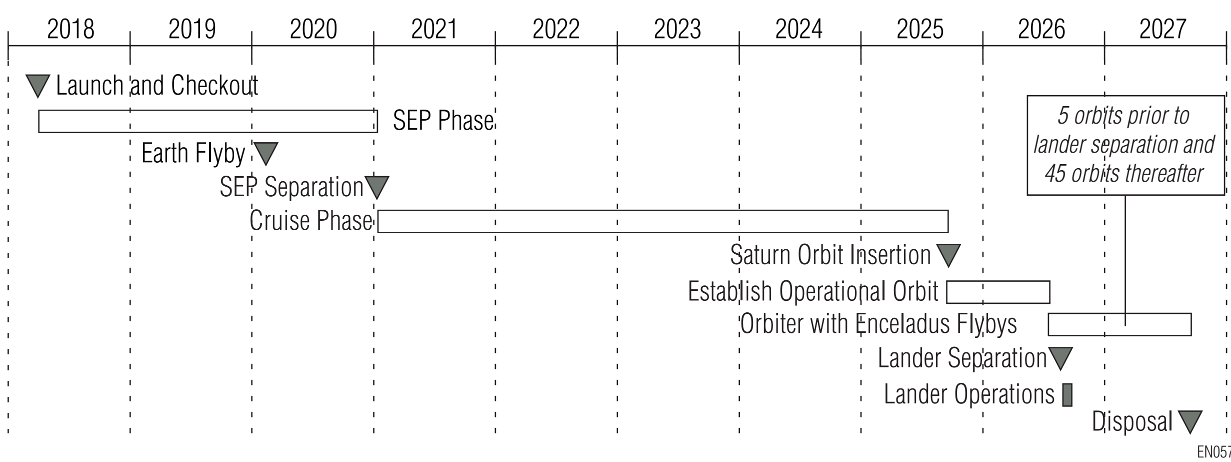

Figure 3.5.3-4: Saturn-OL Key Mission Key Events

for the balance of 45 Enceladus flybys. Breaking the orbiter ΔV of 2797 m/s into two parts allows some propellant savings. Five flybys was selected as a notional time to separate as a compromise between the ability to map the landing site and the propellant required to continue carrying the lander. If five flybys (about 41 Earth days) were found to be insufficient for the science operations center to select a landing site, the number of flybys could be increased with some increase in required propellant mass.

A further breakout of mass by subsystem for each step is provided in **Tables 3.5.3-5** through **3.5.3-7**. Propellant was computed on the basis mass with contingency (i.e., the allocation mass), so no additional contingency was held.

Table 3.5.3-2: Saturn-OL Mission ΔV Budget

Maneuver	ΔV (m/s)	ACS Tax (%)	ΔV (m/s) with ACS Tax	Reserve (%)	Effective ΔV (m/s)
Orbiter Propellant Budget					
Launch	0.0	0.0	0.0	0.0	0.0
Trajectory Control Manuever	50.0	5.0	52.5	10.0	57.8
Saturn Orbital Insertion Maneuver	926.5	5.0	972.8	10.0	1070.1
Trajectory Control Manuever	50.0	5.0	52.5	10.0	57.8
Apogee Burn	645.2	5.0	677.5	10.0	745.2
Trajectory Control Manuever	50.0	5.0	52.5	10.0	57.8
Enceladus Flybys With Lander (5)	55.0	5.0	57.8	10.0	63.5
Deploy Lander (no Δv, just mass change)	0.0	0.0	0.0	0.0	0.0
Enceladus Flybys Without Lander (45)	495.0	5.0	519.8	10.0	571.7
EOL Disposal Maneuver	150.0	5.0	157.5	10.0	173.3
Subtotal Orbiter	**2421.7**		**2542.8**		**2797.1**
Lander Propellant Budget					
Enceladus Orbit Insertion	4000.0	5.0	4200.0	0.0	4200.0
Descent & Landing	100.0	5.0	105.0	10.0	115.5
Subtotal Lander	**4100.0**		**4305.0**		**4315.5**
Total ΔV	**6521.7**		**6847.8**		**7112.6**

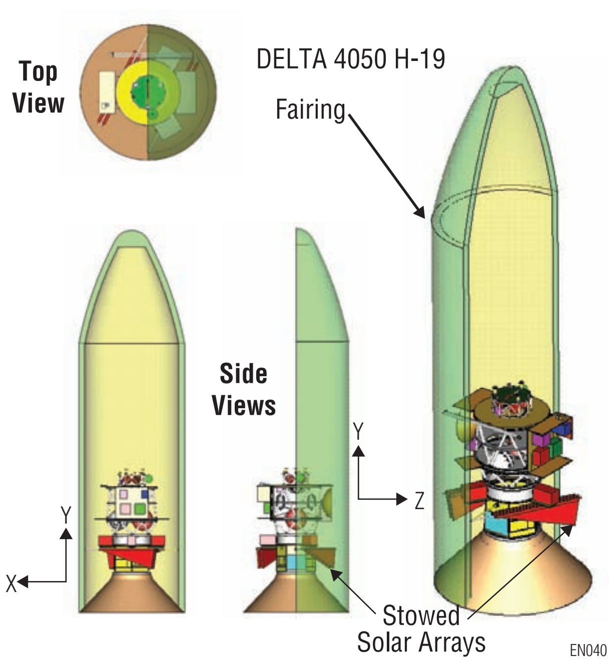

Figure 3.5.3-5: Saturn-OL Stage 1 Stowed Configuration Showing Compatibility with Delta 4050H Fairing Static Envelope

3.5.3.2.3 Saturn-OL SEP Module Description

The SEP module uses three operating and one standby (3+1) xenon ion engines to provide nearly continuous (~90% thrusting duty cycle) thrust along the trajectory arc. Intermittent breaks in thrusting permit updating the navigation solution. At present, using a 10% non-thrusting period for tracking and navigation updates appears sufficient. Were more time needed for tracking and navigation (in particular, for preparation for the Earth gravity assist), the SEP trajectory could be re-designed for a lower thruster duty cycle at the expense of reducing the SEP module performance (reducing the Stage 2 mass available). The SEP system is single fault tolerant, and includes selective cross-strapping.

3.5.3.2.3.1 Saturn-OL SEP Module Mechanical Subsystem

Four carbon over-wrapped titanium tanks, modified from an existing design, provide 700 kg of xenon propellant, which is sufficient to meet the 6525 kg launch mass with a propellant margin of 9%. The hexagonal SEP module structure is made of 2090-T3 aluminum lithium and separates from the orbiter with a clampband separation system and springs. A truncated 1194-5 payload

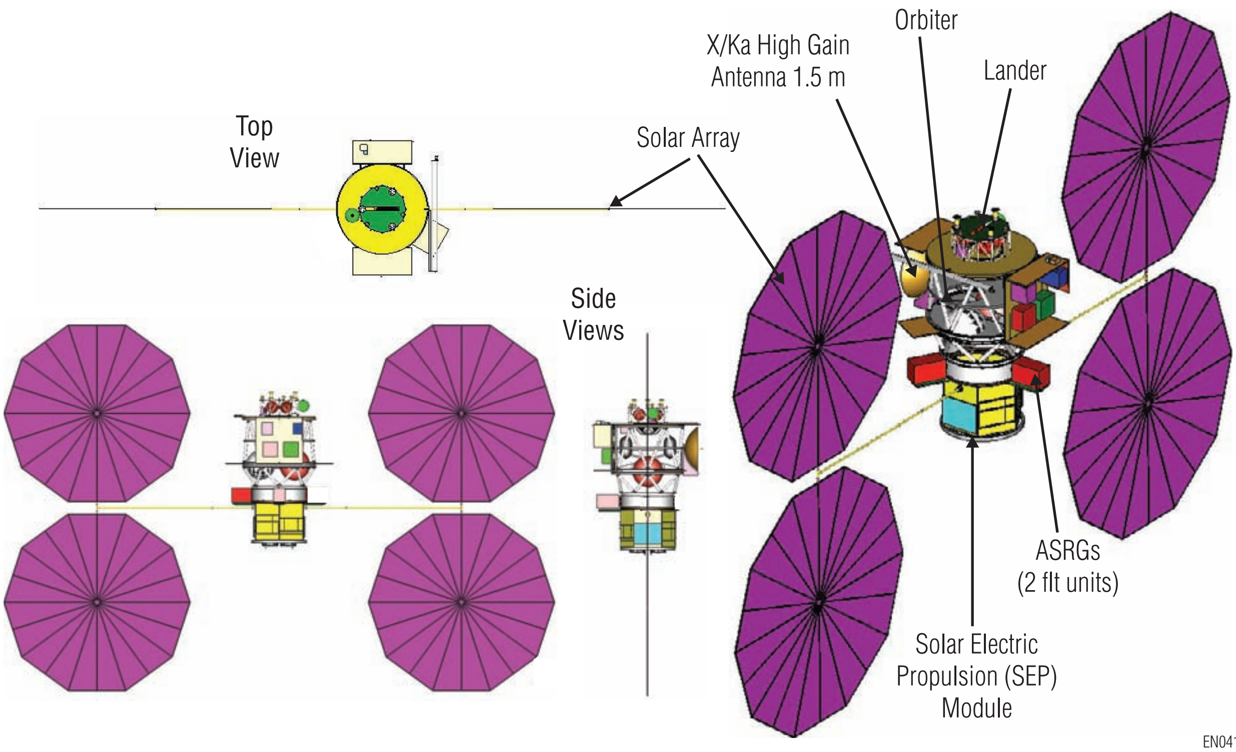

Figure 3.5.3-6: Saturn-OL Stage 1 Showing SEP Solar Arrays Deployed

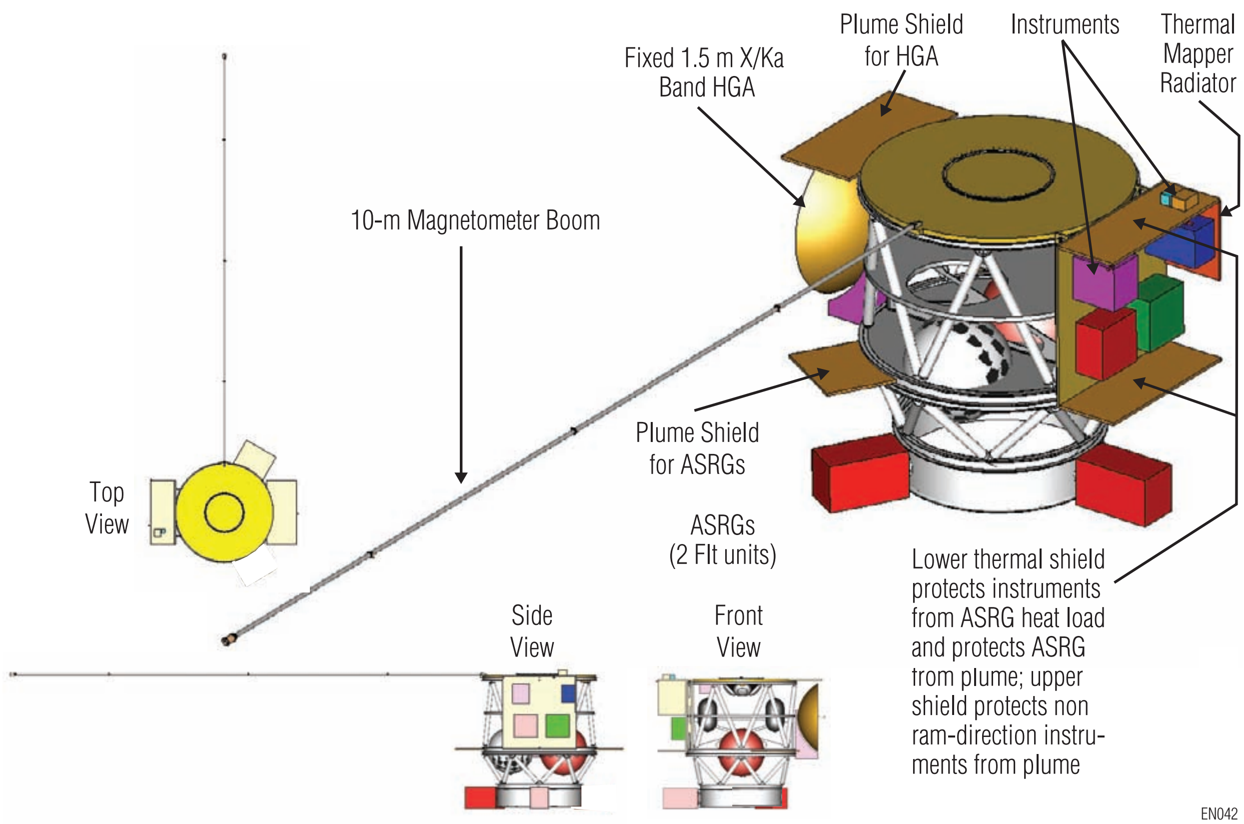

Figure 3.5.3-7: Saturn-OL Orbiter Configuration

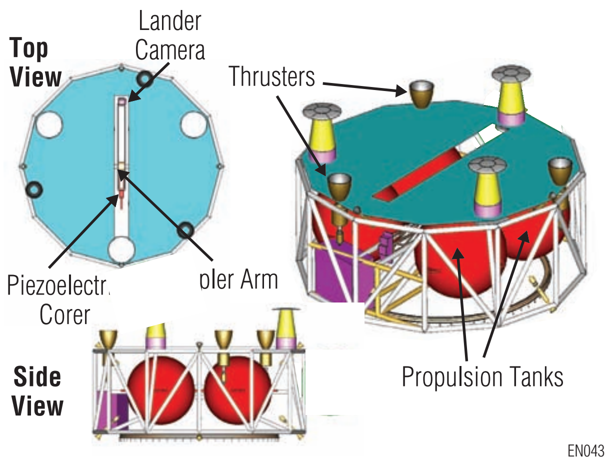

Figure 3.5.3-8: Saturn-OL Lander Configuration

attach fitting (PAF) provides a 1.88m interface that is compatible with the four thrusters which extend about 5 cm into the negotiable fairing envelope volume (after launch, the engines deploy another 10 cm aft). This approach saves the mass associated with adding an adapter to the existing 1194-5 PAF (1.19 m interface) and avoids increasing the center of gravity height.

3.5.3.2.3.2 Saturn-OL SEP Module Power Subsystem

Four triple junction gallium arsenide UltraFlex solar arrays, similar to those planned for the Orion vehicle (Constellation Program), with single axis gimbals provide 25 kW (33 kW with 30% contingency) at BOL and at 1.0 AU to three 7 kW ion thruster strings. The total SEP module power required is 22 kW. When power available exceeds power required, the excess power is shunted. The SEP power system supplies power at 80 - 160 V to the power processing units (PPUs) for the thruster power supplies. Voltage is unregulated and varies with distance from the Sun. The power system also supplies 28V for housekeeping throughout the module. A lithium ion battery provides power during launch and for contingency operations.

3.5.3.2.3.3 Saturn-OL SEP Module Propulsion and Attitude Control Subsystem

The SEP module propulsion system provides a total ΔV of about 3800 m/s at an effective specific impulse of ~3600 s. The purpose of this ΔV is to almost continuously shape the non-Keplerian Earth gravity assist trajectory to enable a fast hyperbolic transfer to Saturn. In doing this, the SEP module ΔV is effectively taking the place of the ΔV gained from the first three gravity assists in the VVEES chemical trajectory discussed in **Section 3.1.1.2.1.2**, but in much less time. The SEP thrusters have +/-19° and +/-17° gimbal capability in orthogonal axes which provides for pitch, yaw and roll control during thruster operation. The orientation of these gimbals can be selected as needed within the spacecraft. Spacecraft attitude is nearly inertial during the Earth flyby phasing orbit, so the thrust vector is only occasionally tangent to the flight path. After Earth flyby, thrust is tangent to the flight path. Plume contamination is not expected to be an issue for surfaces that are outside a 47°-49° half cone angle (30° for the plume and 17°-19° for the gimbal angle). Four Sun sensors that interface directly with the orbiter are included. These sensors provide backup capability in the event the solar arrays block the view of the orbiter navigation instruments. The number of operating thrusters is decreased beyond 1.0 AU, as power available decreases. At approximately 3.0 AU, the SEP system is jettisoned as power available from the arrays falls below that needed to operate the propulsion system effectively.

3.5.3.2.3.4 Saturn-OL SEP Module Thermal Control Subsystem

The thermal system consists of coldplates, heat pipes, louvered radiator panels with embedded heat pipes, body mounted radiators on the faces containing the solar array drives, multi-layer insulation, heaters, coatings, and sensors. Radiators see deep space with ~5% view factor to the

Table 3.5.3-3: Change in Stage 1 Dry Mass with Changes in Step Masses

Δ Stage 1_i Mass / Δ Step_i Dry Mass	For Changes in Step 2 Mass Only	For Changes in Step 3 Mass Only
Δ Stage 1_i / Δ Step 1_{Dry} = $(m_i/m_f)_1$	1.00	1.00
Δ Stage 1_i / Δ Step 2_{Dry} = $(m_i/m_f)_2$ $(m_i/m_f)_1$	2.54	1.92
Δ Stage 1_i / Δ Step 3_{Dry} = $(m_i/m_f)_3$ $(m_i/m_f)_2$ $(m_i/m_f)_1$		8.01

Table 3.5.3-4: Saturn-OL Mission Level Summary Mass Statement

	Saturn OL
Launch Vehicle Margin (%)	**5.3**
Launch Vehicle Capability (kg)	**6525.0**
	Mass (kg)
Stage 1 (SEP+O+L) Initial	6196
- Stage 1 Propellant	700
Stage 1 Dry	5496
- Step 1 (SEP Module) Dry	1323
Stage 2 (O+L) Initial	4173
- Stage 2 Propellant*	2321
Stage 2 Dry w/instruments	1851
- Step 2 (Orbiter) Dry	977
Stage 3 (Lander) Initial	874
- Stage 3 Propellant	676
Stage 3 Dry w/instruments	198
* Includes residuals and loading uncertainty	

solar arrays. Three thermal shields are included to shield the heat radiated by the ASRGs on the orbiter.

3.5.3.2.3.5 Saturn-OL SEP Module Avionics, Flight Software, and Communications Subsystems

A digital control interface unit (DCIU), based on the Dawn DCIU, controls power and propulsion system operation from commands received from the orbiter (the orbiter manages all navigation and communication functions). Data received by the two omni antennas on the aft end of the SEP module are passed to the orbiter for processing. The DCIUs communicate with orbiter using 1553 protocol and communicate with the propulsion system using RS-485 protocol. Flight software, which controls power, propulsion, and thermal control functions, is identical on each DCIU, and each DCIU independently controls all the operating thruster strings. No communication interference from the exhaust plume at is anticipated at X- or Ka-band frequencies. Magnetic fields are not expected to have a significant effect forward above orbiter interface. The SEP separates well before operation of science instruments.

3.5.3.2.3.6 Saturn-OL SEP Module Requirements on Orbiter

The SEP module relies on the orbiter support for guidance, navigation and control, command and data handling and communications. The SEP module, off during launch, is commanded on by the orbiter. After separation, the orbiter nulls launch vehicle tipoff rates, issues the command to deploy the arrays, and puts the vehicle into a safe, power positive attitude (the ASRGs provide power for the orbiter but the solar arrays are required for SEP operation). Navigation solutions will be uplinked to the SEP module periodically (order of every 10 days), but in the interim, the orbiter provides autonomous navigation solutions. The orbiter also provides commanding for the ion thruster and solar array gimbals and provides all attitude control during coasting flight as well as roll control during single ion thruster operation.

3.5.3.2.4 Saturn-OL Orbiter Description

All orbiter subsystems are designed to be 1-fault tolerant for credible failures.

3.5.3.2.4.1 Saturn-OL Orbiter Mechanical Subsystem

The mechanical configuration is shown in **Figures 3.5.3-7**. Materials and construction is similar to that described in **Section 3.3.3.2.3.1**. The magnetometer boom is deployed after SEP separation.

3.5.3.2.4.2 Saturn-OL Orbiter Power Subsystem

Power for the booster and orbiter is provided by two 143 W (BOL) ASRGs and a 20 Ahr rechargeable lithium ion battery. The power system, located in the orbiter, provides 28V DC power to subsystems and instruments on the orbiter. The Saturn-OL orbiter has two ASRGs (shown under the instruments and the antenna in **Figure 3.5.3-7**). Power available from two ASRGs at the 9.5 year point is about 266 W. The maximum steady state power required for Saturn orbiting mission phase (this was the only point evaluated) is 258 W. The battery is used to provide power to transient peaking loads, such as communications and attitude control. After completing the Saturn-OL mission architecture design, it was determined

Table 3.5.3-5: Saturn-OL Step 1 (SEP Module) Mass Statement

Step 1 (SEP Module) Dry Mass				
	Estimate (Kg)	% Total Dry Mass	% Contingency	Allocation (Kg)
Avionics & Communications	14	1	30	18
Guidance, Navigation & Control	1	0	30	1
Electrical Power	500	49	30	650
Thermal Control	61	5	30	79
Structures	117	11	30	152
Propulsion	325	31	30	422
SEP Module Dry Mass	**1018**	**100.0**	**30**	**1323**
Step 1 (SEP Module) Wet Mass				
	Estimate (Kg)	% Total Wet Mass	% Contingency	Allocation (Kg)
SEP Module Dry Mass	1018	59	30	1323
Propellant Mass (Xenon)	700	40	0	700
SEP Module Wet Mass	**1718**	**100.0**		**2023**

Table 3.5.3-6: Saturn-OL Step 2 (Orbiter) Mass Statement

Step 2 (Orbiter) Science Payload				
	Estimate (Kg)	% Total Dry Mass	% Contingency	Allocation (Kg)
Thermal Infrared Mapper	11	1	30	14
Near Infrared Mapper	10	1	30	13
Visible Mapper	10	1	30	13
Laser Altimeter	12	2	30	15
Radio Science	1	0	30	1
Magnetometer	4	1	30	5
IMGCS	10	1	30	13
Dust Analyzer	5	1	30	7
Payload Total	**63**	**8**	**30**	**82**
Step 2 (Orbiter) Spacecraft Bus				
	Estimate (Kg)	% Total Dry Mass	% Contingency	Allocation (Kg)
Mechanical	237	32	30	308
Attitude Control	50	7	30	65
Thermal	32	4	30	42
Propulsion	200	27	30	260
Power	47	6	30	61
C&DH	23	3	30	30
Communications	58	8	30	76
Spacecraft Harness	42	6	30	55
Bus Total	**689**	**92**	**30**	**896**
Step 2 (Orbiter) Dry Mass				
	Estimate (Kg)	% Total Dry Mass	% Contingency	Allocation (Kg)
Science Payload Total	63	8	30	82
Bus Total	689	92	30	896
Obiter Dry Mass	**752**	**100**	**30**	**977**
Step 2 (Orbiter) Wet Mass				
	Estimate (Kg)	% Total Wet Mass	% Contingency	Allocation (Kg)
Orbiter Dry Mass	752	24	30	977
Propellant Mass*	2321	76	0	2321
Orbiter Wet Mass	**3073**	**100**		**3299**
* Includes residuals and loading uncertainty				

Table 3.5.3-7: Saturn-OL Step 3 (Lander) Mass Statement

Step 3 (Lander) Science Payload				
	Estimate (Kg)	% Total Dry Mass	% Contingency	Allocation (Kg)
Lander Camera (2)	0.6	0.4	30	0.8
Surface Transponder	0.0	0.0	30	0.0
Seismometer	2.0	1.3	30	2.6
Surface Chemistry Package	3.0	2.0	30	3.9
LDMS	4.0	2.6	30	5.2
Piezoelectric Corer	1.3	0.9	30	1.7
Surface Ice Oxidant Detector	0.3	0.2	30	0.4
Sample Delivery Mechanism	3.0	2.0	30	3.9
Payload Total	**14.2**	**9.3**	**30**	**18.5**
Step 3 (Lander) Spacecraft Bus				
	Estimate (Kg)	% Total Dry Mass	% Contingency	Allocation (Kg)
Mechanical	24.0	15.8	30	31.2
Attitude Control	4.7	3.1	30	6.0
Thermal	5.0	3.3	30	6.4
Propulsion	71.6	47.0	30	93.0
Power	16.2	10.7	30	21.1
C&DH	7.6	5.0	30	9.9
Communications	9.0	5.9	30	11.7
Bus Total	**138.0**	**90.7**	**30**	**179.4**
Step 3 (Lander) Dry Mass				
	Estimate (Kg)	% Total Dry Mass	% Contingency	Allocation (Kg)
Science Payload Total	14.2	9.3	30	18.5
Bus Total	138.0	90.7	30	179.4
Lander Dry Mass	**152.2**	**100.0**	**30**	**197.8**
Step 3 (Lander) Wet Mass				
	Estimate (Kg)	% Total Wet Mass	% Contingency	Allocation (Kg)
Lander Dry Mass	152.2	18	30	197.8
Propellant Mass	676.0	82	0	676.0
Lander Wet Mass	**828.2**	**100**		**873.8**

per ref. (f) a redundant ASRG would be required. This means a third ASRG would have to be added to the Saturn-OL design spaced 120° apart.

3.5.3.2.4.3 Saturn-OL Orbiter Thermal Control Subsystem

The Saturn-OL design has similar component temperature limits and design implementation to that used for Enceladus-OL with a few exceptions. For example, electronics boxes are mounted directly to the radiator panels, and the panels do not use embedded VCHPs. Also, Whipple-type debris shields used to protect the ASRGs are mounted off the top deck over the instruments and antenna. With the addition of a third ASRG, an additional shield would be needed.

3.5.3.2.4.4 Saturn-OL Orbiter Propulsion Subsystem

Orbiter propulsion is provided by a dual mode N_2O_4/hydrazine system, which is similar to that described in **Section 3.3.3.2.3.4** for the Enceladus-OL orbiter design, except for tank sizing. It operates in monopropellant blowdown mode for Stage 2 pitch, roll, and yaw control, as well as for roll control of Stage 1 up until SOI. Following SOI, all thrusters operate in pressure regulated mode. The combination of maneuvers conducted in bi-propellant and monopropellant mode over the total propellant expended results in an effective I_{sp} for the orbiter of 320 s for manuevers conducted before lander separation, and 272 s for manuevers conducted after lander separation. The large difference in I_{sp} is due to accounting for propellant residuals and loading uncertainty entirely in the post-lander separation maneuver. The propellant quantities in **Table 3.5.3-4** include a 5% ΔV tax to account for propellant used in non-ΔV attitude control maneuvers.

3.5.3.2.4.5 Saturn-OL Orbiter Attitude Control Subsystem

The orbiter ACS provides three axis attitude control for the Stage 2 configuration as well as roll control for the Stage 1 configuration. Four 33.2 Nms reaction wheels and thrusters mounted on the orbiter provide for slew and pointing control; 1.0° for Stage 1 and 0.1° for Stage 2. The attitude control requirement of 0.1° is driven by the laser altimeter instrument. The slew rate (5 mrad/s about the transverse axis for Stage 2) is driven by mapping the Enceladus surface at 4 km/s at an altitude of 200 km. Rather than require the mapper track a fixed position on the surface, which would require a higher slew rate, the target was permitted to move such that the slew rate was within the Cassini experience of ~5 mrad/s. This slew rate is also compatible for communication with the lander since most of that communication window occurs when the orbiter is moving away from Enceladus at altitudes >>200 km. Attitude knowledge is provided by a combination of two star trackers, 12 coarse Sun sensors, and two inertial reference units.

3.5.3.2.4.6 Saturn-OL Orbiter Avionics and Software Subsystem

With some minor exceptions, the avionics and software architecture for the orbiter is similar to that for Enceladus-OL as discussed in **Section 3.3.3.2.3.6**. Some important exceptions are that the Saturn-OL design C&DH system issues commands to SEP actuators, such as SEP thrusters, thruster gimbals, and solar array gimbals and deployment mechanisms.

3.5.3.2.4.7 Saturn-OL Orbiter Communications Subsystem

The orbiter communications system is similar to that used for the Enceladus-OL design. The total data to be downlinked over a single orbit (8.22 days) for orbiter flyby operations and lander operations is 7.0 Gb and 2.3 Gb, respectively. Using an average downlink data rate of 40 kb/s, it takes 48.6 hours, or 6.1 days at eight hours per day to downlink the orbiter data. This meets the need to deliver science data to the science operations center within one week (using a worst case downlink rate of 30 kb/s, this takes 64.8 hrs, or 8.1 days). During lander operations, downlink of lander data will have priority. Using an average downlink rate of 40 kb/s, transmitting data will take 16 hours or 2.0 eight hour contacts. A 9.0 hour per day contact with the DSN is available, and time will be scheduled to avoid any Saturn eclipses. The orbiter will communicate with the lander during descent and again 8.22 days later when the lander mission is complete. Link margins are 3.0 dB or greater except for the orbiter to ground omni antenna link (as discussed in **Section 3.3.3.2.3.7**) and the lander to orbiter uplink (2.8 dB). The geometry for communication with the lander is shown in **Figure 3.5.3-9**, where the orbiter path is from right (acquisition of signal, or AOS) to left (loss of signal, or LOS). The lander's shaped omni antenna is pointed toward the orbiter's receding path, as indicated in purple region. Communication to the lander is limited to several hours due to range. At the closest approach, lander data can be received in about four minutes at 10 Mb/s, but multiple telemetry rates (from 5 Mb/s to 50 kbps) are available to accommodate continuing to receive as the bi d

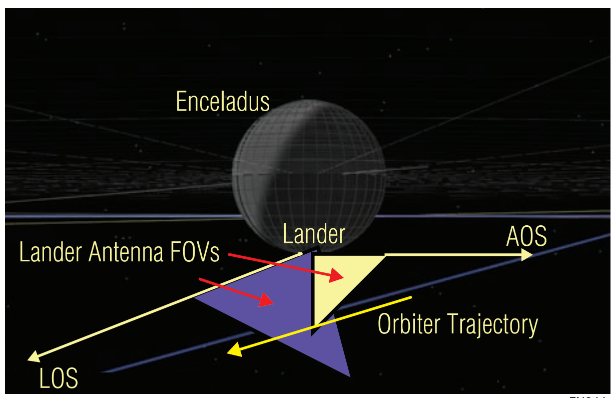

Figure 3.5.3-9: Saturn-OL Lander Communication Field of View to Orbiter

3.5.3.2.5 Saturn-OL Lander Description

The Saturn-OL lander delivers the instruments listed in **Table 3.5.2-2** to the surface of Enceladus to operate for eight days. It needs a large propulsion system to provide the ΔV from Saturn orbit and shares some subsystem design features with the Enceladus-OL lander. The Saturn-OL lander has selective redundancy and is not fully single fault tolerant. The rationale for this was within the short lander lifetime (five days of instrument operation, eight days for communication), it was not clear that designing the capability to execute an autonomous switch to a redundant string would be any more effective than would carefully designing and testing single string system.

3.5.3.2.5.1 Saturn-OL Lander Braking, Descent, Landing, and Surface Operations

The lander is off for most of the ~ nine years between launch and lander deployment. It is turned on periodically to checkout the lander components. While attached to the orbiter, the lander uses the orbiter's power.

The lander is deployed from the orbiter using a clampband separation system and springs. The target landing site is the south polar region, as in the Enceladus-OL concept.

The landing profile is shown in **Figure 3.5.3-10**. The separation is within an hour of landing. At the appropriate point in its trajectory, the lander initiates its major burn. When the lander is within the gravitational sphere of influence of Enceladus, the lander suspends the burn in order to calibrate its accelerometers. When the lander is about 20 km from the surface, it uses its imager and the onboard maps to locate its position. It uses the propulsion system to slow its descent and to translate to the landing target. At a 5-km height, the hazard avoidance software uses the data from the imager to identify and avoid hazards, such as ice blocks larger than ~25 cm that could cause the lander to overturn. The lander turns off the thrusters at a height of 50 meters and the lander descents gently to the surface. The lander retains a small residual horizontal velocity when the thrusters are turned off so thruster plumes do not contaminate the landing site. The lander sends telemetry data to the orbiter from separation through landing.

The instruments start operating immediately upon landing. The camera/antenna mast is deployed and the onboard computer determines the optimal antenna pointing direction based on the received power from the orbiter's signal at various pointing directions. The seismometer couples itself to the surface by placement along a lander leg and takes data for the duration of the lander's lifetime. The imagers take a panoramic picture every two hours over one Enceladus day. The imagers also observe the plumes, with onboard change detection software processing this data to reduce its volume. The sample collection device collects the samples and distributes them to the three sample analysis instruments. The lander's avionics collects the instrument data and stores it until the orbiter returns 8.22 days later. The imaging and sample analysis instruments are turned off on day six to conserve power, but the seismometer stays on for eight days. When the orbiter returns on its next orbit, it commands the lander to uplink the stored data. The data is transmitted at rates that vary up to 10 Mbps. The total transmission time is about 10 minutes.

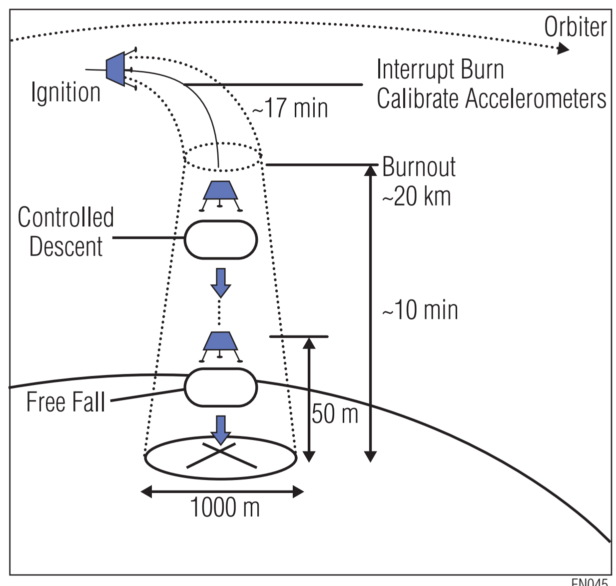

Figure 3.5.3-10: Saturn-OL Landing Profile

3.5.3.2.5.2 Saturn-OL Lander Mechanical Subsystem

The lander structure is a composite tubular truss with supports for experiments and spacecraft components. The camera mast is deployed after reaching the surface. **Figure 3.5.3-8** shows the lander and its components.

3.5.3.2.5.3 Saturn-OL Lander Power Subsystem

The lander is powered by a lithium-ion battery with a capacity of 5000 Watt-hours. The battery is made up of fourteen eight-cell strings.

3.5.3.2.5.4 Saturn-OL Lander Avionics and Flight Software Subsystems

The avionics system is single string. The avionics includes the lander processor, a communications card, propulsion electronics, and power supply electronics. The processor is a PowerPC class unit that provides 240 MIPS at a clock speed of 132 MHz. The avionics uses RS422 connections to the science instrument for science data and a 1553 bus for command and telemetry communication. The lander can store 2.3 Gbits of science and housekeeping data, including 30% contingency and CCSDS overhead.

The lander flight software processes the imager, radar altimeter, and other ACS sensor data to provide for a safe landing. It uses the onboard maps and the imager data to locate itself, then maneuvers the lander to the target while avoiding hazards. Once on the ground, the flight software processes the plume images to detect changes in order to reduce the volume of the data. Flight software margins for the central processor and memory exceed 50%.

The option of using a lower power RISC 68K class processor instead of the PowerPC class unit was evaluated, but the RISC 68K class processor was not powerful enough to perform the image processing required for a safe landing.

3.5.3.2.5.5 Saturn-OL Lander Propulsion Subsystem

Due to the high lander ΔV requirement of 4.3 km/s, the propulsion system for the Saturn-OL lander is a Hydrazine/N_2O_4 bipropellant system. A comparison of a bipropellant system vs. a solid rocket motor (for the deorbit burn) with a monopropellant system (for the soft landing) showed the bipropellant system required 125 kg less mass than the solid rocket motor / monopropellant option.

The propulsion system uses four identical tanks, three 458 N main engines, and eight 9 N attitude control thrusters. The propulsion system is selectively redundant, with dual check valves, pyro valves, and regulators.

3.5.3.2.5.6 Saturn-OL Lander Attitude Control Subsystem

The lander attitude control system consists of an IMU (gyro and accelerometer), radar altimeter, star tracker, and the imaging instruments. The lander uses the IMU for navigation from separation from the orbiter until the lander is about 20 km from the surface. The major burn is interrupted once the lander is within the sphere of influence of Enceladus' gravity in order to calibrate the IMU. At 20 km above the surface the lander transitions to use of the imager and radar altimeter (on the lander bus) to complete navigation for the landing. The attitude control thrusters provide six degree-of-freedom control. The attitude control system is single string.

3.5.3.2.5.7 Saturn-OL Lander Thermal Control Subsystem

The lander thermal control system maintains the temperature of the instruments, battery, electronics, and propulsion systems within operating limits through the use of RHUs. The lander is covered with 18 layers of MLI, including a layer of Kevlar that provides the first layer of the Whipple shield that protects the lander from particle impacts while attached to the orbiter. The lander propulsion module is thermally conditioned prior to separation to minimize the amount of lander battery power required for heaters. The thermal system for the lander is single string.

3.5.3.2.5.8 Saturn-OL Lander Communications Subsystemp

The lander communicates with the orbiter using X-band. The lander's frequencies are reversed from the orbiter, with the lander's transmitter using the same frequency as the orbiter's receiver and vice versa. The lander uses a 5 Watt transmitter and one cross-dipole omni antenna and one shaped omni antenna that points to the orbiter's trajectory. The orbiter uses its high gain antenna to communicate with the lander. The lander telemetry data is convolutionally encoded.

3.5.3.2.5.9 Saturn-OL Lander Integration and Test

The lander is integrated and tested as a unit, in parallel with the orbiter. (see **Section 3.5.3.2.8**) The lander requires cleaning to level IV planetary protection requirements.

3.5.3.2.6 Saturn-OL Mission Reliability

Reliability for this mission lifetime (a total of

10 years was used for this analysis) is moderate. A probability of mission success of .808 is estimated at the 95% confidence level. The SEP module and orbiter ACS are the mission reliability drivers due to their long operating lives in comparison with the lander. The lander is single string with the exception of the power subsystem and some selective redundancy in the propulsion subsystem. A 90% duty cycle was assumed for the SEP module. The limitations of this type of preliminary reliability discussed in **Section 3.3.3.2.5** apply to Saturn-OL.

3.5.3.2.7 Saturn-OL Mission Orbital Debris Protection

Risks due to orbital debris were evaluated for four regimes: 1) asteroid belt, 2) Earth fly-by, 3) Enceladus plume crossings, and 4) Saturn E-ring. The collision probability in the asteroid belt is small and did not require any specific mitigation. For Earth flyby, the orbiter propulsion tanks are protected by MLI as described in **Section 3.3.3.2.6** for the Enceladus-OL configuration, and the risk of penetration is similar. For the plume crossing, Whipple-type shields as described in **Sections 3.1.1.4** and **3.5.3.2.4.3** are oriented: a) on the base of the lander in the ram direction, b) on the orbiter top deck, c) over the ASRGs, and d) over the instrument deck. As a precaution, before lander separation, the orbiter trajectory is offset from the plume to avoid the potential for significant impacts. For the E-Ring crossing, the debris environment is expected to be enveloped by the Enceladus debris environment. In the E-ring, typical particles are expected to be smaller (less than 1.0 micron) and more scattered than in the Enceladus plume.

3.5.3.2.8 Saturn-OL I&T

Parallel fabrication and component test for the orbiter bus, orbiter instruments, lander bus, and lander instruments starts in November 2014 (the longer lead SEP module fabrication starts in August 2014). This is followed by parallel I&T for the same hardware elements starting in November 2015 (this phase includes lander drop testing). Instruments are then integrated with the orbiter bus and lander bus starting in August 2016, fit checks are conducted with the SEP module, and parallel orbiter and lander I&T is conducted. In May 2017, the orbiter and lander are mated for I&T as a combined unit. In September 2017, the SEP module is integrated with the orbiter and lander and combined SEP module/orbiter/lander I&T is conducted. The flight segment is ready for shipment to the launch site in December 2017 for a March 2018 launch.

3.5.4 Saturn-OL Operational Scenarios

Table 3.5.4-1 identifies the driving operational scenarios for this mission concept.

Table 3.5.4-1: Saturn-OL Driving Operations Scenarios

Scenario	Driver
Earth Flyby	Safety, thermal
Saturn Orbit Insertion	Power
Enceladus Flyby	Data Volume
Landing and Data Relay	Lander Design

The Earth flyby drives the spacecraft thermal design. The spacecraft is closest to the Sun during this phase. The orientation of the spacecraft is driven by the need to keep the SEP thrusters pointed in the optimal direction. The spacecraft has some freedom in the roll axis, and positions the spacecraft to minimize the solar heating and to point the radiators toward deep space.

The Enceladus flyby orbit generates the largest data volume. With the exception of the magnetometer, which generates data all of the time, the other instruments only take data for a few minutes around closest approach to Enceladus. **Figure 3.5.4-1** shows the timeline for a typical flyby. Stored data is downlinked once per day to the DSN over the next eight days.

The landing is an operations driver. The lander separates from the orbiter and autonomously lands near the south pole. The lander uses its bipropellant propulsion system to perform the ΔV maneuver to match the Enceladus orbital velocity and to softly land at the surface. The orbiter monitors the landing from separation through landing, ending when the link can no longer support the data rate, an hour or so after landing. The lander instrument timeline is shown in **Figure 3.5.4-2**. The orbiter returns 8.22 days later and collects the lander data. Once the data has been transmitted to the orbiter, the lander's mission is completed.

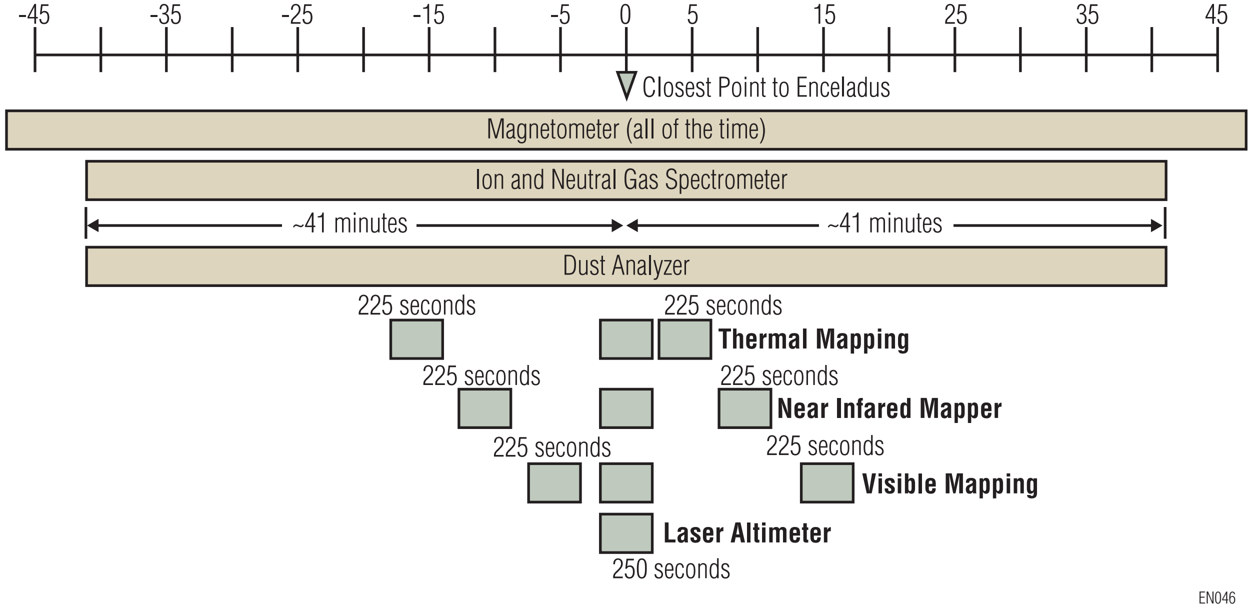

Figure 3.5.4-1: Enceladus Flyby Timeline for Saturn-OL Orbiter

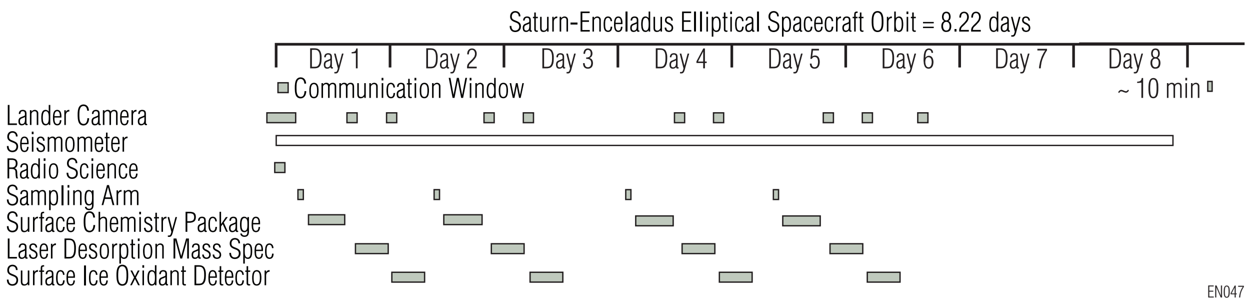

Figure 3.5.4-2: Saturn-OL Lander Timeline

3.5.5 Saturn-OL Planetary Protection (& Disposal)

The lander is disposed of in place on Enceladus, and is designed and cleaned to planetary protection level IV. Analysis that demonstrates the orbiter will have a less than $1x10^{-4}$ probability of inadvertently contaminating any icy moon inside of Titan's radius has not been done, and is recommended for future study. For the purposes of this study, it was presumed the orbiter would need to be cleaned to planetary protection level IV.

3.5.6 Saturn-OL Major Open Issues and Trades

3.5.6.1 SEP Size

The SEP system needs to be optimized, i.e., size of the solar arrays, number of engines to provide the best solution in terms of cost, trip time to Saturn, and V_{hp} at Saturn.

3.5.6.2 IMU Calibration

The calibration of the IMU on the lander needs to take place within Enceladus' gravitational sphere of influence. The details of how this calibration is performed and the impact on the accuracy of the landing need further work.

3.5.6.3 Lander Heaters

The lander heaters are a mix of electrical heaters and RHUs. Further study is required to optimize the combination for the lowest power usage capable of maintaining the appropriate temperatures while the lander is attached to the orbiter and once on Enceladus.

3.5.6.4 Radiation Model

The need for an updated Saturn radiation model (see **Section 3.3.6**) also applies to this design.

3.5.6.5 Debris Shielding

Conduct a study to define whether the Saturn-OL Orbiter needs to include particle shielding on the nadir face (maximum particle size and shield thickness for ~30-second plume transit time).

3.5.6.6 Lander Separation Time

Further investigation will be needed to determine the optimum time to separate the lander. It is likely more than about 40 days will be needed for the science team to evaluate mapping images to select a suitable landing site.

3.5.6.7 SEP Module Requirements on Orbiter

The SEP module relies on the orbiter support for guidance, navigation and control, command and data handling, and communications as discussed in **Section 3.5.3.2.3.6**. The effects associated with these phenomena were not fully addressed in this study. The degree to which these functions need to be implemented should be more fully addressed if this concept is pursued further.

3.5.6.8 Orbiter Power System Sizing

The orbiter has two operating ASRGs, and both are required to deliver power. Even though mission life is 9.5 years, a backup ASRG (and Whipple shield) will be needed. Investigation of additional load cases, such as SOI which has extended transient loads for propulsion, may drive battery size as well as the need for an additional operating ASRG.

3.5.6.9 Thruster Location

One risk in the area of propellant quantity required has to do with positioning thrusters to provide pure pitch, roll and yaw torques with and without the SEP module attached as plume impingent on the orbiter may require larger thruster cant angles. And, there may be an increased reliance on ACS to accommodate the center of gravity shift after lander separation. Each of these can cause a reduction in effective specific impulse and increase ACS propellant required.

3.5.6.10 Lander Fault Tolerance

The lander design is single string with selective redundancy and is not fully one fault tolerant (see **Section 3.5.3.2.5**). The trade between the effectiveness of a 1-fault tolerant system vs. a carefully designed and tested single string system should be addressed for a lander lifetime of eight days, most of which is spent out of communications contact, with respect to reliability and mass estimates.

3.5.6.11 SEP Trajectory Analysis

Determine whether SEP trajectories with C_3 values below that used in this section exist. Trajectories with lower C_3 values (e.g., with more inner planet gravity assists) would increase the allowable launch mass.

3.5.6.12 Lander ΔV Reserve

Re-evaluate the need to hold ΔV reserve on the lander EOI burn.

3.5.7 Saturn-OL Technology Needs

3.5.7.1 SEP

The SEP module is currently at TRL 5 and has the funding from the planetary science technology budget to advance designs to TRL 6 prior to the need date for this mission.

3.5.7.2 Landing

The landing technology is the same as discussed in **Section 3.3.7** for Enceladus-OL.

3.5.8 Saturn-OL Technical Risk Assessment

The orbiter has only one opportunity to collect the lander data, on the next flyby 8.22 days after the landing. The lander has enough autonomy to manage its power. For example, if the power remaining falls below a certain threshold, the lander data system turns off instruments early in order to ensure that enough power remains to transmit the data. Trades that provide enough power to support a second flyby communication opportunity should be pursued in future studies.

3.5.9 Saturn-OL Schedule

The Saturn-OL design uses a development schedule of 73 months from the start of Phase B to launch. The durations of Phase B, C, and D are 12 months, 20 months, and 45 months, respectively. The length of Phase D is driven principally by the length of time need to fabricate, integrate and test the booster and orbiter systems both separately and in combined configurations, and includes the four month period immediately following launch (i.e., the duration of Phase D up until launch is 41 months).

3.6 Other Identified Architectures in the Trade Space

The three mission concepts (Enceladus-OL, Enceladus-O, and Saturn-OL) discussed in **Sections 3.3**, **3.4**, and **3.5** provide insight into key points in the architecture trade space. In this section, the knowledge gained in developing those three concepts is applied to explore the feasibility, advantages, and disadvantages of other mission concepts in the architecture trade space of **Section 3.2**.

3.6.1 Enceladus Orbiter that Lands w/Chemical Propulsion

A spacecraft orbiting Enceladus and a soft lander have similar instruments – imagers, *in-situ* analyzers - and have common needs for some of the subsystems, for example, communications and power. Since the gravity of Enceladus is so weak, would a mission where the entire orbiter lands be better than a mission with a separate orbiter and lander? An orbiter that lands avoids a duplication in instruments and subsystems and would be more robust, having a long-lived radioisotope power source and direct communications to Earth, through a large HGA.

For Enceladus-OL, the orbiter dry mass was 968 kg and the lander wet mass was 228 kg. It would require almost as much propellant mass, 150 kg, to land the orbiter as was saved by eliminating the need for a separate lander. In addition, the instruments and subsystems would be more complex – the imagers would have to articulated, the HGA would have to be on a gimbal, a sampling arm and some method to couple the seismometer to the surface would be needed, the overall center of mass would have to be low enough so that tipping was not a risk, etc. Since the science requirements could be met with a lander with a short lifetime, this architecture was not studied further. It could be considered if there were a need for a large, long-lived lander.

3.6.2 Enceladus Orbiter Using SEP

A trade study was conducted to determine how adding the 2023 kg SEP module would affect the Enceladus-O mission concept. The results are shown in Case 1 of **Table 3.6.1-1**. The top level result is the added mass of the SEP module enables a quicker start for mapping operations at the cost of reducing the mass available for the balance of the flight segment (for a given level of required ΔV). For the purposes of this trade study, the size of the SEP module was assumed fixed.

Flybys of both Dione and Tethys were required to enable a solution with a positive launch margin. They reduced the ΔV by 860 m/s relative to the value of 4977 m/s used in **Section 3.4**. The booster step was removed, and the orbiter was scaled up to meet the total ΔV requirement of 4117 m/s. The resulting lift mass of 6000 kg is marginally heavier than the Enceladus-O configuration of **Section 3.4**. However, with the faster SEP trajectory, mapping begins at 13.25 years, whereas in **Section 3.4**, it begins at 15.0 years. Staging by adding a booster step to reduce launch mass, increase orbiter payload, or increase mapping orbit fuel mass did not appear practical. A booster step dry mass of about 300 kg would be needed in order to provide a benefit. This is about half the dry mass of the booster step for Enceladus-O in **Section 3.4** (see **Table 3.4.3-3**), while the propellant required is about 60% of the Enceladus-O booster propellant in **Section 3.4**.

3.6.3 Enceladus Orbiter with Hard Impactor(s)

One of the science goals is to investigate the internal structure of Enceladus. One method to do this would be to deploy several widely separated seismometers. Using multiple soft landers is not feasible due to the mass that would be required; however, given the low gravitation of Enceladus, hard impactors might be feasible. A hard lander that was dropped from a 200 km altitude impacts the surface at a velocity of about 210 m/s.

A design for a hard lander was looked at briefly during this study. The hard impactor mass was about 15 kg (including the solid rocket motor, but excluding the deployment mechanism). It deploys from the orbiter and is spun up. Then a small solid rocket motor fires to null the orbital velocity. The impactor falls to the surface and uses an airbag or crushable material to absorb the shock of landing. Once the impactor stops rolling, bouncing, or tumbling, it adjusts its orientation and operates for the duration of the battery life (several days). The brief assessment of hard landers in this study identified the need for further definition in battery sizing, thermal design, communication visibility between the orbiter and lander; methods for deploying from the orbiter, spinning up/spinning down before/after solid rocket motor firing, absorbing landing shock, adjusting to

Table 3.6.1-1: Comparison of SEP, Chemical, and Two-Launch Options

Case	Name	Launch Vehicle	Lift Mass (kg)	LV Capab. (kg)	Launch Margin (%)	Major Modules (Steps)	Gravity Assists R Rhea D = Dione T Tethys	Orbiter + Booster[1] ΔV (m/s)	Time at Start of Mapping (yrs)	Instrument Complement
Electric vs. Chemical Propulsion Study Results										
1	SEP for Enceladus-O	Delta 4050 H	6000	6525	9.7	SEP Chem Orbiter	R, D, T	4117	13.25	Enceladus-O
2	All Chemical Saturn-OL	Altas V 551	4460	4460	0.0	Chem Orbiter Bi-prop lander	None	2797	12.5	Saturn-OL + ~240 kg dry mass lander
Two Launch Study Results										
3a	All Chemical Enceladus-O	Atlas V 551	4460	4460	0.0	Chem Booster Chem Orbiter	R, D, T	4117	17.5	Enceladus-OL (no sounding radar)
3b	All Chemical Enceladus-O	Delta 4050 H	6160	6300	2.2	Chem Booster Chem Orbiter	R	4977	15.0	Enceladus-OL with sounding radar added
4	All Chemical Saturn-OL	Atlas V 551	4460	4460	0.0	Chem Orbiter Bi-prop lander	None	2797	12.5	Saturn-OL + ~240 kg dry mass lander
5a	All Chemical Enceladus OL LEO Assy.	Delta 4050 H	23000	23000	0.0	Chem Transfer	R, D	4497	16.0	None - launches part of the chemical transfer module
5b	All Chemical Enceladus OL LEO Assy.	Delta 4050 H	37220	23000	-38	Chem Transfer Chem Booster Chem Orbiter Mono-prop lander	R, D	4497	16.0	Launches remaining part of transfer module + ~ 6300 kg Enceladus-OL (incl. instruments) Stage 1

1. Booster and orbiter ΔV excludes Transfer Module, SEP, & LanderΔV

preferred orientation once on the surface (e.g., use of a clamshell type deployment, use of a sphere with a low center of gravity, etc.), and coupling to the surface for seismometry; and time correlation among the landers and the orbiter. Hard impactors are attractive for their low mass and the ability to create a network of seismometers and/or magnetometers. If pursued in the future, technology investment would be required to develop techniques to survive the landing and couple to the surface.

3.6.4 Saturn Orbiter with Soft Lander Using Chemical Propulsion and Gravity Assists

A trade study was conducted to determine how replacing the 2023 kg SEP module and a single Earth gravity assist trajectory with chemical propulsion and a VVEES trajectory would affect the Saturn-OL mission concept. The results are shown in Case 2 of **Table 3.6.1-1**. The removal of the SEP module extends the time from launch to SOI from 7.5 years to 11.75 years (assuming the middle of the launch window, per **Table 3.3.3-1**), which enables start of mapping at 12.5 years in the Titan-Enceladus elliptical orbit. Since the ΔV budget for the chemical portion of the trajectory is effectively the same with or without the SEP module, removing the SEP module results in a mass credit. In this case, mass reduces sufficiently to permit an Atlas V 551 launch concurrently with a lander dry mass of ~240 kg. Equivalently, the mass reductions could be used to add capabilities to the Saturn orbiter, to increase the C_3 of the trajectory (V_{hp} constraints would need to be considered with respect to braking), or perhaps to eliminate a Venus or Earth flyby and reduce time between launch and SOI. The ΔV budget used for this analysis was the same as used in **Section 3.5**. The lander was assumed deployed after five Enceladus flybys. Should additional flybys be needed to map the landing site, an increase in propellant mass would be required.

3.6.5 Saturn Orbiter with Soft Lander Using SEP and More Saturnian Moon Flybys

The Saturn-OL orbiter is in a Saturn orbit with apoapsis at Titan and periapsis at Enceladus. The science mission starts about nine months after SOI. Rhea, Dione, and Thethys could be used to provide gravity assists to lower the apoapsis and reduce the ΔV required for the soft lander. Lowering apoapsis also would reduce both the periapsis velocity and the relative velocity with respect to the Enceladus orbital velocity (12.63 km/s). **Table 3.6.5-1** summarizes results of an analysis that uses gravity assists from these moons (using the approach described in **Section 3.1.1.2.2**) to lower apoapsis from Titan to: a) Rhea, b) Dione, and c) Tethys. Results show the total residence time in the plume increases with each additional gravity assist due to reductions in spacecraft relative velocity at periapsis. The disadvantage of the gravity assists is the additional time required: 2.5 years for Rhea, 3.5 years for Rhea + Dione, and a 5.0 years for Rhea + Dione + Tethys. However, offsetting this is a total mapping phase time reduction of about six and nine months when apoapsis is at Rhea and Dione, respectively, as these mapping orbits have shorter flyby intervals than orbits with apoapsis at either Titan or Tethys. The apoapsis values selected to achieve the three resonance orbits evaluated is slightly lower than the Rhea orbit, slightly higher than the Dione orbit, and slightly higher than the Tethys orbit, respectively. The apoapsis values used for resonance are: Rhea (517,300 km), Dione (385,500 km), Tethys (299,500 km). A one-time ΔV burn (about 45-60 m/s) adjusts the orbit upon completion of the gravity assist maneuver to achieve the resonant apoapsis. The Enceladus orbit period

Table 3.6.5-1: Total Plume Dwell Time and Total Mapping Orbit Time for Multiple Resonant Orbits

Orbiter Orbit Option	Lander ΔV (km/s)	Time from SOI to Science Ops (yrs)	Flyby Velocity at Periapsis (km/s)	Total Plume Dwell Time (min)	S/C Orbit Period (days)	Orbit Ratio #S/C: #Encel	Flyby Interval (days)	Total Mapping Orbit Time (days)
Titan/Encel.	4.3	0.75	3.82	5.5	8.22	1:6	8.22	411
Rhea/Encel.	2.6	3.25	2.15	9.8	2.74	1:2	2.74	137
Dione/Encel.	1.8	4.25	1.42	14.8	2.06	2:3	4.12	206
Tethys/Encel.	1.1	5.75	0.70	29.9	1.64	5:6	8.22	410

used in this analysis is 1.37 day (where days are specified, they are mean solar days of 86,400 s). A total of 12 plume passes was held fixed among the options. A total of 550 m/s (without reserve) is allocated for mapping orbit operations. Each flyby is assumed to require 10 m/s for targeting. This enables 50 flybys, most of which target locations away from the plume. Total plume dwell time is the total time resident in a 105 km wide plume at an altitude of 200 km over 12 flybys.

The reductions in ΔV resulting from the use of these gravity assists would reduce the mass of the lander propellant. That mass could be reallocated toward more orbiter or lander instruments, a larger lander battery, a larger orbiter high gain antenna, etc. Flyby intervals less than 6.1 days would require enhancements in the communications link or a reduction in data downlinked (see **Section 3.5.3.2.4.7**).

3.6.6 Saturn Orbiter with Hard Impactor(s)

The hard impactors described in **Section 3.6.3** for the Enceladus orbiter were also briefly considered in the Saturn-OL architecture. In this architecture they were to be deployed from the soft lander, so they did not require a separate solid rocket motor. The hard impactors were not defined in any detail due to the modest science utility and the technology risks associated with surviving the impact.

3.6.7 Sample Return with or without an Orbiter

Multiple architectures were identified with sample return capability – a sample return-only mission, a sample return with a Saturn orbiter, and a sample return with an Enceladus orbiter. In the orbiter cases, the sample return vehicle would separate from the orbiter prior to SOI and the two vehicles would operate independently after separation. In all cases, only free return trajectories were considered for the sample return vehicle, where it flies once through the plume on a trajectory that returns it to Earth. As discussed in **Section 3.1.1.2.3**, these architectures were unattractive due to the long mission durations and the risk of having only a single sampling opportunity. None of these architectures was pursued in this concept study. Sample return missions that enter Saturn orbit and allow multiple plume passages at relatively low speed would be worth further study, though mission durations would be long and the required ΔV would increase.

3.6.8 Dual Launch Vehicle Scenarios

Launch mass is a major constraint on this mission. One way to deliver more mass is to use multiple launch vehicles. A trade study was conducted to evaluate the operational utility resulting from the use of two launch vehicles rather than one. Two scenarios were evaluated. The first addresses launching two separate flight segments, one of which has the principal purpose orbiting Enceladus and conducting science operations and the other of which has the principal purpose of delivering a lander to Enceladus. This scenario is addressed in Cases 3a, 3b, and 4 in **Table 3.6.1-1**. Cases 3a and 3b use an Enceladus orbiter equipped in the Enceladus-OL configuration of **Section 3.3**, but Case 3b includes a mass allocation for a sounding radar (equipping it in the Enceladus-OL configuration enables it to function with a lander). Case 3a uses an Atlas V 551 with Rhea, Dione, and Tethys gravity assists and enables start of mapping operations at 17.5 years. Case 3b uses a Delta 4050H with a Rhea gravity assist and enables start of mapping operations at 15.0 years. Case 4 uses an Atlas V 551, as discussed in **Section 3.6.4**, to deliver a lander carrier spacecraft in the Saturn-OL configuration of **Section 3.5** to Saturn orbit and to enable the start of mapping operations at 12.5 years (the lander is deployed after five mapping orbits).

Considering Case 3b and Case 4, the arrival schedules between the lander carrier spacecraft and Enceladus-orbiter differ by 30 months, whereas launch opportunities occur every 18 months. Assuming the lander carrier spacecraft launches 36 months after the Enceladus orbiter, this would require the Enceladus orbiter spacecraft to hold in a safe orbit (radiation exposure should be considered) for about a six-month period before starting joint operations (alternatively, launching 18 months after the Enceladus orbiter would require the lander carrier spacecraft to hold for 12 months).

While the lander spacecraft configuration studied was outfitted the same as the Saturn-OL configuration of **Section 3.5**, launching two spacecraft should enable removal of some instrumentation from the lander carrier spacecraft (though including instrumentation could enhance science return) to further enhance the lander. For example, the Enceladus orbiter could perform the pre-landing survey and would provide the communications relay function. The lander carrier spacecraft would have an HGA and would maintain communications coverage during lander descent, but would not need science data storage or processing functions. The obvious disadvantages to the two-launch approach are cost, e.g., two launch vehicles, two complete spacecraft, and double the number of DSN contacts for at least the cruise phase of the mission, etc., and operational complexity.

The second scenario evaluated the launch capability required to launch two flight segments to LEO, where they would be assembled and placed into the VVEES trajectory by a large bipropellant transfer module. The required C_3 for this is 19.05 km^2/s^2 and the corresponding ΔV is 4.06 km/s. One of the flight segments included the Enceladus-OL configuration (~6300 kg gross mass) and part of the transfer module. The second flight segment included the remainder of the transfer module. Case 5 in **Table 3.6.1-1** shows even if there were a capability to launch two Delta 4050H vehicles within 20 days of each other (currently this capability does not exist), the lift required mass significantly exceeds the capability of the two vehicles. In this analysis, the transfer module dry mass was assumed to be about 20% of the propellant mass. The complexities of rendezvous and docking were not considered. With regard to assembly at non-LEO locations, there are no other locations en-route to Saturn where assembly could be easily performed. Performing rendezvous and docking at Saturn, ~80 light minutes away from Earth, would be complex and risky.

3.7 References

a. Titan Aerocapture Systems Analysis, AIAA Paper 2003-4799, M. Lockwood, NASA/LaRC.

b. Dr. Eric Christiansen, NASA/JSC - KX.

c. Delta IV Payload Planner's Guide, Oct 2000, as updated Apr 2002 and Nov 2002.

d. Mr. Eric Haddox, NASA/KSC Flight Dynamics Branch, VA-H1.

e. Dr. Alan Harmon (Department Of Energy), NASA HQ.

f. Dr. Jacklyn Green, NASA/JPL, Mission Systems Engineering Office (1911).

4.0 CONCLUSIONS AND FINDINGS

A mission to Enceladus would produce science that is highly relevant to NASA goals as laid out in the 2003 Decadal Survey and described in this report. The accessibility of subsurface water enables sampling through conventional means and without complicated drilling scenarios. The SDT defined a comprehensive set of science goals that can be met, to varying degrees, by a wide range of mission configurations.

The highest priority science goal for a future Enceladus mission is the investigation of its biological potential. Of secondary importance are the understanding of Enceladus' tidal heating and interior structure, its composition, its cryovolcanism, and its tectonism. Of tertiary importance is the understanding of surface processes, and the interaction of Enceladus with the rest of the Saturn system.

Cassini can still make valuable contributions towards addressing these questions, but is limited by its instrumentation, its orbit and by its inability to land on Enceladus. Each of the remaining Enceladus flybys can be optimized for only a few of its science instruments. Thus, Cassini cannot adequately address the advanced science goals defined here.

These goals can be met most effectively by both orbiting Enceladus and landing on its surface. Orbiting Enceladus allows comprehensive mapping of its surface morphology, composition, and heat flow, including detailed investigation of the active plume vents. The interior structure and tidal heating mechanisms, including the presence or absence of a subsurface ocean, can also be investigated in detail, by determination of the moon's gravity and global shape, its potential and shape Love numbers, and its magnetic induction signature. Crustal structure can also be probed using sounding radar. Multiple plume passages at the low orbital speed of ~150 m/s will allow collection of intact plume particles and complex organic molecules from the plume for onboard study. One important engineering limitation, which will restrict the number of passages through the plume and over the plume source regions, is that Enceladus orbits with inclination greater than about 50˚ are unstable on short timescales.

A properly-instrumented Enceladus orbiter alone can address all science goals quite well. However, because the total mass of particles that can be collected from the plume is quite small, probably less than 2 x 10^{-7} g/cm^2 per plume passage, analysis of important trace species that require a large sample to process requires a lander. A lander also provides the opportunity for seismic sounding of Enceladus' crust, which is the most robust way to measure crustal thickness, as well as allowing a unique close-up view of surface processes.

Valuable science can also be accomplished from a mission that includes a Saturn orbiter that makes multiple (~50) Enceladus flybys, coupled with a lander. The larger number of flybys, and the use of modern Enceladus-optimized instrumentation, would provide a large increase in our understanding of Enceladus from the Saturn orbiter compared to Cassini, though science from the orbiter alone would not be sufficient to justify a Flagship mission budget. However, the addition of a lander greatly enhances the science return. The detailed analysis of surface samples possible from a lander compensates for the lower-quality plume sampling (compared to an Enceladus orbiter) possible during 4 km/s flybys from Saturn orbit.

The mission design team developed three promising concepts using state of the practice technology: Enceladus-OL, Enceladus-O, and a Saturn-OL, with cost estimates in the two to three billion dollar ($FY07) range. All three present the possibility of providing compelling Flagship mission science, and represent single points in the architecture trade space.

The knowledge accrued from these three concepts was used to gain insight into the remainder of the trade space, including choice of propulsion system, variations in payload, inclusion of sample return, and viability of dual launch vehicle scenarios. For each case, trades can be made that affect mission lifetime and deliverable mass. In addition, common key challenges, risks and technology liens emerged.

In particular, the biggest challenge is in the trajectory design and resultant ΔV budget. First, chemical propulsion or SEP may be used. SEP trajectories usually offer shorter flight times for an equivalent launch mass, at the expense of available payload capacity. Chemical trajectories can be improved to provide increased launch mass with the use of multiple inner solar system flybys, which result in longer flight time. In both cases, the trajectory may be optimized to avoid propulsive maneuvers and propellant use, or to decrease flight time by using such maneuvers. In addition, the gravity assists provided by both the inner solar system moons and Saturn itself, can be optimized with different flyby altitudes, but with the added risk from thermal effects and debris impacts. Finally, aeroassist may also be used to decrease the propellant mass needed in achieving Saturn or Enceladus orbit, but adds to design complexity, and increases risk and complexity.

There is an additional challenge in orbiting Enceladus. Current gravity models of Enceladus do not contain sufficient information, but such information can only be obtained by a mapping mission. This model affects the orbital stability, so such calculations are currently only a best estimate and risk can be mitigated with sufficient propellant reserves. In addition, the Saturn environment radiation model has not been updated since pre-Cassini experience. Current best estimates of the radiation experienced in the vicinity of Enceladus probably over-estimate the total radiation dosage, because mitigation effects of a neutral gas torus are not included. Future work to update this model with flight data is warranted.

The missions presented here all have long required lifetimes, regardless of which trajectory is chosen. One further trade that can reduce the required prime science mission lifetime is in the size and power of the communications system, which can be optimized to return all data in the minimum amount of time. This prevents long data latency or low instrument duty cycles. Nonetheless, a long required mission life also has implications for overall mission reliability, and a technology lien exists for critical spacecraft components to undergo additional long-life testing. This is particularly true in the case of sample return missions which could have lifetimes in excess of 25 years.

Another overall challenge is in meeting planetary protection guidelines. Earth flybys using RPS for power must ensure low probability of Earth re-entry. This should not be insurmountable as this has been done by prior missions. However, in the Saturn system, there are additional planetary protection issues to consider. Beyond the main spacecraft and/or lander impact analysis and cleansing requirements, any propulsion stage has the possibility of a future impact with Enceladus or another moon. Thus, trajectory analysis would be warranted for any booster stages, to determine the probability of impact and planetary protection level that should be met.

Finally, missions containing soft landers or hard impactors have additional challenges and risks. Soft landers must maintain anchoring to the surface during any sample collection and surface coupling for seismometer experiments. The techniques for achieving this require further study, as the surface properties of Enceladus may vary from fluffy snow to hard ice. The soft lander concepts developed here all operated on battery power, resulting in short life. This yields lower science return than would an RPS-powered lander, but in the case of a Saturn orbiter, it also leads to the significant risk of relying on a single opportunity to return science data to the orbiter.

For a hard impactor package, further development is needed in many areas. Further definition in battery sizing, thermal design, communication visibility between the orbiter and lander; methods for deploying from the orbiter, spinning up/spinning down before/after solid rocket motor firing, absorbing landing shock, adjusting to preferred orientation once on the surface, coupling to the surface for seismometry; and time correlation among the landers and the orbiter. If pursued in the future, technology investment will be required to develop techniques to survive the landing and couple to the surface.

In summary, the architecture trade study presented in this report found promising Enceladus mission concepts that would provide valuable, Flagship-level science in the two to three billion dollar ($FY07) range. The three study concepts that were developed use state of the practice technology and could be developed in time to meet the proposed launch dates. Key challenges, considerations and risks have been identified, some which are common to any mission to Saturn and some of which are unique to missions to study Enceladus. Possible mission design trades and their effects were discussed, along with insights gleaned about remaining trade space architectures. The SDT concluded that a Flagship mission to Enceladus can achieve a significant advance in knowledge and several mission concepts were presented that merit further study.

5.0 TEAM MEMBERS AND ROLES

Mission Design Team			
Name		Institution/Expertise	E Mail Address
Bly	Vince	GSFC/Lead Technologist	vincent.t.bly@nasa.gov
Di Pietro	Dave	GSFC/Mission Systems Engineer	david.a.dipietro@nasa.gov
Quinn	Dave	GSFC/Flight Dynamics	david.a.quinn@nasa.gov
Razzaghi	Andrea	GSFC/Study Lead	andrea.i.razzaghi@nasa.gov
Sneiderman	Gary	GSFC/Instrument Systems Engineer	gary.a.sneiderman@nasa.gov
Tompkins	Steve	GSFC/Engineering Coordinator	steve.tompkins@nasa.gov
Via	Lauri	GSFC/Financial Manager	lauri.via@nasa.gov
Science Definition Team			
Barr	Amy	SWRI/Geophysics/interiors	amy@boulder.swri.edu
Brinckerhoff	Will	APL/Astrobiology (in situ surface)	will.brinckerhoff@jhuapl.edu
Buratti	Bonnie	JPL/Spectroscopy	bburatti@scn.jpl.nasa.gov
Dalton	Brad	SETI/Spectroscopy	dalton@mail.arc.nasa.gov
Dombard	Andrew	APL/Geophysics/Geology	andrew.dombard@jhuapl.edu
Glavin	Dan	GSFC/Astrobiology/Instrumentation	daniel.p.glavin@nasa.gov
Helfenstein	Paul	Cornell/Geology	paulhelf@twcny.rr.com
Kirschvink	Joseph	CalTech/Astrobiology (interior)	kirschvink@caltech.edu
Mitchell	Don	APL/Energetic particles	don.mitchell@jhuapl.edu
Nimmo	Francis	UCSC/Geophysics	fnimmo@pmc.ucsc.edu
Simon-Miller	Amy	GSFC/Atmospheres, Co-Chair	amy.a.simon-miller@nasa.gov
Spencer	John	SWRI/Interdisciplinary, Co-Chair	spencer@boulder.swri.edu
Champion Team			
Andary	James	Systems	james.f.andary.1@gsfc.nasa.gov
Barney	Rich	Planetary Instruments	rich.barney@nasa.gov
Cardiff	Eric	Propulsion	eric.h.cardiff@nasa.gov
Folta	Dave	Flight Dynamics	david.c.folta@nasa.gov
Garvin	Jim	Science	jgarvin@milkyway.gsfc.nasa.gov
Niemeyer	Lee	Structures/Mechanical	lee.niemeyer@nasa.gov
Scott	Steve	General/Systems	steven.s.scott@nasa.gov
Steiner	Mark	Systems	mark.steiner@nasa.gov
Watzin	Jim	Planetary Missions	james.g.watzin@nasa.gov

Consultants			
Benson	Scott	Solar Electric Propulsion	Scott.W.Benson@nasa.gov
Cheatwood	Neil	Aerocapture	F.M.Cheatwood@nasa.gov
Christiansen	Eric	Particle Shielding	eric.l.christiansen@nasa.gov
Esposito	Larry	Plume Science	Larry.Esposito@lasp.colorado.edu
Green	Jacklyn	Radioactive Power Sources	jrgreen@jpl.nasa.gov
Haddox	Eric	Launch Vehicles	eric.m.haddox@nasa.gov
Harmon	Alan	Radioactive Power Sources	alan.harmon@hq.doe.gov
Powell	Richard	Aerocapture	r.w.powell@larc.nasa.gov
Prince	Jill	Aerocapture	Jill.L.Prince@nasa.gov
Reh	Kim	Billion Dollar Box Study Lead	Kim.R.Reh@jpl.nasa.gov
Riehl	John	Solar Electric Propulsion	john.p.riehl@nasa.gov
Simms	Jon	Navigation	Jon.A.Simms@jpl.nasa.gov
Spilker	Tom	Navigation	Thomas.R.Spilker@jpl.nasa.gov
Strange	Nathan	Navigation	Nathan.J.Strange@jpl.nasa.gov

Appendix A: Planetary Protection Definitions

NASA Planetary Protection Policy is described in NPD 8020.7F and is summarized as:

"The conduct of scientific investigations of possible extraterrestrial life forms, precursors, and remnants must not be jeopardized. In addition, the Earth must be protected from the potential hazard posed by extraterrestrial sources. Therefore, for certain space-mission/target-planet combinations, controls on organic and biological contamination carried by spacecraft shall be imposed in accordance with directives implementing this policy."

The NASA Planetary Protection Policy Implementing Documents are NPR 8020.12C Planetary Protection Provisions for Robotic Extraterrestrial Missions and NPR 5340.1C NASA Standard Procedures for the Microbial Examination of Space Hardware.

NPR 8020.12C:

- Defines Planetary Protection Mission Categories (summarized in **Table A-1**)
- Details Planetary Protection requirements (summarized in **Table A-2**)
- Establishes schedules for documentation and reviews
- Includes Planetary Protection parameter specifications

Table A-1: Planetary Protection Categories

Planet Priorities		Mission Type	Mission Category
A	Not of direct interest for understanding the process of chemical evolution. No protection of such planets is warranted (no requirements)	Any	I
B	Of significant interest relative to the process of chemical evolution, but only a remote chance that contamination by spacecraft could jeopardize future exploration.	Any	II
C	Of significant interest relative to the process of chemical evolution and/or the origin of life or for which scientific opinion provides a significant chance of contamination which could jeopardize a future biological experiment.	Flyby, Orbiter	III
		Lander, Probe	IV
	All Any Solar System Body	Earth-Return "unrestricted-"or "restricted Earth-return"	V

Table A-2: Planetary Protection Requirements by Mission Category

Category	General Requirement
II	Documentation only • Planetary Protection Plan • Prelaunch Planetary Protection Report • Postlaunch Planetary Protection Report • End-of-Mission Report
III	Implementing Procedures (as required) • Trajectory biasing • Clean room assembly • Microbial reduction or orbital lifetime Documentation • Same as Category II plus • Subsidiary plans (as required)
IV	Implementing Procedures • Trajectory biasing • Clean room assembly • Microbial reduction • Organics inventory and archive Documentation • Same as Category III plus • Subsidiary plans
V	Outbound Implementing Procedures and Documentation as per outbound categorization Inbound requirements if ‘Restricted Earth Return’ are additional documentation, return/reentry certification requirements, and sterilization or containment at Biosafety Level IV.

Appendix B: Reserved

Appendix C: Basic Planetary and Natural Satellite Data

Basic Planetary and Natural Satellite Data for Enceladus Mission						
References for values shown in this table are color coded as shown below:						
a) Report of the IAU Working Group on Cartographic Coordinates and Rotational Elements of the Planets and Satellites (13 July 2001)						
b) AGI STK Version 7						
c) Calculated						
	Sun	**Earth**	**Saturn**	**Titan**	**Enceladus**	**Notes**
Planet / Moon Characteristics						
μ (km^3/s^2)	1.3271E+11	3.9860E+05	3.7931E+07	8.9785E+03	7.2036E+00	
Mean Radius (km)		6.371E+03	5.823E+04	2.575E+03	2.494E+02	
Equatorial Radius (km)		6.378E+03	6.027E+04	2.575E+03	2.563E+02	
Surface Gravity (m/s^2)				1.354E+00	1.158E-01	$(\mu / r_{mean}^2) * 1000$
Escape Velocity @ Surface (km/s)		11.19	36.09	2.641	0.2403	$[2 \mu / r_{mean}]^{0.5}$
Circular Orbit Velocity @ 100 km (km/s)					0.1436	$[\mu / a]^{0.5}$
Circular Orbit Velocity @ 200 km (km/s)					0.1266	$[\mu / a]^{0.5}$
Average Orbit Characteristics						
Semi Major Axis (km)		1.496E+08	1.430E+09	1.221E+06	2.377E+05	
Eccentricity		0.01635	0.05493	0.02942	0.003599	
Period (days)		365.26	10809	15.931	1.3686	
Inclination (deg)		0.002	2.487	0.3567	0.1179	
RA of Ascending Node (deg)		254.65	113.63			
Argument of Perihelion (deg)		207.30	340.39			
Velocity at Apoapsis (km/s)		29.296	9.105	5.412	12.586	
Velocity at Periapsis (km/s)		30.268	10.184	5.740	12.677	
Average Velocity (km/s)		29.782	9.644	5.576	12.632	

Appendix D: Reserved

Appendix E: Comparison of Trade Space Concept Designs

Table E-1: Comparison of Trade Space Concept Designs

	Enceladus OL	Enceladus O	Saturn OL
Operations Summary			
Mission Description	Enceladus Orbiter w/Soft Lander	Enceladus Orbiter	Saturn Orbiter w/Soft Lander
Instruments	Orbiter: imagers & *in-situ* Lander: imager, seismometer, sample analysis	Orbiter: imagers, radar, & *in-situ*	Orbiter: imagers & *in-situ* Lander: imager, seismometer, sample analysis
Required Launch C_3 (km^2/s^2)	19.05	19.05	19.2
Required ΔV (m/s)	4497 (Booster + Orbiter) 415 (Lander)	4977 (Booster + Orbiter)	2797 (Orbiter) 4315 (Lander)
Launch Date	29 Sep 2018[2]	29 Sep 2018[2]	25 Mar 2018
Mission Duration (yrs)	18.3 (18.8 max)	17.3 (17.8 max)	9.5
Launch Window	20 days	20 days	20 days
Trajectory	VVEES + Rhea & Dione gravity assists	VVEES + Rhea gravity assists	Earth gravity assist
Earth/Venus Flyby Altitude (km)	4520 (Venus 1) 1545 (Venus 2) 1558 (Earth 1) 5450 (Earth 2)	4520 (Venus 1) 1545 (Venus 2) 1558 (Earth 1) 5450 (Earth 2)	1000 (Earth)
Saturn Orbit Insertion Date	May 2030	May 2030	Sep 2025
Time to Saturn Arrival (yrs)	11.75 12.25 (max)	11.75 12.25 (max)	7.5
Saturn Flyby Radius (km)	82,000	82,000	210,000
Orbiter Science Ops (yrs)	2.4	2.4	1.3
Plume Passages	12 @ 0.143 km/s	12 @ 0.143 km/s	12 @ 3.8 km/s
Total Time in Plume (min)	~73	~73	5.5
Lander Science Ops (days)	5-8	N/A	5-8
Data Latency (from collection to arrival at SOC)	36 hrs to 1 week	36 hrs to 1 week	36 hrs to 1 week
Mission Complete Date	Jan 2037 (Jul 2037 max)	Jan 2036 (Jul 2036 max)	Sep 2027
Flight Segment Summary			
Number of Stages	3	2	3
Fault Tolerance	1-fault tolerant	1-fault tolerant (except for Orbiter ASRGs)	SEP & Orbiter are 1-fault tolerant, (except for Orbiter ASRGs). Lander has selective redundancy
Structure	Carbon Fiber Composite/ Aluminum Alloy (booster/orbiter/lander)	Carbon Fiber Composite/ Aluminum Alloy (booster/orbiter)	Carbon Fiber Composite/ Aluminum Alloy (orbiter/lander) Aluminum Lithium (SEP)
Power System	Four ASRGs + Li Ion battery (Orbiter) Li Ion battery (Lander)	Three ASRGs + Li Ion battery (Orbiter)	Two ASRGs + Li Ion battery (Orbiter) Li Ion battery (Lander)
Thermal Control System	MLI/heaters + VCHP heat x-port to 2 VCHP panels (orbiter) MLI/heaters + RHUs (lander)	MLI/Heaters + heat pipe x-port to 2 louvered panels (orbiter)	MLI/Heaters + conductive mount to 2 conventional panels (orbiter) MLI + RHUs (lander)

	Enceladus OL	Enceladus O	Saturn OL
Propulsion	Dual-mode chemical (Booster & Orbiter) Mono-prop lander	Dual-mode chemical (Booster & Orbiter)	25 kW SEP module Dual-mode chemical (Orbiter) Bi-prop Lander
Attitude Control System	3-Axis, wheels/thrusters (orbiter) 6-DOF reaction control (lander)	3-Axis, wheels/thrusters	3-Axis, wheels/thrusters (orbiter) 6-DOF reaction control (lander)
Orbiter Pointing Control (deg)	.028	.028	0.10
Communication System	1.5 m fixed HGA X/Ka + Two X-Band omni (orbiter) Two cross dipole omni (lander)	1.5 m fixed HGA X/Ka + Two X-Band omni	1.5 m fixed HGA X/Ka + Two X-Band omni (orbiter) One cross dipole omni + One shaped omni (lander)
Development Schedule (mos)	72	66	73
Flight Segment Masses			
SEP Module Total Mass[1] (kg)	**N/A**	**N/A**	**2023**
Booster Total Wet Mass[1] (kg)	**2939**	**3920**	**N/A**
Orbiter Instrument Mass[1] (kg)	73	85	82
Orbiter Total Wet Mass[1] (kg)	**3153**	**1890**	**3299**
Lander Instrument Mass[1] (kg)	18.9	N/A	18.5
Lander Total Wet Mass[1] (kg)	**228**	**N/A**	**874**
Launch Mass[1] (kg)	**6320**	**5810**	**6196**
Launch Vehicle (LV)	Delta IV Heavy	Delta IV Heavy	Delta IV Heavy
LV Capability to Req'd C_3 (kg)	6300	6300	6525
LV Margin (%)	-0.3	8.4	5.3
Planetary Protection Category			
SEP	N/A	N/A	III
Booster	IV	IV	N/A
Orbiter	IV	IV	IV
Lander	IV	N/A	IV
Mission Cost Range			
Life Cycle Cost (FY07 $B)	**2.8 to 3.3**	**2.1 to 2.4**	**2.6 to 3.0**

1. Includes 30% dry mass contingency

2. Launch window ranges from 19 September to 9 October 2018. The trajectory modeled corresponds to the middle case, 29 September 2018. A 19 September date has a six month longer trip time but gives the highest allowable launch mass (lowest required C_3). A 9 October date has a 12 month shorter trip time, but gives the least allowable launch mass (highest required C_3). The mission is designed to accommodate the least allowable launch mass of the 9 October date and the longest mission duration (denoted "max") of the 19 September date.

Appendix F: Acronyms

ACS ....Attitude Control System
ARTG ....Advanced Radioisotope Thermoelectric Generator
ASRG ....Advanced Stirling Radioisotope Generator
AU ....Astronomical Unit
BOL ....Beginning of Life
C&DH ....Command & Data Handling
C_3 ....Hyperbolic Excess Velocity
CBE ....Current Best Estimate
CCD ....Charge-Coupled Device
CDA ....Cosmic Dust Analyzer
μCE-LIF ....Micro Capilliary Electrophoresis Analyzer with Laser Induced Fluorescence
CIDA ....Cometary Impact Dust Analyzer
CIRS ....Composite Infrared Spectrometer
COMPASS ....Collaborative Modeling for Parametric Assessment of Space Systems
ConOps ....Concept of Operations
CONTOUR ....Comet Nucleus Tour
DCIU ....Digital Control Interface Unit
DLA ....Declination of launch asymptote
DoD ....Depth of Discharge
DOE ....Department of Energy
DSN ....Deep Space Network
E/Q ....Energy per charge
EDX ....Energy Dispersive X-ray
EI ....Electron Ionization
EOI ....Enceladus Orbit Insertion
EOL ....End of Life
EOS ....Earth Observing System
EPO ....Education and Public Outreach
EPS ....Electric Power System
EPS ....Energetic Particle Spectrometer
ESA ....European Space Agency
ESI-TOF-MS ....Electrospray Ionization Time-of-Flight Mass Spectrometer
FIPS ....Fast Imaging Plasma Spectrometer
FSW ....Flight Software
FTE ....Full Time Equivalent
FUV ....Far Ultraviolet
GCMS ....Gas Chromatography and Mass Spectroscopy
GRC ....Glenn Research Center
GSFC ....Goddard Space Flight Center
HiRISE ....High Resolution Imaging Science Experiment
HQ ....NASA Headquarters
HST ....Hubble Space Telescope
I&T ....Integration & Testing
IDT ....Instrument Definition Team
IFOV ....Instantaneous Field of View
IMDC ....Integrated Mission Design Center
INGMS ....Ion and Neutral Gas Mass Spectrometer
INMS ....Ion and Neutral Mass Spectrometer
ISS ....Imaging Science Subsystem
ITAR ....International Traffic in Arms Regulations
JPL ....Jet Propulsion Laboratory

JSC........................Johnson Space Center
JWST....................James Webb Space Telescope
LaRC ....Langley Research Center
LASP ....Laboratory for Atmospheric and Space Physics
LDMS...................Laser Desorption Mass Spectrometer
LEISA ....Linear Etalon Imaging Spectral Array
LIBS......................Laser Induced Breakdown Spectroscopy
LIF........................Laser Induced Fluorescence
LOLA ....Lunar Orbiter Laser Altimeter
LORRI ....Long-Range Reconnaissance Imager
M/Q ....Mass per charge
M³ ....Moon Mineralogy Mapper
MCP.....................Micro-channel Plate
MEMSA ....Micro Electron Microprobe with Sample Analyzer
MESSENGER ......Mercury Surface, Space Environment, Geochemistry, and Ranging
MLI ....Multi Layer Insulation
MMRTG ....Multi-mission Radioisotope Thermoelectric Generator
MOC....................Mars Orbiter Camera
MSL......................Mars Science Laboratory
MVIC...................Multicolor Visible Imaging Camera
NAC ....Narrow-Angle Camera
NAIF ....Navigation and Ancillary Information Facility
NGIMS.................Neutral Gas and Ion Mass Spectrometer
NIR ....Near Infrared
NRC ....National Research Council
NUV ....Near Ultraviolet
OPAG ....Outer Planets Assessment Group
PAF.......................Payload Attach Fitting
PAH......................Polycyclic Aromatic Hydrocarbon
PDS ....Planetary Data System
PEPSSI..................Pluto Energetic Particle Spectrometer Science Investigation
QMS.....................Quadrupole Mass Spectroscopy
RHU ....Radioisotope Heater Units
RPS.......................Radioisotope Power Systems
SAM ....Sample Analysis at Mars
SDT ....Science Definition Team
SEIS ....Seismometer
SEMPA ....Scanning Electron Microscope Particle Analyzer
SEP ....Solar Electric Propulsion
SMA ....Safety & Mission Assurance
SOI ....Saturn Orbit Insertion
SSD.......................Solid State Detector
TDI ....Time-Delay Integration
THEMIS ....Thermal Emission Mapping Spectrometer
TID ....Total Ionizing Dose
TLS.......................Tunable Laser Spectrometer
TOF......................Time of Flight
TOF-MS ....Time of Flight Mass Spectroscopy
USO......................Ultra-Stable Oscillator
UV........................Ultraviolet
UVIS ....Ultraviolet Imaging Spectrometer
VCHP...................Variable Conductance Heat Pipe
VEEJS...................Venus-to-Earth-to-Earth-to-Jupiter-to-Saturn

V_{hp} ....Hyperbolic excess velocity on arrival at the planet
VIMS....................Visible and Infrared Mapping Spectrometer
VVEES.................Venus-to-Venus-to-Earth-to-Earth-to-Saturn
WBS.....................Work Breakdown Structure